Ozonation of amines: Kinetics, stoichiometry, product formation and mechanistic considerations

Dissertation

zur Erlangung des akademischen Grades eines
Doktors der Naturwissenschaften
- Dr. rer. nat. -

vorgelegt von

Agnes Tekle-Röttering

geboren in Lingen (Ems)

Institut für Instrumentelle Analytische Chemie
der
Universität Duisburg-Essen

2015

Die vorliegende Arbeit wurde im Zeitraum von Januar 2010 bis Juli 2015 im Arbeitskreis von Prof. Dr. Torsten C. Schmidt in der Fakultät für Chemie am Institut für Instrumentelle Analytische Chemie der Universität Duisburg-Essen durchgeführt.

Tag der Disputation: 04.04.2016

Gutachter: Prof. Dr. Torsten C. Schmidt
Prof. Dr. Thomas A. Ternes

Vorsitzender: Prof. Dr. Stephan Schulz

Phantasie ist wichtiger als Wissen,
denn Wissen ist begrenzt.

(Albert Einstein)

Summary

Amines are often present in micropollutants because they are an important structural unit of pharmaceuticals or agricultural pesticides. As a consequence of human activity the micropollutants are released in large quantities into the environment. Once released into the environment some of those substances remain in the environment for long periods of time due to their physical and chemical properties. As a result of the several sources of micropollutants in the environment a polishing treatment of wastewater effluents can help to minimize a discharge of micropollutants to receiving waters. For such a treatment, ozonation is often the preferred option. Albeit several studies for the ozonation of micropollutants are available, ozonation of amines in aqueous solution are hardly discussed in current literature. Since for aliphatic amines some knowledge is present, the focus of this work was on the ozonation of three classes of amines such as anilines, aliphatic and aromatic *N*-heterocyles. Thus, the overall objective of the present work is to foster our understanding of the behavior of amines, which also could be archetypes for some kind of pharmaceuticals, in their reaction with ozone.

In this work on the ozonation of anilines, aliphatic and aromatic *N*-heterocyles, kinetics, stoichiometric ratios and structural elucidation of transformation products of the ozone reactions were determined. In addition, advanced mechanistic considerations based on product formation were conducted. It has been demonstrated that anilines (k = 1.2 × 10^5 – 2.4 × 10^6 M^{-1} s^{-1}) and aliphatic *N*-heterocyles (k = 2.6 × 10^4 – 2.4 × 10^5 M^{-1} s^{-1}) can be transformed by ozone in reasonable time periods, as a result of their high reaction rate constants with respect to ozone. In contrast, aromatic *N*-heterocyles react slowly with ozone due to their low ozone rate constants (0.37 – 57 M^{-1} s^{-1}). Nevertheless, compound degradation for anilines (20 – 31%) and aliphatic *N*-heterocyles (13 – 16%) in relation to ozone consumed is small in spite of their high reactivity towards ozone, while the aromatic *N*-heterocyles with lower reactivity partly react even with better compound degradation (22 – 55%). The insufficient compound degradation is most likely due to a chain reaction (presumably induced through aminyl radicals) for which decomposition of ozone without compound degradation is proposed. This implication is derived from $^{\bullet}$OH scavenging results, in which compound transformation is increased almost with all in contrast to the non scavenged system.

Indeed, in the case of pyridine and pyridazine the ozonation resulted in adequate transformation (55 and 54%) in the $^{\bullet}$OH scavenged system. Albeit, pyrimidine and pyrazine have similar structures than pyridazine their reaction behavior to ozone is contradictory. Here, in the $^{\bullet}$OH scavenged system the compound transformation was significantly lower (14 and 2.1%) than in the non scavenged one (25 and 22%). This distinction is confirmed by product formation results.

It has been proposed in literature that for aniline itself ozone attacks to the nitrogen. The present study, however, revealed that ozone attack to the aromatic ring is the preferential reaction, based on substantial formation of *p*- and *o*-hydroxyanilines. However, ozone addition to the lone electron pair at nitrogen must also be envisaged, confirmed through the generation of nitro- and nitrosobenzene. It could be shown that preferentially piperidine and also morpholine (however, not preferentially) react with ozone via an addition reaction at nitrogen to *N*-hydroxypiperidine and *N*-hydroxymorpholine, respectively. In the ozonation of piperazine however, the corresponding *N*-hydroxypiperazine could not be detected. Here it could be revealed, that piperazine (as well as morpholine, although with a lower extent) predominantly reacts via electron transfer with ozone and consecutive reactions in particular with oxygen by releasing formaldehyde and hydrogen peroxide. Pyridine and pyridazine also react with ozone via an addition at nitrogen by forming the corresponding *N*-oxides in high yields. In pyrimidine and pyrazine ozonation the corresponding *N*-oxides are detected as well. However, contrary to expectations ozone adduct formation to the aromatic ring seems to occur in the ozonation of pyrimidine and pyrazine as inferred from hydrogen peroxide yield and reaction stoichiometry results. In the case of pyrazine $^{\bullet}$OH reactions should be a potential process, confirmed through stoichiometric ratio in scavenged and non scavenged systems.

In this study it could be shown that the ozonation of miscellaneous amines does not necessarily result in complete elimination but rather leads to the formation of transformation products. Still, the studies of this thesis exemplify that the amines under study should only be carefully applied as archetypes for pharmaceuticals, because even structurally very similar compounds react substantially different with ozone. This illustrates the importance of fundamental mechanistic considerations in ozone chemistry.

Zusammenfassung

Amine sind häufige Vertreter in Mikroverunreinigungen, da sie eine bedeutende strukturelle Einheit in pharmazeutischen Produkten oder Pestiziden darstellen. Als Folge menschlicher Aktivität gelangen die Mikroverunreinigungen teils in relevanten Konzentrationen in die Umwelt. Einmal in die Umwelt gelangt, können sie hier über einen langen Zeitraum verbleiben. Aufgrund verschiedener Eintragsquellen von Mikroverunreinigungen in die Umwelt, ist eine nachfolgende Behandlung der Abwasserströme von außerordentlicher Bedeutung, um den Eintrag der Mikroverunreinigungen in die Gewässer zu minimieren. Für eine solche Behandlung ist die Ozonisierung eine bevorzugte Technik. Auch wenn etliche Untersuchungen zur Ozonisierung von Spurenstoffen in der Literatur verfügbar sind, ist die Reaktion von Aminen mit Ozon in wässriger Lösung kaum in der aktuellen Literatur diskutiert. Da für aliphatische Amine allerdings bereits ein ausreichender Kenntnisstand vorliegt, ist der Focus dieser Arbeit die Ozonisierung der drei Aminklassen Aniline, sowie aliphatische und aromatische stickstoffhaltige Heterozyklen. Um ein möglichst umfassendes Bild vom Verhalten der Amine in ihrer Reaktion mit Ozon zu erhalten, wurden diese Aminklassen im Rahmen der vorliegenden Dissertation, auch unter dem Aspekt ihres Einsatzes als Modellsubstanzen für bestimmte Arten von Arzneimitteln, untersucht.

In der vorliegenden Arbeit, die sich mit der Ozonisierung von Anilinen, aliphatischen und aromatischen *N*-haltigen Heterozyklen beschäftigt, wurden kinetische und stoichiometrische Untersuchungen der Ozonreaktionen sowie die Bestimmung der Transformationsprodukte durchgeführt. Darüber hinaus wurden weitergehende mechanistische Betrachtungen, die auf der Produktbildung bei der Ozonisierung basierten, vorgenommen. Als Ergebnis ihrer, bezogen auf Ozon, hohen Geschwindigkeitskonstanten konnte gezeigt werden, das die Aniline (1.2×10^5 – 2.4×10^6 M^{-1} s^{-1}) und aliphatischen *N*-Heterozyklen (2.6×10^4 – 2.4×10^5 M^{-1} s^{-1}) in angemessener Zeit mit Ozon umgesetzt werden. Die aromatischen *N*-Heterozyklen hingegen reagieren, aufgrund ihrer niedrigen Geschwindigkeitskonstanten (0.37 – 57 M^{-1} s^{-1}) langsam mit Ozon. Nichtsdestotrotz ist der Substanzabbau der Aniline (20 – 31%) und aliphatischen *N*-Heterozyklen (13 – 16%), trotz ihrer hohen Ozonreaktivität, unzureichend in Bezug zum Ozonverbrauch, während die aromatischen *N*-Heterozyklen mit geringerer

Ozonreaktivität teilweise mit einem besseren Substanzabbau bezogen auf Ozon reagieren (22 − 55%). Der unzureichende Substanzabbau beruht höchstwahrscheinlich auf einer Radikalkettenreaktion, bei der angenommen wird, dass Ozonverbrauch erfolgt ohne einen weiteren Substanzabbau zu gewährleisten. Nachgewiesen werden konnte dies durch steigenden Substanzumsatz beim Abfangen der OH-Radikale bei nahezu fast allen Substanzen. Tatsächlich ergab die Ozonisierung von Pyridin und Pyridazin in einem OH-Radikale abfangendem System einen hinreichenden Umsatz (55 and 54%) im Gegensatz zu Pyrimidin und Pyrazin, auch wenn sie eine ähnliche Struktur wie Pyridazin aufweisen. Es konnte dargelegt werden, dass ihr Reaktionsverhalten mit Ozon gegensätzlich ist, da der Substanzabbau von Pyrimidin und Pyrazin in Systemen, indem die OH-Radikale abgefangen wurden (14 und 2.1%) erheblich niedriger ist, als in Systemen indem OH-Radikale vorhanden sind (25 und 22%). Bestätigt werden konnte dieser Unterschied durch die Ergebnisse der Produktbildung.

Vorschläge in der Literatur postulieren, dass insbesondere beim Anilin der Ozonangriff am Stickstoff erfolgt. Die aktuelle Untersuchung jedoch offenbart, das ein Ozonangriff am aromatischen Ring die bevorzugte Reaktion darstellt, basierend auf eine substanzielle Bildung von *p*- und *o*-Hydroxyanilin. Ein Angriff des Ozons am freien Elektronenpaar des Stickstoffs ist jedoch ebenfalls vorstellbar. Bestätigt werden konnte dies durch die Bildung von Nitro- und Nitrosobenzol. Weiterhin konnte demonstriert werden, das vorzugsweise Piperidin und ebenso Morpholin, wenn auch in geringerem Ausmaß, mit Ozon über eine Additionsreaktion am Stickstoff zu *N*-Hydroxypiperidin bzw. *N*-Hydroxymorpholin reagieren. Bei der Ozonisierung von Piperazin konnte das entsprechende *N*-Hydroxypiperazin nicht detektiert werden. Hier konnte dargelegt werden, dass Piperazin und ebenso Morpholin, jedoch in geringerem Ausmaß, vorzugsweise über einen Elektronentransferprozess mit Ozon reagiert und durch weitergehende Reaktionen insbesondere mit Sauerstoff Formaldehyd und Wasserstoffperoxid freisetzt. Pyridin und Pyridazin reagieren, nachweislich durch die Entstehung der entsprechenden *N*-Oxide mit hoher Ausbeute, mit Ozon über eine Addition am Stickstoff. Bei der Ozonisierung von Pyrimidin and Pyrazin konnten die adäquaten *N*-Oxide ebenfalls detektiert werden. Entgegen den Erwartungen scheint bei der Ozonisierung von Pyrimidin und Pyrazin jedoch auch eine Ozonadduktbildung am aromatischen Ring stattzufinden, welches sich aus den Ergebnissen der

Reaktionsstöchiometrie sowie der Wasserstoffperoxidausbeute ableiten lässt. Beim Pyrazin muss zudem dokumentiert werden, dass wahrscheinlich auch ein OH-Radikalangriff vorliegt, was sich ebenfalls aus den Resultaten der Reaktionsstöchiometrie in Systemen mit und ohne OH-Radikale belegen läßt.

In dieser Studie konnte gezeigt werden, dass die Ozonisierung der untersuchten Amine nicht notwendigerweise in vollständige Eliminierung resultiert, sondern eher zur Bildung von Transformationsprodukten führt. Die Ergebnisse der vorliegenden Arbeit veranschaulichen zudem, dass die untersuchten Amine nur sorgfältig ausgewählt als Modellsubstanzen für bestimmte Arten von pharmazeutischen Produkten verwendet werden können, da sogar strukturell sehr ähnliche Komponenten äußerst unterschiedlich mit Ozon reagieren. Dies zeigt die Bedeutung von grundlegenden mechanistischen Betrachtungen in der Ozonchemie.

Table of Contents

Summary V

Zusammenfassung VII

Table of Contents X

1 General Introduction 1

1.1 Preface 1

1.2 General information on amines 3

1.2.1 Anilines 4

1.2.2 Piperidine, piperazine and morpholine 7

1.2.3 Pyridine, pyridazine, pyrimidine and pyrazine 9

1.3 General information on ozone 13

1.3.1 Ozone reactions in aqueous solution 17

1.3.2 Ozone decay and OH radical ($^{\bullet}$OH) formation in water 22

1.3.3 Kinetics, stoichiometry and product formation 24

1.4 Scope of the thesis 30

1.5 References 31

2 Ozonation of anilines: Kinetics, stoichiometry, product identification and elucidation of pathways 39

2.1 Abstract 39

2.2 Introduction 40

2.2.1 Theoretical background 42

2.3 Experimental part 46

2.3.1 Chemicals and materials 46

2.3.2 Methods 46

2.4 Results and discussion 48

2.4.1 Reaction kinetics 48

2.4.2 Reaction stoichiometry 53

2.4.3 Product formation 56

2.4.4 Mass balances and mechanistic considerations 65

2.5 Conclusions 66

2.6 References 66

2.7 Supporting Information 73

3 Ozonation of piperidine, piperazine and morpholine: Kinetics, stoichiometry, product formation and mechanistic considerations 105

3.1 Abstract 105

3.2 Introduction 106

3.3 Experimental part 110

3.3.1 Chemicals and materials 110

3.3.2 Methods 110

3.4 Results and discussion 112

3.4.1 Reaction kinetics 112

3.4.2 Reaction stoichiometry 115

3.4.3 Product formation 120

3.4.4 Mass balances and mechanistic considerations 130

3.5 Conclusions 131

3.6 References 131

3.7 Acknowledgment 138

3.8 Supporting Information 139

4 Ozonation of pyridine and other *N*-heterocyclic aromatic compounds: Kinetics, stoichiometry, identification of products and elucidation of pathways 164

4.1 Abstract 164

4.2 Introduction 165
4.2.1 Theoretical background 167
4.3 Experimental part 169
4.3.1 Chemicals and materials 169
4.3.2 Methods 169
4.4 Results and discussion 171
4.4.1 Rate constants 171
4.4.2 Reaction stoichiometry 176
4.4.3 Product formation 182
4.4.4 Mass balances and mechanistic considerations 190
4.5 Conclusions 192
4.6 References 192
4.7 Acknowledgment 199
4.8 Supporting Information 200
5 General conclusion and outlook 224
5.1 References 230
6 Supplement A-1
6.1 List of abbreviations A-1
6.2 List of publications A-5
6.3 Curriculum Vitae A-7
6.4 Acknowledgment A-8
6.5 Erklärung A-9

1 General Introduction

1.1 Preface

Anthropogenic organic compounds, commonly also called micropollutants, are ubiquitously present in the aquatic environment. These compounds comprise besides industrial chemicals and pesticides pharmaceuticals, which in the last decades have attracted broad scientific interest. Notably, considerable concern has been raised regarding potential effects on ecotoxicity due to the presence of pharmaceuticals in the aquatic environment. As most human pharmaceuticals are not or incompletely metabolised in treated individuals, large fractions are excreted unmodified and reach the municipal wastewater. Conventional biological treatment in municipal wastewater treatment plants is an insufficient barrier for the release of many of these pharmaceuticals and its metabolites into the receiving waters. Veterinary pharmaceuticals or agricultural pesticides in turn predominantly accomplish the surface waters through agricultural operations. A lot of pharmaceuticals have been identified in relevant concentrations in the aquatic cycle (Ternes & Joss, 2006). Furthermore, water research conducted so far indicates that transformation of pharmaceuticals in the environment as well as in technical processes might result in the formation of potentially toxic transformation products. This bears unforeseen risks for aquatic life and drinking water resources. On this account to minimize a discharge of micropollutants to receiving waters is essential. Micropollutant abatement by ozonation in drinking water and wastewater is, therefore, gaining importance (Ternes et al., 2002, 2015, Huber et al., 2003, Snyder et al., 2006, Schwarzenbach et al., 2006, Benitez et al., 2011).

Amines are an important structural unit of many micropollutants because they are common precursors in several industrial products, e.g., pharmaceuticals (see Scheme 1 for some examples), agricultural pesticides or dyes (Vogt & Geralis, 1985, Koch, 1995, Schmidt et al., 1998, Ternes et al., 2005). Corresponding to their multiple application amines reach the aquatic environment from different sources, e.g., from both, industrial and municipal wastewater (Huber et al., 2005, Gabet-Giraud et al., 2010). In particular aromatic amines are in general more polar than their precursors and thus have a higher solubility in water, which is responsible for the high mobility of aromatic

amines in aquifers (Schmidt et al., 1998). It has to be noted, that several aromatic amines show a high acute and, maybe more important, chronic toxicity (Koch, 1995).

Scheme 1. Pharmaceuticals, containing amine structural units (in dotted circles), e.g., the anti-inflammatory drug dichlofenac, the beta blocker timolol, the antihistamine cetirizin, the antibacterial agent enoxacin, the antimalarial drug pyrimethamine, the bacteriostatic drug pyrazineamide and the decongestant clenbuterol (Ternes & Joss, 2006).

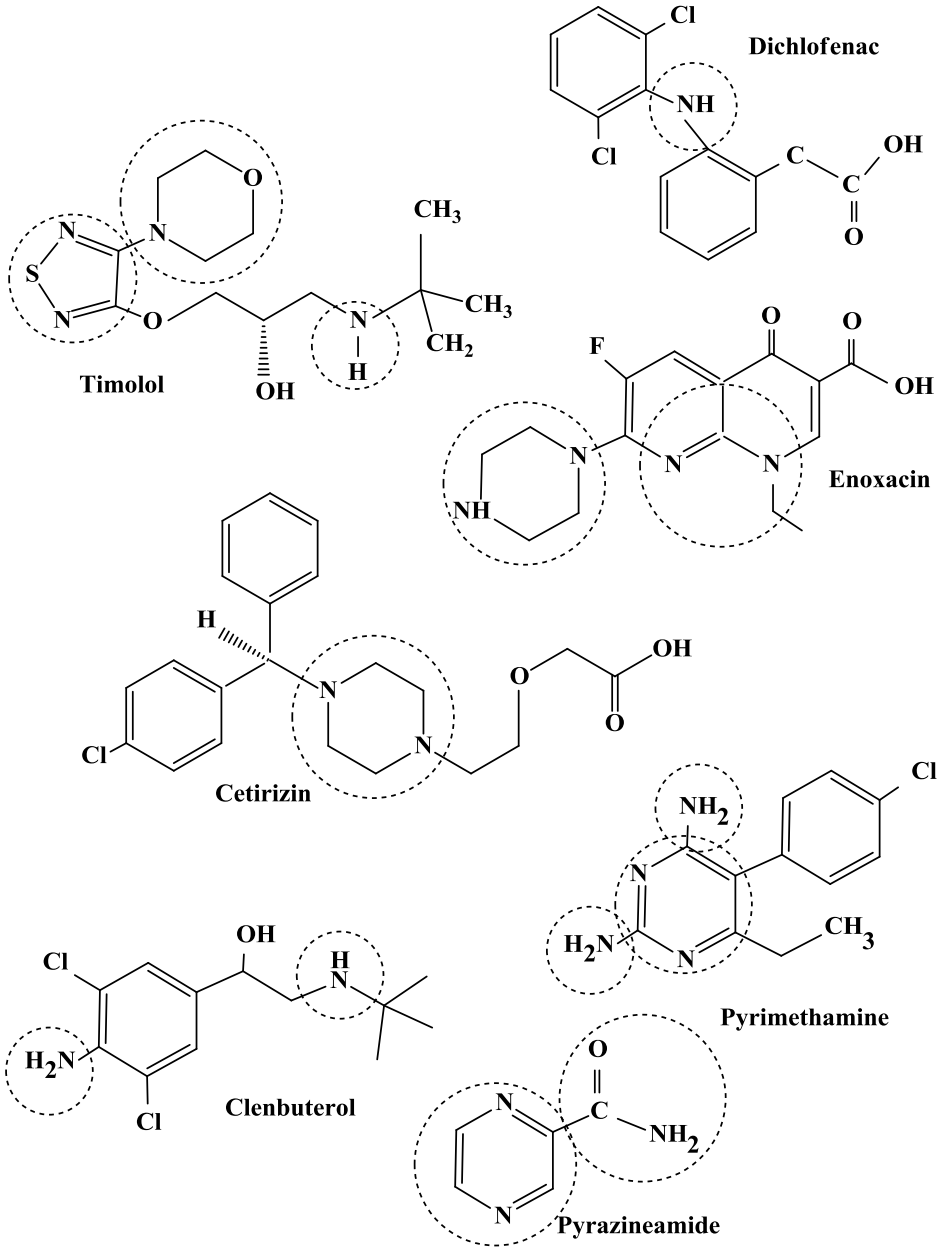

1.2 General information on amines

Amines are organic compounds that contain a nitrogen atom with a lone electron pair, which they can share with another atom, e.g., hydrogen. It has to be noted, that protonation of nitrogen atoms depends on the accessibility of the electron pairs in the sp^3-, sp^2 or sp-orbitals (see Scheme 2), for though from sp^3 over sp^2 to sp the s-character of the orbital increases, while the p-character decreases. Hence, in one s-orbital the electron is close to the nucleus, whereas the electron in one p-orbital is in considerable distance to the nucleus. Thus the attractive force for an electron in one p-orbital is lower than in one s-orbital.

Scheme 2. Orbital scheme of sp, sp^2 and sp^3 hybridisation (taken from wikipedia article: hybridorbital).

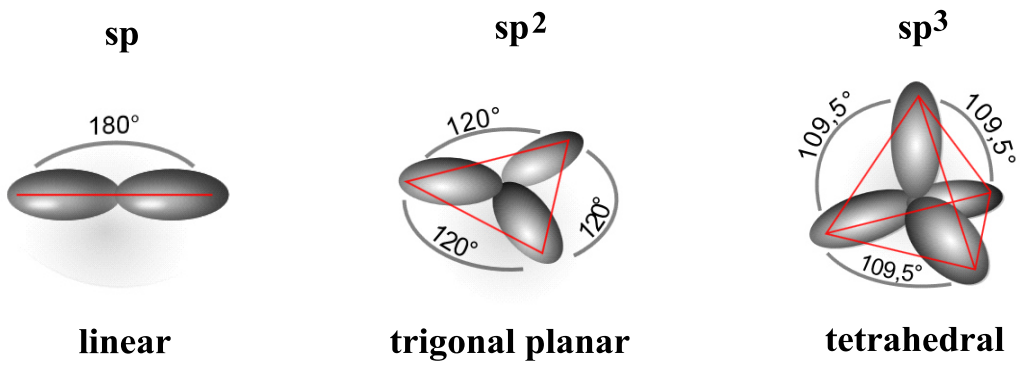

Consequently, the electron pair in a sp^3-orbital is most available and the corresponding molecule is more alkaline (Morrison & Boyd, 1986). Hence, the basicity also increases with electron density at the nitrogen. Thus, the most important characteristic of amines is their basicity, which dictates the chemical behaviour of the amines. Moreover, this characteristic is also responsible for the high reactivity of the aromatic rings with an amino group (Morrison & Boyd, 1986). Aromatic amines are considerably less alkaline than aliphatic amines, because the lone electron pair at nitrogen is delocalized in the aromatic ring and is not so easy available for a proton. Thus, aniline (pK_a of corresponding anilinium ion 4.63) is less alkaline than ammonia (pK_a of ammonium ion 9.25). The delocalization facilitates an electrophilic attack at the benzene ring because of the conjugation of the negative charge into the aromatic ring.

For the reversible addition of a proton at nitrogen, the position of equilibrium depends on the pK_a (see values of the acid dissociation constants (pK_a values) of the corresponding acids of the amines under study in Scheme 5, 7 and 9). The dissociation constant for an acid or base is a direct consequence of the thermodynamics of the dissociation reaction (Morrison & Boyd, 1986). Thus, the pK_a value is directly proportional to the standard Gibbs energy change for the reaction and depends on molecular structure in many ways including the structural factors of inductive or mesomeric effects. Acid dissociation constants are essential in aquatic chemistry, because the behaviour, e.g., of the amines in solution can be understood only if their speciation is known. In principle, for bases the equilibrium constant K_b (or base dissociation constants pK_b) has been defined as the association constant for protonation of the base from the conjugate acid, however, typically K_a is used for bases, too (Perrin et al., 1981, Atkins, 1998). By reason that amines have polarized atomic bonds, which take part in hydrogen bonds the molecules with a low number of C-atoms are mostly soluble in water (Vollhardt & Schore, 2005).

Amines are subdivided into primary (e.g., anilines), secondary (e.g., piperidine) and tertiary amines (e.g., trimethylamine) due to the number of carbon atoms (organic substituents) bound to the nitrogen (Morrison & Boyd, 1986). An organic compound with multiple amino groups is defined by the number of NH_2 - groups as diamine, triamine and so forth. An important group of amines are those in which the nitrogen is part of a cyclic ring. In general, compounds containing in the ring structure at least two different elements as members of its ring (typically besides carbon nitrogen, oxygen or sulphur) are called heterocycles. In particular *N*-heterocyclic compounds contain ring nitrogens, in some the nitrogen may carry a hydrogen. These *N*-heterocycles can be of aromatic (i.e., pyridine) or of aliphatic nature (i.e., piperidine), saturated or non saturated (Davies, 1995). In the following the structure of amines that are in the focus of this work are introduced in more detail.

1.2.1 Anilines

Anilines as the prototypical aromatic amines are consisting of phenyl groups attached to amino groups with a sp^3 hybridisation of the nitrogen atom shown in Scheme 3.

Scheme 3. Orbital scheme of the sp^3 hybridisation nitrogen of aniline.

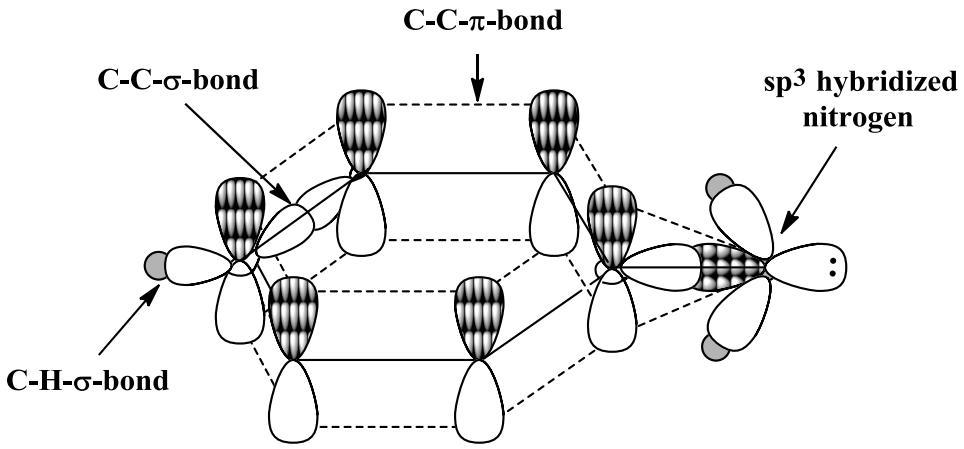

As mentioned above, anilines are in general much weaker bases than aliphatic amines nonetheless they can form anilinium (or phenyl-ammonium) ions. The weak basicity (see pK_a-values of the conjugate acid in water in Scheme 5) is based on both effects, the electron-withdrawing effect (minus inductive effect, (−I)) from the electronegative sp^2 carbon of the phenyl group and the resonance effect (positive mesomeric effect, (+M)). Since the lone pair on the nitrogen is partially delocalized into the π-system of the benzene ring (see above) aniline has higher resonance stability than its ion (see Scheme 4) (Morrison & Boyd, 1986).

Scheme 4. Resonance forms of the aniline molecule (Morrison & Boyd, 1986).

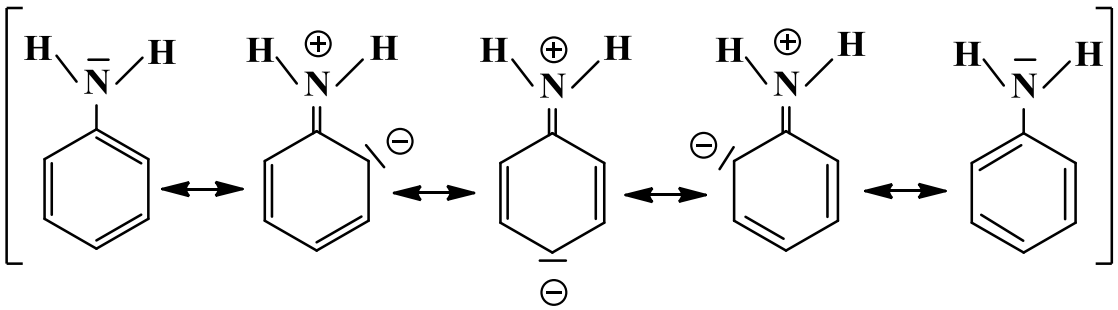

Substituents on the aromatic ring influence the reaction behaviour significantly. Scheme 5 indicates models of substituted anilines investigated in this study. Regarding electrophilic reactions the substituents can generally be divided into two classes: activating and deactivating the aromatic ring (refer to Scheme 6). As expected activating groups (e.g., ^{-}OH, $^{-}CH_3$, $^{-}NH_2$) stabilize the cationic intermediate formed during the substitution by donating electron density into the π system of the ring. This

occurs by either inductive effect or resonance effects and will increase the rate of reaction. On the contrary, deactivating substituents (e.g., −Cl, $-NO_2$, −COOH) destabilize the intermediate action by withdrawing electron density from the aromatic ring and thus decrease the rate of reaction for electrophilic attack.

Scheme 5. Compilation of the investigated anilines (pK_a values depicted from Sims, 1959).

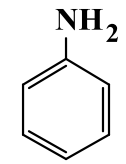

Aniline
pK_a = 4.63

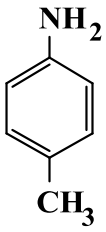

***p*-Methylaniline**
pK_a = 5.08

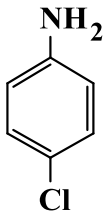

***p*-Chloroaniline**
pK_a = 4.00

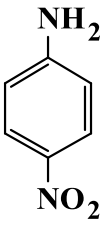

***p*-Nitroaniline**
pK_a = 1.00

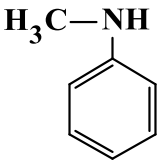

***N*-Methylaniline**
pK_a = 4.85

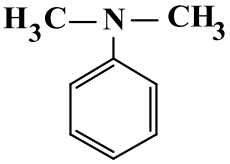

***N,N*-Dimethylaniline**
pK_a = 5.00

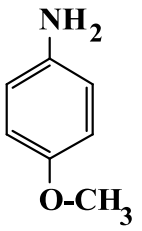

***p*-Methoxyaniline**
pK_a = 5.31

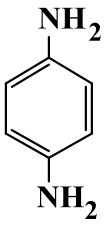

***p*-Phenylenediamine**
pK_{a1} = 6.20
pK_{a2} = 2.67

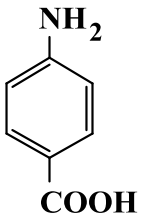

***p*-Aminobenzoic acid**
pK_a = 4.93
p$K_{a(COOH)}$ = 2.38

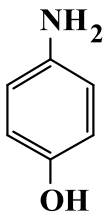

***p*-Hydroxyaniline**
pK_a = 5.14
p$K_{a(OH)}$ = 10.3

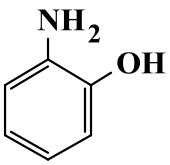

***o*-Hydroxyaniline**
pK_a = 4.84
p$K_{a(OH)}$ = 9.71

Similarly the regioselectivity of the molecules are affected by the substituents already attached to the benzene ring. Groups with unshared pairs of electrons, such as the amino group of aniline promote substitution at the *ortho* or *para* position (*ortho-para*-directing), while deactivating substituents like nitro groups, which cannot donate electron density to the π - system direct the electrophile to the *meta* position (*meta*-

directing). The reason is that in *meta* position the reactivity is not reduced through the negative mesomeric effect. Whereas the pattern of regioselectivity can be explained with resonance structures, the influence on kinetics can be explained by both resonance structures and the inductive effect. The mesomeric effect is negative (−M) when the substituent belongs to an electron-withdrawing group and the effect is positive (+M) when based on resonance the substituent is an electron donating group. The inductive effect on the difference in electronegativity between atoms is negative (−I) when the substituent is an electron-withdrawing group and the effect is positive (+I) when the substituent has an electron donating character (Brückner, 1996, Morrison & Boyd, 1986, Vollhardt & Schore, 2005).

Scheme 6. Activating / deactivating and *ortho* / *para* / *meta* directing effects of substituents.

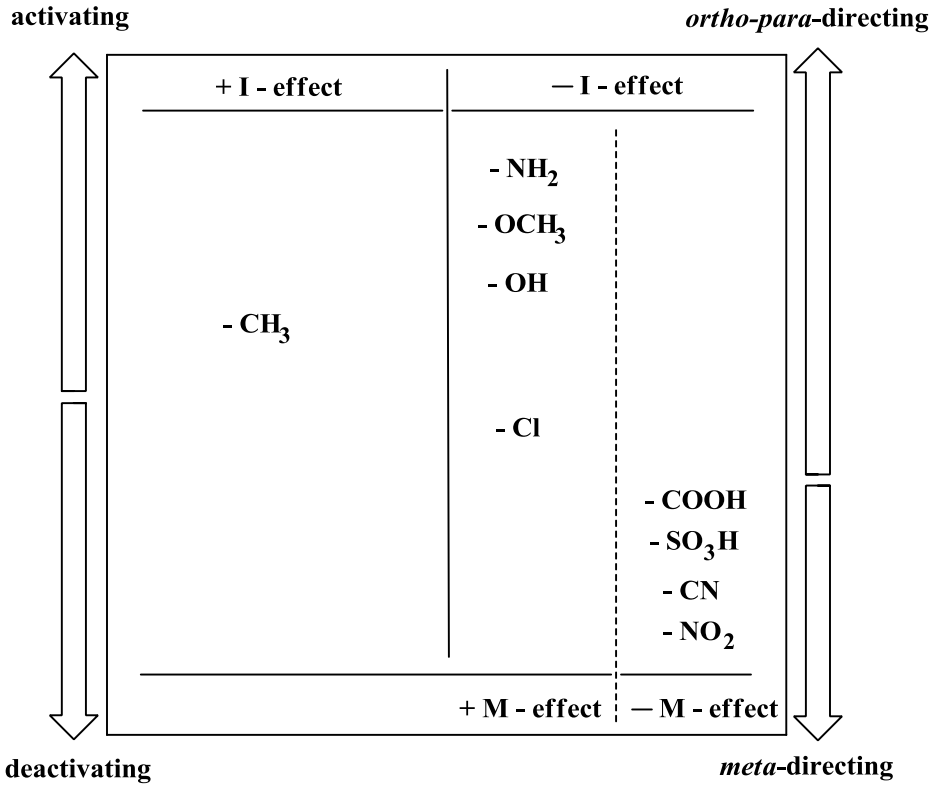

1.2.2 Piperidine, piperazine and morpholine

Piperidine, piperazine and morpholine belong to aliphatic *N*-heterocycles as well as to secondary amines. The three structures of these *N*-heterocycles (azinan after Hantsch-Widmann nomenclature) are closely related to that of cyclohexane (Parkin et. al., 2004). It has to be noted that an aromatic ring is not essential for the stability of

heterocyclic rings, thus saturated rings occur widely. Piperidine and piperazine consist of a six-membered ring containing four or five methylene bridges (-CH_2-), respectively and one (in the case of piperazine two) amine bridges (-NH-) with a sp^3 hybridisation of the nitrogen atom. In addition, morpholine holds an amine (-NH-) and oxygen bridge (-O-). Albeit, in the following the planar structure of the aliphatic *N*-heterocycles are used for describing reactions schemes, the aliphatic *N*-heterocycles have a three-dimensional structure, e.g., the chair conformation as presented in Scheme 7.

Scheme 7. Compilation of the investigated aliphatic *N*-heterocyclic compounds (pK_a values depicted from Lide, 2009).

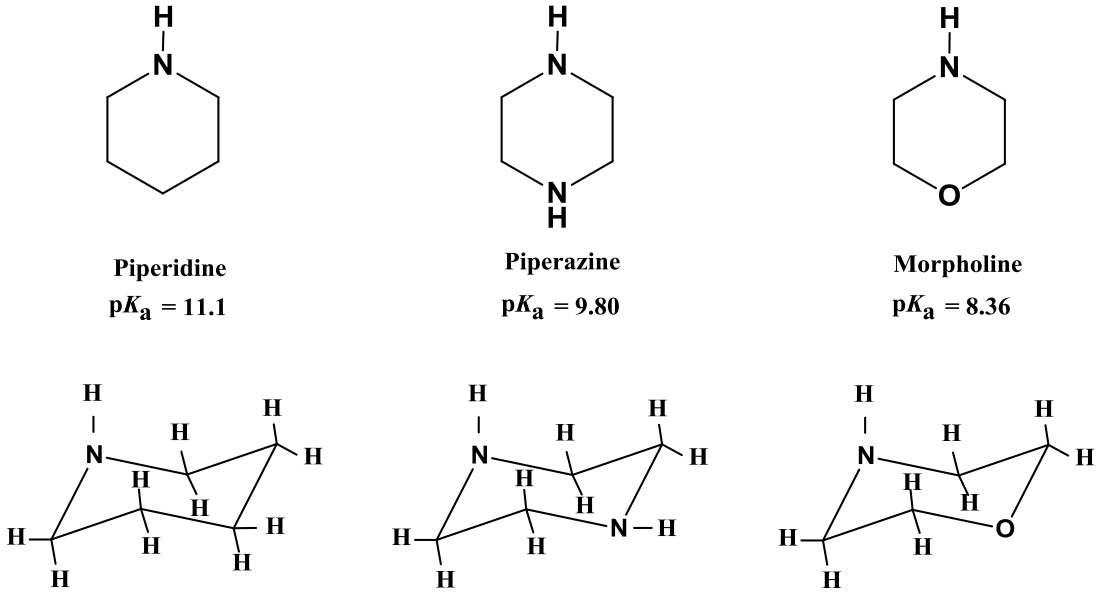

The ring nitrogen of these compounds contains a lone electron pair, which in principle is available for donation to electrophiles. Thus, relating to basicity the saturated heterocyclic hydrocarbons behave like their analogous acyclic compounds. Thereby, piperidine, piperazine and morpholine are strong bases as is to be expected for aliphatic secondary amines. Moreover, the fact that in the heterocycles two alkyl substituents are connected to form a ring has only a slight effect in increasing the strength of the base (see pK_a-values of the conjugate acid in water in Scheme 7) (Rubiralta et. al., 1991).

Referring to reactivity most of the reactions of piperidine are those of a typical secondary amine. Hence, piperidine is an excellent nucleophile (Rubiralta et. al., 1991).

In general also the reactivity of piperazine and morpholine would not be very different from that expected of an amine and hence similar to that of their aliphatic analogues.

1.2.3 Pyridine, pyridazine, pyrimidine and pyrazine

Pyridine, pyridazine, pyrimidine and pyrazine belong to the aromatic *N*-heterocycles, containing nitrogens as an imine unit (C=N) as part of their ring structure. These *N*-heterocycles bear sp^2 hybridized nitrogen (see Scheme 8), in which the lone electron pair is less available than in a sp^3 hybridisation present in aniline and aliphatic *N*-heterocycles. On this account the nitrogen lone electron pair is not much conjugate in the aromatic π-system (Joule & Mills, 2010).

Scheme 8. Orbital scheme of the sp^2 hybridisation nitrogen of pyridine.

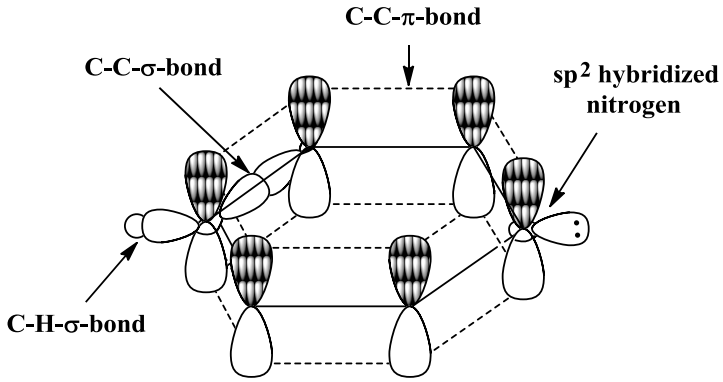

Pyridine (Scheme 9) is structurally related to benzene (Johnson, 1984). One of the CH units in benzene is replaced by nitrogen, which leads to inductive and resonance effects, because the sp^2 hybridized nitrogen is more electronegative than the sp^2 hybridized carbon. Thereby, it gives rise to the canonical forms (1a), (1b) and (1c) of pyridine. Substitution of two carbon atoms of the benzene ring by nitrogen atoms gives rise to three possible isomeric diazines, i.e., pyridazine, pyrimidine and pyrazine (Scheme 9), with the nitrogen atoms occupying a 1,2-, 1,3- or 1,4-position, respectively (Porter, 1984). Pyridazine (1,2-diazine) is represented as a resonance hydrid of two structures (2a) and (2b), however with a larger contribution of the canonical form (2a) with a single bond character between the nitrogen atoms. The replacement of two CH units in benzene by nitrogen atoms to give pyrimidine (1,3-diazine) results in reduced symmetry, however pyrimidine does retain symmetry with regard to the 2,5-axis. The

pyrazine (1,4-diazine) ring in turn may be represented as a resonance hybrid of a number of canonical structures (4a-4d) with charge separated structures such as (4c) contributing significantly, as evidenced by the polar character of the C=N bond in a number of reactions (Porter, 1984). The reactivity of aromatic *N*-heterocycles, which is a combination of that expected from an aromatic system combined with the influence of the nitrogen involved is usually more complex and integrate additional principles (see below and Katrizky, 1984).

Scheme 9. Some resonance hybrid structures of the aromatic *N*-heterocylic compounds (pK_a values depicted from Katrizky et al., 1984).

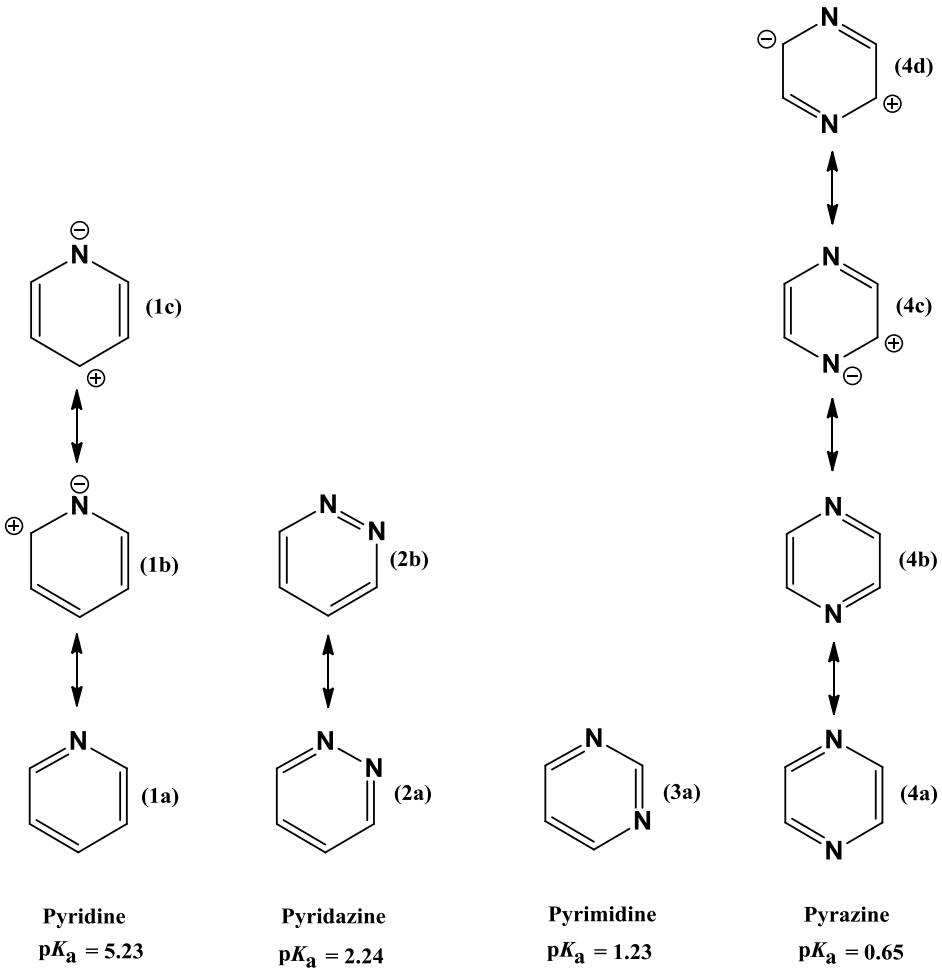

The above mentioned *N*-heterocycles are all in all weak bases, whereat the pK_a-values still differ significantly since many factors can influence the accessibility of the electron pair for protonation (see pK_a-values of the conjugate acid in water in Scheme 9). Pyridine is substantially less basic than aliphatic amines (pK_a ~ 10), nevertheless, the electron pair in the sp^2 orbital (see Scheme 8) of nitrogen is accessible for protonation

(Morrison & Boyd, 1986). Hence, electrophilic addition to the nitrogen generates pyridinium ions, the simplest of which is 1*H*-pyridinium formed by addition of a proton (Joule & Mills, 2010).

In general, the diazines are much weaker bases than pyridine, since the availability of the nitrogen lone pairs is reduced, because the second ring-nitrogen shares the available π-electrons with the first. The reduction in basicity is thereby believed to be largely a consequence of destabilisation of the mono-protonated cations due to a combination of inductive and mesomeric withdrawal by the second nitrogen atom (Joule & Mills, 2010). Secondary effects, however, determine the order of basicity for the three systems. Pyridazine undergoes protonation much easier than the other diazines, a result which is ascribed to the "α-effect", i.e., the increased nucleophilicity is deemed to be due to electron repulsion between the two immediately adjacent nitrogen lone pairs (Joule & Mills, 2010). On this account protonation occurs more readily than if inductive effects were operating. The basicity of pyrimidine is reduced, reflecting the destabilising influence of the second nitrogen on the *N*-protonation (Brown, 1984). In the case of pyrazine mesomeric interaction between the protonated and deprotonated nitrogen atoms in opposite positions in the ring probably destabilizes the cation further. Hence, pyrazine is a weaker base than pyrimidine.

Nevertheless, all aromatic *N*-heterocycles can react with electrophilic species like oxidants such as hydrogen peroxide under mild conditions by addition at nitrogen to form *N*-oxides, respectively, similar to tertiary amines (Joule & Mills, 2010, Johnson, 1984, Tisler & Stanovnik, 1984). These amine oxides, for example pyridine-*N*-oxide are remarkable in that they react easily with both electrophiles and nuceleophiles. Generally speaking, electrophilic addition at aromatic *N*-heterocycles containing two nitrogens takes place only at the first nitrogen, because the presence of the positive charge in the products renders the second nitrogen extremely unreactive towards a second electrophilic addition (Porter, 1984).

The diazines are more resistant to electrophilic substitution at the aromatic ring than is pyridine, because two heteroatoms withdraw electron density from the ring carbons even more than one in pyridine (Joule & Mills, 2010). Consequently, electrophilic substitution of hydrogen at the ring carbon of pyridine is considerable slower than in

benzene, whereas pyridine undergoes electrophilic attack readily at nitrogen (Scriven, 1984). Certainly, there is an increased localization of electron density in the carbon-nitrogen bonds (137 pm), with carbon-carbon bonds being similar in length to those in benzene (139 pm). Thus, the electron density at the pyrazine carbon atom is similar to that at α-position in pyridine and this is manifest in the comparable reactivity of these positions in the two rings. Furthermore, for pyrimidine it is evident that there is considerable depletion of electron density at the 2/4/6- positions, a slight depletion at the 5-position and a greatly enhanced electron density at the nitrogen atoms. Accordingly, electrophilic attack will be confined to C-5 or the ring nitrogen atoms. The depletion of electron density at positions α or γ to the ring-nitrogens are naturally more marked in pyrimidine, where the ring-*N*-atoms act in unison, than in pyridazine or pyrazine, where this is not the case, or in pyridine that has only one electron-withdrawing centre (Tisler & Stanovnik, 1984). In addition, diazines undergo likewise substitution by nucleophilic radicals, in acid solution, with ease (Joule & Mills, 2010). On the other hand radical substitution at pyridine is more frequent than in benzene and often the preferential pathway. All heterocycles, the azin and diazines (as well as the aliphatic *N*-heterocycles and the anilines) are completely miscible with water, as the lone electron pairs on nitrogen atoms are involved in formation of hydrogen bonds with hydroxylic solvents (Tisler & Stanovnik, 1984).

1.3 General information on ozone

Ozone was discovered and named by Christian Schönbein (1799−1896) in 1839 although the chemical structure of the ozone molecule that consists of three oxygen atoms was not confirmed until 1872 (Langlais et al., 1991). In order to combine the three oxygen atoms the ozone molecule represents a resonance hybrid formed by four canonical structures (shown in Scheme 10) which was finally established in 1952 (Trambarulo, 1953, Hoigné, 1998, Beltrán, 2004).

Scheme 10. Resonance forms of the ozone molecule (Hoigné, 1998).

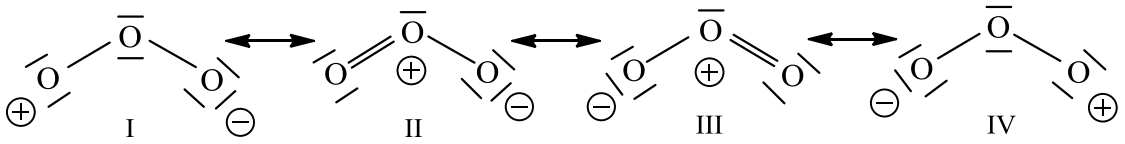

The resonance structures II and III in Scheme 10 basically represent the electronic structure of ozone. Nonetheless, resonance forms I and IV also contribute to some extent to the ozone molecule because the ozone angle is lower than 120° (see Table 1 and Scheme 11 and 12) due to the attraction of positively and negatively charged adjacent oxygen atoms (Beltrán, 2004).

Scheme 11. Orbital scheme of ozone.

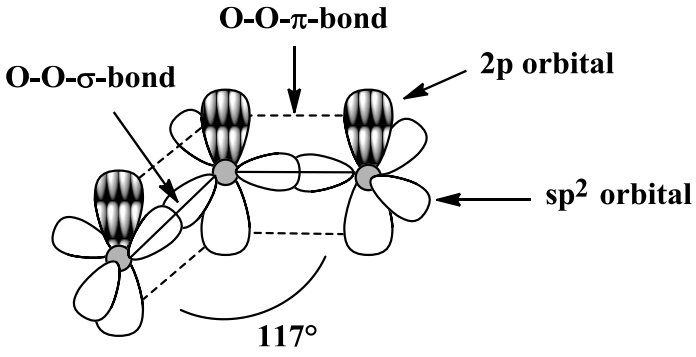

The high reactivity of ozone can be attributed to the electronic configuration of the triatomic oxygen molecule. The reduced electron density in one of the terminal oxygen atoms in some of the resonance hybrid structures confirms the electrophilic character of ozone.

Scheme 12. Scheme of molecular orbitals of ozone (Holleman & Wiberg, 2007).

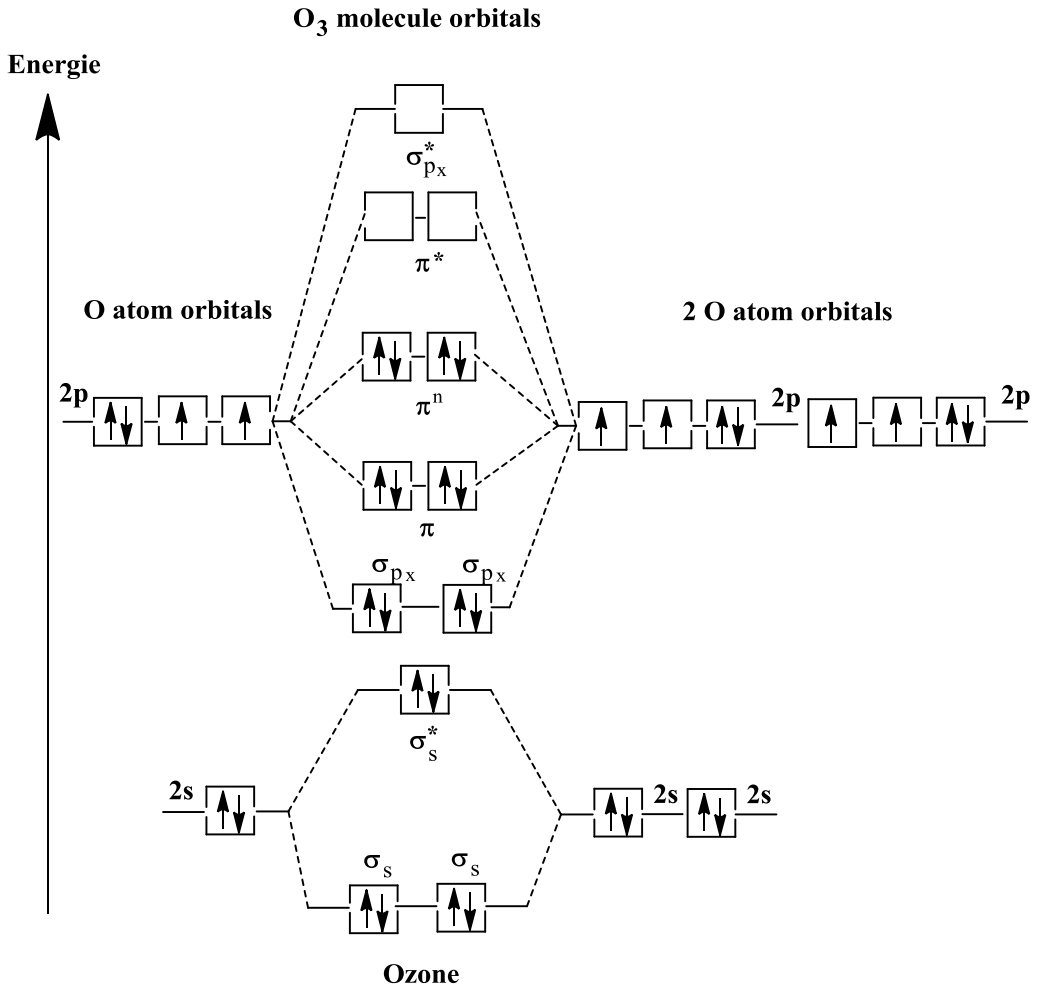

Conversely, the excess negative charge present in some other oxygen atoms imparts a nucleophilic character. Due to these properties ozone is an extremely reactive compound. However, it should be noted, that most of the information related to nucleophilic reactions has been obtained in an organic medium and not in aqueous solution (Beltrán, 2004). Nonetheless the reactivity of ozone, derived from its electrophilic character has been applied in the treatment of water and wastewater. The desinfecting power of ozone (Sonntag, 1890) was already realised practically in the late 19th century. Later on, the oxidation of micropollutants also became an important field of ozone application (von Sonntag & von Gunten, 2012).

Ozone is ten times more soluble in water than oxygen (von Sonntag & von Gunten, 2012). This allows one to obtain rather high concentrations by saturating water with an ozone/oxygen mixture from an ozone generator that is still rich in oxygen. Ozone

solubility strongly depends on temperature and ozone concentration is about twice as high at 0°C than at room temperature (see Table 1).

Table 1. Compilation of some physical properties of ozone (von Sonntag & von Gunten, 2012).

Property	**Value**
Molecular weight	48 Da
Dipole moment	0.537 Debye
Bond length	1.28 Å
Bond angle	117°
Melting point	-192.7°C
Boiling point	-110.5°C
Solubility in water at 0°C	2.2×10^{-2} M
Solubility in water at 20°C	1.19×10^{-2} M
Henry constant at 0°C	35 atm M^{-1}
Henry constant at 20°C	100 atm M^{-1}
Explosion threshold	10% Ozone

The concentration of ozone in aqueous solution can be determined by measuring its absorption at 260 nm (see Figure 1) using a molar absorption coefficient of 3200 M^{-1} cm^{-1} (von Sonntag & von Gunten, 2012).

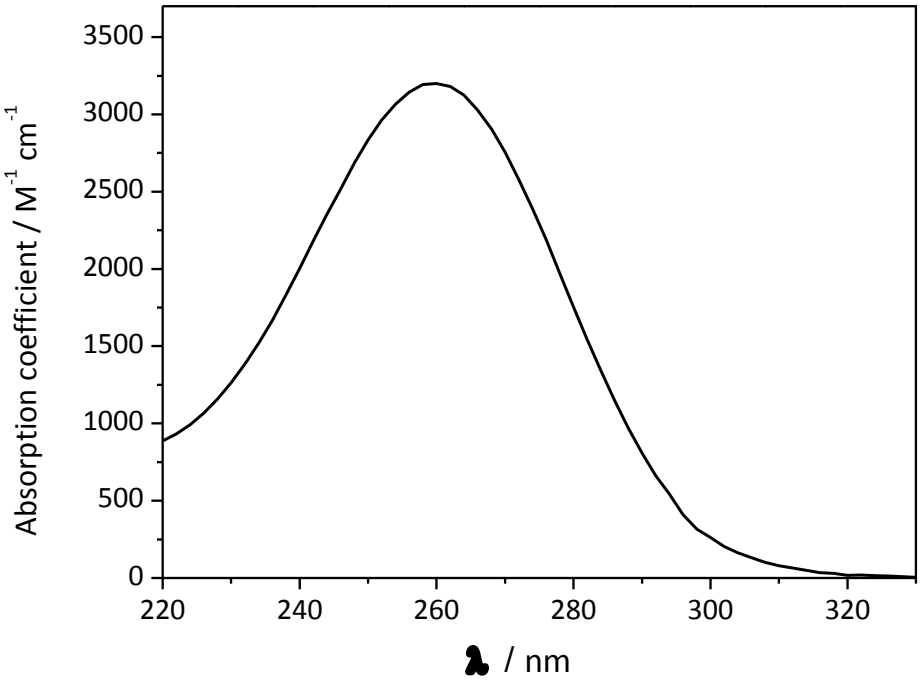

Figure 1. UV-absorption spectrum of ozone with a molar absorption coefficient of 3200 M^{-1} cm^{-1}.

Another method for the quantification of ozone in aqueous solution is the indigo method (Schönbein, 1854, Bader & Hoigné, 1982). In this approach indigotrisulfonate is bleached by ozone (see Scheme 13) and the extent of bleaching is quantified through the residual indigotrisulfonate by measuring its absorption at 600 nm with a molar absorption coefficient of 20000 M^{-1} cm^{-1} (Bader & Hoigné, 1982, Gordon & Pacey, 1986, Muñoz & von Sonntag, 2000a, von Sonntag & von Gunten, 2012). Indigotrisulfonate reacts very quickly with ozone (k (O_3 + indigo) = 9.4×10^7 M^{-1} s^{-1}). Albeit, details of this reaction have not been yet investigated, if the site of ozone attack is the central C-C double bond, sulfonated isatine and the corresponding α-hydroxyhydroperoxide should be formed (see Scheme 13, reaction (1) – (3), von Sonntag & von Gunten, 2012).

Scheme 13. Possible reaction of indigotrisulfonate with ozone by forming sulfonated isatine and the corresponding hydroperoxide.

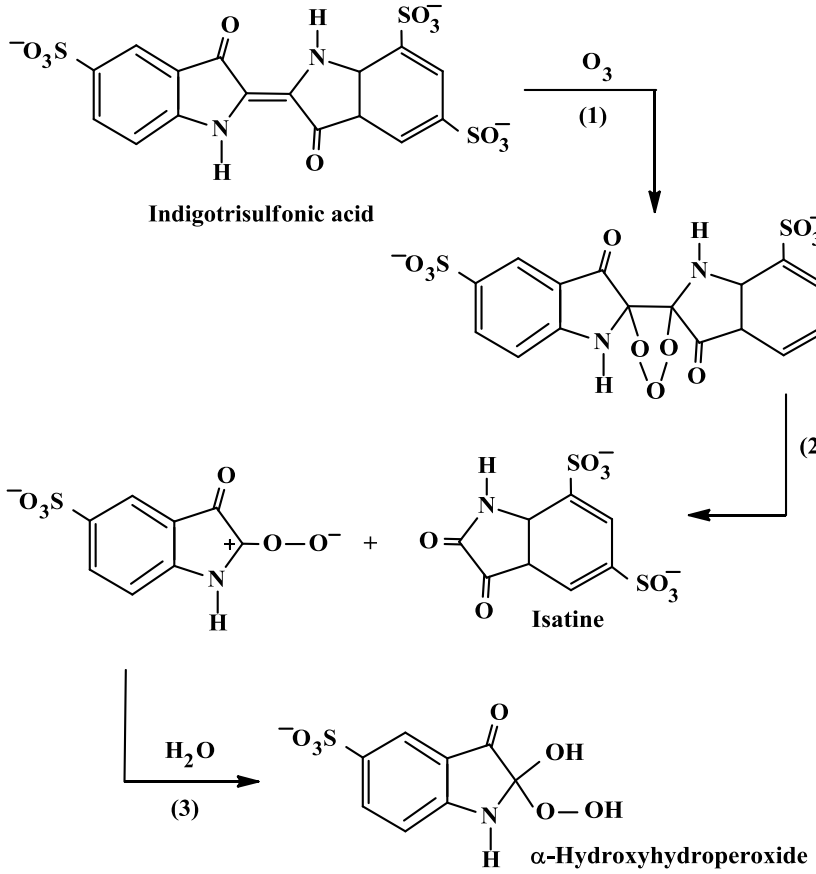

1.3.1 Ozone reactions in aqueous solution

The ozone chemistry of organic compounds was first studied systematically by Carl Friedrich Harries (1866−1923). He coined the name “ozonide” for compounds formed in the reaction of ozone with organic compounds, notably olefins (Rubin, 2003). A breakthrough in the mechanistic understanding of ozone reactions was achieved by Rudolf Criegee (1902-1975). The reactions of olefins with ozone (Criegee, 1975) rightly carry his name. A pioneer in ozone chemistry in aqueous solution was Jürg Hoigné (1930-2014). He realized that ozone reactions in aqueous solution may induce free-radical reactions (Hoigné & Bader, 1975) that seems not to occur in organic solvents (von Sonntag & von Gunten, 2012). Due to its electronic configuration (see above), ozone reacts in different ways with organic compounds in aqueous solution.

These reactions can be dived into three categories:

- **Oxidation-reduction reactions (e.g., electron transfer)**
- **Substitution / elimination reactions (e.g., H-abstraction)**
- **Electrophilic addition reactions (e.g., ozone addition)**

Oxidation-reduction reactions are characterized by the transfer of electrons from one species to another. Among common oxidants used in water treatment, ozone has one of the highest standard redox potentials (E° = 2.07 V), albeit lower than the oxygen atom (E° = 2.42 V) and hydroxyl radical (E° = 2.80 V). Thus, there is a substantial driving force for an electron transfer. Examples of explicit electron transfer reactions are the reactions between ozone and aromatic compounds (see Scheme 14, reaction (4)) by forming a radical cation and an ozonide radical anion (see also Scheme 15, Sehested et al., 1983, Hoigné et al., 1998).

Scheme 14. Electron transfer in the reaction of ozone with an aromatic compound.

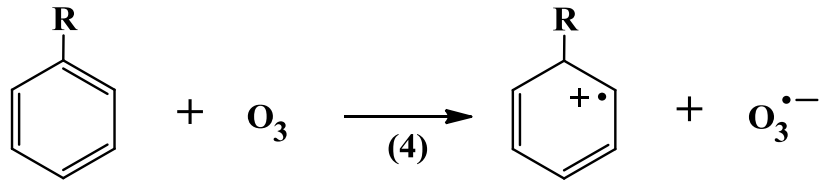

In principle there also could be no explicit electron transfer, but rather an oxygen transfer from the ozone molecule to the other compound (Beltrán, 2004).

Scheme 15. Resonance forms of the ozonide radical anion.

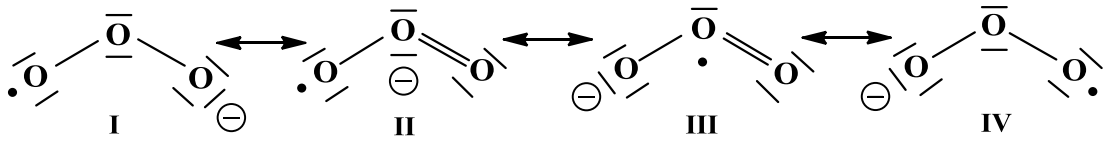

In substitution or elimination reactions, an electrophilic agent (such as ozone) attacks a nucleophilic position of an organic molecule (i.e., an aromatic compound) resulting in the substitution or elimination of one part (i.e., atom, functional group etc., for example H-abstraction) of the molecule (see reactions (5) – (7) in Scheme 16, Morrison & Boyd, 1986, von Sonntag & von Gunten, 2012).

Scheme 16. Electrophilic substitution in the reaction of ozone with an aromatic compound.

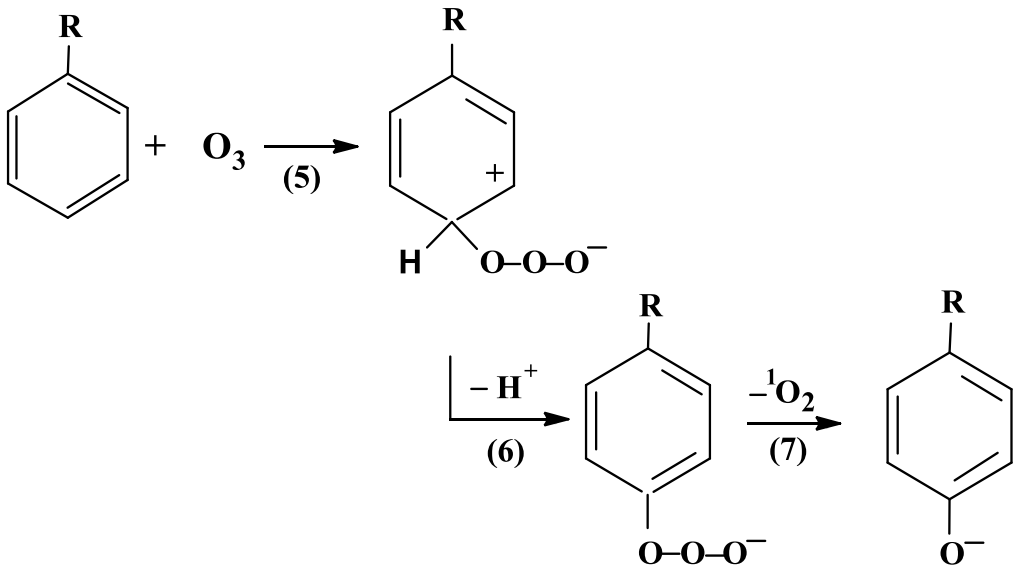

In the breakdown of the ozone adduct singlet oxygen, $^1O_2$, could be released (reaction (7)). Since the ground state of the ozone adduct is a singlet state, the overall spin multiplicity of the products must also be a singlet. This is required from the spin conservation rule. Singlet oxygen has two higher-energy species of molecular oxygen, in which the electrons are paired in contrast to triplet oxygen (see Scheme 17). Triplet oxygen is the ground state of molecular oxygen and its electron configuration has two unpaired electrons occupying two degenerate molecular orbitals with parallel spin. The excited singlet state, $O_2(^1\Delta_g)$, lies 95.5 kJ mol^{-1} above the triplet ground state, $O_2(^3\Delta_{g^-})$ (Muñoz et al., 2001, von Sonntag & von Gunten, 2012).

An important consideration is the presence of substituents in the aromatic molecule (i.e., phenol, toluene, aniline etc.). These groups strongly affect the reactivity of the aromatic ring towards electrophilic agents. Thus, groups such as $^-$HO, $^-$Cl, $^-CH_3$ etc. activate or deactivate the aromatic ring for the electrophilic substitution (see chapter 1.2.1). Depending on the nature of the substituting group, the substitution reaction can take place at different nucleophilic positions of the aromatic ring. Thus, activating groups promote the substitution of hydrogen atoms from their *ortho* and *para* positions with respect to these groups, while the deactivating groups favor substitution in the *meta* position (see chapter 1.2.1).

Scheme 17. Scheme of the molecular orbitals of oxygen (Wikipedia article: oxygen).

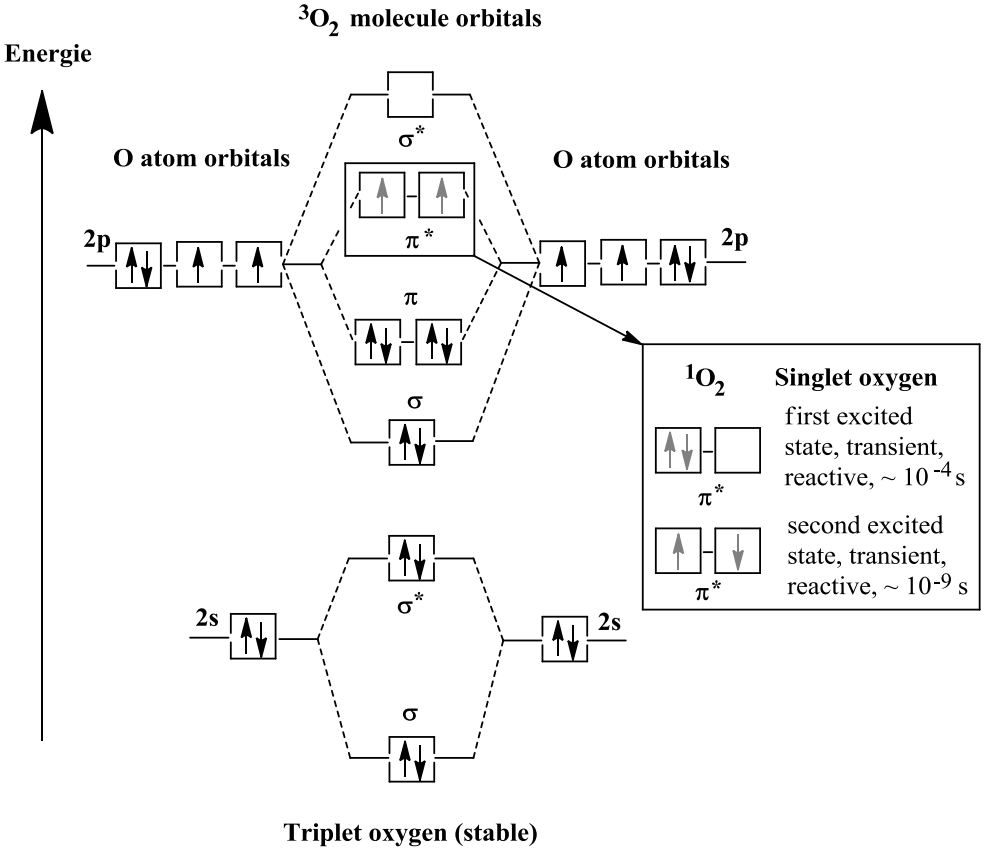

In fact, the activating effect of an OH-group and deactivating effect of a NO_2-group in ozone reactions is reported in the literature. Here, kinetic studies of the ozonation of aromatic compounds show very different rate constants e.g., reactions between ozone and phenol (k = 1.3 × 10^3 M^{-1} s^{-1}, Hoigné & Bader, 1983a, b) and ozone and nitrobenzene (k = 0.09 M^{-1} s^{-1}, Hoigné & Bader, 1983a, b, or 2.2 M^{-1} s^{-1} Beltrán et al., 1998), respectively. It should be noted, however, that these values in particular for phenol correspond to pH 7. Still to mention, the rates of phenol ozonation are largely influenced by the pH of water because of the acidic character of phenols so that the reaction of its anion, the especially reactive species (k = 1.4 × 10^9 M^{-1} s^{-1}, Hoigné & Bader, 1983b) is close to diffusion controlled (Beltrán, 2004, Mvula & von Sonntag, 2003, Ramsmeier & von Gunten, 2009). Thereby, ozone is a highly selective reactant and ozone rate constants with aromatic compounds (Neta et al., 1988) and nitrogen-containing compounds (von Sonntag & von Gunten, 2012) vary strongly with the nature of substituents by ten orders of magnitude. A similar wide spread by as much eight orders of magnitude is also observed with olefins that vary with the nature of the

substituents at the C−C double bond as well (Dowideit & von Sonntag, 1998, von Sonntag & von Gunten, 2012).

Addition reactions are resulting from the combination of two molecules to yield a third one (Morrison & Boyd, 1986). An addition reaction can take place between an electrophilic compound and a compound with π electrons. An example is the Criegee mechanism between ozone and an olefinic compound, which constitutes a cycloaddition reaction. Compounds with different double bonds (C=O or C=N), however, do not react with ozone through this type of reaction (Erikson et al., 1969, White & Bailey, 1965).

Aromatic compounds can also react with ozone through 1,2-cycloaddition reactions (see Scheme 18, reaction (8)). However, the cycloaddition is less likely than the attack from one of the terminal oxygen atoms of the ozone molecule on any nucleophilic center of the aromatic compound. A reason for this is the stability of the aromatic ring that results from the resonance structure. Note that the cycloaddition reaction leads to the breakup of the aromatic ring, then to loss the aromaticity, while the attack from only one oxygen atom retains the aromatic resonance (Beltrán, 2004). Nevertheless, the transfer to a cycloaddition from one oxygen atom attack is also feasible. In many cases, there will be different ozone-reactive sites within a molecule such as an aromatic ring and an aliphatic amino group. In summary, ozone reacts fast with compounds revealing double bonds, activated aromatic systems and deprotonated amines.

Scheme 18. Cycloaddition in the reaction of ozone with an aromatic compound.

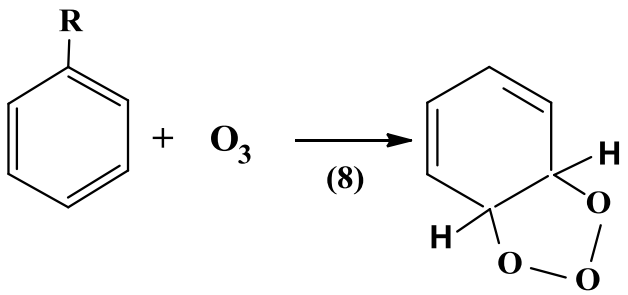

1.3.2 Ozone decay and OH radical ($^{\bullet}$OH) formation in water

Aqueous ozone decomposition plays a very important role in the application of ozonation processes. In conventional ozonation, the stability of dissolved ozone was found to be readily affected by pH, UV light, ozone concentration and the presence of free radical scavengers (Tomiyasu, 1985, Ku et al., 1996). In the research of ozone chemistry in defined aqueous solutions free radicals could be formed in a side reaction of ozone with electron rich moieties of several compounds, i.e. free amines and activated aromatic compounds by yielding hydroxyl radicals, $^{\bullet}$OH (Nöthe et al., 2009, Beltrán, 2004). In these reactions ozone undergoes electron transfer yielding a radical cation and an ozonide radical anion, $O_3^{\bullet-}$ (see Scheme 14, reaction (4)) that is in equilibrium with $O^{\bullet-}$ and O_2 (reaction (12)). The oxide radical anion, $O^{\bullet-}$ can react with water to $^{\bullet}$OH (reaction (13)). However, the protonation of $O^{\bullet-}$ inhibits the reverse reaction since $^{\bullet}$OH does not react with O_2 (pK_a = 11.8, von Sonntag & von Gunten, 2012). Water does not react with ozone (k ($H_2O + O_3$) < 10^{-7} M^{-1} s^{-1}, Neta et al., 1988), but its conjugate base, $^{-}$OH (reaction (9)), does, (k ($^{-}$OH + O_3) = 48 M^{-1} s^{-1}, Forni et al., 1982 or 70 M^{-1} s^{-1}, Staehelin & Hoigné, 1982). The slow reaction of ozone with hydroxyl ions, however, may only yield $^{\bullet}$OH at pH > 8. Note that this reaction (9) might be initiated by formation of HO_4^- which rapidly decomposes into $O_2^{\bullet-}$ and $HO_2^{\bullet}$ (Merényi et al., 2010). Furthermore, ozone decomposition reactions can also contribute to reactions of ozone with further ions e.g., hydroperoxide ions (see reaction (10)) and others. Still to mention, that reaction (10) are initiated by formation of HO_5^- that can decomposes into $O_3^{\bullet-}$ and $HO_2^{\bullet}$, indeed can also yield $^3O_2$ and $^{-}$OH, because both pathways are similar fast (von Sonntag & von Gunten, 2012).

The $^{\bullet}$OH are extremely reactive with any organic (and some inorganic) matter present in water (Buxton et al., 1988). Hence, compounds, which are refractory in ozone chemistry may be degraded in ozone based processes due to the formation of hydroxyl radicals ($^{\bullet}$OH) (von Gunten, 2003). Albeit, in the ozone decomposition mechanisms, the $^{\bullet}$OH could be an responsible species (k ($^{\bullet}$OH + O_3) = 1.1 $\times$ 10^8 M^{-1} s^{-1}, Sehested et al., 1984 or 3.0 $\times$ 10^9 M^{-1} s^{-1}, Bahnemann & Hart, 1982), ozone undergoes reactions more readily with any other type of chemical species, in particular with organic compounds

and other free radicals, e.g. the superoxide radical anion (Lind et al., 2003). Thereby the superoxide radical anion is also the key to propagating free radical species because it rapidly reacts with ozone (k ($O_2^{\bullet -}$) + O_3) = 1.5 × 10^9 M^{-1} s^{-1}, Sehested et al., 1983 or 1.6 × 10^9 M^{-1} s^{-1}, Bühler et al., 1984) to yield free radicals, such as the ozonide radical anion, which in turn can lead to $^{\bullet}OH$ (von Sonntag & von Gunten, 2012, see reactions (10) to (13)).The fast ozone reaction with free radicals is in some cases close to diffusion-controlled (von Sonntag & von Gunten, 2012). The kinetics for diffusion controlled reactions was discussed by Noyes (Noyes, 1954).

$$O_3 + {}^{-}OH \longrightarrow O_2^{\bullet -} + HO_2^{\bullet} \quad k = 70\ M^{-1}s^{-1} \qquad (9)$$

$$O_3 + HO_2^{-} \longrightarrow O_3^{\bullet -} + HO_2^{\bullet} \quad k = 2.8 \cdot 10^6\ M^{-1}s^{-1} \qquad (10)$$

$$O_3 + O_2^{\bullet -} \longrightarrow O_3^{\bullet -} + O_2 \quad k = 1.6 \cdot 10^9\ M^{-1}s^{-1} \qquad (11)$$

$$O_3^{\bullet -} \rightleftharpoons O^{\bullet -} + O_2 \quad k = (1.4 \text{ or } 3.5) \cdot 10^3\ M^{-1}s^{-1} \qquad (12)$$

$$O^{\bullet -} + H_2O \longrightarrow {}^{\bullet}OH + {}^{-}OH \quad k = 1.0 \cdot 10^8\ M^{-1}s^{-1} \qquad (13)$$

Thus, in general compounds of different nature can contribute to the generation or inhibition of free radicals, which are promotors of the decompositition of ozone (von Sonntag & von Gunten, 2012). Promotors are those species that, through their reaction with the $^{\bullet}OH$, yield free radicals and propagate a radical chain reaction. This process is e.g., driven by the release of $HO_2^{\bullet}$/ $O_2^{\bullet -}$ that could react with ozone giving rise to $^{\bullet}OH$. Finally, inhibitors of the decomposition are those species, (i.e., dimethyl sulfoxide) that while reacting with the $^{\bullet}OH$ not yielding $O_2^{\bullet -}$ and thus terminate the radical chain. These inhibitors are called $^{\bullet}OH$ scavengers.

Since in aqueous ozone chemistry experiments are usually performed in air saturated solution the oxygen concentration is sufficiently high. Hence, in particular in its reaction with free radicals, ozone has to compete with oxygen. Yet, oxygen reacts only

with few radical types (e.g., C-centered radicals) rapidly and irreversibly (von Sonntag & Schuchmann, 1997). C-centered radicals could be formed in the reaction of e.g. organic compounds with ozone (see Scheme 14, reaction (4)) by loosing a proton from the radical cation. Thus, ozone reacts with many free radicals effectively, despite the fact that oxygen is typically present in large excess over ozone (von Sonntag & von Gunten, 2012).

Despite the very low rate constant the catalytic action of hydroxyl ions on the ozone decomposition (see above) can play a role at very high pH. Hence, based on the possible importance of radical reactions in ozonation, pH is probably a main variable (Staehelin & Hoigné, 1985, Beltran et al., 1998, von Sonntag & von Gunten, 2012). Moreover, when ozone reacts with a compound that can be present in different protonation states, there will be a pH dependence of the rate constant. When deprotonated the electron density within a given molecule is higher and due to the electrophilicity of ozone the rate constant for the reaction with ozone is also higher. The magnitude of this pH effect strongly depends on the type of ozone reaction. With phenols for example there is already a marked activation of the aromatic ring by the OH group (within the range of 10^3 M^{-1} s^{-1}). This is however, strongly increased upon deprotonation of the phenol, resulting in a high rate constant (around 10^9 M^{-1} s^{-1}) for the phenolate ion (von Sonntag & von Gunten, 2012).

1.3.3 Kinetics, stoichiometry and product formation in ozone reactions

Fundamentals of kinetics. In micropollutant abatement the reactivity between ozone and micropollutants determines the efficiency of elimination by ozone treatment. Thus, an evaluation of the kinetics of the ozone reactions in water is one of the necessary steps to ascertain whether or not ozone is able to remove micropollutants from water. Reaction rates are intuitively defined as how fast or slow a reaction takes place. A main factor influencing the reaction rate includes the concentration of the reactants, because as reactant concentration increases, the frequency of collisions increases. For this reason the kinetic law or rate equation for a chemical reaction is an equation that links the reaction rate with concentrations and constant parameters (normally rate constants). Hence, the main aim of the kinetic study is to determine the

rate constant (*k*) of the ozone-compound reaction. Quantification of the rate constant is achieved by establishing the corresponding kinetic law. Relatively simple rate laws exist for zero order reactions (for which reaction rates are independent of concentration), first order reactions and second order reactions. A first order reaction depends on the concentration of only one reactant. Other reactants can be present, but each will be zero order (because it does not depend on the concentration of the reactant). A second order reaction depends on the concentration of two first order reactants. For example, a bimolecular reaction will be second order overall and first order in each reactant.

$$O_3 + M \longrightarrow P \qquad (14)$$

For a reaction between ozone (O_3) and compound (M) one may write reaction (14). The kinetic law for this ozone reaction is given according to equation (15), in which *k* represent the reaction rate constant (unit: M^{-1} s^{-1}) and $[O_3]$ and [M] are the concentrations of ozone and compound (usually in moles per liter (M)). If the compound concentration is chosen in excess the concentration of (M) does not significantly change during the reaction, [M] becomes a constant and equation (15) can be integrated to equation (16), which links concentrations of reactants or products with time.

$$-\frac{d[O_3]}{dt} = k[O_3] \cdot [M] \qquad (15)$$

$$\ln\frac{[O_3]}{[O_3]_0} = -k[M] \cdot t = -k_{O_3,\,obs} \cdot t \qquad (16)$$

A plot of ln $[O_3]/[O_3]_0$ vs. time (*t*) yields a straight line from the slope of which k_{obs} is calculated and division by [M] yields the bimolecular rate constant *k* (von Sonntag & von Gunten, 2012).

Determination of rate constants. Kinetic laws are empirical and rate constants are derived from experiments by following the concentration of reactants or products. In practice, the reactions are usually carried out in small flasks that act as perfectly mixed batch reactors. In this case ozone and compound are dissolved in water and then mixed and their concentrations over time are observed. Measuring a second order rate constant, k'', with two reactants can be problematic. The concentrations of the two reactants must be followed simultaneously, which is more difficult than following the concentration of only one reactant. A common solution for that problem is the (pseudo)-first order approximation. If the concentration of one reactant remains constant because it is supplied in great excess, its concentration can be combined with the rate constant, obtaining an (pseudo)-first order rate constant, k' or k_{obs} (Conners, 1990, Beltrán, 2004, von Sonntag & von Gunten, 2012). The experiments can be performed in excess of ozone or the selected compound. Typically, a compound concentration is chosen in excess (e.g., tenfold) and the ozone decrease is measured as a function of time. The other way round, ozone in large excess over the substrate is also feasible, but often not as convenient, since the decrease of ozone is easier to observe (Beltrán, 2004, von Sonntag & von Gunten, 2012).

In principle, there are several methods for following the decrease of the ozone concentration for determining the ozone rate constant with a given compound. The most reliable ones are the direct methods, if spectral interferences from the starting material or products are to be excluded. For measuring low to moderate rate constants ($k < 10^3$ M^{-1} s^{-1}) the ozone decay can be followed spectrometrically at 260 nm. A variation of this direct method is the batch quench approach ($k < 10^3$ M^{-1} s^{-1}). Here, aliquots of the solution with the compounds under study are contacted with an appropriate amount of indigotrisulfonate so that the remaining ozone concentration is determined by bleaching of the indigotrisulfonate (Bader & Hoigné, 1981, Hoigné & Bader, 1994, see above). In this case the concentration of indigo has to be high enough to make sure that ozone exclusively reacts with the indigo dye. However, this can be achieved in most cases since indigotrisulfonic acid is very fast (k (indigo + O_3) = 9.4×10^7 M^{-1} s^{-1}, Muñoz & von Sonntag, 2000a). For high rate constants (typically $k > 10^3$ M^{-1} s^{-1}) methods based on competition kinetics are required (von Sonntag & von Gunten, 2012). In competition kinetics two substrates, the substrate (M) and the competitor

substrate (C) react with ozone (Dodd et al., 2006). Here, two valuations are feasible. One competition method requires the measurement of two-endpoints, the residual compound (M) and competitor (C) concentrations remaining after ozone reaction. This rate constant can be evaluated according to equation 17,

$$\ln \frac{[C]}{[C]_0} = \ln \frac{[M]\, k''_{O_3, C}}{[M]_0 k''_{O_3, M}} \qquad (17)$$

where k'' could be determined from the slope of the plot of ln $([C]/[C]_0)$ vs. ln $([M]/[M]_0$. The initial concentration of $[C]_0$ and $[M]_0$ have to be taken from analyses of duplicate controls includes in each experiment. The second competition method requires the measurement of only a single endpoint P, which is typically the degradation of a reactant or the formation of a product resulting from oxidation of either the compound (M) or the competitor (C). The evaluation of the reaction rate constants were conducted using equation 18,

$$\frac{[P]_0}{[P]} = 1 + \frac{k'_{O_3, M}\ [M]_0}{k'_{O_3, C}\ \ [C]_0} \qquad (18)$$

where $[P]_0$ represents the measured endpoint yield in the absence of competitor obtained from controls and [P] represents the endpoint yield in the presence of varying doses of competitor. The rate constant of the investigated compounds was determined from the slopes of plots of equation 19 (Muñoz & von Sonntag, 2000a, Dodd et al., 2006, Zimmermann et al., 2012).

$$\frac{[P]_0}{[P]} - 1 \ \text{vs.} \ \left(\frac{[M]_0}{[C]_0}\right) \qquad (19)$$

For the first approach, it is required that (M) and (C) are degraded by ozone with the same kinetics (i.e. rate constants in the same order of magnitude) to assure that residual concentrations of both compounds can be detected. The other approach is

potentially based on the measurement of just the competitor (C). However, the competitor should have also a similar reactivity towards ozone than the investigated compound (M). Detection can be by transformation of (C) or build-up of the formation of a specific product of (C). While the product of the reaction with (C) can be monitored, the reaction of ozone with (M) remains unobserved. A most convenient competitor is 3-buten-2-ol. Its solubility in aqueous solution is high and one of its oxidation products, formaldehyde, can be readily determined (von Sonntag & von Gunten, 2012). However, interference may occur in the formation of formaldehyde in the reaction of ozone with the compound (M). Furthermore, the determination of ozone rate constants of a given compound (M) with both competition kinetic methods requires the ozone rate constant of the competitor (C), which is known to a high accuracy. For this reason the ozone rate constant of the competitor should have been determined, if it is possible, by a reliable direct method such as pulse radiolysis (von Sonntag & von Gunten, 2012). This is required because a larger error may be involved in this method, as there is already an uncertainty, albeit typically small, in the rate constant of the competitor. The competition methods have the advantage that there is no need for the ozone concentration to be known, however in the second method in each sample the same amount of ozone are dosed.

Stoichiometry and product formation. In micropollutant abatement the stoichiometry of the reaction, which represents the number of moles of compound transformed per mole of ozone consumed, is also important to know. This parameter should be determined to reveal the difference between the consumption rates of ozone and compound. In addition, the reaction stoichiometry is a fundamental parameter to establish a mass balance of the resulting transformation products when ozone undergoes fast reactions in water. The stoichiometry is, as a rule, determined from the mixture of aqueous solutions of different known concentrations of ozone (O_3) and the investigated compound (M). After complete ozone consumption, the ratio of the initial concentration of the resulting solution, $C_{0(M)}/C_{0(O3)}$ becomes $C_{(M)}/C_{(O3)}$, so that the apparent reaction stoichiometry (%) can determined according to equation (20). If the value for the reaction stoichiometry is low, ozone is consumed not only by the compound (M) but also in different reactions with intermediate compounds. For reaction stoichiometry experiments the ratio of $[M]_0 : [O_3]_0$ should be range from 1 to

10, because consumption yields can only be measured at a reasonable transformation of the substrate, otherwise the deviation from the untreated sample is too small (Mvula & von Sonntag, 2003).

$$\textbf{Reaction stoichiometry (\%)} = \frac{C_{0(M)} - C_{(M)}}{C_{0(O_3)} - C_{(O_3)}} \cdot 100 \qquad (20)$$

In micropollutant elimination the oxidative treatment does not usually result in full mineralization but rather leads to transformation products. For a comprehensive environmental assessment it is essential to exemplify the transformation pathways. This is especially important with regard to ecotoxicological concerns, due to the fact that transformation products may be more toxic to aquatic life than their precursors (Shang & Yu, 2002, Schmidt & Brauch, 2008, Boxall et al., 2014). For this reason product formation experiments are indispensable. To quantify the product yields the experiments are as well conducted with a mixture of different defined concentrations of ozone (O_3) and the investigated compound (M) in aqueous solutions. After complete ozone consumption, the product formation ratio of $C_{0(P)}/C_{0(O3)}$ becomes $C_{(P)}/C_{(O3)}$, so that the apparent product formation (%) can determined according to equation (21).

$$\textbf{Product formation (\%)} = \frac{C_{2(P)} - C_{1(P)}}{C_{0(O_3)} - C_{(O_3)}} \cdot 100 \qquad (21)$$

In the case of reaction stoichiometry as well as product formation values are determined from the slope of the straight line resulting from plots which are exemplary shown in Figure 2. In a general case, ozonation experiments aimed at studying the kinetic, stoichiometric and product formation of ozone reactions are carried out both in the presence and absence of scavengers of $^{\bullet}OH$. This is necessary in order to separate reactions of the compound with ozone from those with $^{\bullet}OH$ (see Chapter 1.2.2). In the presence of the scavenger, the kinetics, stoichiometry or product formation of the reaction is due exclusively to the ozone reaction. The reaction of the $^{\bullet}OH$ scavenger (see above) should be well established and it must not react with ozone. If the reaction of the scavenger with $^{\bullet}OH$ is well established the concentration of $^{\bullet}OH$ can be determined.

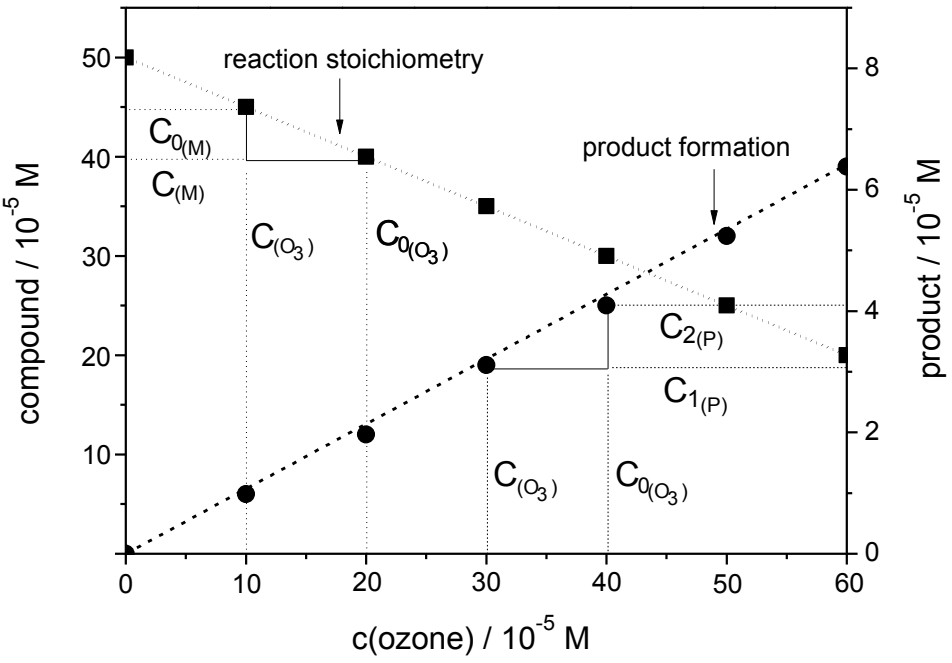

Figure 2. Exemplary representation of the determination of the stoichiometric ratio and product yields in ozone reactions

1.4 Scope of this thesis

The scope of this thesis was to investigate the ozonation of amines in aqueous solutions. A considerable number of papers deal with the ozone chemistry of aromatic compounds (Bailey, 1972, Hoigné & Bader, 1983a, b, Yacobi et al., 1986, Beltrán et al., 1998, Shang & Yu, 2002, Naumov & von Sonntag, 2010), in particular with toluene (Kuo & Chen, 1996, Galatyan et al., 2011, Huang & Li, 2011), phenols (Andreozzi et al., 1999, Fang et al., 2000, Benitez, 2003, Mvula et al., 2003, Huber et al., 2004) or anisoles (Mvula et al., 2009). Many papers also deal with reactions of ozone with olefins (Dowideit & von Sonntag, 1998, Theruvathu et al., 2001, Leitzke et al., 2003). Even though there is quite a lot of information on amines (Bailey et al., 1970, Bailey & Carter, 1972, Kerr & Meth-Cohn, 1971, Keinan & Masur, 1976, Elmghari-Tabib et al., 1982, Cocheci et al., 1989, Andreozzi et al., 1991, Vedprakash et al., 1994, Hon et al., 1995, Muñoz & von Sonntag, 2000b, Sein et al., 2008, Benner & Ternes, 2009a, b) or nucleobases (Theruvathu et al., 2001, Flyunt, 2002) either, most of these studies are

not embedded in a general mechanistical concept of ozone chemistry of the investigated amines in aqueous solution. Reactions of aniline with ozone have been rather extensively studied in organic solvents whereas investigations in aqueous solutions are scare (Gilbert & Zinecker, 1980, Doré et al., 1980, Turhan & Uzman, 2007, Caprio & Insola, 1985). Studies on reactions of aromatic (Andreozzi et al., 1990-92) and aliphatic *N*-heterocycles (Pietsch et al., 1999) with ozone do not give a satisfactory picture of the reactive behavior as they disregard the possible overlapping of different transformation pathways, when ozone and $^{\bullet}$OH are present as oxidants. The present work aims at elucidating fundamental chemical patterns related to the nitrogen atom in aniline (Chapter 2), aliphatic (Chapter 3) and aromatic *N*-containing heterocycles (Chapter 4). Special emphasis is given to a kinetic examination for assessing ozone rate constants in the reaction of ozone with the amines under study. A main focus of the research is also to exemplify reaction stoichiometry and product formation including most abundant primary and advanced oxidation pathways. The investigated compounds should be archetypes for amines, a structural unit that is often present in micropollutants in aqueous solution. Thus, the information on the quantitative generation of transformation products during ozonation of the amines may also help in the evaluation of ozone reactions with micropollutants.

1.5 References

Andreozzi, R., Caprio, V., D`Amore, M. G., Insola, A., 1990. Quinoxaline ozonation in aqueous solution. Ozone Sci Eng 12, 329-340.

Andreozzi, R., Insola, A., Caprio, V., D`Amore, M. G., 1991. Ozonation of pyridine in aqueous solution: mechanistic and kinetic aspects. Wat Res 25, 655-659.

Andreozzi, R., Insola, A., Caprio, V., D`Amore, M. G., 1992. Quinoline ozonation in aqueous solution. Wat Res 26, 639-643.

Andreozzi, R., Marotta, R., 1999. Ozonation of *p*-chlorophenol in aqueous solution. J Hazard Mater B69, 303-317.

Atkins, P. W., 1998. Physical chemistry. Oxford University Press, Oxford, Melbourne, Tokyo.

Bader, H., Hoigné, J., 1981. Determination of ozone in water by the indigo method. Wat Res 15, 449-456.

Bader, H., Hoigné, J., 1982. Determination of ozone in water by the indigo method: a submitted standard method. Ozone Sci Eng 4, 169-176.

Bahnemann, G., Hart, E. J., 1982. Rate constants of the reaction of the hydrated electron and hydroxyl radical with ozone in aqueous solution. J Phys Chem 86, 252-255.

Bailey, P. S., Keller, J. E., Carter, T. P., 1970. Ozonation of amines. IV. Di-t-butylamine. J Org Chem 35, 2777-2782.

Bailey, P. S., Carter, T. P., Southwick, L. M., 1972. Ozonation of amines. VI. Primary amines. J Org Chem 37, 2997-3004.

Bailey, P. S., 1972. Organic groupings reactive toward ozone mechanisms in aqueous media. In: Ozone in water and wastewater treatment. F. L. Evans (ed.), Ann Arbor Science, Ann Arbour, Michigan, pp. 29-59.

Beltrán, F. J., Encinar, J. M., Alonso, M. A., 1998. Nitroaromatic hydrocarbon ozonation in water: 1: Single ozonation. Ind End Chem Res 37, 25-31.

Beltrán, F. J., 2004. Ozone reaction kinetics for water and wastewater systems. Lewis Publishers, Boca Raton, London, New York, Washington D.C.

Benitez, F. J., Acero, J. L., Real, F. J., Garcia, J., 2003. Kinetics of pentachlorophenol ozonation. 226th AC national meeting, New York, ENVR-191.

Benitez, F. J., Acero, J. L., Real, F. J., Roldan, G., Casas, F., 2011. Comparison of different chemical oxidation treatments for the removal of selected pharmaceuticals in water matrices. Chem Eng J 168, 1149–1156.

Benner, J., Ternes, T. A., 2009a. Ozonation of metoprolol: elucidation of oxidation pathways and major oxidation products. Environ Sci Technol 43, 5472-5480.

Benner, J., Ternes, T. A., 2009b. Ozonation of propranolol: formation of oxidation products. Environ Sci Technol 43, 5086-5093.

Boxall, A., Keller, V. D. J., Straub, J. O., Monteiro, S. C., Fussell, R., Williams, R. J., 2014. Exploiting monitoring data in environmental exposure modelling and risk assessment of pharmaceuticals. Environ Int, 73, 175-185.

Bühler, R. E., Staehelin, J., Hoigné, J., 1984. Ozone decomposition in water studied by pulse radiolysis. HO_2/O_2^- and HO_3/O_3^- as intermediates. J Phys Chem 88, 2560-2564.

Brown, D. J., 1984. Pyrimidines and their benzo derivatives. In: Katritzky, A. R., 1984. Comprehensive heterocyclic chemistry / the structure, reactions, synthesis and uses of heterocyclic compounds, Pergamon Press, Oxford, pp. 57-77.

Brückner, R., 1996. Reaktionsmechanismen. Organische Reaktionen, Stereochemie, moderne Synthesemethoden. Spektrum Akademischer Verlag, Heidelberg, Berlin, Oxford.

Buxton, G. V., Greenstock, C. L., Helman, W. P., Ross, A. B., 1988. Critical review of rate constants for reactions of hydrated electrons, hydrogen atoms and hydroxyl radicals (OH/O^{-}) in aqueous solution. J Phys Chem Ref Data 17, 513-886.

Caprio, V., Insola, A., 1985. Aniline and anilinium ion ozonation in aqueous solution. Ozone Sci Eng 7, 169-179.

Cocheci, V., Gherasimov, E., Csunderlik, C., Cotarca, L., Nov, A., 1989. Ozone oxidation of alkylamines in aqueous solution. - I. Rate constants of ozone reactions with primary, secondary and tertiary amines. Revue roumaine de chimie, 749-757.

Connors, K. A., 1990. Chemical kinetics. The study of reaction rates in solution. VCH Publishers, New York.

Criegee, R., 1975. Mechanismus der Ozonolyse. Angew Chem 87, 765-771.

Davies, D. T., 1995. Aromatische Heterocyclen. Verlag Chemie, Weinheim, New York, Basel, Cambridge, Tokyo.

Dodd, M. C., Buffle, M.-O., von Gunten, U., 2006. Oxidation of antibacterial molecules by aqueous ozone: moiety-specific kinetics and application to ozone-based wastewater treatment. Environ Sci Technol 40, 1969-1077.

Doré, M., Langlais, B., Legube, B., 1980. Mechanism of the reaction of ozone with soluble aromatic pollutants. Ozone Sci Eng 2, 39-54.

Dowideit, P., von Sonntag, C., 1998. The reaction of ozone with ethene and its methyl- and chlorine-substituted derivatives in aqueous solution. Environ Sci Technol 32, 1112-1119.

Elmghari-Tabib, M., LaPlanche, A., Venien, F., Martin, G., 1982. Ozonation of amines in aqueous solutions. Wat Res 16, 223-229.

Erikson, R. E., 1969. Mechanismen of ozonation reactions. IV. Carbon-nitrogen double bonds. J Org Chem 34, 2961-2966.

Fang, X., Schuchmann, H.-P., von Sonntag, C., 2000. The reaction of the OH radical with pentafluoro-, pentachloro-, pentabromo- and 2,4,6-triiodophenol in water: electron vs. addition to the ring. J Chem Soc, Perkin Trans 2, 1391-1398.

Flyunt, R., Theruvathu, J. A., Leitzke, A., von Sonntag, C., 2002. The reactions of thymine and thymidine with ozone. J Chem Soc, Perkin Trans 2, 1572-1582.

Forni, L., Bahnemann, D., Hart, E. J., 1982. Mechanism of the hydroxide ion initiated decomposition of ozone in aqueous solution. J Phys Chem 86, 255-259.

Gabet-Giraud, V., Miège, C., Choubert, J. M., Ruel, S. M., Coquery, M., 2010. Occurrence and removal of estrogens and beta blockers by various processes in wastewater treatment plants. Sci Total Environ 408, 4257-4269.

Galstyan, A. G., Galstyan, S. G., Lysak, V. V., 2011. Kinetics and products of the reaction of ozone with toluene and its derivatives in acetic anhydride. Kinetics and catalysis 52, 493-498.

Gilbert, E., Zinecker, H., 1980. Ozonation of aromatic amines in water. Ozone Sci Eng 2, 65-74.

Gordon, G., Pacey, G. E., 1986. Analytical measurements of ozone in aqueous solution. Advances in water analysis and treatment / Technology Conference Proceedings 13, 181-190.

Hoigne, J., Bader, H., 1975. Ozonation of water. Role of hydroxyl radicals as oxidizing intermediates. Science / America Association for the Advancement of Science 190, 782-784.

Hoigné, J., Bader, H., 1983a. Rate constants of reactions of ozone with organic and inorganic compounds in water. - I. Non-dissociating organic compounds. Wat Res 17, 173-183.

Hoigné, J., Bader, H., 1983b. Rate constants of reactions of ozone with organic and inorganic compounds in water. - II. Dissociating organic compounds. Wat Res 17, 185-194.

Hoigné, J., 1998. Chemistry of aqueous ozone and transformation of pollutants by ozonation and advanced oxidation processes. In: The Handbook of Environmental Chemistry 5 (C), Quality and Treatment of Drinking Water II, in J. Hrubec, Ed., Springerverlag, Heidelberg pp. 83-141.

Hoigné, J., Bader, H., 1994. Characterization of water quality criteria for ozonation processes. Part II: lifetime of added ozone. Ozone Sci Eng 16, 121-134.

Holleman, A. F., Wiberg, E., 2007. Lehrbuch der anorganischen Chemie. Verlag Walter de Gruyter, Berlin, New York.

Hon, Y.-S., Lin, S.-W., Lu, L., Chen, Y.-J., 1995. The mechanistic study and synthetic applications of the base treatment in the ozonolytic reactions. Tetrahedron 51, 5019-5034.

Huang, H., Li, W., 2011. Destruction of toluene by ozone-enhanced photocatalysis: performance and mechanism. Applied Catalysis B: Environmental 102, 449-453.

Huber, M. M., Canonica, S., Park, G.-Y., von Gunten, U., 2003. Oxidation of pharmaceuticals during ozonation and advanced oxidation processes. Environ Sci Technol 37, 1016-1024.

Huber, M. M., Ternes, T. A., von Gunten, U., 2004. Removal of estrogenic activity and formation of oxidation products during ozonation of 17α-ethinylestradiol. Environ Sci Technol 38, 5177-5186.

Huber, M. M., Göbel, A., Joss, A., Hermann, N., Löffler, D., McArdell, C. S., Ried, A., Siegrist, H., Ternes, T. A., von Gunten, U., 2005. Oxidation of pharmaceuticals during ozonation of municipal wastewater effluents: a pilot study. Environ Sci Technol 39, 4290-4299.

Johnson, C. D., 1984. Pyridines and their benzo derivatives: Structure. In: Katritzky, A. R., 1984. Comprehensive heterocyclic chemistry / the structure, reactions, synthesis and uses of heterocyclic compounds, Pergamon Press, Oxford, pp. 99-119.

Joule, J. A., Mills K., 2010. Heterocyclic chemistry. Blackwell Publishing. John Wiley & Sons LTD. The Atrium, Southern Gato, Chichester, West Sussex, United Kingdom.

Katritzky, A. R., 1984. Comprehensive heterocyclic chemistry, Pergamon Press, Oxford.

Keinan, E., Masur, Y., 1976. Dry ozonation of amines. Conversion of primary amines to nitro compounds. J of Org Chemisty, 844-847.

Kerr, G. H., Meth-Cohn, O., 1971. Ozonation of tertiary aromatic amines. J Chem Soc C, 1369-1374.

Koch, R., 1995. Umweltchemikalien. Verlag Chemie, Weinheim, New York, Basel, Cambridge, Tokyo.

Ku, Y., Su, W.-J., Shen, Y.-S., 1996. Decomposition kinetics of ozone in aqueous solution. Ind Eng Chem Res 35, 3369-3374.

Kuo, C.-H., Chen, S.-M., 1996. Ozonation and peroxone oxidation of toluene in aqueous solutions. Ind Eng Chem Res 35, 3973-3983.

Langlais, B., Reckhow, D. A., Brink, D. R., 1991. Ozone in water treatment: application and engineering. Lewis Publishers, Chelsea, MI.

Leitzke, A., Flyunt, R., Theruvathu, J. A., von Sonntag, C., 2003. Ozonolysis of vinyl compounds, CH_2=CH-X, in aqueous solution – The chemistries of the ensuing formyl compounds and hydroperoxides. Org Biomol Chem 1, 1012-1019.

Lide, D. R., 2009. Handbook of Chemistry and Physics. 89th Edition.

Lind, J., Merényi, G., Johansson, E., Brinck, T., 2003. The reaction of peroxyl radicals with ozone in water. J Phys Chem A 107, 676-681.

Merényi, G., Lind, J., Naumov, S., von Sonntag, C., 2010. The reaction of ozone with the hydroxide ion. Mechanistic considerations based on thermokinetic and quantum-chemical calculations. The role of HO_4^- in superoxide dismutation. Chem Eur J 16, 1372-1377.

Morrison, R. T., Boyd, R. N., 1986. Lehrbuch der organischen Chemie. Verlag Chemie, Weinheim, New York, Basel, Cambridge, Tokyo.

Muñoz, F., von Sonntag, C., 2000a. Determination of fast ozone reactions in aqueous solution by competition kinetics. J Chem Soc, Perkin Trans 2, 661-664.

Muñoz, F., von Sonntag, C., 2000b. The reaction of ozone with tertiary amines including the complexing agents nitrilotriacetic acid (NTA) and ethylenediaminetetraacetic acid (EDTA) in aqueous solution. J Chem Soc, Perkin Trans 2, 2029-2033.

Muñoz, F., Mvula, E., Braslavsky, S. E., von Sonntag, C., 2001. Singlet dioxygen formation in ozone reactions in aqueous solution. J Chem Soc, Perkin Trans 2, 1109-1116.

Mvula, E., von Sonntag, C., 2003. Ozonolysis of phenols in aqueous solution. Org Biomolec Chem 1, 1749-1756.

Mvula, E., Naumov, S., von Sonntag, C., 2009. Ozonolysis of lignin models in aqueous solution: anisole, 1,2-dimethoxybenzene, 1,4-dimethoxybenzene and 1,3,5-trimethoxybenzene. Environ Sci Technol, 43, 6275-6282.

Naumov, S., von Sonntag, C., 2010. Quantum chemical studies on the formation of ozone adducts to aromatic compounds in aqueous solution. Ozone Sci Eng 32, 61-65.

Neta, P., Huie, R. E., Ross, A. B., 1988. Rate constants for reactions of inorganic radicals in aqueous solution. J Phys Chem Ref Data 17, 1027-1284.

Nöthe, T., Fahlenkamp, H., von Sonntag, C., 2009. Ozonation of wastewater: rate of ozone consumption and hydroxyl radical yield. Environ Sci Technol 43, 5990-5995.

Noyes, R. M., 1954. A treatment of chemical kinetics with special applicability to diffusion controlled reactions. J Chem Phys 22, 1349-1359.

Parkin, A., Oswald, I. D. H., Parsons, S., 2004. Structures of piperazine, piperidine and morpholine. Acta Cryst B60, 219-227.

Perrin, D. D., Dempsey, B., Serjeant, E. P., 1981. p*K*a Prediction for organic acids and bases. Chapmann and Hall, London and New York.

Pietsch, J., Schmidt, W., Brauch, H.-J., Worch, E., 1999. Kinetic and mechanistic studies of the ozonation of alicyclic amines. Ozone Sci Eng 21, 23-37.

Porter, A. E. A., 1984. Pyrazines and their benzo derivatives. In: Katritzky, A. R., 1984. Comprehensive heterocyclic chemistry / the structure, reactions, synthesis and uses of heterocyclic compounds, Pergamon Press, Oxford, pp. 157-199.

Ramseier, M. K., von Gunten, U., 2009. Mechanism of phenol ozonation – Kinetics of formation of primary and secondary reaction products. Ozone Sci Eng 31, 201-215.

Rubin, M. B., Harries, C. H., 2003. History of ozone and the introduction of ozone into organic chemistry. Part III. Helv Chim Acta 86, 930-940.

Rubiralta, M., Giralt, E., Diez, A., 1991. Piperidine: structure, preparation, reactivity and synthetic applications of piperidine and its derivatives. Elsevier Science Publishers, Amsterdam, New York.

Scriven, E. F. V., 1984. Pyridines and their benzo derivatives: reactivity at ring atoms. In: Katritzky, A. R., 1984. Comprehensive heterocyclic chemistry / the structure, reactions, synthesis and uses of heterocyclic compounds, Pergamon Press, Oxford, pp. 165-185.

Schmidt, C. K., Brauch, H.-J., 2008. *N*,*N*-Dimethylsulfamide as precursor for *N*-nitroso-dimethylamine (NDMA) formation upon ozonation and its fate during drinking water treatment. Environ Aci Technol 42, 6340-6346.

Schmidt, T. C., Less, M., Haas, R., von Löw, E., Steinbach, K., Stork, G., 1998. Gas chromatographic determination of aromatic amines in water samples after solid-phase

extraction and derivatization with iodine I. Derivatization. J Chromatogr A, 810, 161-172.

Schönbein, C. F., 1854. Über verschiedene Zustände des Sauerstoffs. Ann Chem Pharm 89, 257-300.

Schwarzenbach, R. P., Escher, B. I., Fenner, K., Hofstetter, T. B., Johnson, C. A., von Gunten, U., Wehrli, B., 2006. The challenge of micropollutants in aquatic systems. Science 313, 1072-1077.

Sehested, K., Holcman, J., Hart, E. J., 1983. Rate constants and products of the reactions of e^-, O_2^- and H with ozone in aqueous solutions. J Phys Chem 87, 1951-1954.

Sehested, K., Holcman, J., Bjergbakke, E., Hart, E. J., 1984. A pulse radiolytic study of the reaction OH + O_3 in aqueous medium. J Phys Chem 88, 4144-4147.

Sein, M. M., Zedda, M., Tuerk, J., Schmidt, T. C., Golloch, A., von Sonntag, C., 2008. Oxidation of diclofenac with ozone in aqueous solution. Environ Sci Technol 42, 6656-6662.

Shang, N.-C., Yu, Y.-H., 2002. Toxicity and color formation during ozonation of mono-substituted aromatic compounds. Environ Technol, 43-52.

Sims, P., 1959. In: Handbook of tables for organic compound identification. 3rd ed, CRC press, Boca Raton, United states.

Snyder, S. A., Wert, E. C., Rexing, D. J., Zegers, R. E., Drury, D. D., 2006. Ozone oxidation of endocrine disrupters and pharmaceuticals in surface water and wastewater. Ozone Sci Eng 28, 445-460.

Staehelin, J., Hoigné, J., 1982. Decomposition of ozone in water: rate of initiation by hydroxide ions and hydrogen peroxide. Environ Sci Technol 16, 676-681.

Staehelin, J., Hoigné, J., 1985. Decomposition of ozone in water in the presence of organic solutes acting as promoters and inhibitors of radical chain reactions. Environ Sci Technol 19, 1206-1213.

Sonntag, H., 1890. Über die Bedeutung des Ozons als Desinficiens. Z Mediz Microbiol Imunol 8, 95-136.

Ternes, T. A., Meisenheimer, M., McDowell, D., Sacher, F., Brauch, H.-J., Haist-Gulde, B., Preuss, G., Wilme, U., Zulei-Seibert, N., 2002. Removal of pharmaceuticals during drinking water treatment. Environ Sci Technol 36, 3855-3863.

Ternes, T., Joss, A., Kreuzinger, N., Miksch, K., Lema, J. M., von Gunten, U., Mc Ardell, C. S., Siegrist, H., 2005. Removal of pharmaceuticals and personal care products: results of the Poseidon project. WEFTEC, Conference Proceedings 78, 227-243.

Ternes, T. A., Joss, A., 2006. Human pharmaceuticals, hormones and fragrances. The challenge of micropollutants in urban water management. IWA Publishing, London, New York.

Ternes, T. A., 2015. Occurrence, fate, removal and assessment of emerging contaminants in water in water cycle (from wastewater to drinking water). Wat Res 72, 1-2.

Theruvathu, J. A., Flyunt, R., Aravindakumar, C. T., von Sonntag, C., 2001. Rate constants of ozone reactions with DNA, its constituents and related compounds. J Chem Soc, Perkin Trans 2, 269-274.

Tisler, M., Stanovnik, B., 1984. Pyridazines and their benzo derivatives. In: Katritzky, A. R., 1984. Comprehensive heterocyclic chemistry / the structure, reactions, synthesis and uses of heterocyclic compounds, Pergamon Press, Oxford, pp. 1-56.

Tomiyasu, H., Fukutomi, H., Gordon, G., 1985. Kinetics and mechanism of ozone decomposition in basic aqueous solution. Inorg Chem 24, 2962-2966.

Trambarulo, R., 1953.The molecular structure, dipole moment and g factor of ozone from its microwave spectrum, J Phys Chem 21, 851-855.

Turhan, K., Uzmann, S., 2007. The degradation products of aniline in the solutions with ozone and kinetic investigations. Ann Chim 97, 1129-1138.

Vedprakash, S. M., Jyeshtharaj, B. J., Vijaykumar V. M., 1994. Kinetics of wet air oxidation of diethanolamine and morpholine. Wat Res 28, 1601-1608.

Vogt, P. F., Geralis, J. J., 1985. In: Ullmann`s Encyclopedia of Industrial Chemisty A2, 5th ed., Verlag Chemie, Weinheim, New York, Basel, Cambridge, Tokyo, p. 37.

Vollhardt, K. P. C., Schore, N. E., 2005. Organische Chemie. Verlag Chemie, Weinheim, New York, Basel, Cambridge, Tokyo.

von Gunten, U., 2003. Ozonation of drinking water. Part I. Oxidation kinetics and product formation. Wat Res 37, 1443-1467.

von Sonntag, C., Schuchmann, H.-P., 1997. Peroxylradicals in aqueous solution. In: Peroxyl Radicals, Z. B. Alfassi (ed.), Wiley Chichester, 173-234.

von Sonntag, C., von Gunten, U., 2012. Chemistry of ozone in water and wastewater treatment. From basic principles to applications. IWA Publishing.

White, H. M., Bailey, P. S., 1965. Ozonation of aromatic aldehydes, J Org Chem 30, 3037-3041.

Yakobi, V., Shpak, L. P., Ivanova, N. N., 1986. Kinetics and mechanism of oxidation of some benzenes derivatives with ozone. Communications of the department of chemistry 2, 206-214.

Zimmermann, S. G., Schmukat, A., Schulz, M., Benner, J., von Gunten, U., Ternes, T. A., 2012. Kinetic and mechanistic investigations of the oxidation of tramadol by ferrate and ozone. Environ Sci Technol 46, 876-884.

2 Ozonation of anilines: Kinetics, stoichiometry, product identification and elucidation of pathways

Agnes Tekle-Röttering, Clemens von Sonntag, Erika Reisz,
Claudia vom Eyser, Holger V. Lutze, Jochen Türk, Sergej Naumov,
Winfried Schmidt, Torsten C. Schmidt

submitted to Water Research

2.1 Abstract

Anilines as archetypes for aromatic amines, which play an important role in the production of, e.g., dyestuffs, plastics, pesticides or pharmaceuticals were investigated in their reaction with ozone. Due to their high reactivity towards ozone (1.2×10^5 – 2.4×10^6 M^{-1} s^{-1}) the investigated aniline bearing different substituents are readily degraded in ozonation. However, around 4 to 5 molecules of ozone are needed to yield a successful transformation of aniline, most likely due to a chain reaction that decomposes ozone without compound degradation. This is inferred from OH radical scavenging experiments, in which compound transformation per ozone consumed is increased. Mechanistic considerations based on product formation indicate that addition to the aromatic ring is the preferential reaction in the case of aniline, *p*-chloroaniline and *p*-nitroaniline (high amounts of *o*-hydroxyaniline, *p*-hydroxyaniline, chloride, nitrite and nitrate, respectively were found). For aniline an addition to the nitrogen happens but to a small extent, since nitroso- and nitrobenzene were observed as well. In the case of *N*-methylaniline and *N*,*N*-dimethylaniline, an electron transfer reaction from nitrogen to ozone was proven due to the formation of formaldehyde. In contrast, for *p*-methylaniline and *p*-methoxyaniline the formation of formaldehyde may result from an electron transfer reaction at the aromatic ring. Additional oxidation pathways for all of the anilines under study are reactions of hydroxyl radicals formed in the electron transfer of ozone with the anilines (OH radical yields = 34 – 59%). These reactions may form aminyl radicals which in the case of aniline can terminate in

bimolecular reactions with other compounds such as the determined *o*-hydroxyaniline by yielding the detected 2-amino-5-anilino-benzochinon-anil.

2.2 Introduction

Investigations of the ozonation of anilines in aqueous solution can help to elucidate the mechanisms involved in the oxidation of many micropollutants by ozone. Compounds belonging to the class of anilines are often present as micropollutants in water since some of them are widely used as pesticides or pharmaceuticals. According to their manifold utilisations, anilines can reach the environment through several input paths, e.g., from municipal wastewater effluents (Huber et al., 2005, Gabet-Giraud et al., 2010). However, anilines are also found in groundwater and leachate water (Schmidt et al., 1998). Micropollutants in turn are of major concern in surface and ground water that are used as source for drinking water supply (Nöthe et al., 2007, Ternes et al., 2002). Even at low concentrations in surface water, they can be harmful to aquatic life (Huggett et al., 2002, Küster et al., 2010). Therefore, advanced wastewater treatment with ozone or powered activated carbon is frequently discussed as means to abate micropollutant emissions (Snyder et al., 2006, Schwarzenbach et al., 2006, Hollender et al., 2009, Benitez et al., 2011). Reaction rate constants of micropollutants with ozone are an important tool for a first assessment of their degradability in ozonation of waste- and drinking water (Lee & von Gunten, 2010). To assess the importance of OH radical ($^{\bullet}$OH) reactions the determination of $^{\bullet}$OH yield is crucial (von Sonntag & von Gunten, 2012). In addition, the amount of ozone needed for full compound degradation is of fundamental importance (Nöthe et al., 2009). Furthermore, the knowledge of possible reaction pathways and quantitative formation of transformation products during ozonation, especially with regard to ecotoxicological concerns, will allow assessing the treatment (Shang & Yu, 2002, Schmidt & Brauch, 2008, Boxall et al., 2014).

The purpose of this study is to elucidate the rate constants of the following aromatic amines bearing different substituents: aniline, *p*-methylaniline, *p*-chloroaniline, *p*-nitroaniline, *p*-methoxyaniline, *p*-hydroxyaniline, *o*-hydroxyaniline, *p*-phenylene-diamine, *p*-aminobenzoic acid, *N*-methylaniline and *N*,*N*-dimethylaniline in their

reaction with ozone in aqueous solution. The investigated amines should be archetypes for assessing kinetic data in the degradation of micropollutants (e.g., diclofenac as an anti-inflammatory drug, the decongestant and bronchodilator clenbuterol, the chemotherapy agent cytarabine or the antibiotic sulfamethoxazole used for urinary tract infections (Sein et al., 2008, Ternes & Joss, 2006). A considerable number of papers deal with the ozone chemistry of anilines (Gilbert & Zinecker, 1980, Doré et al., 1980, Elmghari-Tabib et al., 1982, Caprio & Insola, 1985, Pierpoint et al., 2003, Turhan & Uzman, 2007, 2008, Galstyan et al., 2008, Machulek et al., 2009). Thus, for ozone reactions with anilines some basic principles are well-known. Since ozone is a strong electrophile the ozone-reactive sites of aromatic amines are the electron-rich aromatic ring and/or the lone electron pair at nitrogen. In case the amines are deprotonated (pK_a in general around 5) the free electron pair can either conjugate into the aromatic ring system (activation) or be attacked by ozone at the nitrogen moiety. Hence, the ozone reactivity of aromatic amines depends on pH (von Sonntag & von Gunten, 2012). Besides, ozone is a highly selective reactant and ozone rate constants with aromatic compounds (Neta et al., 1988) and nitrogen-containing compounds (von Sonntag & von Gunten, 2012) vary strongly with the nature of substituents by up to ten orders of magnitude.

Mechanistic information on ozonation products formed trough the investigated anilines is of high interest since it could be transferred subsequently to more complex micropollutants. Literature information allow us to consider addition of ozone and electron transfer as conceivable for the ozone-amine-reactions in aqueous solution (Doré et al., 1980, Muñoz & von Sonntag, 2000b, Muñoz et al., 2001, Mvula & von Sonntag, 2003, Mvula et al., 2009, von Sonntag, 2008, Ramseier & von Gunten, 2009, von Gunten et al., 2010, von Sonntag & von Gunten, 2012, Tekle-Röttering et al., 2016). Ozone addition is often exergonic and may yield oxidized nitrogen moieties or hydroxylation of the benzene moiety by oxygen transfer as well as by forming an ozonide in a Criegee type reaction (von Sonntag & von Gunten, 2012). Outer and inner sphere electron transfer as well as H-abstraction is also possible. A mechanistic discussion and a mechanistic demonstration are presented in the theoretical background in Scheme 1 and 2, reactions (1) – (26).

Even though there is quite a lot of qualitative information about oxidation products and possible reaction pathways in the oxidation of anilines, complementary knowledge about the quantitative contribution of the different transformation pathways, when ozone and $^{\bullet}OH$ are present as oxidants, is still missing. Furthermore, with the current literature at hand it is still unknown if ozone prefers attack at the nitrogen or the aromatic moiety in its reaction with aniline. Thus, in the present paper the kinetics, stoichiometry and product formation including most abundant primary and advanced oxidation pathways in the reaction of anilines bearing different substituents with ozone were investigated. The substituents on the aromatic ring should influence the reaction behaviour significantly by activating or deactivating the aromatic ring. The information on the quantitative generation of transformation products (TPs) during ozonation will allow the assessment or prediction of TPs of micropollutants with similar structural elements and functional groups.

2.2.1 Theoretical background

The following primary processes are conceivable for the ozone-amine-reactions in aqueous solution. The examples in Scheme 1 and Scheme 2 are for aniline, but all reactions are effectual for the investigated compounds as well.

The initial step of the ozone addition at nitrogen (Scheme 1, reaction (1), pathway 1) is well-established for aliphatic amines (Muñoz & von Sonntag, 2000b, Muñoz et al., 2001). The first step of ozone addition to the aromatic ring (Scheme 2, reaction (13), pathway 5) is well-known for the electron-rich benzene derivative, phenol, which also can lead to the formation of an ozone adduct (Mvula & von Sonntag, 2003, Ramseier & von Gunten, 2009). In the breakdown of the ozone adduct singlet oxygen, $^1O_2$, is released (Scheme 1, reaction (2) and Scheme 2, reaction (14)). This is followed by a proton shift by forming hydroxylated products (Scheme 2, reaction (15)) for ozone addition at the aromatic ring. For phenols and some other aromatic compounds singlet oxygen yields in ozone reactions were measured (Muñoz et al., 2001). In the case of *N*,*N*-dimethylaniline a yield of 7% singlet oxygen was obtained (Muñoz et al., 2001). For further details on singlet oxygen see Supporting Information Text S1.

Scheme 1. Proposed reaction scheme of the reaction of ozone with the lone electron pair at nitrogen of aniline

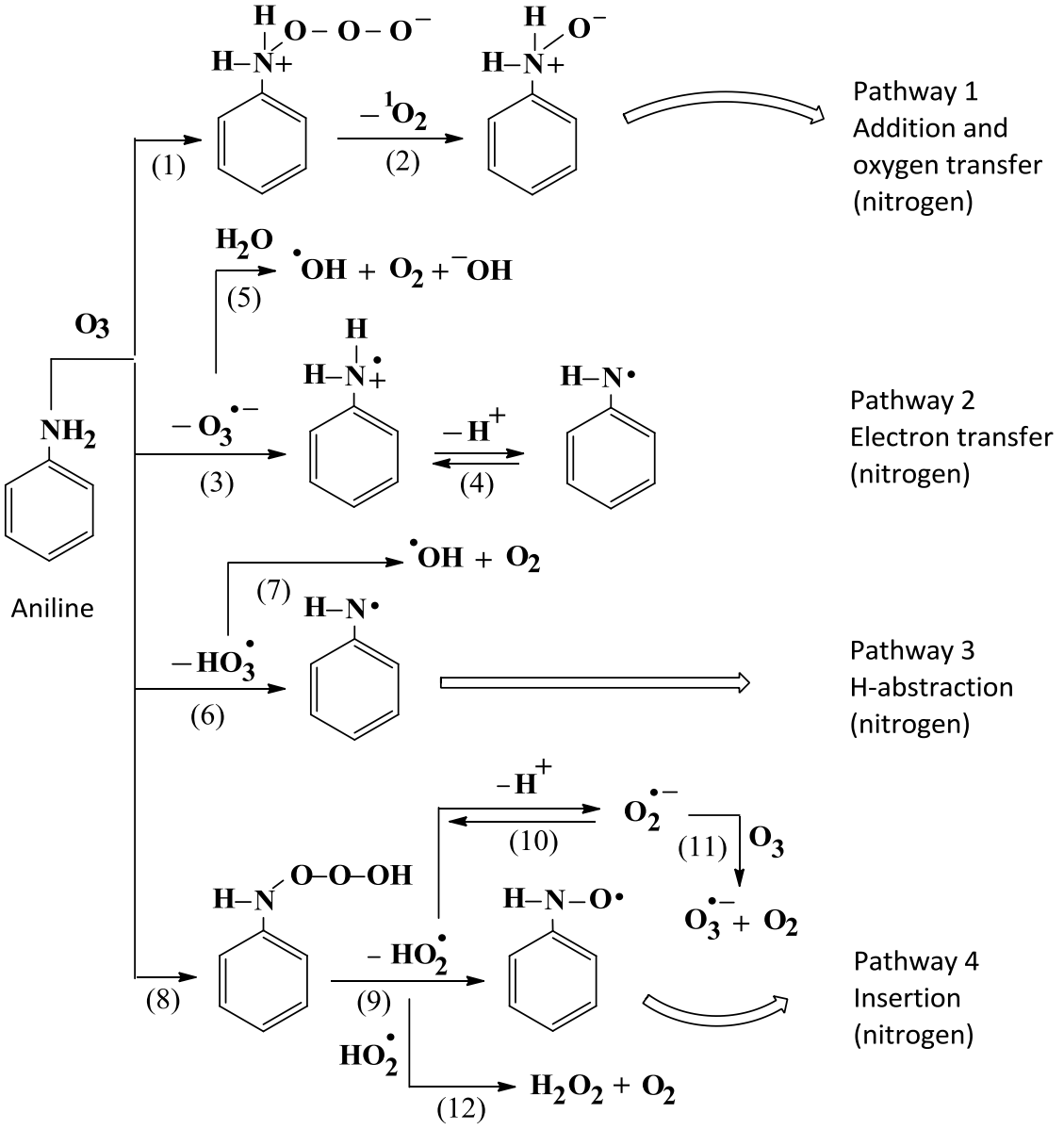

In competition, the ozone adduct may dissociate by forming different radicals through reactions like electron transfer or H-abstraction (von Sonntag & von Gunten, 2012). In principle these radical processes could also proceed directly via an outer sphere electron transfer without adduct as intermediate (von Sonntag & von Gunten, 2012). However, in experiments the direct pathway and the adduct pathway cannot be distinguished. The electron transfer leads to a radical cation (Scheme 1, reaction (3), pathway 2 and Scheme 2, reaction (16), pathway 6) and ozonide radical anion, $O_3^{\bullet-}$ (adduct of the hydrated electron to ozone (Elliot & McCracken, 1989, reaction see

there). The amine radical cation, formed after electron transfer at nitrogen is in equilibrium with an aminyl radical (reaction (4)). The pK_a value for the acidic dissociation of the amine radical cation is 7.05 (Qin et al., 1985) so that in neutral solution based on equilibrium 50% of each amine radical cation and aminyl radical are present. From the H-abstraction process an aminyl radical and hydrotrioxyl radical, $HO_3^{\bullet}$ (Scheme 1, reaction (6), pathway 3) are generated. The above mentioned ozonide radical anion, $O_3^{\bullet-}$ reacts with water (Scheme 1, reaction (5) and Scheme 2, reaction (17)) giving rise to $^{\bullet}OH$ whereas $HO_3^{\bullet}$ decomposes to $^{\bullet}OH$ and oxygen (reaction (7), Bühler et al., 1984).

Furthermore, ozone attack can lead to an insertion via ozone addition concomitant with proton transfer (Scheme 1, reaction (8), pathway 4 and Scheme 2, reaction (20), pathway 8). The insertion process on nitrogen can lead to a nitroxyl radical (Scheme 1, reaction (9)) or oxyl radical at the aromatic ring (Scheme 2, reaction (21)) and hydroperoxyl radical, $HO_2^{\bullet}$. The latter is in equilibrium with its conjugate base, $O_2^{\bullet-}$ (equilibrium reaction (10) and (22), pK_a ($HO_2^{\bullet}$) = 4.8) and dominates even in slightly acid solution (Bielski et al., 1985, Ragnar et al., 1999a, b). The superoxide radical anion, $O_2^{\bullet-}$ in turn can react with ozone to the ozonide radical anion, $O_3^{\bullet-}$ (reaction (11)) (Sehested et al., 1983)). Likewise, the superoxide radical anion, $O_2^{\bullet-}$ can be generated from the decay of the ozone adduct at the aromatic ring by forming phenoxyl radicals (reaction (18) – (19), pathway 7, Ragnar et al., 1999a, b), but this reaction seems to be of minor importance (von Sonntag & von Gunten, 2012). With respect to mechanisms a distinction between the formation of the ozonide radical anion, $O_3^{\bullet-}$ and other radical reactions, e.g., formation of superoxide radical anion, $O_2^{\bullet-}$, is not feasible because they can both lead to $^{\bullet}OH$. This, therefore, may be formed in substantial yields in the ozone reaction with aromatic compounds (von Sonntag & von Gunten, 2012). Another reaction that can occur with the aromatic ring (Scheme 2, reaction (23) – (26), pathway 9), well-documented in the reaction of olefins with ozone (Criegee, 1975), is the formation of an ozonide. With its breakdown (Dowideit & von Sonntag, 1998) into the intermediate hydroxyhydroperoxide, it typically looses hydrogen peroxide (H_2O_2). However, water elimination is also feasible by forming pyridine-2-carboxylic acid upon closing of the *ortho* ozone adduct (von Sonntag & von Gunten, 2012).

Scheme 2. Proposed reaction scheme of the reaction of ozone with the electron-rich aromatic ring of aniline

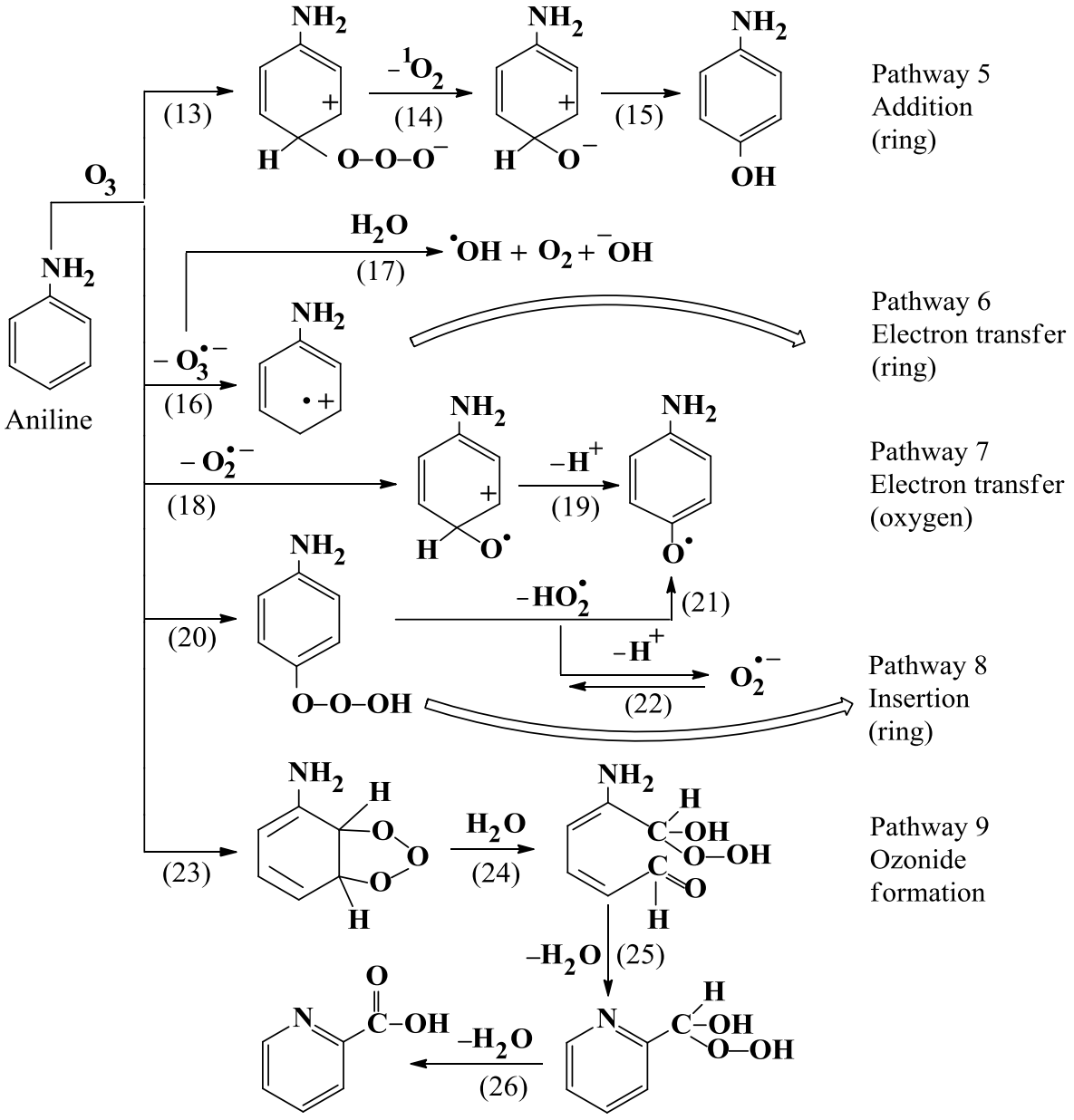

The resulting highly reactive intermediates from all of the above mentioned reactions, like aminyl radicals, nitroxyl radicals, hydrotrioxyl radicals, hydroperoxyl radicals, amine radical cations or ozonide radical anions will undergo different further reactions and the products that are formed may indicate the initial mechanism.

2.3 Experimental part

2.3.1 Chemicals and materials

All chemicals were commercially available in analytical grade (> 95%) and used as received. Further information on chemicals is given in Supporting Information in Text S2. Ozone solutions (max. 1×10^{-3} M) were freshly prepared by purging ozone-containing gas from an ozonator (Sander, Uetze-Eltze, Germany) fed with oxygen (6.0 from Linde) through ultra-pure water. If high ozone concentrations were required ice-bath-cooled water was used. The ozone concentration of this solution was determined spectrophotometrically taking ε(260nm) = 3200 M^{-1} cm^{-1} (Forni et al., 1982, Hart et al., 1983) using a Shimadzu UV 1800 device.

2.3.2 Methods

Sample preparation. The experiments were performed as batch experiments in bench-scale with 10^{-4} – 10^{-1} M solutions of investigated compounds. Solutions containing the investigated compounds with or without additives were made up in ultra-pure water (Merck Millipore, Darmstadt, Germany) and mixed in various ratios with freshly prepared ozone solutions. All experiments were carried out at room temperature in duplicate or triplicate. Before product determination or others, the change in pH was measured and completion of the ozone reaction was verified with indigotrisulfonate. Experiments with exclusion of $^{\bullet}OH$ reactions were conducted by addition of an $^{\bullet}OH$ scavenger that reacts slowly with ozone but fast with $^{\bullet}OH$ (von Sonntag, 2007). In the tertiary butanol (t-BuOH) assay $^{\bullet}OH$ are scavenged by its reaction with t-BuOH that ultimately leads to formaldehyde formation (k(t-BuOH + $^{\bullet}OH$) = 6×10^{8} M^{-1} s^{-1} and k(t-BuOH + O_3) = 0.003 M^{-1} s^{-1}, Schuchmann & von Sonntag, 1979, Buxton et al., 1988, Reisz et al., 2003). Further details are given in Supporting Information in Text S3 and Scheme S1).

Reaction kinetics. The rate constants of the ozone-amine reactions were determined with a competition method without scavenging $^{\bullet}OH$. Here, the ozone decay (ozone under substoichiometric conditions) was followed by product formation with a competitor. In this case, a competition with 3-buten-2-ol (k = 7.9×10^{4} M^{-1} s^{-1}, Muñoz & von Sonntag, 2000a, Dowideit & von Sonntag, 1998) was selected, since a similar reactivity towards ozone as for the investigated compounds was expected. The

competitor 3-buten-2-ol reacts with ozone to formaldehyde, which was determined with the 2,4-dinitrophenylhydrazine (DNPH) method (Lipari & Swarin, 1982). The formed 2,4-dinitrophenylhydrazone was measured by HPLC-DAD (LC20, Shimadzu, Duisburg, Germany) at a wavelength of 353 nm (refer to Supporting Information Text S4 and Scheme S2).

Reaction stoichiometry. The stoichiometry of the ozone reaction was determined by quantification of the residual compounds after complete ozone consumption, calibrated with the original compounds and measured by using a HPLC–DAD system (see above and Supporting Information Text S6).

Product formation. Product identification was done by GC-MS (Thermo Trace GC Ultra coupled to a Thermo DSQ II single quadrupole mass spectrometer, Thermo Fisher, Waltham, USA) after solid phase microextraction (SPME) as well as by LC-MS (LC 20 AD, Shimadzu, Duisburg, Germany coupled to an hybrid tandem mass spectrometer 3200 QTRAP, SCIEX, Darmstadt, Germany). For both systems refer to Supporting Information Text S8 and S9. Quantification of products was carried out with HPLC-DAD in the same way as reaction stoichiometry experiments described above (refer to Supporting Information Text S7 and S9). The determination of chloride, nitrite and nitrate was performed by ion chromatography (883 basic Metrohm, Filderstadt, Germany), verified by retention time (refer to Supporting Information Text S10). The determination of $^{\bullet}OH$ yields was carried out with the dimethyl sulfoxide (DMSO) method, as $^{\bullet}OH$ scavenger present in excess (k(DMSO + $^{\bullet}OH$) = 7×10^9 M^{-1} s^{-1}, Flyunt et al., 2001, Veltwisch et al., 1980). The DMSO assay leads to methanesulfinic acid and methanesulfonic acid. The combined yield of both acids, which was quantified by ion chromatography (as described above) is equivalent to 92% of the $^{\bullet}OH$ yield (Flyunt et al., 2001, refer to Supporting Information Text S11 and Scheme S6). Formaldehyde (CH_2O) from the ozone-amine reaction was determined with the DNPH method (refer to Supporting Information Text S4 and Text S12). In all analytical methods blanks were performed in the same manner with ultra-pure water instead of ozone solution to determine the initial concentration. Calibration experiments were performed in the same manner.

Quantum chemical method. The Gibbs energies were calculated using the Density Functional Theory (DFT) as implemented in Jaguar 8.3 program. For further information refer to Supporting Information Text S5.

2.4 Results and Discussion

2.4.1 Reaction kinetics

The rate constants of the aromatic amines with ozone are high and range between 1.2×10^5 and 2.4×10^6 M^{-1} s^{-1} (determined by competition kinetics from slopes of the plots, see Experimental part, Figure 1 and Supporting Information Figure S1 and S2). The pH value of the initial solution of the selected amines was in the range of 6 – 7 (see Supporting Information Text S4). Table 1 summarizes the results.

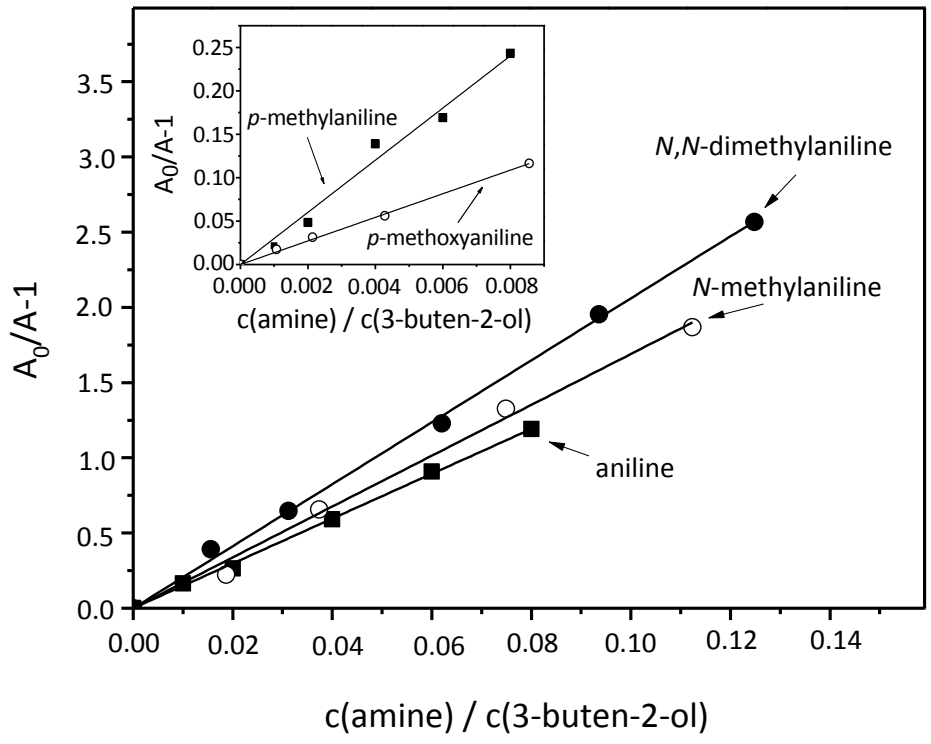

Figure 1. Determination of ozone rate constants in the reaction of investigated aromatic amines c_0(1×10^{-3} M – 8×10^{-3} M) with 3-buten-2-ol (1×10^{-2} M – 1×10^{-1} M) as competitor. The resulted formaldehyde yield from the ozone reaction with 3-buten-2-ol is determined with DNPH at appropriate pH. The ratio of the peak areas of

formaldehyde in the absence of competitor (A_0) and in the presence of varying concentrations of competitor (A) is plotted against the amine to 3-buten-2-ol ratio. The -1 is only necessary for scaling of the y-axis (see Supporting Information Text S4).

Taking into account the structure of the investigated amines, e.g., *p*-methylaniline contains an electron-donating substituent in contrast to aniline, while *p*-nitroaniline has a strongly electron-withdrawing one. As a consequence, the ozone reactivity of the first is higher and of the latter is much lower than that of aniline (see below, Table1). However, in general, the logarithm of the rate constants does not correlate well with the acid dissociation constants (pK_a) of the corresponding acids (see Figure 2).

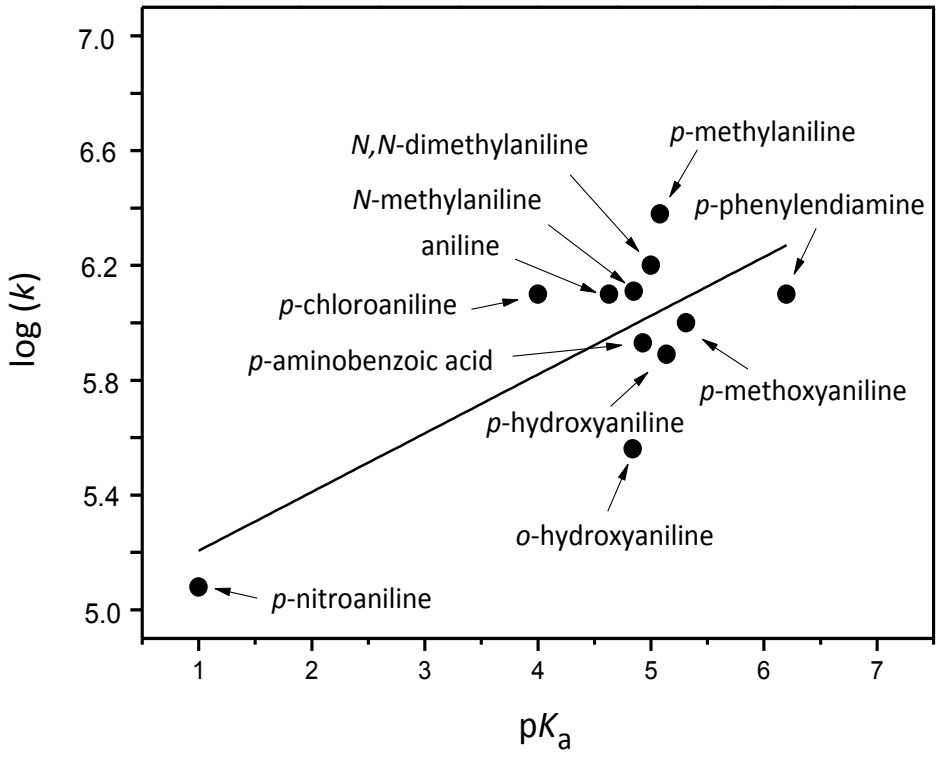

Figure 2. Correlation plot of the logarithm of the ozone rate constants vs. the acid dissociation constant (p*K*a) of the anilines with substituent in *para* position according to Hammett-type

In this correlation the value of the rate constant of *p*-methoxyaniline is lower than predicted, whereas the values of *p*-methylaniline and *p*-chloroaniline are higher than predicted. In experiments with *o*-hydroxyaniline and *p*-hydroxyaniline the kinetic data display a drop in the ozone rate constant by a factor of 3.3 and 5.7 in comparison with

aniline and are located between the rate constant of phenol and phenolate ion (for further details see Supporting Information Text S4, last paragraph). The rate constant of *p*-phenylenediamine displays the same value as aniline, despite the insufficient deprotonation at apparent pH for the second nitrogen. Calculated under the conditions of completely deprotonated amine species (i.e. the protonated species is neglected) a somewhat higher value of $k = 1.5 \times 10^6\ M^{-1}\ s^{-1}$ is obtained (the error of the pK_a–value contributes to the standard error of the rate constants, see Supporting Information Text S4, paragraph 2).

There is a good correlation between log(*k*) and Gibbs energy (ΔG^0) for adduct formation in the reaction of ozone with the benzene ring substituted in *para* position as shown in Figure S3 (see Supporting Information and Naumov & von Sonntag, 2010). For aniline, a Gibbs energy of $\Delta G^0 = -53\ kJ\ mol^{-1}$ for the ozone adduct at the aromatic moiety has been calculated and this value falls well on the predicted correlation line shown in Figure S3 (taken from von Sonntag & von Gunten, 2012, see Supporting Information). This further indicates that in particular for aniline ozone adduct formation to the ring seems possible (cf. Scheme 2). Therefore, the same Hammett-type plot was constructed for the anilines under study. However, a correlation plot of the log(*k*) of anilines vs. standard Gibbs energy of adduct formation at the *ortho* position to the amine group does not yield a comparably good correlation as for the benzenes (see above and Supporting Information Figure S4). Note that the *ortho* position in *o*-hydroxyaniline is blocked and ozone attack probably takes place at the *para* position, thus for this compound the standard Gibbs energy was calculated for an adduct at *para* position.

Since Hammett plot correlations of log(*k*) of aromatic compounds vs. the substituent constant (σ values) have been described in literature (Hoigné & Bader, 1983a, Pierpoint et al., 2001, Lee & von Gunten, 2012) this kind of correlation plot was also constructed for the anilines. As the p value (slope) in Hammett plot is negative, ozone must react as an electrophilic agent, whereupon the magnitude of the value reflects the sensitivity of the reaction to the substituent effect (von Sonntag & von Gunten, 2012). Even though the Hammett plot gives a better correlation (p slope is -1.44), it does not as well correlate linearly as benzenes or phenols does (see Figure 3). One

reason for the poorer correlation for the ozone-amine rate constants could be the two opportunities for ozone attack on anilines in contrast to benzene, where only the aromatic ring can be attacked (Naumov & von Sonntag, 2010, p slope is -2.65). Hammett plots of anilines vs. $\Sigma\ \bar{\sigma}_{o,\,m,\,p}$ described by Lee & von Gunten, 2012 (p slope is -1.54) and Pierpoint et al., 2001 (p slope is -1.48) indicate that the reactions are not very sensitive to the substituent effects.

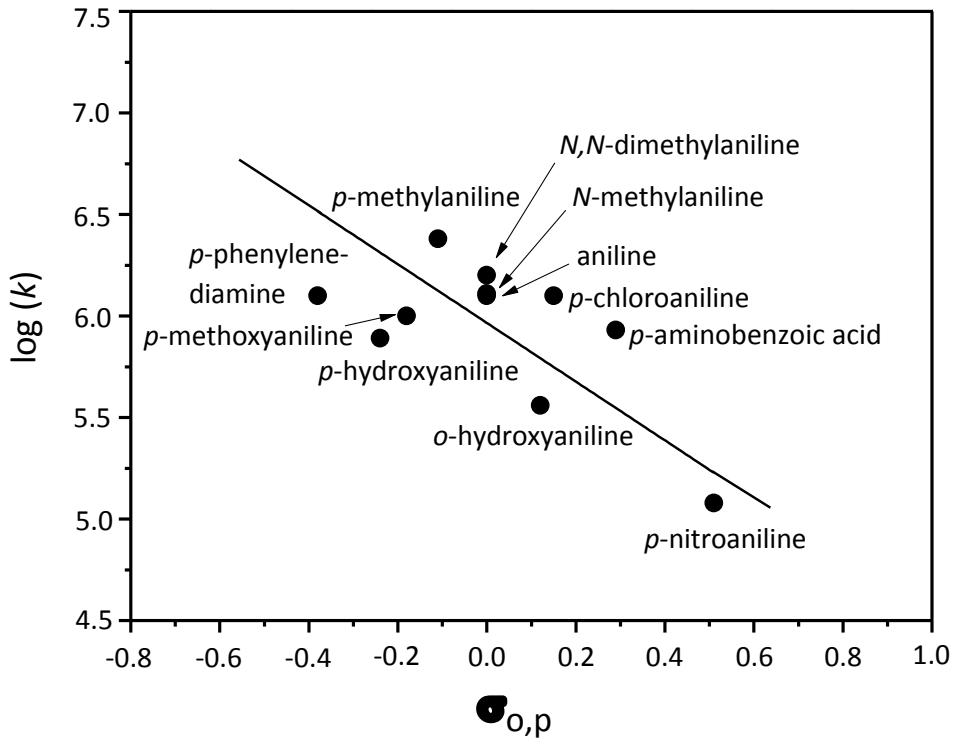

Figure 3. Hammett-type plot of the logarithm of the rate constants vs. the $\sigma_{o,p}$ values of the substituents (σ_p values taken from Hansch et al., 1991, Perrin et al., 1981, σ_o values were calculated from the relationship $\sigma_o = 0.66\sigma_p$, Lee & von Gunten, 2012).

Kinetic data of the above mentioned amines (Table 1) resulted in mostly 10 times lower values of the rate constant compared to literature reports. Previously reported findings show rate constants of aniline ($k = 1.4 \times 10^7$ M^{-1} s^{-1}), *m*-chloroaniline ($k = 1.04 \times 10^7$ M^{-1} s^{-1}), *p*-chloroaniline ($k = 7.84 \times 10^6$ M^{-1} s^{-1}), *o*-methoxyaniline ($k = 1.7 \times 10^7$ M^{-1} s^{-1}), *m*-methylaniline ($k = 1.9 \times 10^7$ M^{-1} s^{-1}), *m*-nitroaniline ($k = 2.4 \times 10^6$ M^{-1} s^{-1}) and *p*-nitroaniline ($k = 1.4 \times 10^5$ M^{-1} s^{-1}) which are all higher with the exception of

p-nitroaniline (all from Pierpoint et al., 2001). *N*,*N*-dimethylaniline, however, is in good accordance with *N*,*N*-dimethylcyclohexylamine ($k = 3.7 \times 10^6$ M^{-1} s^{-1}, Dodd et al., 2006). In the case of *p*-aminobenzoic acid ($k = 8.5 \times 10^5$ M^{-1} s^{-1}) in comparison with benzoate ion ($k = 1.2$ M^{-1} s^{-1}, Hoigné & Bader, 1983b), salicylic acid ($k < 500$ M^{-1} s^{-1}, Hoigné & Bader, 1983b) and salicylic acid anion ($k = 2.8 \times 10^4$ M^{-1} s^{-1}, Hoigné & Bader, 1983b) the ozone rate constant of *p*-aminobenzoic acid is much higher, which indicate that the free electron pair at nitrogen enhances the reactivity.

Table 1. Compilation of ozone rate constants (in the absence of $^{\bullet}OH$ scavenger) and compound degradation (in % of mole ozone consumed) in the reaction of ozone with anilines (deprotonated amine species). The compound degradation is presented in the absence and presence (scav.) of tertiary butanol (pooled data of various experiments, standard deviation in parenthesis).

Compounds	***k* /** M^{-1} s^{-1}	**Compound degradation / %** (per ozone consumed)		**pK_a (**Amine**)** (of corres-ponding acid) depicted from Sims, 1959
			scav.	
Aniline	$1.3 (\pm 0.57) \times 10^6$	23 (± 2)	40 (± 2)	4.63
p-Methylaniline	$2.4 (\pm 0.37) \times 10^6$	31 (± 4)	37 (± 2)	5.08
p-Chloroaniline	$1.4 (\pm 0.32) \times 10^6$	22 (± 2)	31 (± 1)	4.00
p-Nitroaniline	$1.2 (\pm 0.23) \times 10^5$	20 (± 2)	23 (± 1)	1.00
p-Methoxyaniline	$1.1 (\pm 0.67) \times 10^6$			5.31
p-Phenylenediamine	$1.3 (\pm 0.72) \times 10^6$	62 (±4)		6.20 (pK_{a2}: 2.67)
o-Hydroxyaniline	$3.7 (\pm 0.62) \times 10^5$			4.84 (p$K_{a(OH)}$ 9.71)
p-Hydroxyaniline	$7.8 (\pm 1.2) \times 10^5$			5.14 (p$K_{a(OH)}$ 10.3)
p-Aminobenzoic acid	$8.5 (\pm 1.4) \times 10^5$	76 (±6)		4.93 (p$K_{a(COOH)}$ 2.38)
N-Methylaniline	$1.4 (\pm 0.15) \times 10^6$			4.85
N,N-Dimethylaniline	$1.6 (\pm 0.78) \times 10^6$			5.00

2.4.2 Reaction stoichiometry

Considering the quite high ozone rate constants of the anilines, reaction stoichiometry is also of special interest for detailed mechanistic studies. The reaction stoichiometry was determined for selected anilines at pH of 6 – 7 (apparent pH). In addition pH values of 2 and 12 were used. Figure 4 shows that the concentration of the compounds under study in both the scavenged and non scavenged system decreases linearly with the ozone concentration using the example of aniline and *p*-nitroaniline. The reaction stoichiometry data for the reaction of ozone with the anilines are derived from the slopes of such correlations and compiled in Table 1.

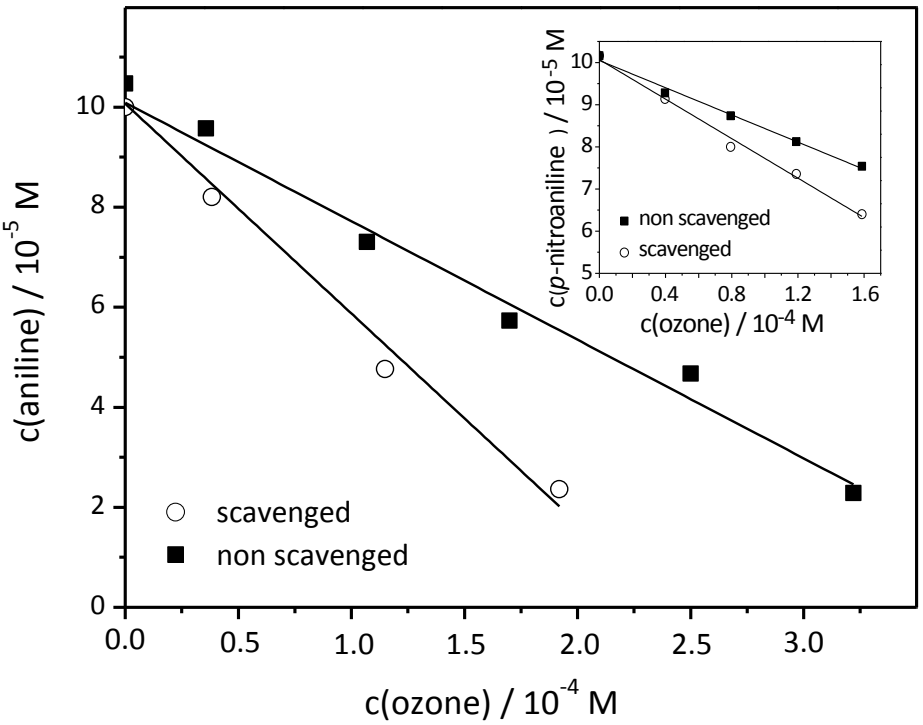

Figure 4. Degradation of aniline $c_0(1 \times 10^{-4}$ M) and *p*-nitroaniline $c_0(1 \times 10^{-4}$ M) in the reaction with ozone. Aniline (main graph) and *p*-nitroaniline (inset) concentrations in the absence and presence of tertiary butanol are plotted vs. the ozone dose.

The data in Table 1 indicate that the reaction stoichiometry, in other words the aniline transformation per ozone consumed, is in most cases similar (20 – 31%) in the absence of $^{\bullet}$OH scavenger of the selected different substituted anilines. Only *p*-aminobenzoic acid and *p*-phenylenediamine show much higher values of 76% and

62%, respectively. In particular, the aniline transformation in relation to 100% ozone yields 23%. Therefore, for the complete elimination of 1 mole aniline approximately 4.5 mole of ozone are required. Using the $^{\bullet}$OH scavenger tertiary butanol, the degradation of aniline per ozone consumed is 40%. Hence, for the same degradation more or less the half of ozone is needed. *p*-Methylaniline, *p*-chloroaniline and *p*-nitroaniline react in the same manner, however, with a lower difference in compound degradation in absence or presence of the $^{\bullet}$OH scavenger (Table 1).

On balance a higher ozone dosage is needed for complete compound elimination mainly for aniline when the $^{\bullet}$OH scavenger is absent. This is a surprising effect, as one would expect further amine degradation when both ozone and $^{\bullet}$OH react with the amine. The importance of radical-forming processes can be explained by $^{\bullet}$OH induced chain reactions accelerating ozone degradation (Staehelin & Hoigné, 1985). The chain reaction is presented in Scheme 3 (reaction (27) – (34)) using the example aniline. In this scheme the reactions (27) – (28) and (30) – (31) are identical to the primary pathways 4 and 5 from Scheme 1 and 2. Ozone addition to nitrogen or aromatic ring can lead to an amine radical cation and $O_3^{\bullet-}$. The amine radical cation is in equilibrium with its conjugate base the aminyl radical (reaction (29), Merényi et al., 2010). Aminyl radicals as N-centered radicals do not react with O_2, but can react with ozone (reaction (32), von Sonntag & von Gunten, 2012). $^{\bullet}$OH react with a high rate constant with aniline (reaction (34), $k = 1.4 \times 10^{10}$ M^{-1} s^{-1}, Buxton et al., 1988) by yielding the amine radical cation in acidic solution (pH 5, examined by optical pulse radiolysis methods, Qin et al., 1985). In basic solution the aminyl radical (cf. Scheme 3, reaction (28)) is formed (confirmed by in-situ radiolysis-ESR studies, Qin et al., 1985). The aminyl radicals react more quickly with ozone than the anilines by forming nitroxyl radicals (von Gunten, 2003, Sehested et al., 1984). Rate constants for the reaction of aminyl radicals with ozone are as yet not known, but the exergonicity of this reaction is remarkable and this reaction may be quite fast (Naumov & von Sonntag, 2010, 2011). Thus, upon $^{\bullet}$OH attack on aniline, further aminyl radicals are formed (reaction (34)), which initiate a chain reaction that consumes ozone (reaction (32) and (33), von Gunten, 2003, Sehested et al., 1984). This chain reaction is less pronounced if $^{\bullet}$OH is scavenged, albeit such reactions are still initiated by ozone. The $^{\bullet}$OH scavenging

experiments may be taken as an indication that the $^{\bullet}OH$ precursor reactions can be considered as important side reactions. Deficits in the stoichiometry between ozone and aniline transformation are similar to that reported for diclofenac (Sein et al., 2008). There, it has been suggested, that there may be a chain reaction that consumes ozone in competition with its reactions with diclofenac in analogy to reaction (32) - (33) in Scheme 3.

Scheme 3. Proposed reaction scheme of a chain reaction in the ozonation of aniline

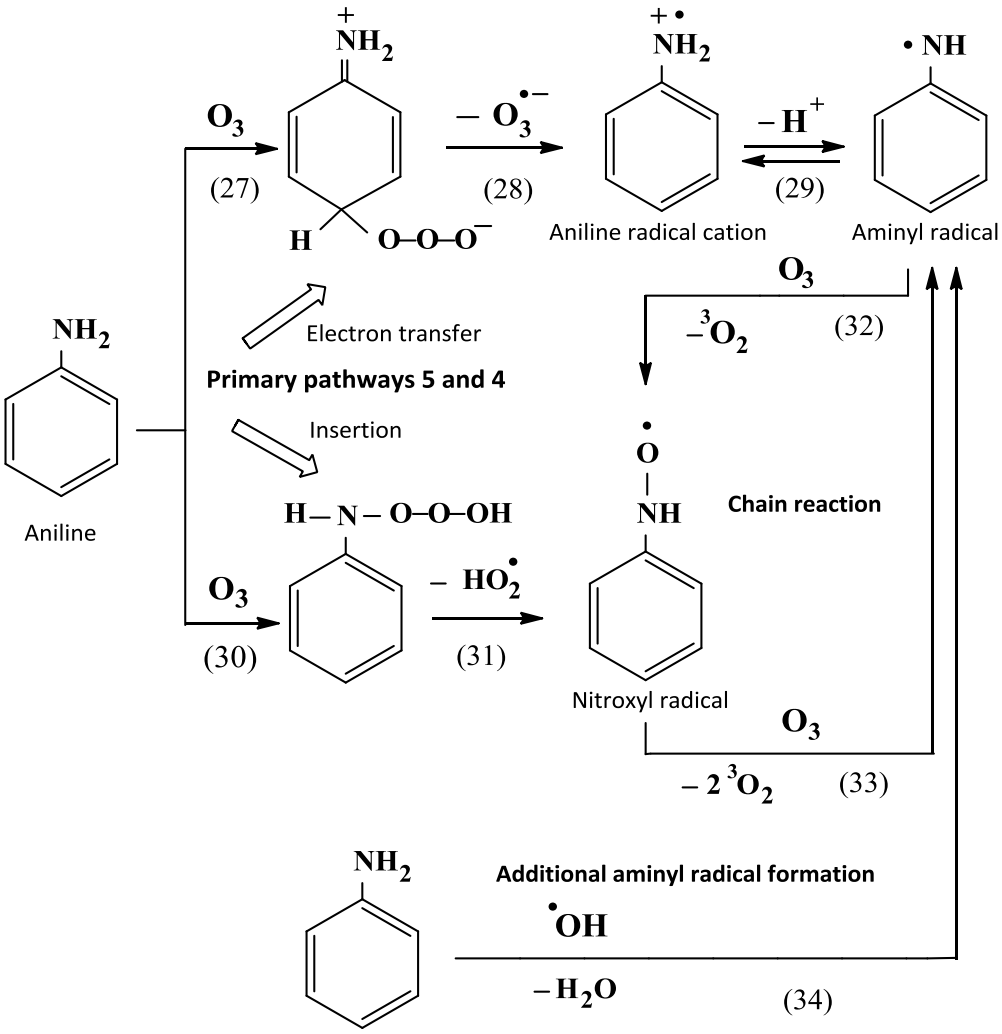

Experiments in non scavenged systems where pH was adjusted with sulfuric acid and sodium hydroxide to pH values of 2 and 12, respectively, revealed differences in reaction stoichiometry depending on pH (see Supporting Information Table S1). At pH 2 where the deprotonated fraction of the nitrogen is very low (less than 1%,

protonated amine species prevail) with the exception of *p*-nitroaniline (90%, due to the low pK_a value) no substantial difference in stoichiometry to experiments at neutral pH is observed. This observation suggests that ozone attack mostly occurs at the aromatic ring. However, at pH 12 where the deprotonation ratio in all cases is high (always 100%) the results are distinguished in the case of aniline (13%), *p*-chloroaniline (10%) and *p*-methylaniline (20%). Here less compound transformation was observed. An apparent reason could be the catalytic action of hydroxyl ions ($^{-}$OH), which react with ozone and give rise to $^{\bullet}$OH. However, due to the high rate constant of the ozone-amines reaction this reaction is not relevant (refer to Supporting Information Text S3, paragraph 3), so that other reasons must prevail. This will need further elucidation, but is beyond the scope of this study.

2.4.3 Product formation

Anilines react fast with ozone. This fast reaction is compatible with an addition to the activated aromatic ring but also with an addition to the nitrogen (von Sonntag & von Gunten, 2012). Stoichiometry experiments displayed that the fast reaction of aniline with ozone leads to three main transformation products (RT 3.2, 3.9 and 12.2 min) and several minor products at various ozone doses detectable by HPLC-DAD at 200 nm (see Supporting Information Figure S6). Using t-BuOH as radical scavenger, to suppress the influence of $^{\bullet}$OH reactions, also three main products and several minor products (with identical RT) at lower and higher ozone doses were detected as will be discussed below.

***o*-Hydroxyaniline and *p*-hydroxyaniline yields in aniline-ozone reactions.** Ozone attack at the aromatic ring can lead to hydroxylation (von Sonntag & von Gunten, 2012). In the case of aniline the hydroxylation may yield *o*-hydroxyaniline and *p*-hydroxyaniline (Scheme 2 illustrates the suggested reaction of aniline with ozone to *p*-hydroxyaniline, which is shown in pathway 5, reaction (13) – (15)). In contrast, *m*-hydroxyaniline should not be formed, because the amine group of the aniline as an electron donating group has a positive mesomeric effect, which is *ortho-para* directing (Beyer et al., 1981). The product formation experiments (with and without using an $^{\bullet}$OH scavenger and with pH of ~7) indeed confirmed the expected formation of

p-hydroxyaniline and *o*-hydroxyaniline (see Supporting Information Text S7). The product yields increased linearly with the ozone dose. From the slope of the resulting graph (see Figure 5) a 3-fold higher yield of *p*-hydroxyaniline than for *o*-hydroxyaniline in systems without using an $^{\bullet}OH$ scavenger could be quantified. In scavenged systems *p*-hydroxyaniline yields to 1.5-fold higher value than *o*-hydroxyaniline. Yields of hydroxyanilines in the scavenged system were determined in total nearly 40% per aniline transformation (see Table 2).

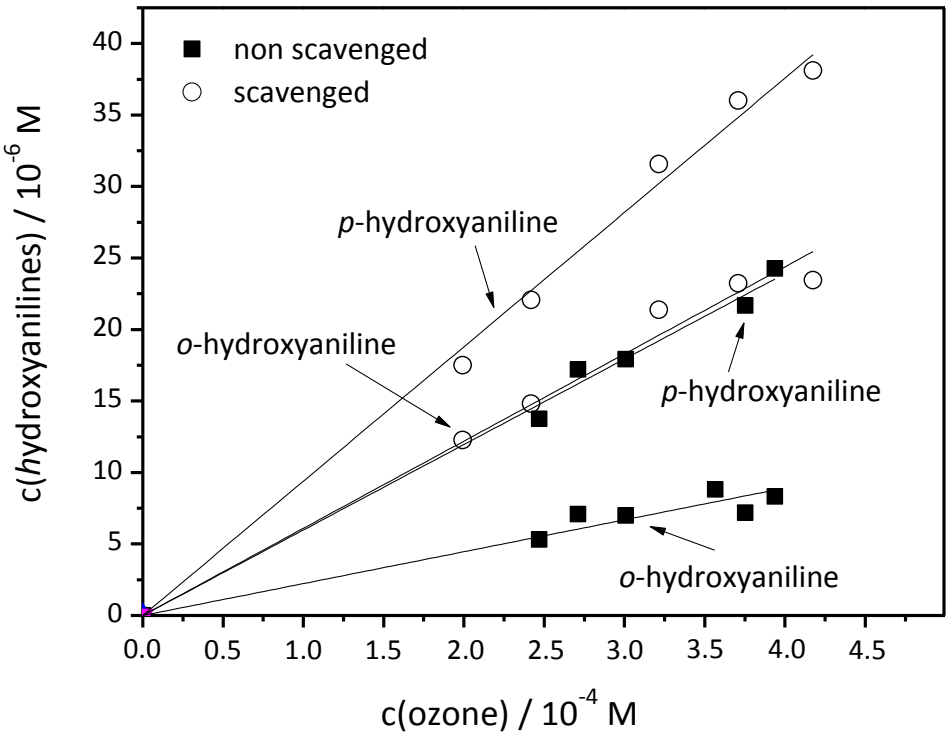

Figure 5. Plot of the determination of *o*-hydroxyaniline and *p*-hydroxyaniline in the reaction of aniline $c_0(1 \times 10^{-3}$ M) with ozone in the scavenged and non scavenged system as a function of ozone concentration.

As a result of these high values of hydroxyanilines, ozone addition at the aromatic ring of aniline takes place preferentially according to primary pathway 5 in Scheme 2. The formation of an ozonide after ozone attack at the aromatic ring should not occur, because pyridine-2-carboxylic acid was not found (see Scheme 2, primary pathway 9, reaction (23) – (26)).

Table 2. Ozonation of anilines. Oxidation products including $^{\bullet}$OH and their yields in % of ozone consumed (first column, standard deviation in parentheses) as well as in % of compound degradation (second column). $^{\bullet}$OH yields can not be related to compound degradation as well as the calculation of some formaldehyde yields was not possible, because reaction stoichiometry results are missing, denoted as not available. The product formation experiments are mostly carried out without $^{\bullet}$OH scavenger. The sum of stable products is denoted in rectangular brackets.

Compounds	**Product yield / %** First column: Per ozone consumed. Second column: Calculated per degraded compound. In rectangular brackets: Sum of stable products in relation to 100% compound.	
Aniline		[49]
p-Hydroxyaniline / (scavenged)$^{\bullet}$	5.9 (± 0.36) / (9.4 (± 0.32))$^{\bullet}$	26 / (24)$^{\bullet}$
o-Hydroxyaniline / (scavenged)$^{\bullet}$	2.2 (± 0.18) / (6.1 (± 0.23))$^{\bullet}$	9.6 / (15)$^{\bullet}$
Nitrobenzene	0.42 (± 0.029)	1.8
Nitrosobenzene	1.9 (± 0.24)	8.3
Azobenzene	0.085 (± 0.026)	0.37
$^{\bullet}$OH	34 (± 3.1)	
Formaldehyde	0.67 (± 0.021)	2.9
***p*-Methylaniline**		
$^{\bullet}$OH	46 (± 2.4)	
Formaldehyde	2.9 (± 0.26)	9.4
***p*-Chloroaniline**		[100]
Chloride	21 (± 0.012)	95
$^{\bullet}$OH	42 (± 6.9)	
Formaldehyde	1.0 (± 0.38)	4.6

***p*-Nitroaniline**		[71]
Nitrite	3.7 (± 0.061)	16
Nitrate	12 (± 0.043)	52
$^{\bullet}$OH	35 (± 4.7)	
Formaldehyde	0.43 (± 0.38)	2.2
***p*-Methoxyaniline**		
$^{\bullet}$OH	51 (± 1.2)	
Formaldehyde	3.1 (± 0.06)	not available
***p*-Phenylenediamine**		
$^{\bullet}$OH	59 (± 1.0)	
Formaldehyde	0.53 (± 0.05)	0.89
***o*-Hydroxyaniline**		
$^{\bullet}$OH	44 (± 1.1)	
Formaldehyde	1.2 (± 0.26)	not available
***p*-Hydroxyaniline**		
$^{\bullet}$OH	53 (± 2.1)	
Formaldehyde	2.1 (± 0.55)	not available
***p*-Aminobenzoic acid**		
$^{\bullet}$OH	43 (± 1.4)	
Formaldehyde	0.43 (± 0.031)	0.57
***N*-Methylaniline**		
$^{\bullet}$OH	39 (± 2.0)	
Formaldehyde	6.3 (± 0.49)	not available
***N*,*N*-Dimethylaniline**		
$^{\bullet}$OH	46 (± 2.6)	
Formaldehyde	6.1 (± 0.85)	not available

2-Amino-5-anilino-benzochinon-1,4-anil in aniline-ozone reactions. In addition to the determined hydroxylated products one more main oxidation product peak (RT 12.2 min, absorption maximum 346 nm) was detected in stoichiometric experiments in aniline-ozone reactions (see Supporting Information Figure S6). Identification of this product was carried out with LC-MS measurements (see Experimental part and Supporting Information Text S8). From these measurements a mass of *m*/*z* 290 $[M+H]^+$ was obtained in solutions at pH 7.2 and without an $^{\bullet}OH$ scavenger (refer to Supporting Information Scheme S3). This nominal mass fits with 2-amino-5-anilino-benzochinon-anil and 2,5-dianilino-*p*-benzochinon-imin. In previous studies these compounds were also identified in the reaction of aniline with other oxidation reagents (Tanabe, 1959, Dobarganes Garcia & González-Quijano, 1983, Gupta et al., 1984).

In a secondary process the most likely formed aminyl radicals (see Scheme 1, primary pathway 2 and 3, reaction (3) – (6)) can further react with other intermediates, products or with one another in neutral solution (Qin et al., 1985). By this reason 2-amino-5-anilino-benzochinon-anil could be formed by an aminyl radical attack to *o*-hydroxyaniline (see Scheme 4, reaction (35) – (36)), while 2,5-dianilino-*p*-benzochinon-imin could be formed with *p*-hydroxyaniline (cf. Scheme 4, reaction (37) – (38)). However, from the fragmentation pattern of the product ion scans, 2-amino-5-anilino-benzochinon-anil is suggested to be the more likely product (refer to Supporting Information Scheme S3). This is further confirmed by the fact that the UV-spectrum (absorption maximum 346 nm) from the HPLC-DAD measurements of the aniline-ozone reaction matches that one from literature (Teuber & Jellinek, 1954), which is not the case for 2,5-dianilino-*p*-benzochinon-imin. Quantification of 2-amino-5-anilino-benzochinon-1,4-anil was not possible since no reference standard was available. However, based on peak areas, it is clear that formation of 2-amino-5-anilino-benzochinon-1,4-anil (with experiments in the non scavenged system) is not linearly dependent on ozone concentration (refer to Supporting Information Figure S7).

Scheme 4. Proposed reaction scheme of the reaction of aminyl radicals with *o*-hydroxyaniline and *p*-hydroxyaniline by forming 2-amino-5-anilino-benzochinon-1,4-anil or 2,5-dianilino-*p*-benzochinon-imin

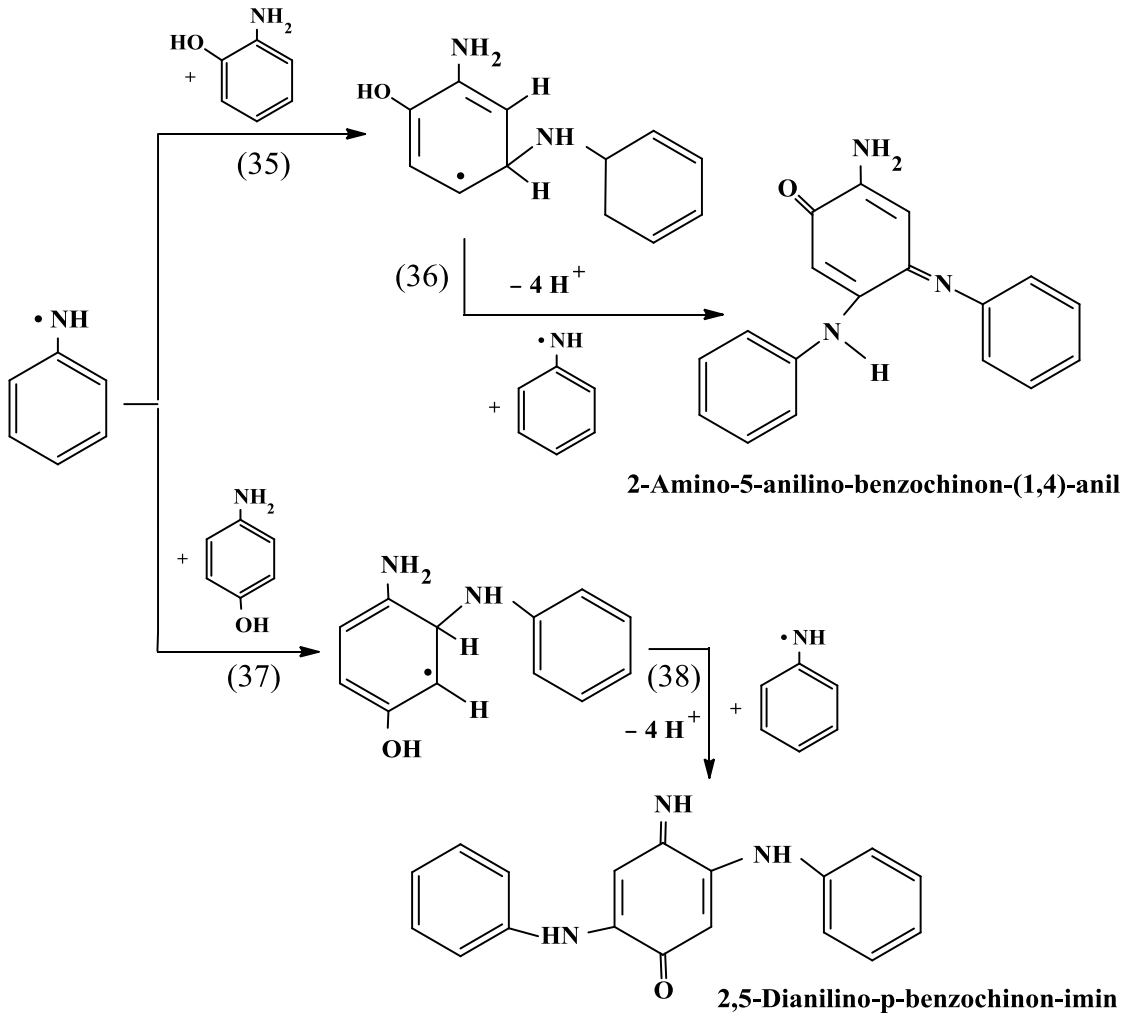

Benzidine and 1,2-diphenylhydrazine from a combination reaction of two aminyl radicals as described by Qin et al., 1985 as well from a combination of two amine radical cations (Merényi & Lind, 1998) could not be found, neither in LC-MS measurements nor with HPLC-DAD and the use of reference material (refer to Supporting Information Scheme S4, reaction (39) – (40)). Thus, the reaction of aminyl radicals with one another cannot be confirmed.

Nitrobenzene, nitrosobenzene and azobenzene yields in aniline-ozone reactions. Ozone attack at nitrogen can lead to nitrobenzene, nitrosobenzene (Sarasa et al., 2002, Turhan & Uzman, 2007) and azobenzene (from the reaction of nitrosobenzene with aniline, for the kinetics see Dalmagro et al., 1994, Chan & Larson, 1991, 1995). Indeed, these compounds were identified in the aniline-ozone reaction with GC-MS measurements as the minor products detected by HPLC-DAD in stoichiometric experiments (see above and Figure S6 in Supporting Information). For further details refer to Experimental part and Supporting Information Text S9 and Figure S8. The proposed mechanism is demonstrated in Scheme 5.

A calculation of nitrobenzene, nitrosobenzene and azobenzene yields as a function of the aniline degradation leads to a total product yield near 10%. This and the above data indicate that a second primary oxidation pathway is addition of ozone at nitrogen accompanied by a concomitant proton transfer (according to pathway 1 and 4 in Scheme 1). However, this pathway is a minor reaction, in contrast to previously reported findings, in which these components are documented as main reaction products (Sarasa et al., 2002, Turhan & Uzman, 2007, identified after liquid-liquid extraction with GC-FID, however without quantification). The above mentioned processes are confirmed with quantum-chemical calculations, which indicate that addition to the aniline ring is markedly exergonic (ΔG^0 = –53 kJ mol^{-1}), but an addition to the nitrogen is slightly endergonic (ΔG^0 = +15 kJ mol^{-1}, Naumov & von Sonntag, 2010). The low yields of nitrobenzene and nitrosobenzene fairly reflect the thermodynamic data.

Concerning the mechanism of the formation of nitrobenzene, it could on the one hand be generated by an insertion reaction of ozone at nitrogen (Scheme 5, reaction (41), see also Scheme 1, reaction (8) – (9), pathway 4). The intermediate would readily release a hydroperoxyl radical, $HO_2^{\bullet}$, by forming a nitroxyl radical (reaction (42)). A biomolecular decay of the nitroxyl radical, assisted by water (reaction (43) – (44)) giving rise to aniline and nitrobenzene is energetically feasible (ΔG^0 = –83 kJ mol^{-1}, von Sonntag & von Gunten, 2012).

Scheme 5. Proposed scheme in the reaction of ozone with aniline (at nitrogen) by forming nitrobenzene, nitrosobenzene and azobenzene

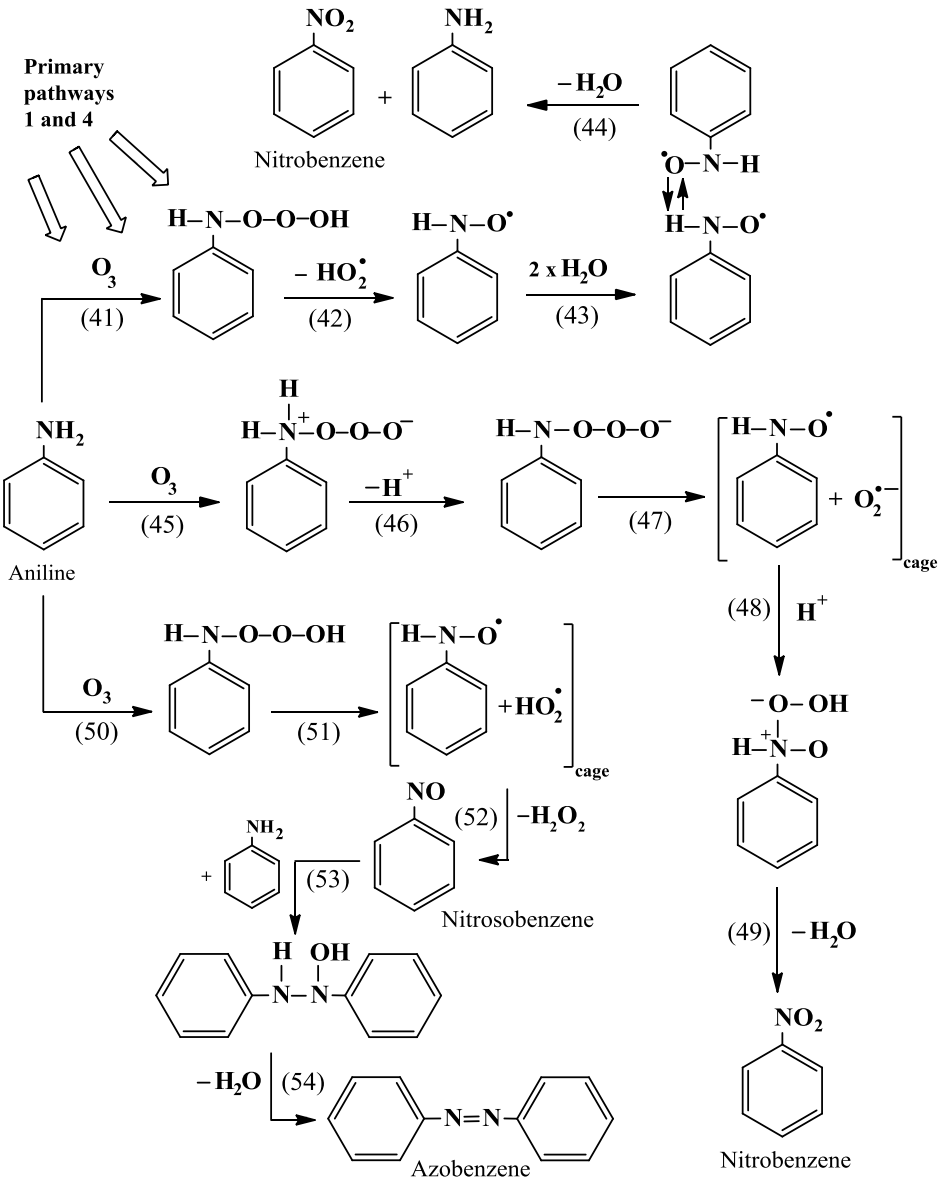

On the other hand nitrobenzene could be formed if ozone reacts as an H-abstractor after addition (cf. pathway 1 and reaction (45) – (49)), whereby a radical pair would be formed. Whenever two radicals are formed side by side, they are held together for a short time by the solvent cage (reaction (47)), where they can react by combination (or diffusing out of the cage, Rabinowitch & Wood, 1936, Rabinowith, 1937). After the release of water nitrobenzene is formed. One has to take into account that nitrobenzene is a primary product despite the fact that it requires two oxidation equivalents (von Sonntag & von Gunten, 2012). Nitrosobenzene as well may be

generated by the insertion reaction of ozone at nitrogen (reaction (50) – (52)) and subsequent disproportionation of the nitroxyl radical with hydroperoxyl radical ($HO_2^{\bullet}$), e.g., in the cage. Thus, the release of hydrogen peroxide could result from formation of nitrosobenzene. The reaction of nitrosobenzene with aniline to form azobenzene (reaction (53) – (54)) in water is a slow postozonation process for which reaction kinetics are well documented (k = 8.4 × 10^{-6} M^{-1} s^{-1}, Dalmagro et al., 1994, Ueno & Akiyoshi, 1954, Ogata & Takagi, 1957, Yunes et al., 1975). However, nitrosobenzene takes part in further reactions (not yet identified), because of its degradation in time based experiments (see above and Figure S9).

Chloride, nitrite and nitrate yields in reactions of *p*-chloroaniline and *p*-nitroaniline with ozone. Ozone attack at the aromatic ring of *p*-chloroaniline and *p*-nitroaniline can potentially release chloride (Cl^-) and nitrite (NO_2^-). The latter can be further oxidized to nitrate (NO_3^-). For further details see Experimental part and Supporting Information Text S10 and Figure S10, S11 and S12. The proposed mechanism is presented in Supporting Information Scheme S5 (reaction (55) – (61)). As a result of the high chloride or nitrite and nitrate yields as a function of *p*-chloroaniline (95%) or *p*-nitroaniline transformation (in total near 70%, see Table 2) ozone addition at the aromatic ring (according to pathway 5) with subsequent abstraction of chloride or nitrite takes place to a large extent. Comparing *p*-chloroaniline and *p*-nitroaniline with chlorobenzene and nitrobenzene, respectively (for which product formation experiments were additionally carried out) it is shown that the chloride, nitrite and nitrate yields resemble one another, in spite of the low ozone rate constants of the benzenes in contrast to the anilines (see Supporting Information Text S10, last paragraph and Figure Inset S11 and S12). These results point out that in the ozonation of *p*-chloroaniline and *p*-nitroaniline the effect of the amino group is negligible with respect to transformation products. This is in accordance to the observation that mostly addition at the aromatic ring of anilines and not at nitrogen takes place.

Yield of $^{\bullet}$OH and formaldehyde. The reactions of ozone with the anilines can lead to $^{\bullet}$OH, provided that ozone reacts via a radical mechanism, i.e., electron transfer, H-abstraction or insertion with the amines either from ring addition or nitrogen addition or from both (von Sonntag & von Gunten, 2012). For aniline, this is shown in

scheme 1 and 2 (reactions (3), (6) or (9) and reactions (16), (18) or (21)). In all cases the $^{\bullet}OH$ yield is calculated by plotting $^{\bullet}OH$ concentrations against the ozone concentration, which increases linearly with increasing ozone concentration (refer to Supporting Information Text S11, Figure S13 and Scheme S6). From the slope of the resulting graph high $^{\bullet}OH$ yields of 34% to 59% are deduced, whereupon aniline displays the lowest and *p*-phenylenediamine the highest value (shown in Table 2). Based on these high values a direct radical mechanism upon ozonation of anilines in aqueous solution is likely.

In ozonation experiments of the investigated amines, a secondary product can be formaldehyde (shown in Schemes S7, S8 and S9). The formaldehyde yields were calculated and the corresponding data are summarized in Table 2. On account of the low formaldehyde yields (0.4% up to 6%) mechanistic considerations are only made for *N*-methylaniline, *N*,*N*-dimethylaniline, *p*-methoxyaniline and *p*-methylaniline with yields higher than 3%. For further details refer to Supporting Information Text S12. The proposed mechanisms are also presented in Supporting Information. Here, for *N*,*N*-dimethylaniline see Scheme S7 (reaction (62) – (67)), for *p*-methoxyaniline see Scheme S8 (reaction (68) – (73)) and for *p*-methylaniline see Scheme S9 (reaction (74) – (79)). As a result of the formaldehyde yield electron transfer reactions at nitrogen after ozone adduct formation (cf. Scheme1, pathway 2) take place in the case of *N*-methylaniline and *N*,*N*-dimethylaniline. For *p*-methoxyaniline and *p*-methylaniline it is proposed that on the basis of the formaldehyde yield in an initial step ozone adduct formation at the aromatic ring occurs and according to pathway 6 (cf. Scheme 2) electron transfer reactions take place.

2.4.4 Mass balances and mechanistic considerations

The mass balance in the reaction of ozone with aniline is near 50% with respect to compound transformation (see Table 2). This can be explained by the 2-amino-5-anilino-benzochinon-anil, which could not be quantified and that may close the gap. For *p*-chloroaniline a product yield of chloride near 95% in relation to oxidized *p*-chloroaniline point out that more or less a complete mass balance is obtained. In the reaction of *p*-nitroaniline with ozone a sum of nitrite and nitrate yield near 70%

referring to degraded *p*-nitroaniline points out that the mass balance is not fully complete.

The mass balance of product formation (without scavenging $^{\bullet}$OH) in relation to 100% ozone consumption is only 10% in the case of aniline. For *p*-chloroaniline and *p*-nitroaniline the corresponding values are about 20% and 16%, respectively. A reason is that the ozone consumption for compound degradation is low (see reaction stoichiometry), so that approximately 80% to 90% of the dosed ozone reacts by forming radicals such as $^{\bullet}$OH (34% – 42%) and other products which could not be detected. In the case of *p*-nitroaniline further oxidation of nitrite to nitrate (12%) consumes ozone, which has to be taken into account. Thus, approximately 30% ozone is used for nitrite and nitrate formation (see Table 2, 12% is required for nitrate and around 16% for transformation of *p*-nitroaniline yielding nitrite). The remaining 70% in the case of *p*-nitroaniline comprises 35% of ozone, which is converted to $^{\bullet}$OH. Finally, in the case of aniline approximately 56% of ozone (e.g., 100% ozone minus 10% ozone for aniline degradation minus 34% ozone for $^{\bullet}$OH formation, see Table 1 and 2) and about 38% for *p*-chloroaniline and 35% for *p*-nitroaniline could be consumed in unknown reactions, possibly chain reactions (see Scheme 3, reaction (32) – (33)). The ratio of the product yield in absence and presence of scavenger is, however, in good accordance with the ratio of the consumption in absence and presence of scavenger.

2.5 Conclusions

The present study has shown that the generally fast reactions of eleven substituted anilines with ozone arise from several radical and non radical processes. The reaction pathways of particularly aniline in its reaction with ozone could be proposed. Ozone attack at the aromatic ring, alter the anilines structure by forming several transformation products. Hammett plots for the reaction of ozone with the anilines indicate that the reactions are less sensitive to substituent effects in contrast to benzenes and phenols. This is probably due to the two opportunities for ozone attack at anilines on the one hand at nitrogen and on the other hand at the aromatic ring. The presented results may help to explain the complexity of transformation pathways of micropollutants containing an aniline group as structural unit. An important role in transformation plays $^{\bullet}$OH and other free radical reactions.

2.6 References

Benitez, F. J., Acero, J. L., Real, F. J., Roldan, G., Casas, F., 2011. Comparison of different chemical oxidation treatments for the removal of selected pharmaceuticals in water matrices. Chem Eng J 168, 1149–1156.

Beyer, H., Walter, W., Francke, W., 1981. Lehrbuch der organischen Chemie. S. Hirzel Verlag, Stuttgart.

Bielski, B. H. J., Cabelli, D. E., Arudi, R. L., Ross, A. B., 1985. Reactivity of HO_2/O_2^- radicals in aqueous solution. J Phys Chem Ref Data 14, 1041-1100.

Boxall, A., Keller, V. D. J., Straub, J. O., Monteiro, S. C., Fussell, R., Williams, R. J., 2014. Exploiting monitoring data in environmental exposure modelling and risk assessment of pharmaceuticals. Environ Int, 73, 175-185.

Bühler, R. E., Staehelin, J., Hoigné, J., 1984. Ozone decomposition in water studied by pulse radiolysis. HO_2/O_2^- and HO_3/O_3^- as intermediates. J Phys Chem 88, 2560-2564.

Buxton, G. V., Greenstock, C. L., Helman, W. P., Ross, A. B., 1988. Critical review of rate constants for reactions of hydrated electrons, hydrogen atoms and hydroxyl radicals (OH/O^-) in aqueous solution. J Phys Chem Ref Data 17, 513-886.

Caprio, V., Insola, A., 1985. Aniline and anilinium ion ozonation in aqueous solution. Ozone Sci Eng 7, 169-179.

Chan, W. F., Larson, R. A., 1991. Mechanisms and products of ozonolysis of aniline in aqueous solution containing nitrite ion. Wat Res 25, 1539-1544.

Chan, W. F., Larson, R. A., 1995. Formation of azobenzenes and azoxybenzenes from the aqueous reactions of anilines and ozone. Ozone Sci Eng 17, 619-625.

Criegee, R., 1975. Mechanismus der Ozonolyse. Angew Chem 87, 765-771.

Dalmagro, J., Yunes, R. A., Simionatto, E. L., 1994. Mechanism of reaction of azobenzene formation from aniline and nitrosobenzene in basic conditions. General base catalysis by hydroxide ion. J Phys Org Chem 7, 399-402.

Dobarganes Garcia, M. C., González-Quijano, R., 1983. Formation of aniline oxidation products in oils related to the toxic syndrome. Grasas y aceites 32, 91-94.

Dodd, M. C., Buffle, M.-O., von Gunten, U., 2006. Oxidation of antibacterial molecules by aqueous ozone: moiety-specific kinetics and application to ozone-based wastewater treatment. Environ Sci Technol 40, 1969-1077.

Doré, M., Langlais, B., Legube, B., 1980. Mechanism of the reaction of ozone with soluble aromatic pollutants. Ozone Sci Eng 2, 39-54.

Dowideit, P., von Sonntag, C., 1998. The reaction of ozone with ethene and its methyl- and chlorine-substituted derivatives in aqueous solution. Environ Sci Technol 32, 1112-1119.

Elliot, A. J., McCracken, D. R., 1989. Effect of temperature on $O^{\bullet -}$ reactions and equilibria: a pulse radiolysis study. Radiat Phys Chem 33, 69-74.

Elmghari-Tabib, M., LaPlanche, A., Venien, F., Martin, G., 1982. Ozonation of amines in aqueous solutions. Wat Res 16, 223-229.

Flyunt, R., Makogon, O., Schuchmann, M. N., Asmus, K.-D., von Sonntag, C., 2001. The OH-radical-induced oxidation of methanesulfinic acid. The reactions of the methyl-sulfonyl radical in the absence and presence of dioxygen. J Chem Soc, Perkin Trans 2, 787-792.

Forni, L., Bahnemann, D., Hart, E. J., 1982. Mechanism of the hydroxide ion initiated decomposition of ozone in aqueous solution. J Phys Chem 86, 255-259.

Gabet-Giraud, V., Miège, C., Choubert, J. M., Ruel, S. M., Coquery, M., 2010. Occurrence and removal of estrogens and beta blockers by various processes in wastewater treatment plants. Sci Total Environ 408, 4257-4269.

Galstyan, A. G., Bushuev, A. S., Solomyannyi, R. N., 2008. Oxidation of 4-aminotoluene with ozone in acetic acid solution. Russ J App Chem 81, 1198-1201.

Gilbert, E., Zinecker, H., 1980. Ozonization of aromatic amines in water. Ozone Sci Eng 2, 65-74.

Gupta, V. K., Bhushan, R., Kaushik, R. D., Jain, M. C., Srivastava, S. P., 1984. Kinetics and mechanism of the oxidation of aromatic amines by periodate ion – oxidation of aniline and *N*,*N*-dimethylaniline. Oxid Commun 7, 409-423.

Hansch, C., Leo, A., Taft, R. W., 1991. A survey of Hammett substituent constants and resonance and field parameter. Chem Rev 91, 165-195.

Hart, E. J., Sehested, K., Holcman, J., 1983. Molar absorptivities of ultraviolet and visible bands of ozone in aqueous solutions. Anal Chem 55, 46-49.

Hoigné, J., Bader, H., 1983a. Rate constants of reactions of ozone with organic and inorganic compounds in water. - I. Non-dissociating organic compounds. Wat Res 17, 173-183.

Hoigné, J., Bader, H., 1983b. Rate constants of reactions of ozone with organic and inorganic compounds in water. - II. Dissociating organic compounds. Wat Res 17, 185-194.

Hollender, J., Zimmermann, S. G., Koepke, S., Krauss, M., McArdell, C. S., Ort, C., Singer, H., von Gunten, U., Siegrist, H., 2009. Elimination of organic micropollutants in a municipal wastewater treatment plant upgraded with a full-scale post-ozonation followed by sand filtration. Environ Sci Technol 43, 7862-7869.

Huber, M. M., Göbel, A., Joss, A., Hermann, N., Löffler, D., McArdell, C. S., Ried, A., Siegrist, H., Ternes, T. A., von Gunten, U., 2005. Oxidation of pharmaceuticals during ozonation of municipal wasterwater effluents: a pilot study. Environ Sci Technol 39, 4290-4299.

Huggett, D. B., Brooks, B. W., Peterson, B., Foran, C. M., Schlenk, D., 2002. Toxicity of select beta adrenergic receptor-blocking pharmaceuticals (b-blockers) on aquatic organisms. Arch Environ Contam Toxicol 43, 229–235.

Küster, A., Alder, A. C., Escher, B. I., Duis, K., Fenner, K., Garric, J., Hutchinson, T. H., Lapen, D. R., Péry, A., Römbke, J., Snape, J., Ternes, T. A., Topp, E., Wehrhan, A., Knacker, T., 2010. Environmental risk assessment of human pharmaceuticals in the European union: a case study with the b-blocker atenolol. Integr Environ Assess Manage 6, 514–523.

Lee, Y., von Gunten, U., 2010. Oxidative transformation of micropollutants during municipal wastewater treatment: comparison of kinetic aspects of selective (chlorine, chlorine dioxide, ferrateVI, and ozone) and non-selective oxidants (hydroxyl radical). Wat Res 44, 555-566.

Lee, Y., von Gunten, U., 2012. Quantitative structure−activity relationships (QSARs) for the transformation of organic micropollutants during oxidative water treatment. Wat Res 46, 6177-6195.

Lipari, F., Swarin, S. J., 1982. Determination of formaldehyde and other aldehydes in automobile exhaust with an improved 2,4-dinitrophenylhydrazine method. J Chrom 247, 297-306.

Machulek, A., Gogritchiani, E., Moraes, J. E. F., Quina, F. H., Braun, A. M., Oliveros, E., 2009. Kinetic and mechanistic investigation of the ozonolysis of 2,4-xylidine (2,4-dimethyl-aniline) in acidic aqueous solution. Sep & Pur Technol 67, 141-148.

Merényi, G., Lind, J., 1998. Anilinyl radicals. In N-centered radicals, ed. by Zeev B. Alfassi, John Wiley & Sons, 599-613

Merényi, G., Lind, J., Naumov, S., von Sonntag, C., 2010. The reaction of ozone with the hydroxide ion. Mechanistic considerations based on thermokinetic and quantum-chemical calculations. The role of HO_4^- in superoxide dismutation. Chem Eur J 16, 1372-1377.

Muñoz, F., von Sonntag, C., 2000a. Determination of fast ozone reactions in aqueous solution by competition kinetics. J Chem Soc, Perkin Trans 2, 661-664.

Muñoz, F., von Sonntag, C., 2000b. The reaction of ozone with tertiary amines including the complexing agents nitrilotriacetic acid (NTA) and ethylene-diaminetetraacetic acid (EDTA) in aqueous solution. J Chem Soc, Perkin Trans 2, 2029-2033.

Muñoz, F., Mvula, E., Braslavsky, S. E., von Sonntag, C., 2001. Singlet dioxygen formation in ozone reactions in aqueous solution. J Chem Soc, Perkin Trans 2, 1109-1116.

Mvula, E., von Sonntag, C., 2003. Ozonolysis of phenols in aqueous solution. Org Biomolec Chem 1, 1749-1756.

Mvula, E., Naumov, S., von Sonntag, C., 2009. Ozonolysis of lignin models in aqueous solution: anisole, 1,2-dimethoxybenzene, 1,4-dimethoxybenzene and 1,3,5-trimethoxybenzene. Environ Sci Technol, 43, 6275-6282.

Naumov, S., von Sonntag, C., 2010. Quantum chemical studies on the formation of ozone adducts to aromatic compounds in aqueous solution. Ozone Sci Eng 32, 61-65.

Naumov, S., von Sonntag, C., 2011. Standard Gibbs free energies of reactions of ozone with free radicals in aqueous solution- quantum chemical calculations. Environ Sci Technol 45, 9195-9204.

Neta, P., Huie, R. E., Ross, A. B., 1988. Rate constants for reactions of inorganic radicals in aqueous solution. J Phys Chem Ref Data 17, 1027-1284.

Nöthe, T., Hartmann, D., von Sonntag, J., von Sonntag, C., Fahlenkamp, H., 2007. Elimination of the musk fragrances galaxolide and tonalide from wastewater by ozonation and concomitant stripping. Wat Sci Tech 55, 287-292.

Nöthe, T., Fahlenkamp, H., von Sonntag, C., 2009. Ozonation of wastewater: Rate of ozone consumption and hydroxyl radical yield. Environ Sci Technol 43, 5990-5995.

Ogata, Y., Takagi, Y.,1958. Kinetics of the condensation of anilines with nitrosobenzenes to form azobenzenes. J Am Chem Soc 80, 3591-3595.

Perrin, D. D., Dempsey, B., Serjeant, E. P., 1981. pK_a prediction for organic acids and bases. Chapmann and Hall, London, New York.

Pierpoint, A. C., Hapemann, C. J., Torrents, A., 2001. Linear free energy study of ring-substituted aniline ozonation for developing treatment of aniline-based pesticide waters. J Agric Food Chem 49, 3827-3832.

Pierpoint, A. C., Hapeman, C. J., Torrents, A., 2003. Ozone treatment of soil contaminated with aniline and trifluralin. Chemosphere 50, 1025-1034.

Qin, L., Tripathi, G. N. R., Schüler, R. H., 1985. Radiation chemical studies of the oxidation of aniline in aqueous solution. Z Naturforsch A 40, 1026-1039.

Rabinowitch, E., Wood, W. C. 1936. The collision mechanism and the primary photochemical process in solutions. Trans Faraday Soc 32, 1381-1387.

Rabinowitch, E., 1937. Collision, co-ordination, diffusion and reaction velocity in condensed systems. Trans Faraday Soc 33, 1225-1233.

Ragnar, M., Eriksson, T., Reitberger, T., 1999a. Radical formation in ozone reactions with lignin and carbohydrate model compounds. Holzforschung 53, 292-298.

Ragnar, M., Eriksson, T., Reitberger, T., Brandt, P., 1999b. A new mechanism in the ozone reaction with lignin like structures. Holzforschung 53, 423-428.

Ramseier, M. K., von Gunten, U., 2009. Mechanism of phenol ozonation – kinetics of formation of primary and secondary reaction products. Ozone Sci Eng 31, 201-215.

Reisz, E., Schmidt, W., Schuchmann, H.-P., von Sonntag, C., 2003. Photolysis of ozone in aqueous solution in the presence of tertiary butanol. Environ Sci Technol 37, 1941-1948.

Sarasa, J., Cortés, S., Ormad, P., Garcia, R., Ovelleiro, J. L., 2002. Study of the aromatic by-products formed from ozonation of anilines in aqueous solution. Wat Res 36, 3035-3044.

Schmidt, C. K., Brauch, H.-J., 2008. *N*,*N*-Dimethylsulfamide as precursor for *N*-nitrosodimethylamine (NDMA) formation upon ozonation and its fate during drinking water treatment. Environ Sci Technol 42, 6340-6346.

Schmidt, T. C., Less, M., Haas, R., von Löw, E., Steinbach, K., Stork, G., 1998. Gas chromatographic determination of aromatic amines in water samples after solid-phase extraction and derivatization with iodine I. Derivatization. J Chromatogr A, 810, 161-172.

Schuchmann, M. N., von Sonntag, C., 1979. Hydroxyl radical-induced oxidation of 2-methyl-2-propanol in oxygenated aqueous solution. A product and pulse radiolysis study. J Phys Chem 83, 780-784.

Schwarzenbach, R. P., Escher, B. I., Fenner, K., Hofstetter, T. B., Johnson, C. A., von Gunten, U., Wehrli, B., 2006. The challenge of micropollutants in aquatic systems. Science 313, 1072-1077.

Sehested, K., Holcman, J., Hart, E. J., 1983. Rate constants and products of the reactions of e^-, O_2^- and H with ozone in aqueous solutions. J Phys Chem 87, 1951-1954.

Sehested, K., Holcman, J., Bjergbakke, E., Hart, E. J., 1984. A pulse radiolytic study of the reaction OH + O_3 in aqueous medium. J Phys Chem 88, 4144-4147.

Sein, M. M., Zedda, M., Tuerk, J., Schmidt, T. C., Golloch, A., von Sonntag, C., 2008. Oxidation of diclofenac with ozone in aqueous solution. Environ Sci Technol 42, 6656-6662.

Shang, N.-C., Yu, Y.-H., 2002. Toxicity and color formation during ozonation of mono-substituted aromatic compounds. Environ Technol, 23, 43-52.

Sims, P., 1959. In: Handbook of tables for organic compound identification. 3rd ed, CRC press, Boca Raton, United states.

Snyder, S. A., Wert, E. C., Rexing, D. J., Zegers, R. E., Drury, D. D., 2006. Ozone oxidation of endocrine disrupters and pharmaceuticals in surface water and waste-water. Ozone Sci Eng 28, 445-460.

Staehelin, J., Hoigné, J., 1985. Decomposition of ozone in water in the presence of organic solutes acting as promoters and inhibitors of radical chain reactions. Environ Sci Technol 19, 1206-1213.

Tanabe, H., 1959. Studies on the periodic acid oxidation of anilines. Chem & Pharm Bull 7, 177-183.

Tekle-Röttering, A., Jewell, K. S., Reisz, E., Lutze, H., Ternes, T. A., Schmidt, W., Schmidt, T. C., 2016. Ozonation of piperidine, piperazine and morpholine: Kinetics, stoichiometry, product formation and mechanistic considerations. Wat Res 88, 960-971.

Ternes, T. A., Meisenheimer, M., McDowell, D., Sacher, F., Brauch, H.-J., Haist-Gulde, B., Preuss, G., Wilme, U., Zulei-Seibert, N., 2002. Removal of pharmaceuticals during drinking water treatment. Environ Sci Technol 36, 3855-3863.

Ternes, T. A., Joss, A., 2006. Human pharmaceuticals, hormones and fragrances. The challenge of micropollutants in urban water management. IWA Publishing, London, New York.

Teuber, H., Jellinek, G., 1954. Reaktionen mit Nitrosodisulfonat. Oxidation von primären aromatischen Aminen. (Reactions with nitrosodisulfonate. Oxidation of primary aromatic amines.) Chem Ber 87, 1841-1848.

Turhan, K., Uzmann, S., 2007. The degradation products of aniline in the solutions with ozone and kinetic investigations. Ann Chim-Rome 97, 1129-1138.

Turhan, K., Uzmann, S., 2008. Oxidation of aniline using different reactions pathways. Asian J Chem 20, 1295-1302.

Ueno, B. K., Akiyoshi, S., 1954. Kinetic study on the condensation reaction of aniline and nitrosobenzene. J Am Chem Soc 76, 3670-3672.

Veltwisch, D., Janata, E., Asmus, K.-K., 1980. Primary processes in the reactions of •OH radicals with sulphoxides. J Chem Soc, Perkin Trans 2, 146-153.

von Gunten, U., 2003. Ozonation of drinking water. Part I. Oxidation kinetics and product formation. Wat Res 37, 1443-1467.

von Gunten, U., Salhi, E., Schmidt, C. K., Arnold, W. A., 2010. Kinetics and mechanismus of *N*-nitrosodimethylamine formation upon ozonation of *N*,*N*-dimethylsulfamide-containing waters: bromide catalysis. Environ Sci Technol 44, 5762-5768.

von Sonntag, C., 2007. The basics of oxidants in water treatment. Part A: OH radical reactions. Wat Sci Tech, 19-23.

von Sonntag, C., 2008. Advanced oxidation processes: mechanistic aspects. Wat Sci Tech 58, 19-23.

von Sonntag, C., von Gunten, U., 2012. Chemistry of ozone in water and wastewater treatment. From basic principles to applications. IWA Publishing

Yunes, R. A., Terenzani, A. J., do Amaral, L., 1975. Kinetics and mechanism of azobenzene formation. J Am Chem Soc 97, 368-373.

2.7 Supporting Information of Chapter 2

Ozonation of anilines:

Kinetics, stoichiometry, product

Identification and elucidation of pathways

Agnes Tekle-Röttering, Clemens von Sonntag, Erika Reisz,
Claudia vom Eyser, Holger V. Lutze, Jochen Türk, Sergej Naumov,
Winfried Schmidt, Torsten C. Schmidt

submitted to Water Research

32 pages of Supporting Information, including 12 narrations, 13 figures, 9 schemes and 1 table

Text S1. Theoretical background (singlet oxygen) 75

Text S2. Chemicals 75

Text S3. Sample preparation 76

Text S4. Competition kinetics 78

Text S5 Calculation of Gibbs energy and Hammett-Plots 82

Text S6. Reaction stoichiometry 84

Text S7. Quantification of *p*-hydroxyaniline and *o*-hydroxyaniline with HPLC-DAD 86

Text S8. Identification of 2-amino-5-anilino-benzochinon-1,4-anil with LC-MS 87

Text S9. Identification and quantification of nitrobenzene, nitrosobenzene and azobenzene with GC-MS and HPLC-DAD 90

Text S10. Quantification of chloride, nitrite and nitrate with IC 92

Text S11. Determination of OH radicals ($^{\bullet}$OH 97

Text S12. Determination of formaldehyde 98

Figure S1. Determination of ozone rate constants in the reaction of *p*-hydroxyaniline, *o*-hydroxyaniline and *p*-aminobenzoic acid with ozone

Figure S2. Determination of ozone rate constants in the reaction of *p*-chloroaniline and *p*-nitroaniline with ozone

Figure S3. Plot of the log(*k*) vs. calculated standard Gibbs energy for the reaction of ozone with benzene derivatives

Figure S4. Correlation plot of the log(*k*) vs. the calculated standard Gibbs energy of adduct formation in the *para* position to the amine group

Figure S5. Calibration curves for reaction stoichiometry of aniline and *p*-chloroaniline

Figure S6. HPLC-Chromatogram in the ozonation of aniline in the absence of t-BuOH

Figure S7. Peak area of the formation of 2-amino-5-anilino-benzochinon-1,4-anil in the ozonation of aniline

Figure S8. Determination of nitrobenzene, nitrosobenzene and azobenzene in the reaction of aniline with ozone

Figure S9. Time based experiments in the reaction of aniline with ozone

Figure S10. Calibration curves of chloride, nitrite and nitrate

Figure S11. Determination of chloride in the reaction of *p*-chloroaniline and chlorobenzene with ozone

Figure S12. Determination of nitrite and nitrate in the reaction of *p*-nitroaniline and nitrobenzene with ozone

Figure S13. Calibration curves of methanesulfinic and methanesulfonic acid

Scheme S1. Scavenging of $^{\bullet}OH$ with tertiary butanol

Scheme S2. Competition in the reaction of aniline and 3-buten-2-ol with ozone plus derivatization of the developed formaldehyde with DNPH

Scheme S3. Proposed fragmentation pathway from MS^2 spectra of 2-amino-5-anilino-benzochinon-1,4-anil

Scheme S4. Reaction scheme of the reaction of aminyl radicals with each other by forming 1,2-diphenylhydrazine and benzidine

Scheme S5. Proposed reaction scheme in the ozonation of *p*-chloro- and *p*-nitroaniline with the release of chloride and nitrite

Scheme S6. Determination of $^{\bullet}OH$ with dimethyl sulfoxide (DMSO)

Scheme S7. Proposed reaction scheme in the ozonation of *N,N*-dimethylaniline with release of formaldehyde

Scheme S8. Proposed reaction scheme in the ozonation of *p*-methoxyaniline with release of formaldehyde

Scheme S9. Proposed reaction scheme in the ozonation of *p*-methylaniline with release of formaldehyde

Table S1. Compilation of compound degradation at pH values of 2 and 12

Text S1. Theoretical background (singlet oxygen)

Triplet oxygen is the ground state of molecular oxygen. The electron configuration of the molecule has two unpaired electrons occupying two degenerate molecular orbitals with parallel spin. Singlet oxygen has two higher-energy species of molecular oxygen, in which the electrons are paired. Since the ground state of the ozone adduct is a singlet state, the overall spin multiplicity of the products must also be a singlet. This is required from the spin conservation rules. The excited singlet state, $O_2(^1\Delta_g)$, lies 95.5 kJ mol^{-1} above the triplet ground state, $O_2(^3\Delta_{g^-})$ (Muñoz et al., 2001, von Sonntag & von Gunten, 2012).

Text S2. Chemicals

Aniline (98%, Merck, Darmstadt, Germany), *p*-methylaniline (*p*-toluidine) (99%, Fluka, Buchs, Switzerland), *p*-chloroaniline (98%, Aldrich, Seelze, Germany), *p*-nitroaniline (99%, Fluka), *p*-methoxyaniline (*p*-anisidine) (98%, Merck), *p*-hydroxyaniline (4-amino-phenol) (99%, Merck), *o*-hydroxyaniline (2-aminophenol) (99%, Merck), *p*-phenylene-diamine (1,4-diaminobenzene) (98%, Merck) *p*-aminobenzoic acid (99%, Merck), *N*-methylaniline (98%, Merck) and *N*,*N*-dimethylaniline (99%, Merck) were commercially available of analytical grade and used as received. In addition for product quantification nitrobenzene (98%, Merck), nitrosobenzene (98%, Merck), azobenzene (96%, Merck), benzidine (4,4-diaminobiphenyl) (98%, Aldrich), 1,2-diphenylhydrazine (p.a. Aldrich) and chlorobenzene (99%, Merck) were available as reference material. Tertiary butanol (t-BuOH) (p.a., Merck) and dimethyl sulfoxide (DMSO) (99.9%, J.T. Baker, Griesheim, Germany) were applied as radical scavenger. Potassium indigo-trisulfonate (p.a. Aldrich) was required for the determination of the concentration of

dissolved ozone in water. 3-buten-2-ol (97%, Alfa Aesar, Karlsruhe, Germany) was used for competitions experiments. Acetylacetone (99%), ammonium acetate (p.a.), acetic acid (100%), 2,4-dinitrophenylhydrazine (DNPH) (p.a.) (all from Merck) and perchloric acid (70%, p.a. Aldrich) were applied for measuring formaldehyde. Methanesulfinic acid (95%, Alfa Aesar) and methanesulfonic acid (p.s., Merck) were used for quantification of OH radicals. All further required chemicals were of analytical grade. Sulfuric acid and sodium hydroxide (both from Merck) were required for pH adjustment. For chromatography acetonitrile (Fisher Scientific, Schwerte, Germany or Th. Geyer, Renningen, Germany) and ultra-pure water were used.

Text S3. Sample preparation

Glass test tubes, bottles or volumetric flasks (20 − 25 mL) closed with ground-in glass stoppers were used as reaction vessels. In order to limit losses of ozone, the flasks were kept closed during all the experimental time. The ozone solution was added (with a glass syringe, under rapid mixing) to the reaction solution containing the investigated compounds resulting in ozone to compound ratios of 1:0.1 – 1:10 at apparent pH (pH of the aqueous solutions with the investigated amines at the applied concentration) or adjusted pH (with sodium hydroxide or sulfuric acid). All samples were prepared without phosphate buffer, because the relevant buffer species scavenge $^{\bullet}OH$ (Andreozzi et al., 2000). The pH of experimental solutions was measured by a Metrohm 620 pH meter with a glass electrode (Metrohm, Filderstadt, Germany), calibrated every time before use.

Tertiary butanol (k (t-BuOH + O_3) = 0.003 M^{-1} s^{-1}) reacts with ozone at negligible rates even if present at reasonable excess (Flyunt et al., 2003). Taking into account the concentration of tertiary butanol (at most 0.1 M) and amines (at least 1×10^{-4} M and k(nitroaniline + O_3) = 1.2×10^5 M^{-1} s^{-1}, lowest k in this study) in their reaction with ozone (k_{app}(t-BuOH + O_3) = 3×10^{-4} s^{-1} and k_{app}(nitroaniline + O_3) = 12 s^{-1}), the latter is still favored.

Scheme S1. Scavenging of $^{\bullet}OH$ with tertiary butanol

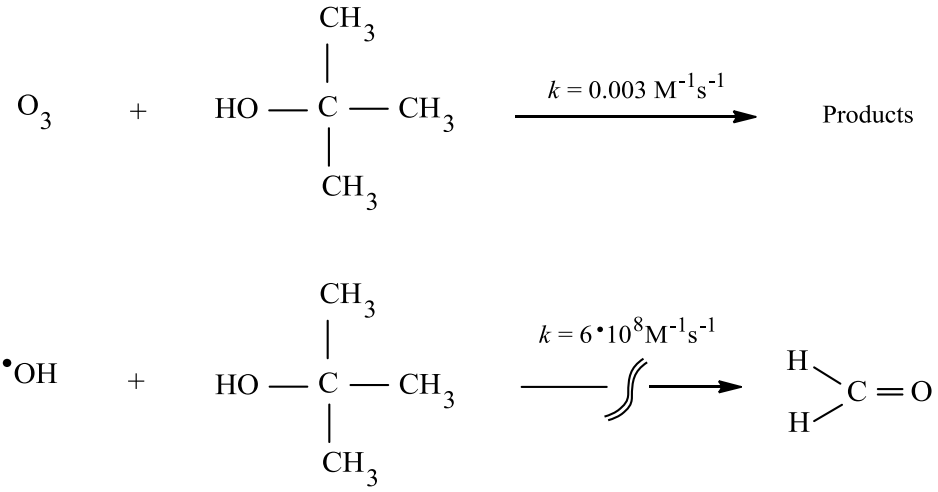

Dissociation of hydroxyl radicals into the oxygen anion radical ($O^{\bullet-}$) occurs through the equilibrium $^{\bullet}OH \rightleftharpoons O^{\bullet-} + H^+$ (Buxton et al., 1988). However, due to the high pK_a–value of $^{\bullet}OH$ (pK_a ($^{\bullet}OH$) = 11.8, Merényi et al., 2010) the radicals are converted to oxygen anion radical ($O^{\bullet-}$) only at high pH. Especially, in its reaction with free radicals, ozone has to compete with oxygen, as well known free radical scavenger. Yet, oxygen reacts only with few radical types (e.g. C-centered radicals) rapidly and irreversibly (von Sonntag & Schuchmann, 1997). Thus, ozone reacts with many free radicals effectively, despite the fact that oxygen is typically present in large excess over ozone (von Sonntag & von Gunten, 2012). In addition, water does not react with ozone (k ($H_2O + O_3$) < 10^{-7} M^{-1} s^{-1}, Neta et al., 1988), but its conjugate base, ^{-}OH does, (k ($^{-}OH + O_3$) = 48 M^{-1} s^{-1}, Forni et al., 1982 or 70 M^{-1} s^{-1}, Staehelin & Hoigné, 1982), albeit slowly and gives rise to $^{\bullet}OH$ (Staehelin & Hoigné, 1982, Merényi et al., 2010). This could be relevant at pH 12. Hence, based on the possible importance of radical reactions in ozonation, pH is possibly a main variable (Gilbert & Zinecker, 1980, Staehelin & Hoigné, 1985, Beltrán et al., 1998, von Sonntag & von Gunten, 2012). However, in this case decomposition of ozone at pH 12 is irrelevant due to the high rate constants of the amines with ozone (see Table S1). Taking into account the concentration of the hydroxide ion (e.g. 10^{-2} M at adjusted pH of 12 with NaOH) in its reaction with ozone (k_{app}($^{-}OH + O_3$) = 0.48 s^{-1} or 0.70 s^{-1}) this reaction can be neglected since the reaction of ozone with the amines (at least 1 × 10^{-4} M and k(nitroaniline + O_3) = 1.2 × 10^5 M^{-1} s^{-1}, lowest k in this study) that occurs in competition is sufficiently faster (k_{app}(nitroaniline + O_3) ≥ 12 s^{-1}) under all

investigated conditions and therefore still favored. Thus, $^{\bullet}OH$ formation from this reaction does not take place.

Text S4. Competition kinetics

Free amines react very fast with ozone so that the rate of reaction under pseudo-first-order conditions (amine in excess) is too fast to follow the reaction spectrophotometrically (Muñoz & von Sonntag, 2000b). Protonation of amines reduces the ozone reactivity, which therefore depends on pH (von Sonntag & von Gunten, 2012). Thus, it is common practice for the determination of the ozone rate constant of aliphatic amines to follow the ozone decay at 260 nm at low pH and extrapolate to high pH. Anilines however absorb strongly in the UV-spectrum, and the kinetics can no longer be followed under conditions of pseudo-first-order kinetics at low pH. Thus, a competition with 3-buten-2-ol (k = 7.9 × 10^4 M^{-1} s^{-1}, Muñoz & von Sonntag, 2000a, Dowideit & von Sonntag, 1998) was carried out. In the literature the rate constant of aniline with ozone was estimated from 10^7 up to 10^8 M^{-1} s^{-1} (k = 1.4 × 10^7 M^{-1} s^{-1}, Pierpoint et al., 2001, k = 9 × 10^7 M^{-1} s^{-1}, Hoigné & Bader, 1983a). However, a competition with 3-buten-2-ol at low pH by determining the resulting formaldehyde (see below) with the Hantzsch method (Nash, 1953) does not yield reliable values, even if this value with k around 10^7 is reported in von Sonntag & von Gunten, 2012. One reason is that there were interferences in the Hantzsch method with the colored products from the ozonation of aniline, which cannot ignored. Thus, formaldehyde as product from the competition reaction of ozone with 3-buten-2-ol was determined as their 2,4-dinitrophenyl-hydrazones by HPLC-DAD after derivatization with 2,4-dinitrophenylhydrazine (DNPH) (Lipari & Swarin, 1982, Olson & Swarin, 1985) in neutral pH range according to Scheme S2.

Due to the moderate pK_a values of the investigated amines (see paper Table 1) the degree of protonation is low at pH values in neutral range. Thus, under these conditions 98 up to 100% of the investigated anilines are present as deprotonated amines at the appropriate pH of 6 – 7 by the applied concentration (except phenylene-diamine with 86%). Besides, for setting up adequate conditions for the competition with 3-buten-2-ol experiments were carried out with different amine-competitor ratios.

Scheme S2. Competition in the reaction of aniline and 3-buten-2-ol with ozone plus derivatization of the developed formaldehyde with DNPH

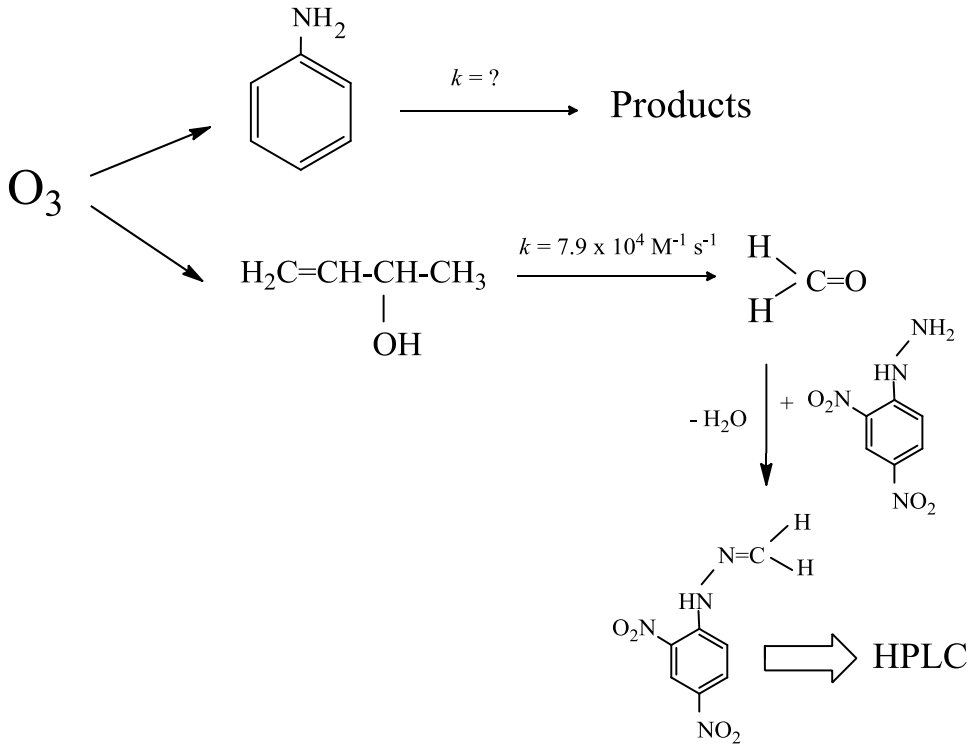

Competition experiments require the measurement of only a single endpoint P, which is typically the degradation of a reactant or the formation of a product resulting from oxidation of either the compound (M) or the competitor (C). The evaluation of the reaction rate constants were conducted using equation 1 (Muñoz & von Sonntag, 2000a, Dodd et al., 2006, Zimmermann et al., 2012),

$$\frac{[\mathrm{P}]_0}{[\mathrm{P}]} = 1 + \frac{k_{\mathrm{O_3,M}}\ [\mathrm{M}]_0}{k_{\mathrm{O_3,C}}\ \ [\mathrm{C}]_0} \qquad (1)$$

where $[P]_0$ represents the measured endpoint yield in the absence of competitor obtained from controls and [P] represents the endpoint yield in the presence of varying doses of competitor.

The rate constant of the investigated compounds was determined from the slopes of plots of equation 2.

$$\frac{[P]_0}{[P]} - 1 = f\left(\frac{[M]_0}{[C]_0}\right) \qquad (2)$$

The experiments were carried out in a series of volumetric flasks (20 mL) each containing 1 mL solution of 3-buten-2-ol (10^{-2} – 10^{-3} M) as competitor and different volumes (0–8 mL) of compound solution (10^{-2} – 10^{-3} M) to obtain various ratios of $[M]:[C]_0$ (both in at least 10-fold molar excess of ozone). After adding appropriate volumes of pure water to complete the solution volume to 9 mL, a fixed dosage of 1 mL ozone solution was added with a glass syringe under rapid mixing. All experiments were performed at apparent pH values (see Text S3). After complete ozone consumption the developed formaldehyde (according to Scheme S2) was measured by withdrawn 1.5 mL sample from the batch and transferred into HPLC-vials. After that 0.2 mL 2,4-dinitrophenylhydrazine solution (30 mg/ 25 mL acetonitrile) and 0.1 mL $HClO_4$ (0.1 M) were added. After a reaction time of 45 minutes (in the dark) the formed 2,4-dinitrophenylhydrazone was measured by HPLC (LC20, Shimadzu, Duisburg, Germany) and DAD at a wavelength of 353 nm. The separation occurs on a C_{18} column (Prontosil, NC-04, 250 mm x 4.0 mm I.D., 5.0 µm, Bischoff, Leonberg, Germany) with the following gradient: water/acetonitrile (ACN): 35% ACN/ 2 min, 45% ACN/ 5 min, 100% ACN. The elution flow rate was 0.5 mL min^{-1} and the injection volume was 50 µL for all samples. In all cases blanks were processed in the same manner with water instead of ozone solution to determine the initial concentration. Taking this into account ozone rate constants were calculated from the slope by plotting the resulted formaldehyde yield against the amine-competitor ratio according to equation 2 (see Figure 1 and Figure S1 and S2).

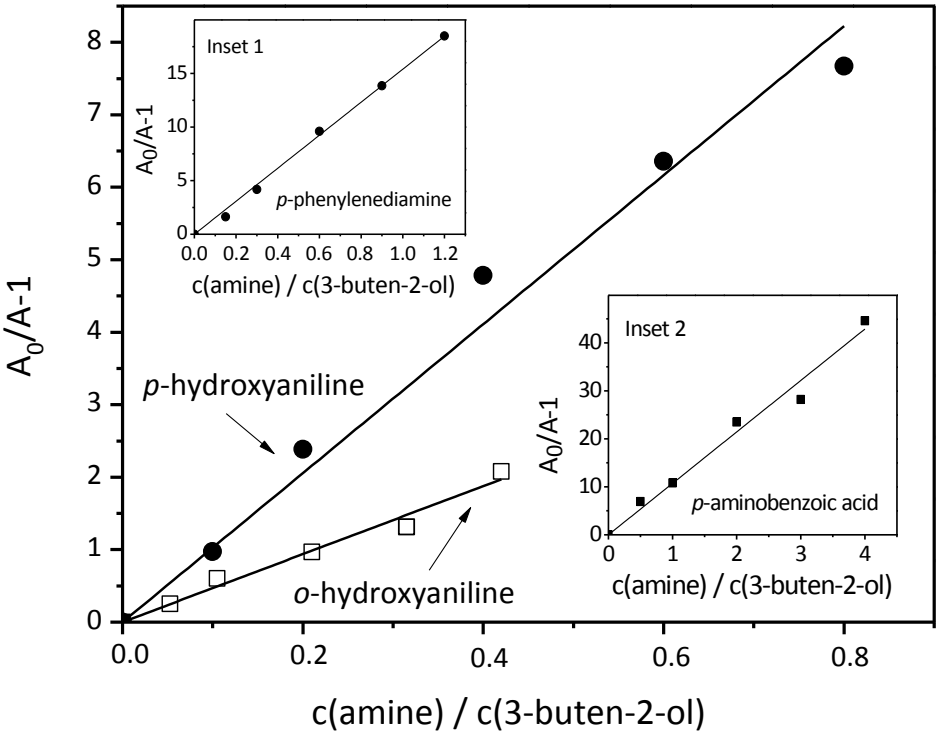

Figure S1. Determination of ozone rate constants in the reaction of investigated aromatic amines c_0(1×10^{-3} M – 8×10^{-3} M) with 3-buten-2-ol (1×10^{-3} M – 1×10^{-2} M) as competitor. The resulted formaldehyde yield from the competition with 3-buten-2-ol was determined with DNPH at apparent pH and plotted against the amine-competitor ratio. Main graph: *p*-hydroxyaniline, *o*-hydroxyaniline. Inset 1-2: *p*-phenylenediamine, *p*-aminobenzoic acid.

With p$K_{a(amine)}$ values of 4.84 and 5.14 for the two aminophenols, *o*-hydroxaniline and *p*-hydroxyaniline, respectively, the ozone reaction at the amino group observed at pH 7 is not much hindered through protonation. Phenol (pK_a = 9.9) reacts moderately rapid with ozone (k = 1300 M^{-1} s^{-1}, Hoigné & Bader, 1983b) but the reaction of its anion (k = 1.4×10^9 M^{-1} s^{-1}, Hoigné & Bader, 1983b) is close to diffusion controlled (Mvula & von Sonntag, 2003, Ramsmeier & von Gunten, 2009). With p$K_{a(phenol\ moiety)}$ values of 9.71 for *o*-hydroxyaniline and 10.3 for *p*-hydroxyaniline the rate of reaction observed at pH 7 is hence determined by the fraction of the phenolate anion.

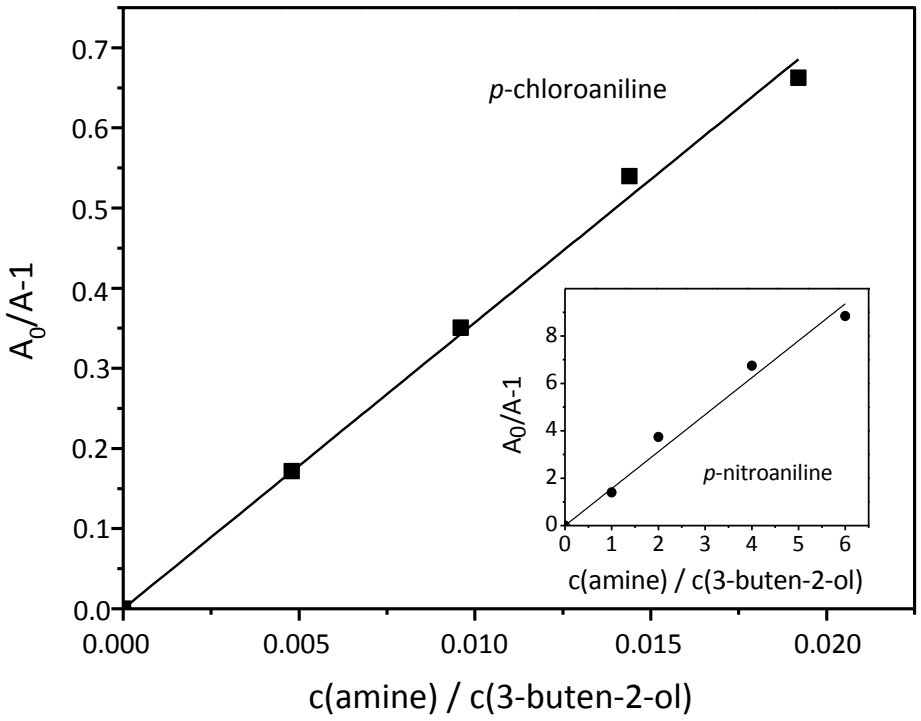

Figure S2. Determination of ozone rate constants in the reaction of investigated aromatic amines $c_0(1 \times 10^{-3}\,M - 8 \times 10^{-3}\,M)$ with 3-buten-2-ol $(1 \times 10^{-3}\,M - 1 \times 10^{-2}\,M)$ as competitor. The resulted formaldehyde yield from the competition with 3-buten-2-ol was determined with DNPH at apparent pH and plotted against the amine-competitor ratio. Main graph: *p*-chloroaniline. Inset: *p*-nitroaniline.

Text S5. Calculation of Gibbs energy and Hammett-plots

By means of quantum chemical method, the energetics various reactions was studied using Density Functional Theory (DFT) B3LYP method (Becke, 1996, Lee et al., 1988) as implemented in Jaguar 8.3 program (Jaguar, 2014). The structures were optimized in water at B3LYP/6-311+G(d,p) level of theory, which was successfully used in our previous works (Naumov & von Sonntag, 2010, 2011, Naumov et al., 2010). To take solvent effect (water in this case) on the structure and reaction parameters of studied molecules into account the calculation were done using Jaguar's dielectric continuum Poisson-Boltzmann solver (PBF) (Tannor et al., 1994), which fits the field produced by the solvent dielectric continuum to another set of point charges. The frequency analysis

was made at the same level of theory to characterize the stationary points on the potential surface and to obtain thermodynamic parameters such as total enthalpy (H) and Gibbs energy (G) at 298 K. The reaction enthalpies (ΔH) and Gibbs energies of reaction (ΔG) were calculated as the difference of the calculated total enthalpies H and Gibbs energies (G) between the reactants and products respectively.

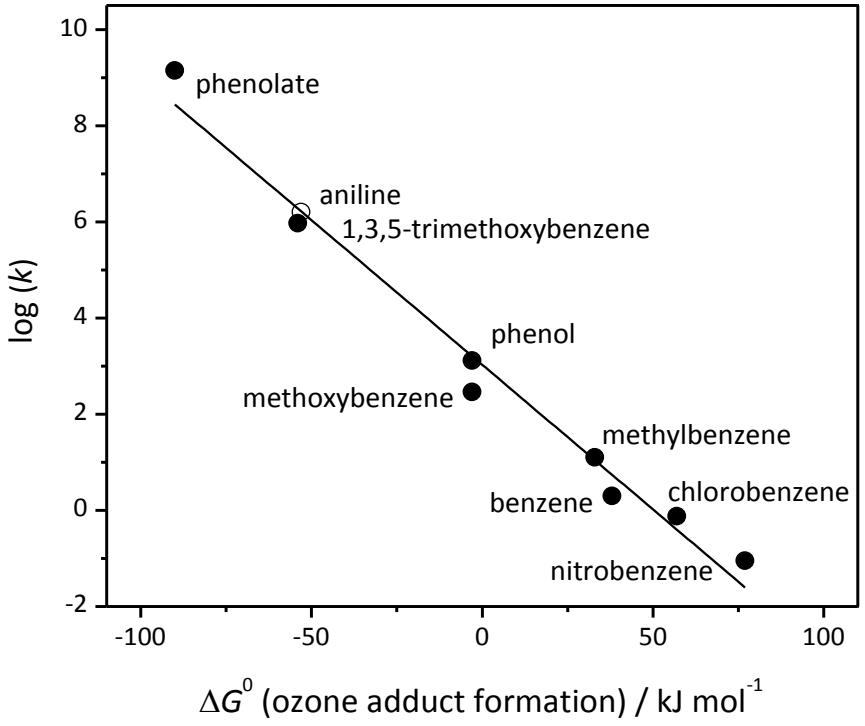

Figure S3. Plot of the log(*k*) vs. calculated standard Gibbs energy of adduct formation at the *para* position to the substituent for the reaction of ozone with benzene derivatives. Adapted from Naumov & von Sonntag, 2010 and taken from von Sonntag & von Gunten, 2012. The aniline rate constant (○) was corrected.

Hammett-plots are based on van`t Hoff equation at equilibrium ($\Delta G^0 = - R T \times \ln K$) and thus on the linear dependence between standard Gibbs energy and the logarithm of the rate constant (von Sonntag & von Gunten, 2012). Figure S3 and Figure S4 show this dependence for the formation of ozone adducts of benzene and its derivatives and of anilines, respectively. The log used in all figures is related to the base 10 (common logarithm).

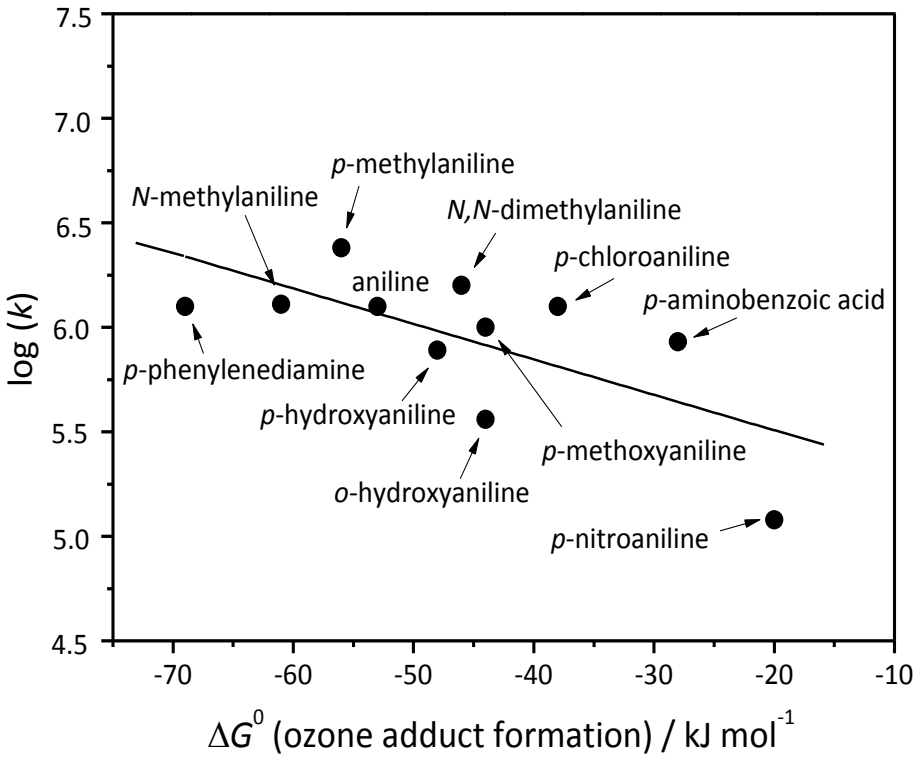

Figure S4. Correlation plot of the logarithm of the rate constants vs. the calculated standard Gibbs energy of adduct formation in the ozone reaction of the *para* substituted amines.

Text S6. Reaction stoichiometry

For measuring the stoichiometry of the reaction lower compound concentrations have to be used, because consumption yields can only be measured at a reasonable transformation of the substrate, otherwise the deviation from the untreated sample is too small (Mvula & von Sonntag, 2003). Hence for these experiments a substrate concentration around 10^{-4} M was used, resulting in ozone to compound molar concentration ratios of 1:0.3 – 1:3. To terminate free radical mechanisms, like $^{\bullet}$OH radical reactions, all samples were prepared in parallel as described above, however, with containing tertiary butanol (0.05 – 0.1 M) as a radical scavenger (see Text S3).

The experiments were carried out in a series of volumetric flasks (20 mL) each containing 1 mL of the investigated compound solution, with scavenger (1 mL) and without scavenger and different volumes (0–8 mL) of ozone solution to obtain various ozone concentrations. Appropriate volumes of pure water were added to complete the solution volume to 10 mL. All experiments were realized at apparent pH of the selected amines by the applied concentration (pH 6 – 7) and in addition at pH values of 2 (acidized with H_2SO_4) and 12 (alkalinized with NaOH). The apparent pH of the initial solution decreased gradually more or less one pH unit and dropped to pH 5 – 6 as the ozone was consumed as a function of the molar ratio of ozone to compound.

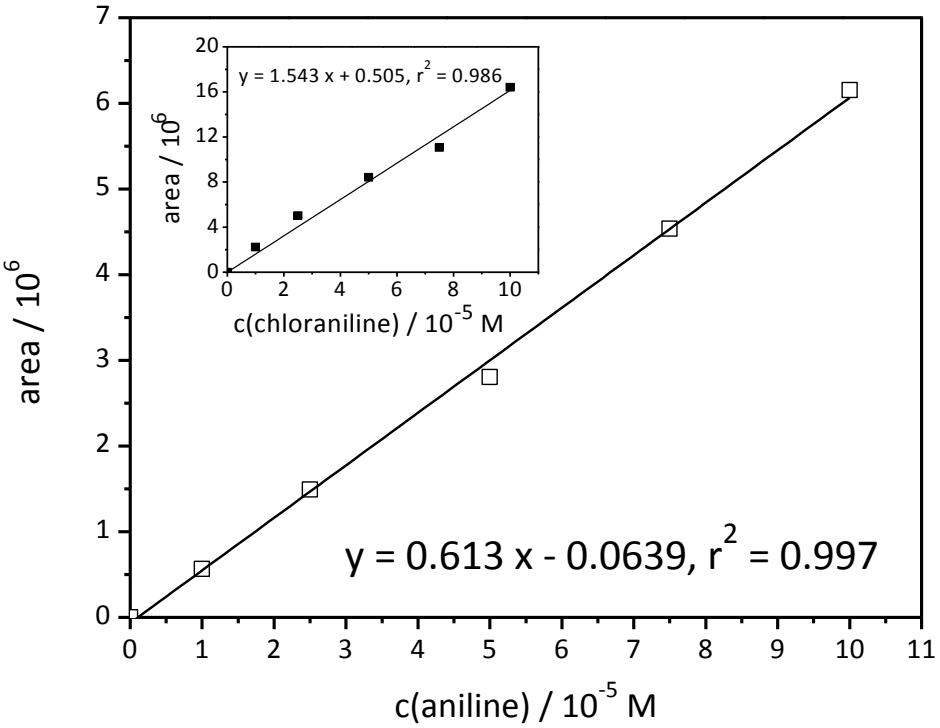

Figure S5. Calibration curves for reaction stoichiometry experiments of aniline (main graph) and *p*-chloroaniline (inset). Areas are plotted vs. amine concentrations.

After complete ozone consumption the quantification was realized in the batch sample through compound-degradation using a HPLC – DAD system, equipped with a C_{18} column (Prontosil, as described above, Text S4). The compounds were eluted with a water/acetonitrile gradient system (35% ACN/ 5 min, 45% ACN/ 10 min, 100% ACN) and verified by retention time and the appropriate UV-spectra. The quantification was

carried out at wavelengths of 200 nm. In these HPLC analytics the elution flow rate was 1.0 mL min^{-1} and the injection volume was 50 µL in all samples. Blanks were processed in the same manner with water instead of ozone solution to determine the initial concentration. Calibration experiments (cf. Figure S5) were performed in the same manner with the investigated compounds as reference material.

Table S1. Compilation of compound degradation (in % of mole ozone consumed) in the reaction of ozone with anilines. The compound degradation is presented at pH values of 2 and 12 in the absence of tertiary butanol (pooled data of various experiments, standard deviation in parenthesis).

Compounds	**Compound degradation / %** (per ozone consumed)	
	pH 2	pH 12
Aniline	21 (± 2)	13 (± 2)
***p*-Methylaniline**	32 (± 4)	20 (± 2)
***p*-Chloroaniline**	28 (± 2)	10 (± 1)
***p*-Nitroaniline**	20 (± 2)	24 (± 1)

Text S7. Quantification of *p*-hydroxyaniline and *o*-hydroxyaniline with HPLC-DAD

The quantification of the hydroxylated products was performed with HPLC-DAD (see Experimental part and stoichiometry experiments) with the use of reference material, verified by retention time and UV-spectra (cf. Figure S6). In these HPLC analytics the elution flow rate was 0.8 mL min^{-1} and the injection volume was 50 µL in all samples. It has to be noted, that due to the normal autooxidation of the hydroxyanilines HPLC measurements of calibrations and aniline-ozone-experiments were made directly after preparation respectively after addition of ozone.

By reason of a potential competition of the generated hydroxy products in its reaction with ozone against aniline with ozone ($k(O_3 + \text{aniline}) = 1.3 \times 10^6\ M^{-1}\ s^{-1}$) , the rate constants of *o*-hydroxyaniline ($k(O_3 + o\text{-hydroxyaniline}) = 3.7 \times 10^5\ M^{-1}\ s^{-1}$) and

p-hydroxyaniline $k(O_3$ + *p*-hydroxyaniline) = 7.8 × 10^5 M^{-1} s^{-1}) are determined (see Chapter rate constants). Thus, in the product formation experiments aniline was in constant high concentration (at least 10^{-3} M) to avoid ozone reaction with the hydroxyanilines. Taken into account the concentration of *p*-hydroxyaniline (at most near 4 × 10^{-5} M, highest rate constant and highest concentration from both hydroxyanilines) in the reaction with ozone (k_{app} (O_3 + *p*-hydroxyaniline) = 31 s^{-1}), the reaction of aniline with ozone (k_{app} (O_3 + aniline) = 1300 s^{-1}) is still favored.

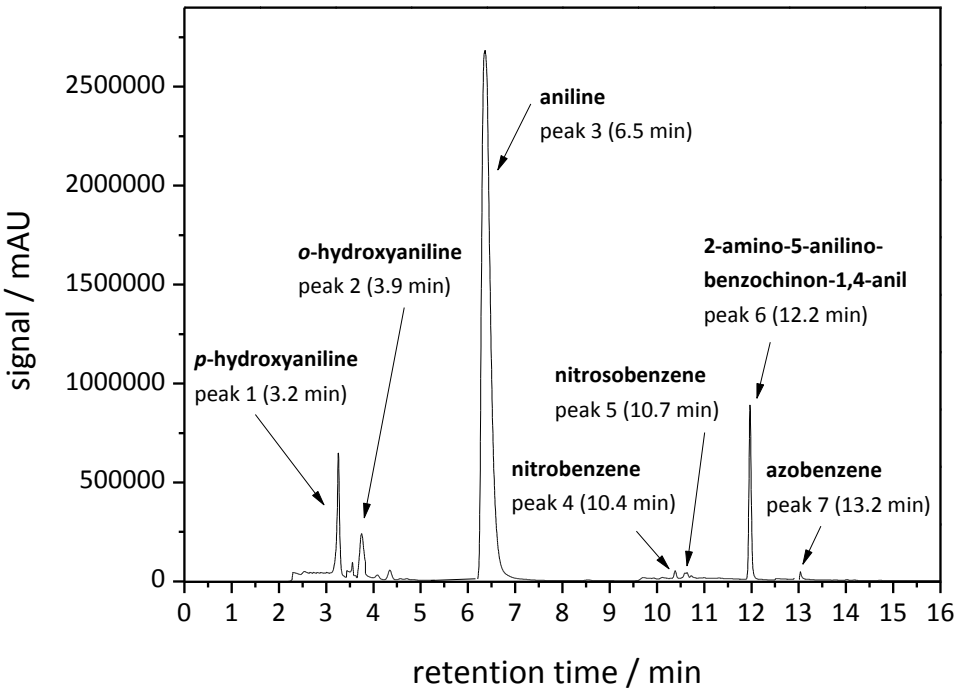

Figure S6. HPLC-Chromatogram in the ozonation of aniline and in the absence of t-BuOH

Text S8. Identification of 2-amino-5-anilino-benzochinon-1,4-anil with LC-MS

Further product identification was performed through molecular mass. The molecular weights and hence sum formula were determined by LC-MS (Linear triple quadrupole ion trap mass spectrometer (3200 QTrap, SciEx, Darmstadt, Germany, LC 20 AD, Shimadzu, Duisburg, Germany)) with performing scans in positive and negative mode.

Scheme S3. Proposed fragmentation pathway from MS^2 spectra of 2-amino-5-anilino-benzochinon-1,4-anil

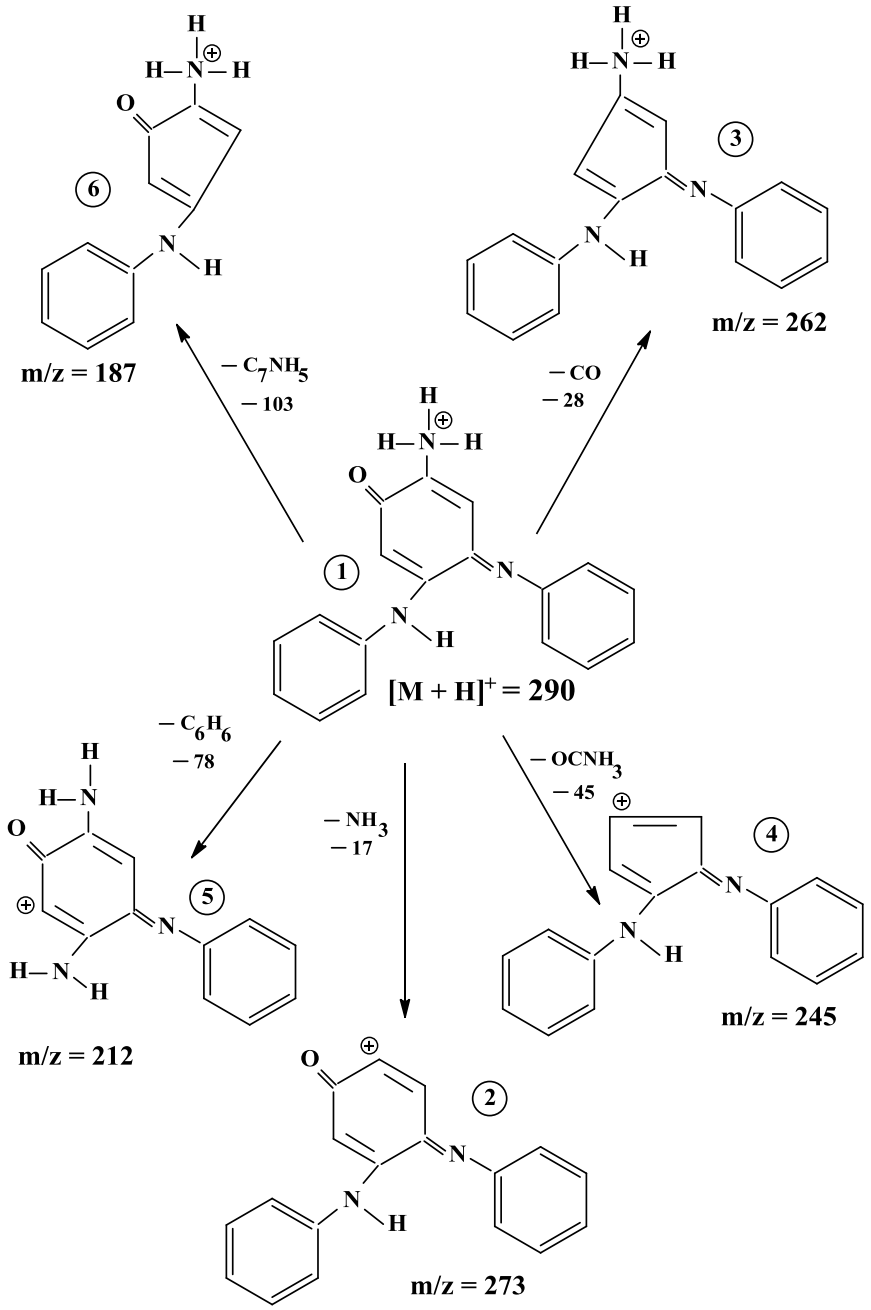

Structural elucidation (Scheme S3) of the oxidation products was based on their MS^2 fragmentation pathways obtained from product ion. The MS-System was equipped with an electrospray ionization source (ESI). The excitation energy was optimized for each experiment and varied between 20−100 V, with a collision energy spread of 5 V. In the LC-System the sample compounds were separated on a C_{18} column (Synergi Polar-RP 80 A, 150 mm x 2.0 mm I.D., 4.0 µm, Phenomenex, Aschaffenburg, Germany) at

25°C. As eluents ultra-pure water and acetonitrile were used in gradient system (35% ACN/ 2 min, 45% ACN/ 5 min, 100% ACN). In these HPLC analytics the elution flow rate was 1.0 mL min^{-1} and the injection volume was 50 µL in all samples.

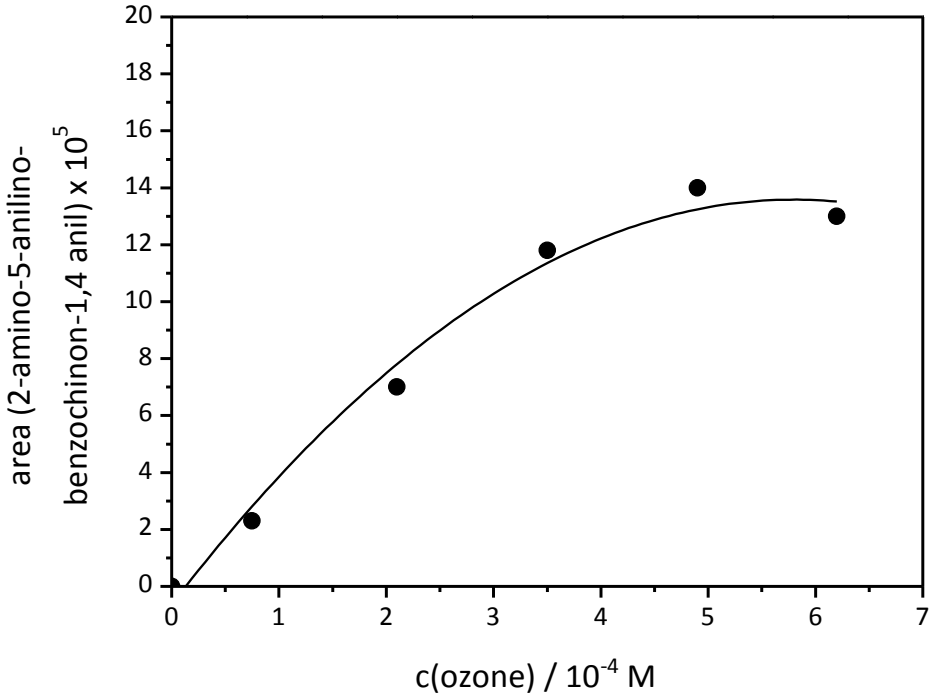

Figure S7. Plot of peak area of the formation of 2-amino-5-anilino-benzochinon-1,4-anil in the ozonation of aniline c_0(1 × 10^{-3} M) as a function of ozone concentration (without scavenger).

Scheme S4. Reaction scheme of the reaction of aminyl radicals with each other by forming 1,2-diphenylhydrazine and benzidine

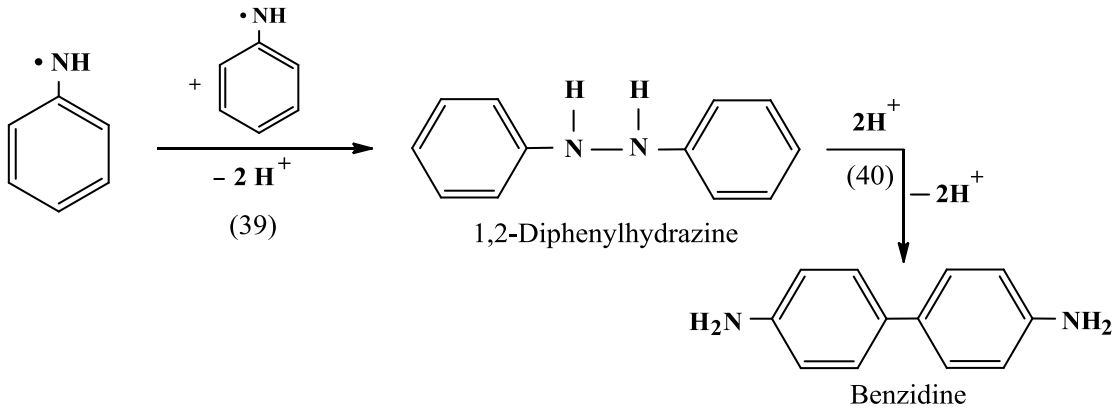

Text S9. Identification and quantification of nitrobenzene, nitrosobenzene and azobenzene with GC-MS and HPLC-DAD

The identification of nitrobenzene, nitrosobenzene and azobenzene was carried out with GC-MS using a Thermo Trace GC Ultra coupled to a Thermo DSQ II single quadrupole mass spectrometer (Thermo Fisher, Waltham, USA). Helium was used as carrier gas with a constant flow of 1.5 mL min^{-1}. The split/splitless injector was used in splitless mode (1 minute splitless time) with constant septum purge. Separation of compounds was performed on a fused-silica capillary column (DB-5) with 20 m length, 0.18 mm I.D. and 0.4 µm film thickness (Restek GmbH, Bad Homburg, Germany). Initial GC oven temperature was 40 °C for 2 min, than heated with 10 °C min^{-1} to 250 °C with a hold time of 5 min. The MS transfer line and ion source temperatures were set to 250 °C. Electron ionization mode (EI) with an ionization energy of 70 eV was used in scan mode (*m*/*z* = 20-200) with a scan rate of 500 amu s^{-1}. Automatic tuning of the instrument was carried out regularly. The extraction of the compounds was performed with solid phase micro extraction (SPME), utilized a fused silica fiber core, coated with a film of a polydimethysiloxane (PDMS) sorptive phase (Supleco, Aldrich). Quantification was made with HPLC-DAD (see above), equipped with a C_{18} column (Prontosil, as described above). The compounds were eluted with a water/acetonitrile gradient system (35% ACN/ 5 min, 45% ACN/ 10 min, 100% ACN) and verified by retention time and the appropiate UV-spectra with the use of reference material. The quantification was carried out at wavelengths of 280 – 312 nm. In this HPLC analytics the elution flow rate was 0.8 mL min^{-1} and the injection volume was 50 µL in all samples.

The several minor products in aniline-ozone reactions identified as nitrobenzene, nitrosobenzene and azobenzene with GC-MS measurements (see above) were quantified by HPLC-DAD in experiments without using an $^{\bullet}OH$ scavenger. In these experiments the product yields increased linearly with the ozone dose and from the slope of the resulting graph (Figure S8) one calculates a low nitrobenzene yield of 0.42% (determined at 280 nm). In the case of nitrosobenzene (280 nm) a somewhat higher yield of 1.9% could be quantified, however, for azobenzene (312nm) a much lower yield of 0.085% was calculated.

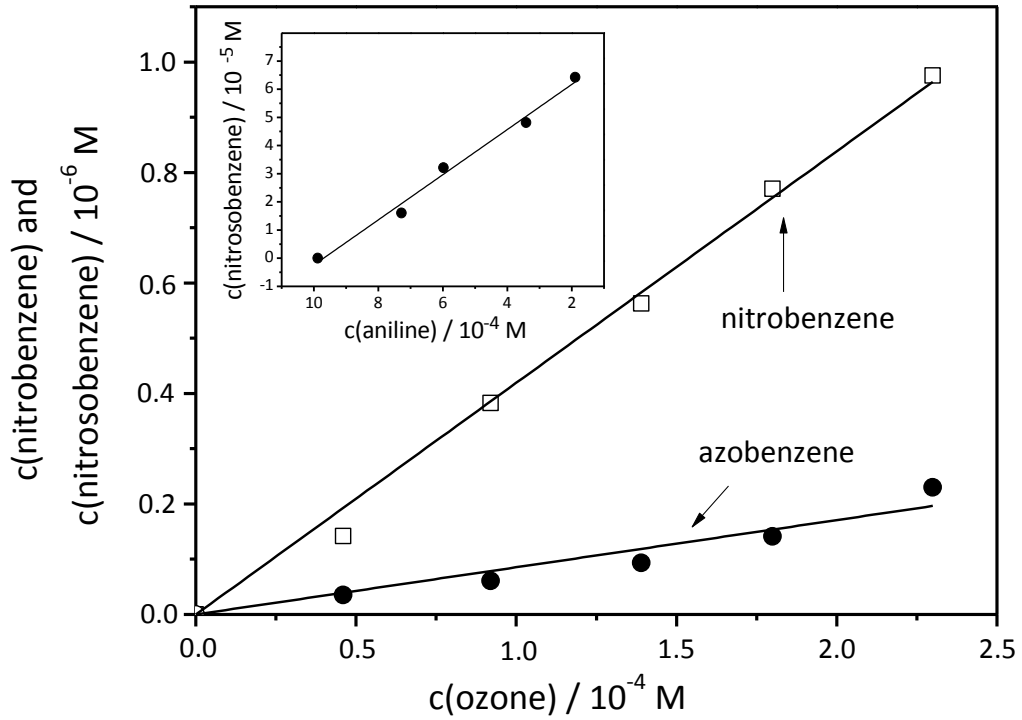

Figure S8. Yield determination of nitrobenzene, nitrosobenzene and azobenzene in the reaction of aniline $c_0(1 \times 10^{-3}$ M) with ozone. Main graph: nitrobenzene and azobenzene concentrations vs. the ozone concentration. Inset: nitrosobenzene concentrations vs. aniline transformation

With aniline in excess (at least 10^{-3} M), above mentioned minor products do not take part in further reactions with ozone, because compared to aniline, their ozone rate constants are low (nitrobenzene, k = 0.09 M^{-1} s^{-1}, Hoigné & Bader, 1983a, azobenzene, k = 220 M^{-1} s^{-1}, Yao & Haag, 1991). The ozone rate constant of nitrosobenzene is supposed to be between the rate constant of benzene (k = 2 M^{-1} s^{-1}, Hoigné & Bader, 1983a) and nitrobenzene. This assumption is based on the linear correlation of substituted benzenes with the σ_p^+ values of the substituents according to Hoigné (Hoigné & Bader, 1983a) and the Hammett-type plot for ozone reactions with benzene and its derivates corresponding to Naumov & von Sonntag, 2010.

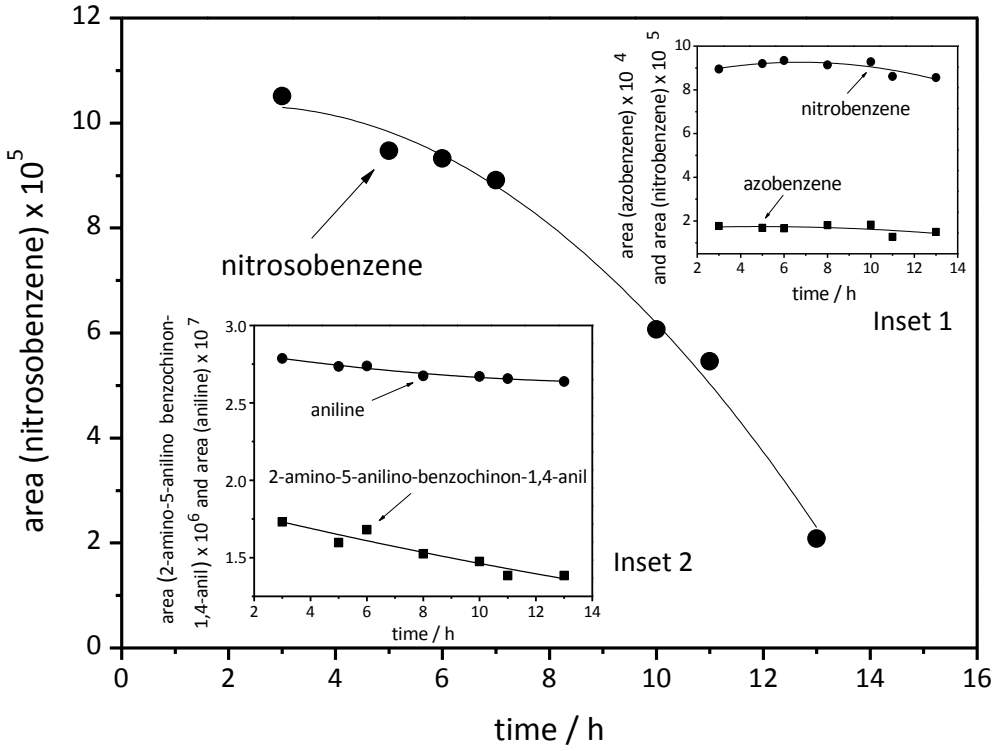

Figure S9. Time based experiments in the reaction of aniline $c_0(1 \times 10^{-3}$ M) with ozone $c_0(8 \times 10^{-4}$ M). Main graph: area of nitrosobenzene vs. time. Inset 1: area of nitrobenzene and azobenzene vs. time. Inset 2: aniline and 2-amino-5-anilino-benzochinon-1,4-anil area vs. time.

It has to be noted, that due to the nitrosobenzene-aniline reaction (generating azobenzene, see paper Scheme 5) nitrosobenzene concentration may be not constant. For this reason time based measurements were made (Figure S9) in which it is seen, that nitrobenzene and azobenzene concentrations as well aniline concentration (due to the high concentration in comparison to products) are mostly constant over time, however nitrosobenzene and 2-amino-5-anilino-benzochinon-anil (see above) are not. Thus, quantification measurements with HPLC-DAD were made directly after preparation respectively after addition of ozone.

Text S10. Quantification of chloride, nitrite and nitrate with IC

The quantification of chloride, nitrite and nitrate were carried out by ion chromatography, equipped with a conductivity detector and ion suppression. The

separation occurs on an anion exchange column with quaternary ammonium groups (Metrosep A Supp 4, 250/4.0 mm). The following eluent: Na_2CO_3: 1.8×10^{-4} M, $NaHCO_3$: 1.7×10^{-4} M was used at a flow rate of 1 mL min^{-1} and the injection volume was 2 mL. The products were verified by retention time with the use of chloride, nitrite and nitrate calibrations, which was performed in the same manner (see Figure S10).

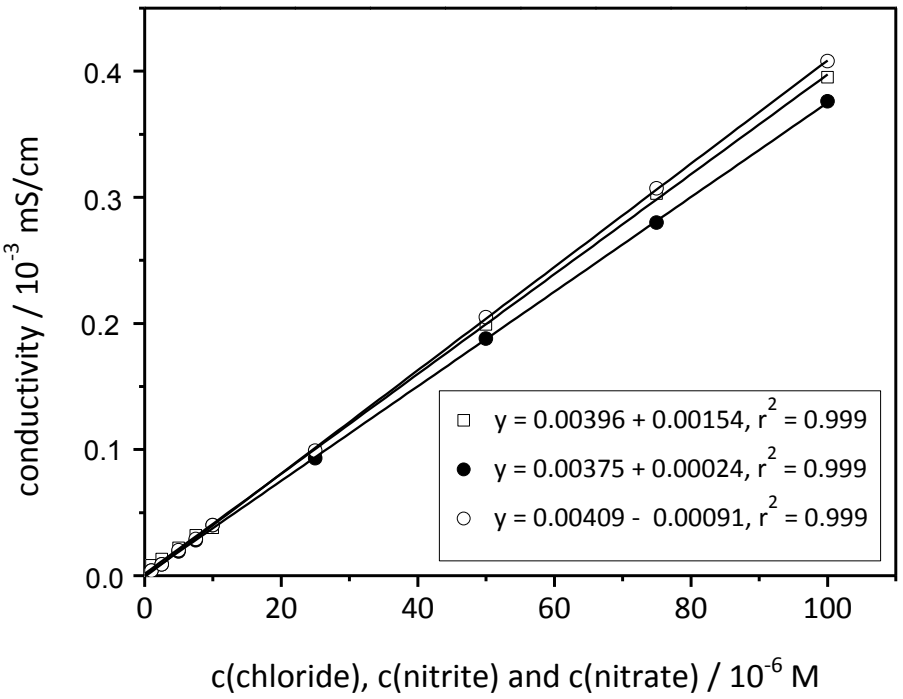

Figure S10. Calibration curves of chloride (□), nitrite (○) and nitrate (●). Conductivity is plotted vs. concentrations.

Stoichiometry experiments showed that the reaction of *p*-chloroaniline and *p*-nitroaniline with ozone led to one main oxidation product and several minor products at lower and higher ozone doses detectable by HPLC-DAD at 200 nm. In the presence of tertiary butanol as radical scavenger also one main product with identical retention time at various ozone doses was detected. Experiments used for the determination of chloride, nitrite and nitrate were conducted at the appropriate pH (~ 7) and in the absence of tertiary butanol (see Experimental part and Supporting Information Text S3).

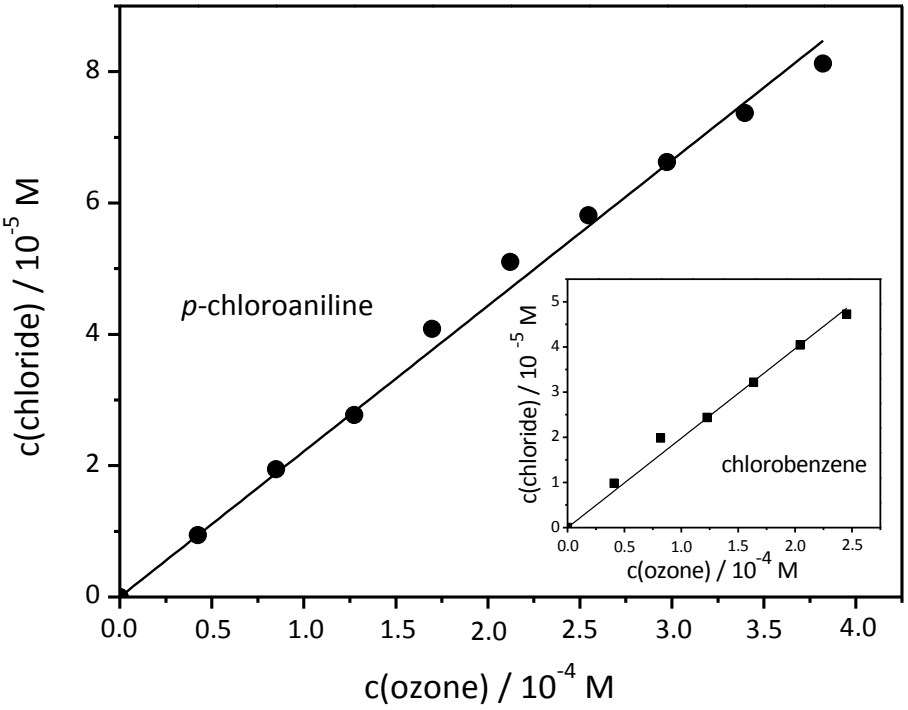

Figure S11. Plot of the determination of chloride in the reaction of *p*-chloroaniline (main graph) and chlorobenzene (inset) with ozone as a function of ozone concentration.

The chloride yield in the case of *p*-chloroaniline (Figure S11, for chlorobenzene in the inset, see above) increased linearly with the ozone dose and from the slope of the resulting graph one calculates a high chloride yield of 21%. A calculation of the chloride yield as a function of the *p*-chloroaniline transformation leads to a product yield of 95%. With *p*-chloroaniline in excess (at least 10^{-3} M), chloride reactions with ozone can be neglected, since its ozone rate constant is low ($k(O_3 + \text{chloride}) < 3 \times 10^{-3}$ M^{-1} s^{-1}, Hoigné et al., 1985).

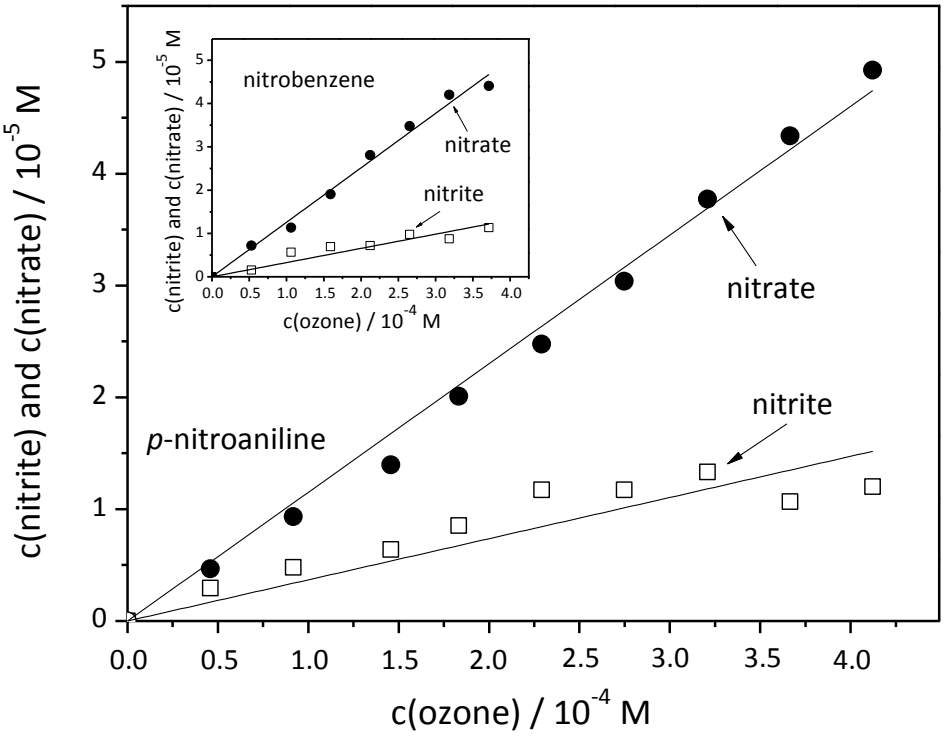

Figure S12. Plot of the determination of nitrite and nitrate in the reaction of *p*-nitroaniline (main graph) and nitrobenzene (inset) with ozone as a function of ozone concentration

In the case of *p*-nitroaniline a low nitrite yield of 3.7% and somewhat higher nitrate yield of 12% (certainly from further oxidation of nitrite with ozone, see below) were quantified (Figure S12, for nitrobenzene in the inset, see above). Taken into account the rate constants of nitrite and nitrate, with *p*-nitroaniline in excess (at least 10^{-3} M), nitrate does not take part in further reactions with ozone, since its ozone rate constant is keenly low ($k(O_3 + \text{nitrate}) < 10^{-4}$ M^{-1} s^{-1}, Hoigné et al., 1985). Nitrite, however, reacts rapidly with ozone ($k(O_3 + \text{nitrite}) = 5.83 \times 10^5$ M^{-1} s^{-1}, Liu et al., 2001 or 1.8×10^5 M^{-1} s^{-1}, Hoigné et al., 1985) resulting to nitrate as main product.

In an initial step the generated ozone adduct separates (see Scheme S5, reaction (55) – (57) or (58) – (60)) and subsequently releases chloride or nitrite with a feasible formation of C-centered chinonimine cations. The released oxygen must be in its singlet

state (Scheme S5, reaction (56) and (59)). The C-centered chinonimine cations in turn can further react with H_2O.

Scheme S5. Proposed reaction scheme of the reaction of ozone at the electron-rich aromatic ring of *p*-chloroaniline and *p*-nitroaniline with the release of chloride, nitrite and nitrate

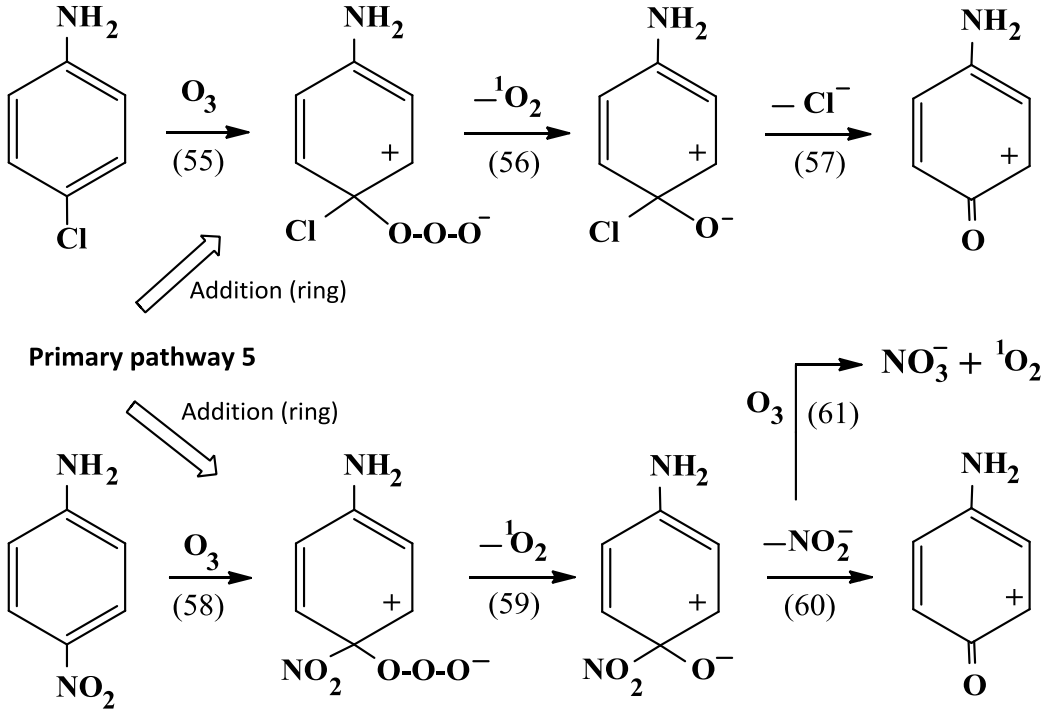

For comparison of *p*-chloroaniline and *p*-nitroaniline with chlorobenzene (k(O_3 + chlorobenzene) = 0.75 M^{-1} s^{-1}, Hoigné & Bader, 1983a, Vysokikh et al., 2007) and nitrobenzene (k(O_3 + nitrobenzene) = 0.09 M^{-1} s^{-1}, Hoigné & Bader, 1983a or 2.2 M^{-1} s^{-1}, Caprio et al., 1984, Akata & Gurol, 1994, Beltrán et al., 1998, Wang & Yin, 1988, Shen et al., 2006), experiments were carried out with chlorobenzene and nitrobenzene in parallel manner (as described above). In both cases the product yields increased linearly with the ozone dose and from the slope of the resulting graph (Figure S11 + S12, Inset) chloride in a yield of 20% is calculated. In the case of nitrobenzene a nitrite yield of 3.3% and a nitrate yield of 13% were quantified.

Text S11. Determination of OH radicals ($^{\bullet}$OH)

The yield of $^{\bullet}$OH radicals was quantified by using DMSO (according to Scheme S6), because in the tertiary butanol assay potential interference of the colored products from the aniline/ozone reaction with the tertiary butanol assay can be obtained.

Scheme S6. Determination of $^{\bullet}$OH with dimethyl sulfoxide (DMSO)

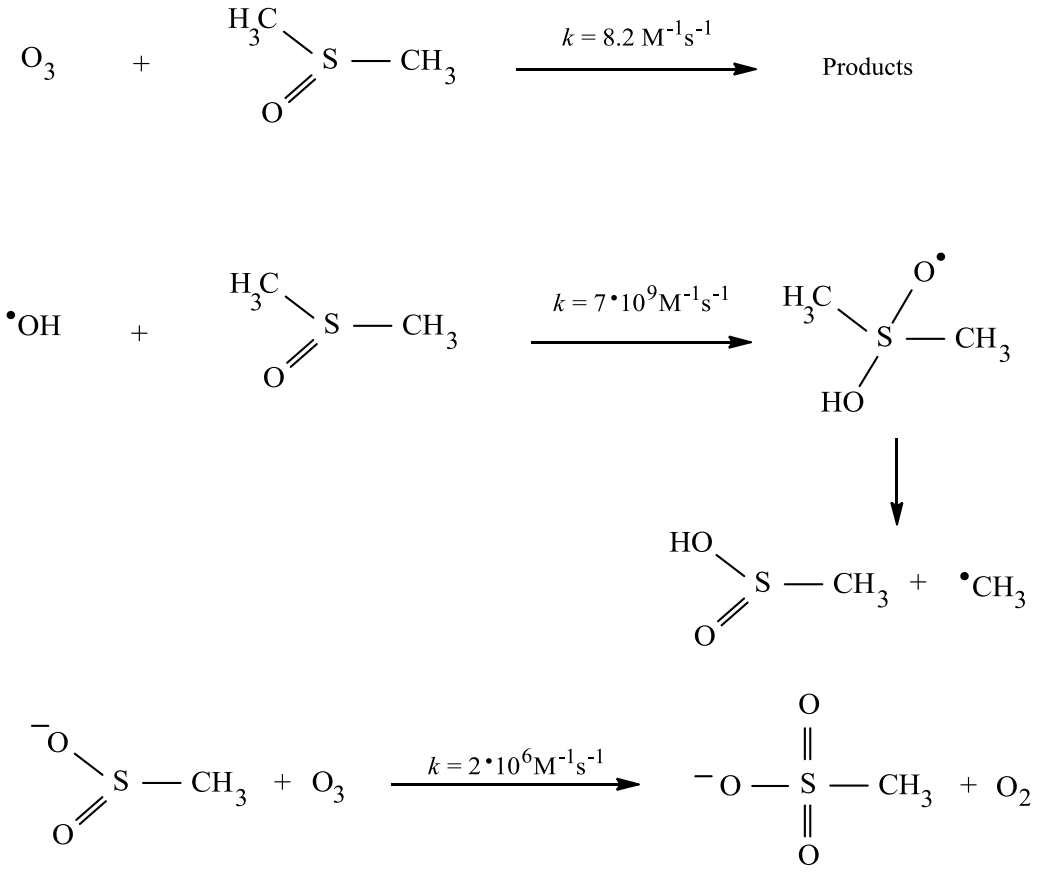

Note that this approach is limited to highly ozone-reactive substrates, which is given for the anilines, since dimethyl sulfoxide itself reacts with ozone with a rate constant of 8.2 M^{-1} s^{-1} (Veltwisch et al., 1980). In addition, methanesulfinic acid (k (O_3 + MSIS) = 2 × 10^6 M^{-1} s^{-1}) react fast with ozone (Flyunt et al., 2001, Veltwisch et al., 1980). Thus, in experiments by determination the combined yield of methanesulfinic and methanesulfonic acids, in the reaction of anilines with ozone the substrate was in constant high concentration (at least 10^{-3} M) and DMSO in large excess (0.1 M) over ozone (1 × 10^{-4} M − 4 × 10^{-4} M) to avoid ozone reaction with the methanesulfinic acid and the $^{\bullet}$OH radicals. Taken into account the concentration of methanesulfinic acid (at

most 2.5 × 10^{-5} M) in the ozone reaction (k_{app} (O_3 + MSIS) = 50 s^{-1}), the reaction of *p*-nitroaniline with ozone (k (O_3 + *p*-nitroaniline) = 1.2 × 10^5 M^{-1} s^{-1}, lowest k in this study and at least 10^{-3} M) is still favored (k_{app} (O_3 + *p*-nitroaniline) = 120 s^{-1}). In due consideration in the reaction of DMSO (0.1 M) with ozone (k_{app} (O_3 + DMSO) = 0.82 s^{-1}) or with $^{\bullet}$OH radicals (k_{app} ($^{\bullet}$OH + DMSO) = 7 × 10^8 s^{-1}) the reaction of ozone with *p*-nitroaniline and the reaction of DMSO with $^{\bullet}$OH radicals are clearly favored. The quantification of the acids by ion chromatography (as described above) was carried out with the following eluent concentration: Na_2CO_3: 1.8 × 10^{-3} M, $NaHCO_3$: 1.7 × 10^{-3} M. Calibration experiments (Figure S13) with methanesulfinic and methanesulfonic acid were performed in the same manner.

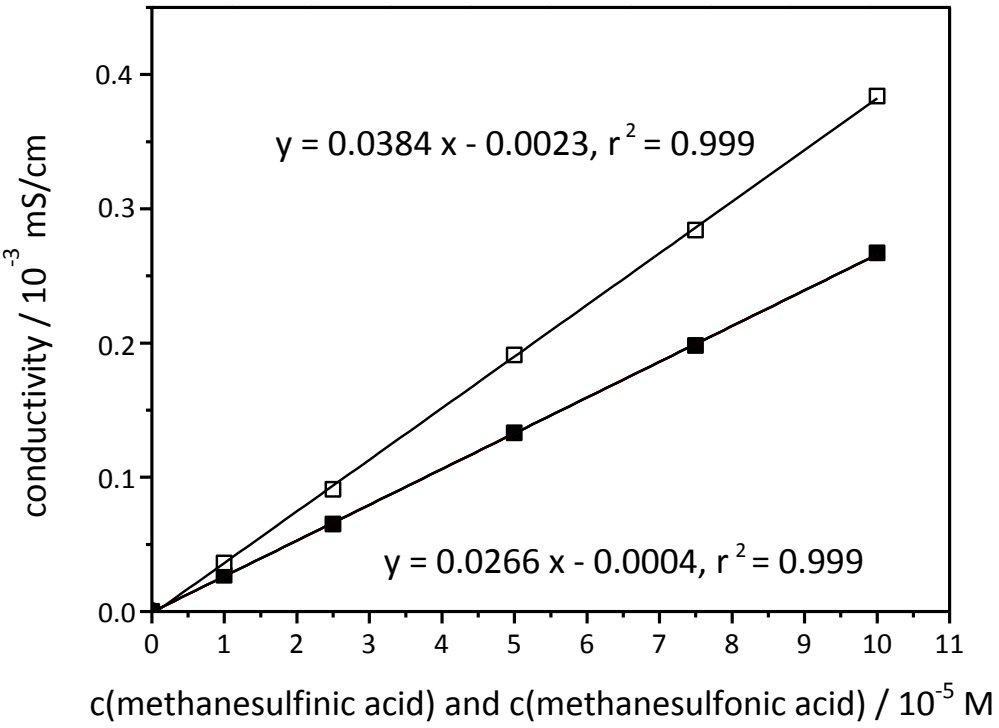

Figure S13. Calibration curves of methanesulfinic acid (■) and methanesulfonic acid (□). Conductivity is plotted vs. concentrations.

Text S12. Determination of formaldehyde

Formaldehyde (k(CH_2O + O_3) = 0.1 M^{-1} s^{-1}, Hoigné & Bader, 1983a) react with ozone at low rates, even if present at reasonable excess. Anyway, in all of these experiments

(formaldehyde was determined with DNPH method, see Experimental part and Text S4) the substrate was in constant high concentration to reduce ozone reaction with formaldehyde. Taking into account the concentration of formaldehyde (at most 6×10^{-5} M) in their reaction with ozone ($k_{app}(O_3 + CH_2O) = 6 \times 10^{-6}$ s^{-1}) and the reaction of *p*-nitroaniline with ozone (k (O_3 + *p*-nitroaniline) = 1.2×10^5 M^{-1} s^{-1}, lowest k in this study and at least with substrate concentration of 10^{-3} M) the latter ($k_{app}(O_3$ + *p*-nitroaniline) = 120 s^{-1}) is still favored.

A plot of formaldehyde formation vs. ozone concentration in the non scavenged system allows quantifying yields by a linear regression. This leads in most cases to low formaldehyde yields between 0.4% up to 3%. Only in the case of *N*-methylaniline and *N*,*N*-dimethylaniline a somewhat higher value of around 6% was obtained. For this reason mechanistic considerations are only made for *N*-methylaniline, *N*,*N*-dimethyl-aniline (see Scheme S7, reaction (62) – (67)), *p*-methoxyaniline (see Scheme S8, reaction (68) – (73)) and *p*-methylaniline (see Scheme S9, reaction (74) – (79)), with around 3%, respectively. Furthermore, the low formaldehyde yields indicate that competition experiments with 3-buten-2-ol (see kinetics) were not biased.

Scheme S7. Proposed reaction scheme of the ozonation of *N*,*N*-dimethylaniline with release of formaldehyde (the reactions are also effectual for *N*-methylaniline)

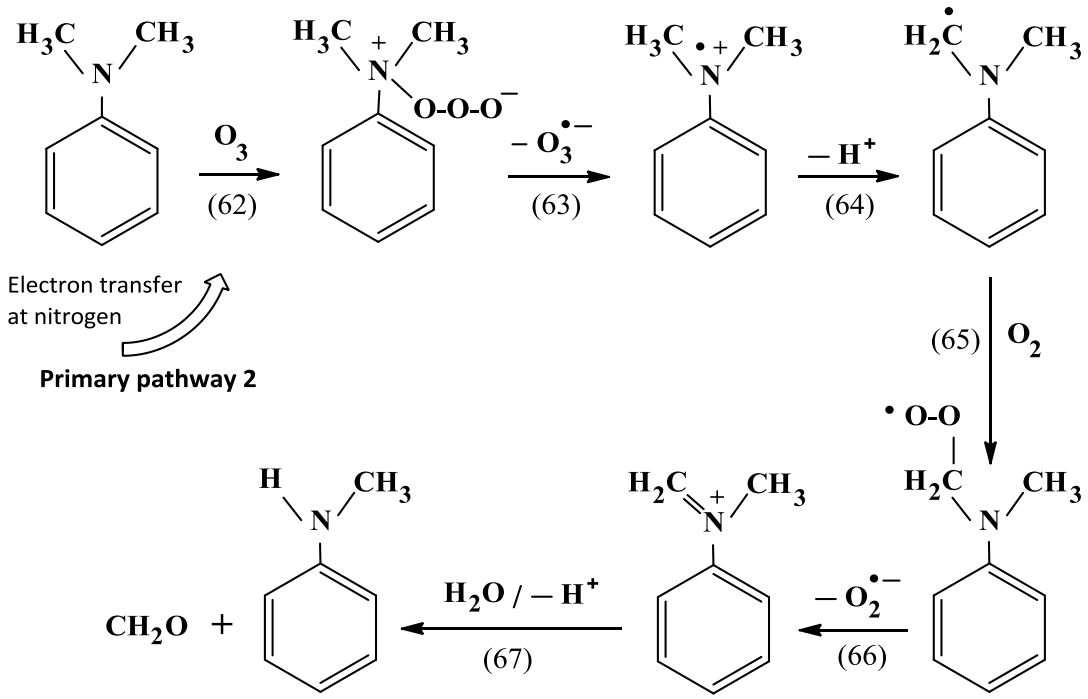

In the case of *N*,*N*-dimethylaniline and *N*-methylaniline it is suggested that based on the primary pathway 2 the amine radical cation (Scheme S7, reaction (63)) can rearrange into a carbon-centered radical (reaction (64)) according to the decay of aliphatic amine radical cations (Das & von Sonntag, 1986, Das et al., 1987). The C-centered radical can react rapidly by addition with oxygen (Tauber & von Sonntag 2000), that is abundant in ozone solution (reaction (65)). The resulting short-lived peroxyl radical looses $O_2^{\bullet-}$ (reaction (66), Das et al., 1987). Subsequently, the developed N-centered cation can react with water and releases formaldehyde and *N*-methylaniline (reaction (67)) in the case of *N*,*N*-dimethylaniline or aniline in the case of *N*-methylaniline (reaction not shown).

Scheme S8. Proposed reaction scheme of the ozonation of *p*-methoxyaniline with release of formaldehyde

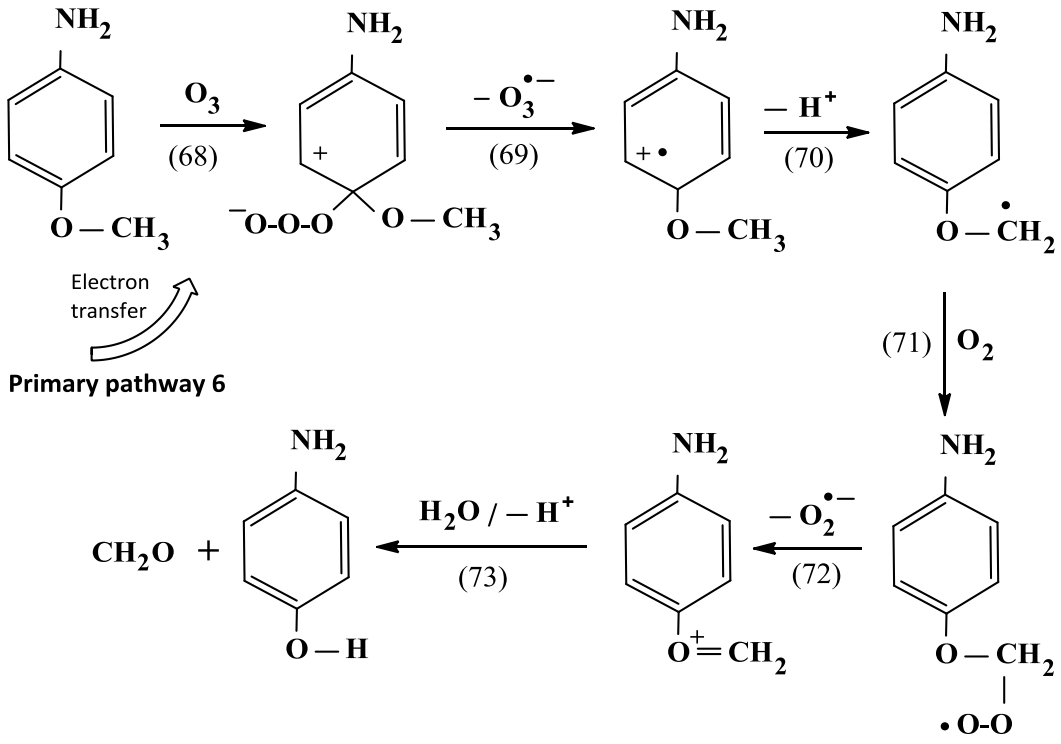

In the case of *p*-methoxyaniline and *p*-methylaniline it is proposed that after ozone adduct formation electron transfer takes place at the aromatic ring by forming a carbon-centered radical cation (see Scheme S8, reaction (68) – (73) and Scheme S9, reaction (74) – (79)). After the release of hydrogen the C-centered radical can react rapidly with oxygen (Tauber & von Sonntag 2000) according to the decay of aliphatic amine radical cations (Das & von Sonntag, 1986, Das et al., 1987) as mentioned above.

The resulting short-lived peroxyl radical looses $O_2^{\bullet-}$ (Das et al., 1987) and the subsequently developed O-centered cation can react with water and releases formaldehyde and *p*–hydroxyaniline (reaction (73)) in the case of *p*-methoxyaniline or aniline in the case of *p*-methylaniline (reaction (79)).

Scheme S9. Proposed reaction scheme of the ozonation of *p*-methylaniline with release of formaldehyde

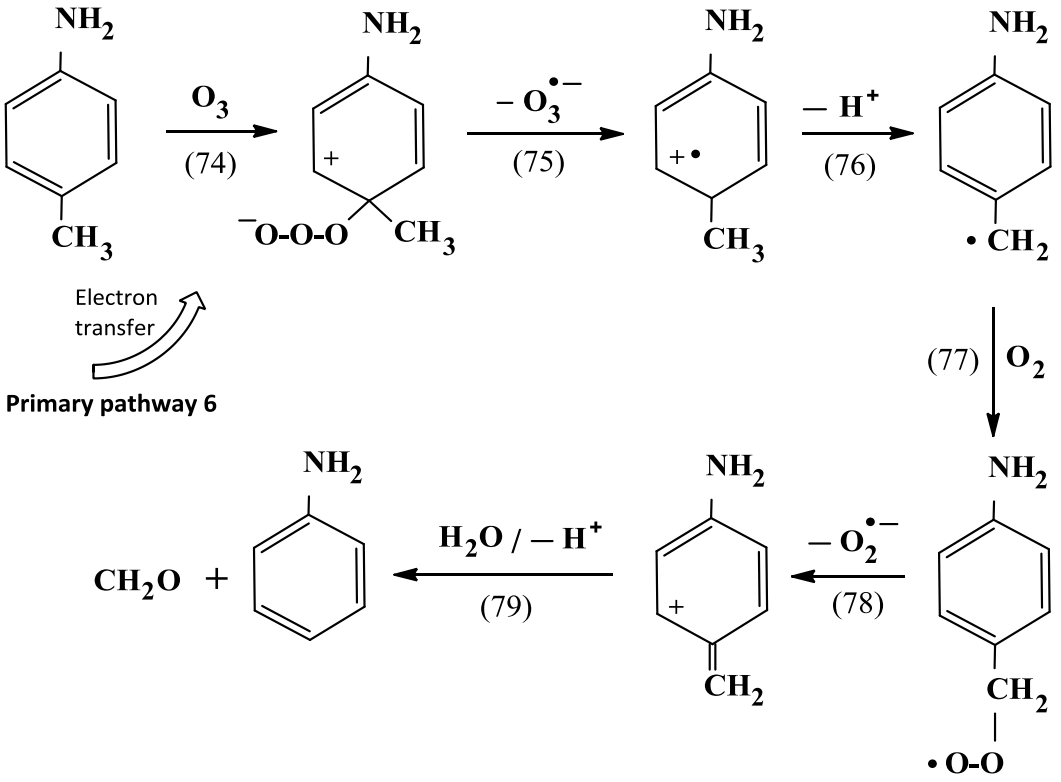

References

Akata, A., Gurol, M. D., 1994. Oxidation of nitrobenzene by ozone and ozone/UV processes. Chem oxid/technol for the nineties 2, 140-160.

Andreozzi, R., Caprio, V., Insola, A., Marotta, R., 2000. The oxidation of metol (*N*-methyl-*p*-aminophenol) in aqueos solution by UV/H2O2 photolysis. Wat Res 34, 463-472.

Becke, A. D., 1996. Density-Functional Thermochemistry. IV. A new dynamical correlation functional and implications for exact-exchange mixing. J Chem Phys, 104, 1040-1046.

Beltrán, F. J., Encinar, J. M., Alonso, M. A., 1998. Nitroaromatic hydrocarbon ozonisation in water: 1: single ozonation. Ind Eng Chem Res 37, 25-31.

Buxton, G. V., Greenstock, C. L., Helman, W. P., Ross, A. B., 1988. Critical review of rate constants for reactions of hydrated electrons, hydrogen atoms and hydroxyl radicals (OH/O^-) in aqueous solution. J Phys Chem Ref Data 17, 513-886.

Caprio, V., Insola, A., Volpicelli, G., 1984. Ozonation of aqueous solution of nitro-benzene. Ozone Sci Eng 6, 115-121.

Das, S., von Sonntag, C., 1986. Oxidation of trimethylamine by OH radicals in aqueous solution, as studied by pulse radiolysis, ESR and product analysis. The reactions of the alkylamine radical cation, the aminoalkyl radical and the protonated aminoalkyl radical. Z Naturforsch B 41, 504-513.

Das, S., Schuchmann, M. N., Schuchmann, H.-P., von Sonntag, C., 1987. The production of the superoxide radical anion by the OH radical-induced oxidation of trimethylamine in oxygenated aqueous solution. The kinetics of the hydrolysis of (hydroxymethyl)-dimethyl amine. Chem Ber 120, 319-323.

Dodd, M. C., Buffle, M.-O., von Gunten, U., 2006. Oxidation of antibacterial molecules by aqueous ozone: moiety-specific kinetics and application to ozone-based wastewater treatment. Environ Sci Technol 40, 1969-1077.

Dowideit, P., von Sonntag, C., 1998. The reaction of ozone with ethene and its methyl- and chlorine-substituted derivatives in aqueous solution. Environ Sci Technol 32, 1112-1119.

Flyunt, R., Makogon, O., Schuchmann, M. N., Asmus, K.-D., von Sonntag, C., 2001. The OH-radical-induced oxidation of methanesulfinic acid. The reactions of the methyl-sulfonyl radical in the absence and presence of dioxygen. J Chem Soc, Perkin Trans 2, 787-792.

Flyunt, R., Leitzke, A., Mark, G., Mvula, E., Reisz, E., Schick, R., von Sonntag, C., 2003. Determination of $^{\bullet}OH$ and $O_2^{\bullet-}$, and hydroperoxide yields in ozone reactions in aqueous solutions. J Phys Chem B 107, 7242-7253.

Forni, L., Bahnemann, D., Hart, E. J., 1982. Mechanism of the hydroxide ion initiated decomposition of ozone in aqueous solution. J Phys Chem 86, 255-259.

Gilbert, E., Zinecker, H., 1980. Ozonization of aromatic amines in water. Ozone Sci Eng 2, 65-74.

Hoigné, J., Bader, H., 1983a. Rate constants of reactions of ozone with organic and inorganic compounds in water. - I. Non-dissociating organic compounds. Wat Res 17, 173-183.

Hoigné, J., Bader, H., 1983b. Rate constants of reactions of ozone with organic and inorganic compounds in water. - II. Dissociating organic compounds. Wat Res 17, 185-194.

Hoigné, J., Bader, H., Haag, W. R., Staehelin, J., 1985. Rate constants of reactions of ozone with organic and inorganic compounds in water. - III. Inorganic compounds and radicals. Wat Res 19, 993-1004.

Jaguar, version 8.3, 2014, Schrodinger, Inc., New York, NY.

Lee, C., Yang, W., Parr, R. G., 1988. Development of the Colle-Salvetti correlation-energy formula into a functional of the electron-density. Phys Rev B, 37, 785-789.

Lipari, F., Swarin, S. J., 1982. Determination of formaldehyde and other aldehydes in automobile exhaust with an improved 2,4-dinitrophenylhydrazine method. J Chrom 247, 297-306.

Liu, Q., Schurter, L. M., Muller, C. E., Aloisio, S., Francisco, J. S., Margerum, D. W., 2001. Kinetics and mechanisms of aqueous ozone reactions with bromide, sulfite, hydrogen sulfite, iodide and nitrite ions. Inorg Chem 40, 4436-4442.

Merényi, G., Lind, J., Naumov, S., von Sonntag, C., 2010. The reaction of ozone with the hydroxide ion. Mechanistic considerations based on thermokinetic and quantum-chemical calculations. The role of HO_4^- in superoxide dismutation. Chem Eur J 16, 1372-1377.

Muñoz, F., von Sonntag, C., 2000a. Determination of fast ozone reactions in aqueous solution by competition kinetics. J Chem Soc, Perkin Trans 2, 661-664.

Muñoz, F., von Sonntag, C., 2000b. The reaction of ozone with tertiary amines including the complexing agents nitrilotriacetic acid (NTA) and ethylenediaminetetraacetic acid (EDTA) in aqueous solution. J Chem Soc, Perkin Trans 2, 2029-2033.

Muñoz, F., Mvula, E., Braslavsky, S. E., von Sonntag, C., 2001. Singlet dioxygen formation in ozone reactions in aqueous solution. J Chem Soc, Perkin Trans 2, 1109-1116.

Mvula, E., von Sonntag, C., 2003. Ozonolysis of phenols in aqueous solution. Org Biomol Chem 1, 1749-1756.

Nash, T., 1953. The colorimetric estimation of formaldehyde by means of the Hantzsch reaction. Biochem J 55, 416-421.

Naumov, S., von Sonntag, C., 2010. Quantum chemical studies on the formation of ozone adducts to aromatic compounds in aqueous solution. Ozone Sci Eng 32, 61-65.

Naumov, S., Mark, G., Jarocki A., von Sonntag, C., 2010. The reactions of nitrite ion with ozone in aqueous solution – new experimental data and quantum-chemical considerations. Ozone Sci Eng 32, 430-434

Naumov, S., von Sonntag, C., 2011. Standard Gibbs free energies of reactions of ozone with free radicals in aqueous solution- quantum chemical calculations. Environ Sci Technol 45, 9195-9204.

Neta, P., Huie, R. E., Ross, A. B., 1988. Rate constants for reactions of inorganic radicals in aqueous solution. J Phys Chem Ref Data 17, 1027-1284.

Olson, K. L., Swarin, S. J., 1985. Determination of aldehydes and ketones by derivatization and liquid chromatography- mass spectrometry. J Chrom 333, 337-347.

Pierpoint, A. C., Hapemann, C. J., Torrents, A., 2001. Linear free energy study of ring-substituted aniline ozonation for developing treatment of aniline-based pesticide waters. J Agric Food Chem 49, 3827-3832.

Ramseier, M. K., von Gunten, U., 2009. Mechanism of phenol ozonation – kinetics of formation of primary and secondary reaction products. Ozone Sci Eng 31, 201-215.

Shen, J., Chen, Z., Li, X., Qi, F., Ye, M., 2006. The efficiency and mechanism of the degradation of nitrobenzene in aqueous solution by O_3/H_2O_2. Wat Sci & Technol: Water Supply 6, 153-162.

Staehelin, J., Hoigné, J., 1982. Decomposition of ozone in water: rate of initiation by hydroxide ions and hydrogen peroxide. Environ Sci Technol 16, 676-681.

Staehelin, J., Hoigné, J., 1985. Decomposition of ozone in water in the presence of organic solutes acting as promoters and inhibitors of radical chain reactions. Environ Sci Technol 19, 1206-1213.

Tannor, D. J., Marten, B., Murphy, R., Friesner, R. A., Sitkoff, D., Nicholls, A., Honig, B., Ringnalda, M., GoddardIII, W. A., 1994. Accurate first principles calculation of molecular charge distributions and solvation energies from ab initio quantum mechanics and continuum dielectric theory. J Am Chem Soc, 116, 11875-11882.

Tauber, A., von Sonntag, C., 2000. Products and kinetics of the OH-radical-induced dealkylation of atrazine. Acta Hydrochim Hydrobiol 28, 15-23.

Veltwisch, D., Janata, E., Asmus, K.-K., 1980. Primary processes in the reactions of •OH radicals with sulphoxides. J Chem Soc, Perkin Trans 2, 146-153.

von Sonntag, C., Schuchmann, H.-P., 1997. Peroxylradicals in aqueous solution. In: Peroxyl Radicals, Z.B. Alfassi (ed.), Wiley Chichester, 173-234.

von Sonntag, C., von Gunten, U., 2012. Chemistry of ozone in water and wastewater treatment. From basic principles to applications. IWA Publishing

Vysokikh, T. A., Yagodovskaya, T. V., Savilov, S. V., Lunin, V. V., 2007. The interaction of ozone with chlorobenzene. Russ J Phys Chem A81, 878-882.

Wang, B., Yin, J., 1988. Removal of aromatic nitro-compounds from water by ozonation. Ozone Sci Eng 10, 1-23.

Yao, C. C. D., Haag, W. R., 1991. Rate constants for direct reactions of ozone with several drinking water contaminats. Wat Res 25, 761-773.

Zimmermann, S. G., Schmukat, A., Schulz, M., Benner, J., von Gunten, U., Ternes, T. A., 2012. Kinetic and mechanistic investigations of the oxidation of tramadol by ferrate and ozone. Environ Sci Technol 46, 876-884.

3 Ozonation of piperidine, piperazine and morpholine: Kinetics, stoichiometry, product formation and mechanistic considerations

Agnes Tekle-Röttering, Kevin S. Jewell, Erika Reisz, Holger V. Lutze,
Thomas A. Ternes, Winfried Schmidt, Torsten C. Schmidt

Water research (2016), 88, 960-971

3.1 Abstract

Piperidine, piperazine and morpholine as archetypes for secondary heterocyclic amines, a structural unit that is often present in pharmaceuticals (e.g., ritalin, cetirizine, timolol, ciprofloxacin) were investigated in their reaction with ozone. In principle the investigated compounds can be degraded with ozone in a reasonable time, based on their high reaction rate constants (1.9×10^4 – 2.4×10^5 M^{-1} s^{-1}) with respect to ozone. However, transformation is insufficient (13 – 16%) most likely due to a chain reaction, which decomposes ozone. This conclusion is based on $^{\bullet}OH$ scavenging experiments, leading to increased compound transformation (18 – 27%). The investigated target compounds are similar in their kinetic and stoichiometric characteristics. However, the mechanistic considerations based on product formation indicate various reaction pathways. Piperidine reacts with ozone via a nonradical addition reaction to *N*-hydroxypiperidine (yield: 92% with and 94% without scavenging, with respect to compound transformation). However, piperazine degradation with ozone does not lead to *N*-hydroxypiperazine. In the morpholine-ozone reaction, *N*-hydroxymorpholine was identified. Additional oxidation pathways in all cases involved the formation of $^{\bullet}OH$ with high yields. One important pathway of piperazine and morpholine by ozonation could be the formation of C-centered radicals after ozone or $^{\bullet}OH$ attack. Subsequently, O_2 addition forms unstable peroxyl radicals, which

in one pathway loose superoxide radicals by generating a carbon-centered cation. Subsequent hydrolysis of the carbon-centered cation leads to formaldehyde, whereby ozonation of the *N*-Hydroxy products can proceed in the same way and in addition give rise to hydroxylamine. A second pathway of the short-lived peroxyl radicals could be a dimerization to form short-lived tetraoxides, which cleave by forming hydrogen peroxide. All three products have been found.

3.2 Introduction

Amino groups are among the most common structural units in micropollutants, since many biologically active compounds, e.g., pharmaceuticals, contain aromatic and aliphatic amino groups. Micropollutants in turn are of major concern in drinking water and wastewater (Nöthe et al., 2007, Deblonde et al., 2011, Ternes et al., 2015). In wastewater treatment plants, they are not fully biodegraded and thus reach the environment (Huber et al., 2005, Gabet-Giraud et al., 2010). Hence, in surface water micropollutants have been found (Ternes, 1998, Benotti et al., 2009, Martínez Bueno et al., 2012). Even at low concentrations, they may be harmful to aquatic life (Huggett et al., 2002, Küster et al., 2010). Therefore, in drinking water and wastewater treatment, micropollutant abatement by ozonation is gaining importance (Ternes et al., 2002, Huber et al., 2003, Ternes & Joss, 2006, Schwarzenbach et al., 2006, Benner et al., 2008, Kim et al., 2009, Benitez et al., 2011, Zimmermann et al., 2012). The degradation of micropollutants with ozone is, however, in competition with the reaction of ozone with the water matrix and only micropollutants with high ozone rate constants are readily eliminated (Lee & von Gunten, 2010). This requires the determination of ozone rate constants of the micropollutants. An important degradation path involves the formation of OH radicals ($^{\bullet}$OH) (von Gunten, 2003a,b, von Sonntag, 2007). Hence, $^{\bullet}$OH yield is a relevant reaction parameter. In addition, the reaction stoichiometry, the amount of ozone needed for full compound degradation, is to be determined (Nöthe et al., 2009). There is, however, now also a raising interest in the ozonation products, due to the fact that transformation products may be also toxic to aquatic life (Shang & Yu, 2001, Huber et al., 2004, Schmidt & Brauch, 2008, Boxall et al., 2014).

In the present study, the reactions of piperidine, piperazine and morpholine with ozone in aqueous solution were investigated. These compounds are archetypes for micropollutant degradation, in particular for heterocyclic amines (e.g., the pharmaceuticals: ADHD (attention deficit hyperactivity disorder) medicine ritalin, the antihistamine cetirizine, the antibiotic ciprofloxacin as well as timolol or other beta blockers). The reactions of ozone with olefins (Dowideit & von Sonntag, 1998, Theruvathu et al., 2001, Leitzke et al., 2003), aromatic compounds (Dorè et al., 1980, Hoigné & Bader, 1983a,b, Beltrán et al., 1998, Mvula & von Sonntag, 2003, Naumov & von Sonntag, 2010) and some amines (Gilbert & Zinecker, 1980, Elmghari-Tabib et al., 1982, Cocheci et al., 1989, Muñoz & von Sonntag, 2000b, Flyunt et al., 2002, Sein et al., 2008, Benner & Ternes, 2009a,b) have already been investigated in detail. Thus, when considering ozone reactions some basic principles relating to amines are well established. First, it is well-known that ozone reacts strongly electrophilic. Hence the ozone-reactive site of amines is the lone electron pair at nitrogen. Protonation reduces the otherwise high ozone reactivity and so reactivity depends strongly on pH and the corresponding speciation of the amines (Tyupalo & Yakobi, 1980, von Sonntag & von Gunten, 2012). Compounds that contain two amino groups (such as EDTA), show a high rate constant, when both amino groups are deprotonated, but reaction rates drop when one of them is protonated. Obviously, protonation of one of the nitrogens also influences the electron density of the other, thereby reducing its reactivity towards ozone (Muñoz & von Sonntag, 2000b, von Sonntag & von Gunten, 2012). In addition, ozone is a highly selective reactant and its rate constants with aromatic compounds (Neta et al., 1988), nitrogen-containing compounds (von Sonntag & von Gunten, 2012), electron-rich and electron-deficient olefins (Dowideit & von Sonntag, 1998) vary by ten orders of magnitude.

In ozone reactions mechanistic considerations are of growing interest and this includes product studies. The investigated amines in this study could refer to more complex micropollutants. In the literature several primary ozone reactions with miscellaneous compounds have been discussed (Muñoz et al., 2001, von Sonntag, 2008, von Gunten, 2010, von Sonntag & von Gunten, 2012), so that on the basis of these studies four conceivable primary processes (presented in Scheme 1) are feasible for the three investigated amines in aqueous solution: Addition (reaction (1)), electron transfer

(reaction (4)), H-abstraction (reaction (7)) and insertion (reaction (9)). Piperidine is exemplarily shown in Scheme 1 but all reactions are applicable to morpholine and piperazine as well.

Scheme 1. Primary processes in the reaction of piperidine with ozone.

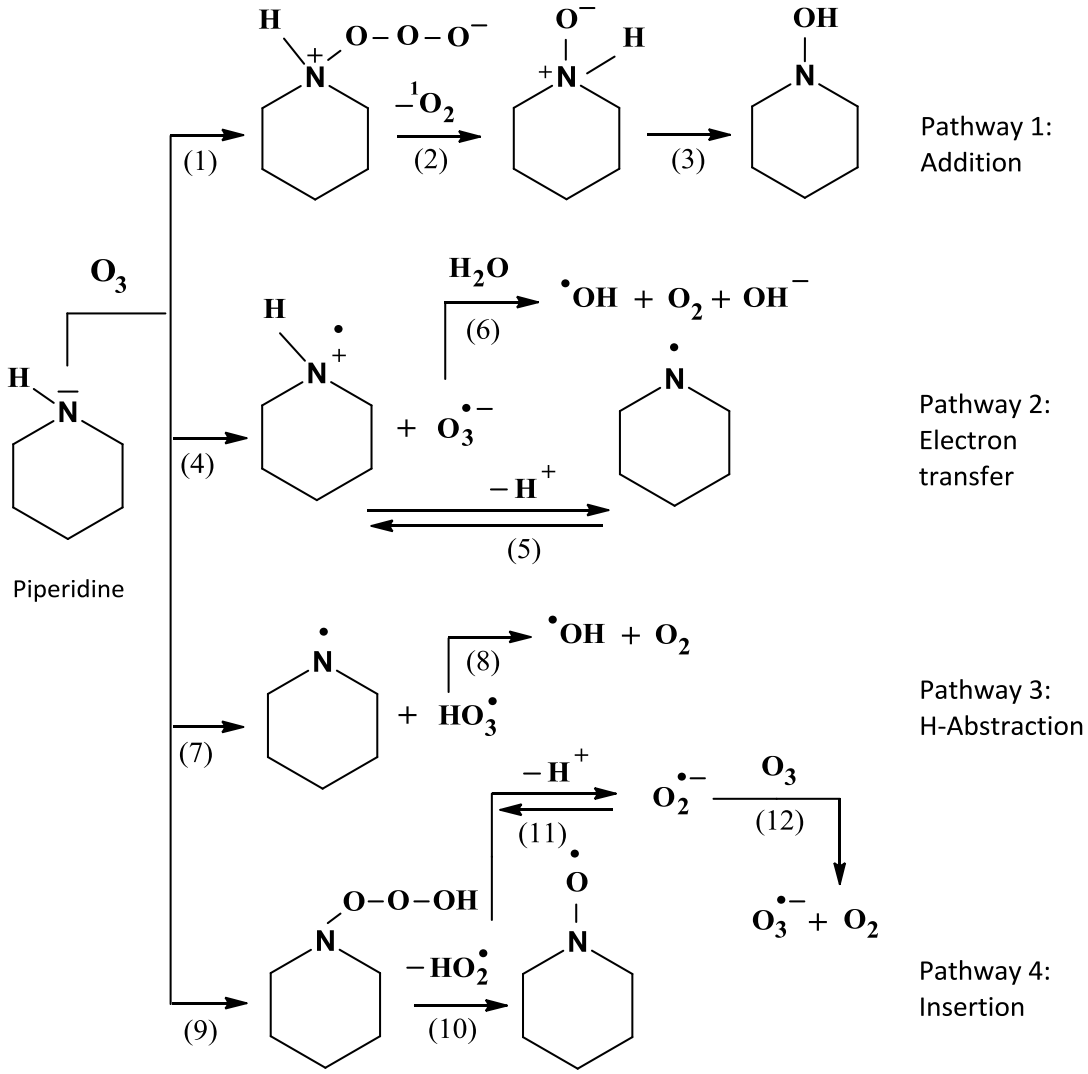

The initial step of the ozone addition to the lone electron pair of the nitrogen atom is well-established (Muñoz & von Sonntag, 2000b) and leads to the formation of an ozonide ammonium zwitterion (reaction (1)). This zwitterion subsequently can eliminate singlet oxygen ($^1O_2$, see Supporting Information Text S8, Muñoz et al., 2001) by yielding *N*-hydroxy products (similar to propranolol, Benner & Ternes, 2009b) (shown in Scheme 1, reaction (2) – (3)). In competition with the singlet oxygen elimination, the initially formed ozonide ammonium zwitterion may also separate by

forming different radicals through reactions such as electron transfer, H-abstraction and insertion (von Sonntag & von Gunten, 2012). In principle, these radical processes could also proceed via a direct reaction pathway without adduct as intermediate (von Sonntag & von Gunten, 2012). However, in experiments the direct pathway and the adduct pathway cannot be distinguished. From the electron transfer reaction an amine radical cation (reaction (4)), (which is in equilibrium with an amine radical (reaction (5)) (von Sonntag & von Gunten, 2012) and an ozonide radical anion, $O_3^{\bullet-}$ (adduct of the hydrated electron to ozone, Elliot & McCracken, 1989, see reaction therein) are formed. The ozonide radical anion, $O_3^{\bullet-}$ reacts with water giving rise to $^{\bullet}OH$ (reaction (6), Bühler et al., 1984). In the H-abstraction process an amine radical and hydrotrioxyl radical, $HO_3^{\bullet}$ (reaction (7)) are formed and the latter likewise decomposes to $^{\bullet}OH$ and oxygen (reaction (8), Bühler et al., 1984). One further radical pathway is after insertion (reaction (9)) the subsequent formation of a nitroxyl radical and a hydroperoxyl radical, $HO_2^{\bullet}$ (reaction (10)). The latter is in equilibrium with its conjugate base, the superoxide radical anion, $O_2^{\bullet-}$ (equilibrium reaction 11, pK_a ($HO_2^{\bullet}$) = 4.8) which dominates even in slightly acid solution (Bielski et al., 1985, Ragnar et al., 1999a). $O_2^{\bullet-}$ can react with ozone to the ozonide radical anion, $O_3^{\bullet-}$ (reaction (12)), the precursor of $^{\bullet}OH$ (Sehested et al., 1983, Staehelin et al., 1984). Under alkaline experimental conditions the hydrotrioxyl radical (pK_a ($HO_3^{\bullet}$) = -2, Naumov & von Sonntag et al., 2011b) and hydroperoxyl radical ($HO_2^{\bullet}$, pK_a see above and in Scheme 1 the equilibrium reaction (11)) exist mostly as their conjugated bases, $O_3^{\bullet-}$ and $O_2^{\bullet-}$, respectively. Which of the above mentioned primary reactions take place preferentially, can be inferred from products that are formed in the ozone-compound reactions.

Some previous studies have investigated ozone reactions with tertiary (Muñoz & von Sonntag, 2000b, Zimmermann et al., 2012) and secondary amines (Benner & Ternes, 2009a, b). A study about the ozonation of pyrrolidine, piperidine, morpholine and piperazine has already reported rate constants determined from the decrease of the amine concentration vs. the reaction time at pH 7.0 (Pietsch et al., 1999). One study investigating the regioselective oxidation of *N*-phenylmorpholine by ozone in dichloromethane or acetonitrile has reported the formation of lactam and a diformylderivative (Suarez-Bertoa et al., 2012). However, these studies and even the most comprehensive textbook (von Sonntag & von Gunten, 2012) have not included

details on the kinetics, stoichiometry and products of the ozonation of secondary heterocylic amines. Thus, the objectives of the present work are kinetic studies and stoichiometry in the reaction of ozone with piperidine, piperazine and morpholine. These compounds should be archetypes for secondary heterocyclic amines, a structural unit that is often present in pharmaceuticals in aqueous solution. Furthermore, the most abundant primary pathways of scheme 1 as well as advanced mechanistic considerations are provided as a result of product yields.

3.3 Experimental part

3.3.1 Chemicals and materials

All chemicals were commercially available in high purity (> 97%). Further information on chemicals is given in Supporting Information in Text S1. Ozone solutions (max. 1×10^{-3} M) were freshly prepared by bubbling ozone-containing gas from an ozonator (Sander, Uetze-Eltze, Germany) fed with oxygen (6.0 from Linde, München, Germany) through ultra-pure water (Merck Millipore). If high ozone concentrations were required ice-bath-cooled water was used. The ozone concentration of the stock solution was determined spectrometrically (Photometer UV 1800, Shimadzu, Duisburg, Germany) taking ε(260nm) = 3200 M^{-1} cm^{-1} (Forni et al., 1982, Hart et al., 1983). For chromatography acetonitrile (Fisher Scientific, Schwerte, Germany) and ultra-pure water were used. Solutions were at all times freshly prepared from ultra-pure water or water in HPLC-grade (Merck, Darmstadt, Germany) which sometimes was preozonated by adding ozone, in order to ensure that the water is absolutely free from ozonation competing organic and inorganic compounds.

3.3.2 Methods

Sample preparation. The experiments were performed as batch experiments in bench-scale with 10^{-4} – 10^{-2} M of investigated compounds and at different pH-values (9.5 – 12.5). All experiments were carried out at room temperature in duplicate or triplicate. The samples were analyzed 3 – 5 h after the addition of ozone to ensure that no more ozone was present, sometimes tested with indigotrisulfonate. To exclude $^{\bullet}OH$ reactions, for example the decomposition of ozone with $^{\bullet}OH$ (k ($^{\bullet}OH + O_3$) = 1.1×10^8 M^{-1} s^{-1}, Buxton et al., 1988) or (k ($^{\bullet}OH + O_3$) = 3.0×10^9 M^{-1} s^{-1}, Staehelin & Hoigné,

1982) samples were prepared in parallel as described above but containing tertiary butanol (t-BuOH) (0.05 - 0.1 M) or dimethyl sulfoxide (DMSO) (0.1 M) as $^{\bullet}OH$ scavengers, that terminate the free radical mechanisms (Staehelin & Hoigné, 1985). Provided that no interferences were observed, tertiary butanol was used, otherwise DMSO was chosen. Dissociation of hydroxyl radicals into the oxide radical anion occurs through the equilibrium $^{\bullet}OH \rightleftharpoons O^{\bullet-} + H^{+}$ (Buxton et al., 1988). This could play a role at high pH values. However, due to the high pK_a–value of hydroxyl radicals (pK_a ($^{\bullet}OH$) = 11.8, Merényi et al., 2010b) at a pH value of 12.5 more than 80% is present as $^{\bullet}OH$. In addition, the hydroxyl ion (^{-}OH) can react with ozone, (k ($^{-}OH + O_3$) = 48 M^{-1} s^{-1}, Forni et al., 1982 or 70 M^{-1} s^{-1}, Staehelin & Hoigné, 1982), albeit slowly and gives rise to $^{\bullet}OH$ (Staehelin & Hoigné, 1982, Merényi et al., 2010b). This could in principle be relevant in the used pH range of 9.5 − 12.5. However, despite the very high pH in the experiments this is not relevant for the presented results. Further details for this paragraph are given in Supporting Information in Text S2.

Reaction kinetics. The ozone rate constants for the investigated compounds were determined by a competition kinetic method, in which the ozone decay (ozone under substoichiometric conditions) was followed by quenching with competitor (refer to Supporting Information Text S3). Here, a competition with 3-buten-2-ol (k(3-buten-2-ol + O_3) = 7.9 × 10^4 M^{-1} s^{-1}, Muñoz & von Sonntag, 2000a, Dowideit & von Sonntag, 1998) and cephalexin (k(ceph.$_{monoprotonated}$ + O_3 = 8.2 (± 2.9) × 10^4 M^{-1} s^{-1} and k(ceph.$_{deprotonated}$ = 9.3 (± 2.2) × 10^4 M^{-1} s^{-1} , Dodd et al., 2006a, pK_a = 7.1, Takacs-Novak et al., 1997) was selected since a rate constant of ozone with the investigated compounds was expected in the same order of magnitude. 3-buten-2-ol reacts with ozone to formaldehyde (see Supporting Information Text S3 and Scheme S5), which was determined with the Hantzsch assay (Nash, 1953) or DNPH (2,4-dinitrophenyl-hydrazine) method (Lipari & Swarin, 1982). In the case of cephalexin as competitor the residual cephalexin was determined with HPLC–DAD (LC20, Shimadzu, Duisburg, Germany, refer to the Supporting Information Text S3).

Reaction stoichiometry. The stoichiometry of the ozone reaction was carried out by adding different understoichiometric concentrations of ozone followed by a determination of the residual compound concentrations after complete ozone consumption (measured and calibrated with the original compound and derivatized

according to Pietsch et al., 1996, using a HPLC–DAD system, see Supporting Information Text S4 and Scheme S6).

Product formation. Identification of products was performed through molecular mass, which were determined by LC-HRMS (Linear triple quadrupole ion trap Fourier transformation mass spectrometer (LTQ Orbitrap Velos, Thermo Scientific, Bremen, Germany)). The quantification of the identified products was carried out with HPLC-DAD (refer to Supporting Information Text S5). One method to determine $^{\bullet}OH$ is to use an $^{\bullet}OH$ scavenger that reacts slowly with ozone but fast with $^{\bullet}OH$. The determination of $^{\bullet}OH$ yields was conducted by choosing the dimethyl sulfoxide (DMSO) method (k(DMSO + $^{\bullet}OH$) = 7×10^9 M^{-1} s^{-1}, Flyunt et al., 2001a, 2003a, Veltwisch et al., 1980), with the chemical as $^{\bullet}OH$ scavenger present in excess. The reaction of DMSO with $^{\bullet}OH$ leads to methanesulfinic and methanesulfonic acid, which were quantified by ion chromatography (refer to Supporting Information Text S6). Formaldehyde (CH_2O), as reaction product was determined with the Hantzsch method (see description above, kinetics and refer to Supporting Information Text S7). In order to corroborate the formaldehyde yield a Hach-Lange test kit (LCK 325) was used. Hydroxylamine (NH_2OH) was determined by its oxidation with iodate (IO_3^-, 4.7×10^{-2} M) to nitrite (Afkhami et al., 2006, see Supporting Information Text S7). Hydrogen peroxide (H_2O_2) was quantified with Allen`s reagent (Allen et al., 1952, Flyunt et al., 2003b, Kitsuka et al., 2007, see Supporting Information Text S7). In all analytical methods blanks were performed in the same manner with ultra-pure water instead of ozone solution to determine the initial concentration. Calibration experiments were performed in the same manner.

3.4 Results and Discussion

3.4.1 Reaction kinetics

The rate constants for the reaction of ozone with the investigated nitrogen-containing heterocyclic compounds range between 1.9×10^4 and 2.4×10^5 M^{-1} s^{-1} (Table 1, description see below, with DNPH at pH 11.5 see Figure 1). The ozone rate constants were determined by competition kinetics (from slopes of the plots, see Supporting Information Text S3) using two competitors (see Experimental part) at various experimental conditions, in particular different pH, that are compiled in Table S1 in

Supporting Information. The values obtained, as well the values from literature, were calculated for the conditions of completely deprotonated amine species and averaged (the protonated species are neglected, the error of the pK_a–values falls into the margin of deviation, see Supporting Information Text S3). Results are summarized in Table 1.

Table 1. Compilation of ozone rate constants of heterocyclic compounds in aqueous solution under conditions of deprotonated amine species (pH values: 11.5 – 12.5). $^{\bullet}$OH were scavenged with DMSO or tertiary butanol. Standard deviation is reported in parenthesis.

Compound	***k*** / M^{-1} s^{-1}	pK_a (of corresponding acid)
Piperidine	$2.4 (\pm 0.95) \times 10^5$ $1.4 (\pm 0.55) \times 10^5$ (scavenged) 2.9×10^5 (Pietsch et al., 1999)	11.1*
***N*-Hydroxypiperidine**	$9.4 (\pm 0.27) \times 10^4$ $6.3 (\pm 0.38) \times 10^4$ (scavenged)	
Piperazine	$2.6 (\pm 0.22) \times 10^4$ $1.9 (\pm 0.05) \times 10^4$ (scavenged) 1.4×10^5 (Pietsch et al., 1999)	9.80* pK_{a2}: 5.57**
Morpholine	$8.3 (\pm 0.37) \times 10^4$ $6.2 (\pm 0.25) \times 10^4$ (scavenged) 1.2×10^5 (Pietsch et al., 1999)	8.36*

*Handbook of Chemistry and Physics, David R. Lide, 89th Edition, 2008-2009

** (chemie-online (D`Ans-Lax))

Comparing the reactions of ozone with piperidine, piperazine and morpholine at different experimental conditions (see Supporting Information Text S3 and Table S1) revealed similar rate constants, with piperidine displaying the highest one. The high ozone rate constants are in accordance with the high ozone reactivity of the corresponding deprotonated species of the amines. Lower rate constants were

obtained by using a radical scavenger because •OH reactions are excluded. Overall, the reactivity of the azinane-ozone system drops only to a small extent if •OH is scavenged, so radical formation has only a minor contribution on the oxidative degradation in non scavenged systems and can be neglected. However, it has to be taken into account that even in the experiments without scavenger, •OH could be scavenged by the compounds under study (with ozone in substoichiometric addition, for some rate constants see Buxton et al., 1988). In experiments without scavengers but either buffered or alkalinized the rate constants are approximately equal (see Supporting Information Table S1). The rate constants determined with cephalexin are in good accordance with those determined with 3-buten-2-ol (see Supporting Information Table S1). *N*-hydroxypiperidine as the first transformation product following pathway 1 in Scheme 1 reacts as fast with ozone as piperidine.

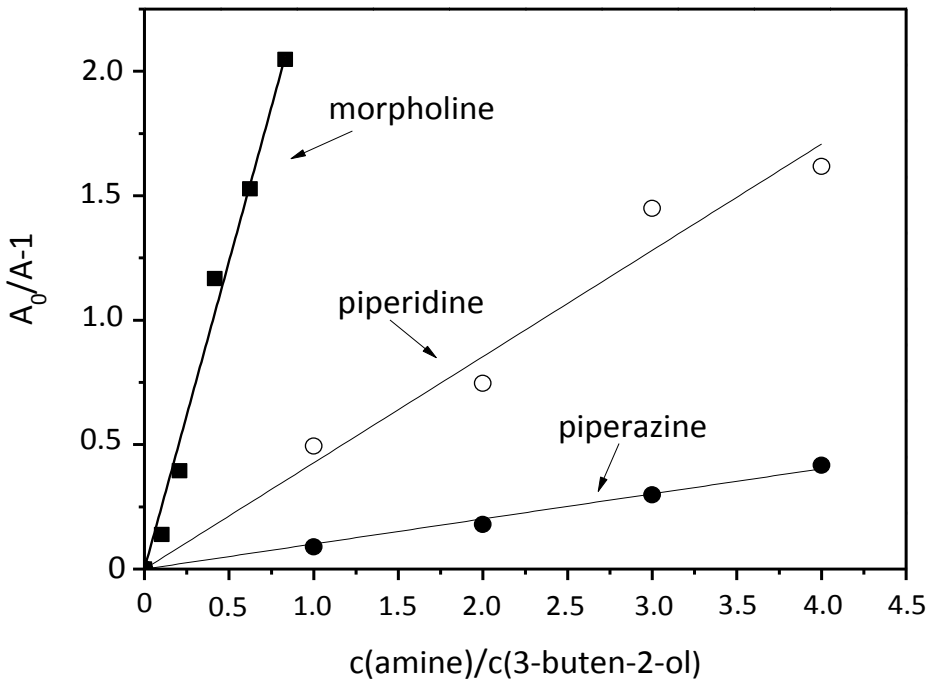

Figure 1. Determination of the rate constants in the reaction of secondary amines $c_0(1 \times 10^{-2}$ M – 8×10^{-2} M) with ozone $c_0(4.2 \times 10^{-5}$ M). The experiments were carried out with 3-buten-2-ol $c_0(1 \times 10^{-3}$ M) and without pH adjustment (pH 9.8 – 11.2). Formaldehyde, as product from 3-buten-2-ol in its reaction with ozone is determined with DNPH. The ratio of the peak areas of formaldehyde from the yield in the absence of competitor (A_0) and in the presence of varying does of competitor (A) is plotted against the amine-3-buten-2-ol ratio (see Supporting Information Text S3).

Kinetic analysis of the azinane-ozone system resulted in comparable rate constants for the deprotonated amine species containing one nitrogen atom such as piperidine and morpholine as reported in the literature (see Table 1 and Supporting Information Table S1). The rate constant of 1.9×10^4 M^{-1} s^{-1} measured for piperazine is not in accordance with a previously reported finding, which leads to a higher value (k = 1.4×10^5 M^{-1} s^{-1}, calculated for completely deprotonated species from a value at pH 7 from Pietsch et al., 1999). However, in spite of the second pK_a–value of 5.57 the piperazine molecule is almost completely protonated at pH 7 just as piperidine and morpholine (see Supporting Information Figure S1). Furthermore, the previous study was performed monitoring the disappearance of the compound (with ozone in excess) at a pH of 7, while our data were obtained monitoring the disappearance of ozone at pH values between 9.8 and 12.5. In comparison to imidazole (5-membered ring also with two nitrogen atoms, $k = 2.4 \times 10^5$ M^{-1} s^{-1}, Pryor et al., 1984) piperazine has a 10 times lower rate constant. Other comparable amines (with one or more nitrogens), e.g., *N*-methylpyrrolidine ($k = 2.0 \times 10^6$ M^{-1} s^{-1} Dodd et al., 2006a), Ciprofloxacin ($k_{monoprotonated} = 7.5 \times 10^3$ M^{-1} s^{-1}, $k_{deprotonated} = 9.0 \times 10^5$ M^{-1} s^{-1}, Dodd et al., 2006a), metoprolol ($k = 8.6 \times 10^5$ M^{-1} s^{-1}, Benner & Ternes, 2009a) and propranolol (k = ~ 1×10^5 M^{-1} s^{-1}, Benner & Ternes, 2009b) have somewhat higher rate constants. The high reactivity of the monoprotonated species of ciprofloxacin indicates that ozone attack probably does not take place at the protonated amine, but rather on another moiety. By comparison of the investigated aliphatic nitrogen-containing heterocyclic compounds to aromatic nitrogen-containing heterocyclic compounds, the rate constants of the former are orders of magnitude higher (cf. pyridine $k = 2.0$ M^{-1} s^{-1}, Hoigné & Bader, 1983a). A reason should be that the lone electron pair at nitrogen in aromatic systems is delocalized and thus not well available for the reaction with ozone.

3.4.2 Reaction stoichiometry

Kinetic experiments showed that the investigated nitrogen-containing heterocyclic compounds are very reactive to ozone and hence reaction stoichiometry is also of special interest for detailed mechanistic studies. The degradation of the *N*-heterocycles (refer to Supporting Information Text S4) at molar ratios and the selected pH (11.5) depends linear on ozone concentration in the absence and

presence of scavenger (Figure 2, morpholine and piperidine are shown as examples). Results are summarized in Table 2 (refer also to Supporting Information Figure S7 and Figure S8).

Table 2. Ozonation of piperidine, piperazine and morpholine. Compound degradation in percentage of ozone consumed (%) in scavenged (t-BuOH) and non scavenged systems in reference to 100% ozone (pH values: adjusted to 11.5). Products and their yields (including $^{\bullet}OH$) in % of ozone consumed as well as in % of degraded compound in scavenged (t-BuOH and DMSO) and non scavenged systems (standard deviation in parenthesis).

Compound	**Compound degradation / %** (per ozone consumed) [Scavenged system in rectangular brackets]	**Product yield / %** (per ozone consumed) [Scavenged system in rectangular brackets]	**Product yield / % (calculated)** (per degraded compound) [Scavenged system in rectangular brackets]	**Sum of stable products in relation to 100% of compound / %**
Piperidine	13 (± 1) [18 (± 2)]			104*
N-Hydroxy-piperidine	18 (± 3) [31 (± 5)]	12 (± 2) [17 (± 1)]	92 [94]	
$^{\bullet}OH$		28 (± 3)		
Formaldehyde		1.2 (± 0.1) [2.5 (± 0.2)]	9.2 [14]	
Hydroxylamine		1.1 (± 0.1) [0.64 (± 0.03)]	8.5 [3.5]	
Hydrogen peroxide		0.17 (± 0.1) [0.43 (± 0.1)]	2.6 [4.6]	

Piperazine	14 (± 4) [24 (± 7)]			115*
•OH		30 (± 1)		
Formaldehyde		10 (± 0.5) [19 (± 0.5)]	71 [79]	
Hydroxylamine		7.8 (± 0.05) [6.6 (± 0.1)]	56 [28]	
Hydrogen peroxide		3.1 (± 0.3) [7.2 (± 1)]	44 [60]	
Morpholine	16 (± 5) [27 (± 5)]			61*
N-Hydroxy-morpholine		detected, not quantified		
•OH		33 (± 1)		
Formaldehyde		4.3 (± 0.2) [8.2 (± 0.3)]	27 [30]	
Hydroxylamine		1.9 (± 0.09) [1.8 (± 0.04)]	12 [6.7]	
Hydrogen peroxide		2.7 (± 0.1) [3.8 (±3)]	34 [28]	

* Calculated for non scavenged system and without hydroxylamine yield
(Explanation see paragraph last but two in chapter formaldehyde, hydroxylamine and hydrogen peroxide and scheme 3)

The data in Table 2 show that in all three cases the degradation of the compounds (without addition of •OH scavenger) is low and yields only 16% of morpholine and even less piperidine and piperazine in relation to ozone consumption. Therefore, for the complete elimination of one mole morpholine approximately six moles of ozone are required. For piperazine and piperidine the ozone consumption increased to around seven to eight moles of ozone. Using the •OH scavenger tertiary butanol, morpholine degradation in relation to ozone consumption is 27%, somewhat higher

than without scavenger (explanation see below). Piperidine and piperazine react in an analogous manner (Table 2). Thus, in the absence of •OH, for the elimination of one mole morpholine or piperazine ozone consumption decreased to approximately four moles ozone, for piperidine a value of six moles is calculated. The oxidation product *N*-hydroxypiperidine (see below) displays a similar reaction stoichiometry than the original azinanes (Table 2). In all cases a higher ozone dosage is needed for complete compound elimination when the •OH scavenger is absent. The difference in compound degradation between solutions with the presence and absence of •OH indicates that ozone consuming reactions, which do not contribute to compound degradation are much more important in the presence of •OH. This is a surprising effect, as one would expect higher yields of amine degradation when both ozone and •OH react with the amine.

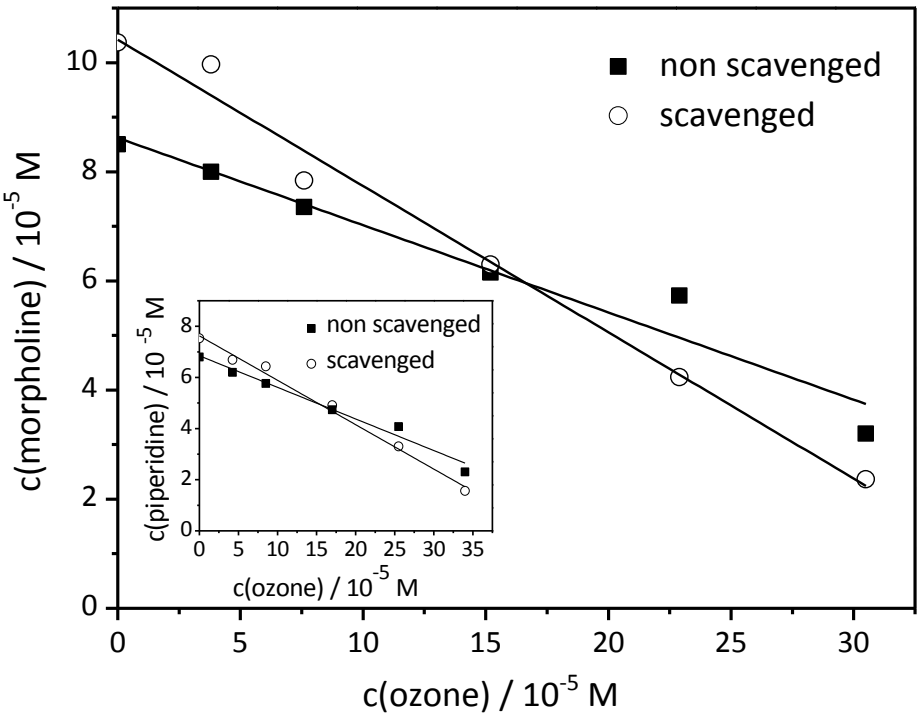

Figure 2. Amine degradation in the reaction of morpholine (main graph) and piperidine (inset) with ozone in the absence and presence of tertiary butanol c_0(0.1 M). Amine concentrations are plotted vs. the ozone concentration.

The low amine degradation is rationalized by assuming a chain reaction initiated by the radical reactions shown in Scheme 1. The chain reaction is presented in Scheme 2 (reactions (13) - (20)) using the example of piperazine. In this Scheme the reactions (13) – (14) and (16) – (17) are identical to the pathways 2 and 4 from Scheme 1 supplemented with chain reaction (15) and (18)).

Scheme 2. Chain reaction in the ozonation of piperazine.

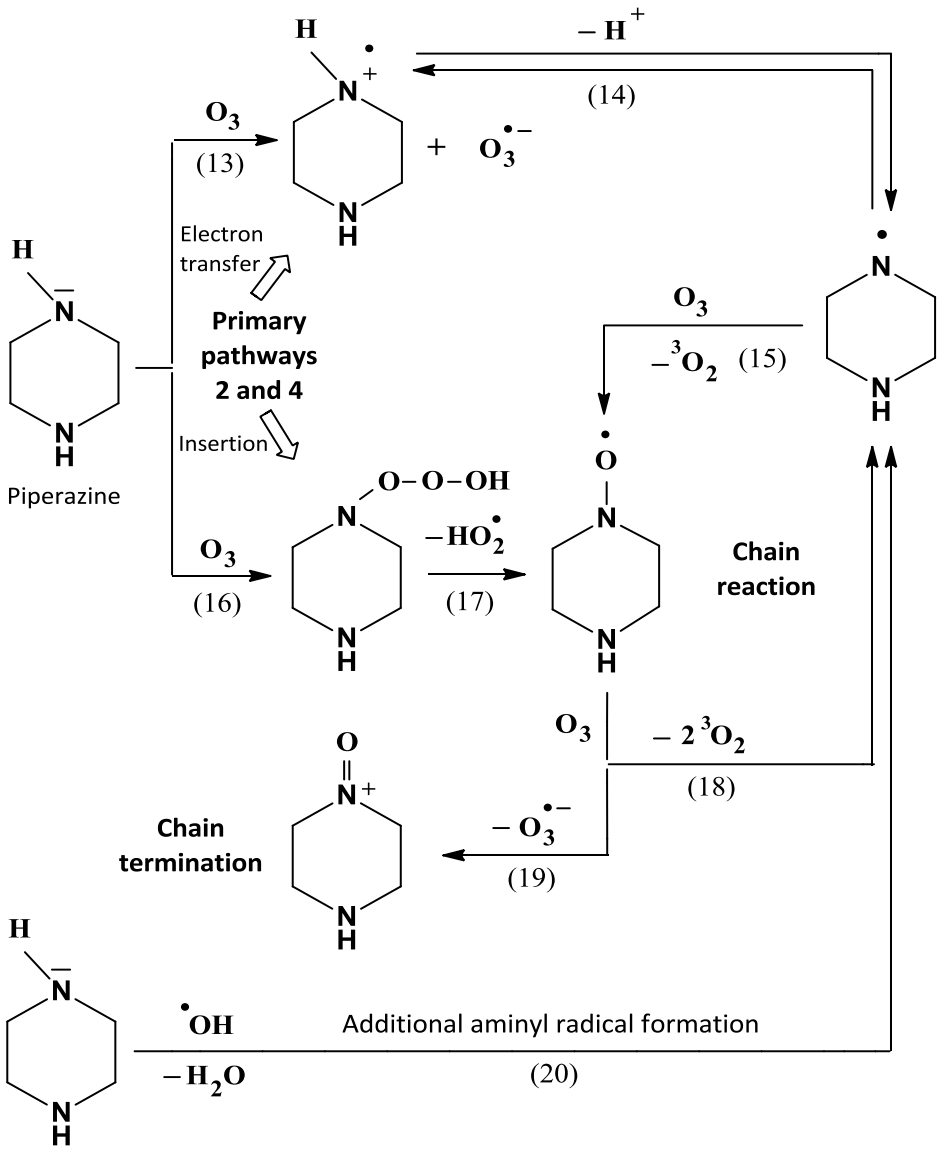

The chain reaction is most likely due to the fact that the intermediates like aminyl radicals (additionally formed in the $^{\bullet}OH$ mediated reaction (20)) react more quickly with ozone than the *N*-heterocycles. This in turn consumes ozone without further compound degradation (von Gunten, 2003a, b, Sehested et al., 1984). Aminyl radicals as N-centered radicals do not react with O_2, but can react with ozone. Rate constants

for the reaction of aminyl radicals with ozone are as yet not known, but the exergonicity of this reaction (ΔG^0 = - 77 kJ mol^{-1} for the aminyl radical of morpholine, Naumov & von Sonntag, 2011a) is remarkable and this reaction may be quite fast (von Sonntag & von Gunten, 2012). $^{\bullet}OH$ scavenging prevents the additional formation of aminyl radicals (reaction (20)) and thus reduces the concentration of chain carriers. This must lead to a higher compound degradation as observed. The chain reaction may be terminated if the nitroxyl radicals react with ozone in a possible electron transfer (reaction (19)) in competition to oxygen transfer (reaction (18)). In this reaction additional $^{\bullet}OH$ are generated. Deficits in the stoichiometry between ozone and heterocycles degradation are similar to that reported for diclofenac (Sein et al., 2008), for which it has been tentatively suggested that a chain reaction consumes ozone in competition with its reaction with the compound.

3.4.3 Product formation

***N*-Hydroxy products.** The reaction of secondary amines with ozone can give rise to their corresponding *N*-hydroxy products (similar to propranolol, Benner & Ternes, 2009b) according to the suggested reactions in Scheme 1, resulting from an ozone attack to nitrogen and subsequent addition (pathway 1). Kinetic and reaction stoichiometry experiments showed that the investigated secondary *N*-heterocycles are very reactive towards ozone (10^4 up to 10^5 M^{-1} s^{-1}), however with a moderate transformation leading to two main oxidation products in the case of piperidine detectable by HPLC-DAD (see Experimental part). For piperazine and morpholine three main products are detectable. Using t-BuOH to suppress the influence of $^{\bullet}OH$ reactions, in all cases three main products at lower and higher ozone doses were detected. The experiments were performed without pH adjustment (pH 9.8 for example for morpholine, see Table S1) and a adjusted pH of 11.5. The product formation at different pH is similar, so that further differentiations are not made. To identify these oxidation products in scavenged and non scavenged systems (without pH-adjustment) LC-HRMS measurements were used (see Experimental part and Supporting Information Text S5). In the case of piperidine and morpholine one main oxidation product, i.e., the corresponding *N*-hydroxy products (cf. *N*-hydroxy-piperidine, *m/z* 102.09122 $[M+H]^+$ and *N*-hydroxymorpholine, *m/z* 104.07040 $[M+H]^+$) could be identified by obtaining the exact masses (refer to Supporting Information Text

S5, Figure S3 and S4). In contrast, *N*-hydroxypiperazine could not be identified. Since *N*-hydroxypiperidine was available as pure compound standard, the quantification of this identified oxidation product was carried out with HPLC-DAD. The product yields increased linearly with the ozone dose, so that from the slope of the resulting graph *N*-hydroxypiperidine yields of 12% in non scavenged and 17% in the scavenged system were determined in relation to ozone concentration as shown in the main graph of Figure 3 (listed in Table 2).

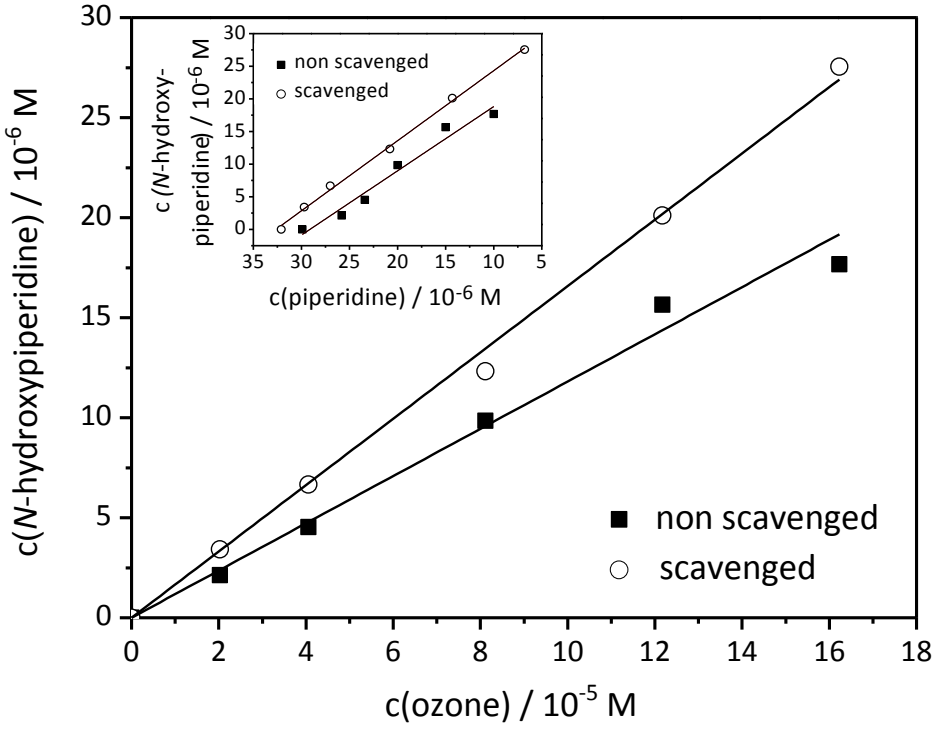

Figure 3. Main graph: *N*-Hydroxypiperidine in the reaction of piperidine $c_0(1 \times 10^{-3}$ M) with ozone. The *N*-hydroxypiperidine concentration in the presence and absence of scavenger is plotted vs. the ozone concentration, pH: 11.2, c(ozone): c(piperidine) = 1:1 – 1:5. Inset: Formation of *N*-hydroxypiperidine vs. degradation of piperidine by ozonolysis, pH: 11.2, c(ozone): c(piperidine) = 1:1 – 1:5.

A plot of the formation of *N*-hydroxypiperidine vs. piperidine degradation allows quantifying product yields in relation to compound consumption by a linear regression as illustrated in the inset of Figure 3. Here, high yields of 92% in the non scavenged and 94% in the scavenged system are deduced (on account of the low piperidine transformation, see reaction stoichiometry). Thus, referring to Scheme 1 in the reaction of piperidine with ozone the suggested addition (see above and pathway 1) is

preferential. Quantum-chemical calculations for the secondary dimethylamine by Naumov & von Sonntag (2010) indicate that the precursor of the *N*-hydroxy product of the dimethylamine is the corresponding *N*-oxide (reaction (2) in the case of the investigated piperidine), which is only a short-lived intermediate and rearranges into the isomeric *N*-hydroxy product (von Sonntag & von Gunten, 2012). Also for morpholine, ozone addition is a feasible process, since *N*-hydroxymorpholine could be detected with LC-HRMS, although to a minor extent in comparison with *N*-hydroxypiperidine (see Supporting Information Figure S3 and S4). In the reaction of piperazine with ozone, addition seems not evident, since formation of *N*-hydroxypiperazine was not observed (explanation see below). It has to be noted that a pure standard for *N*-hydroxypiperazine and *N*-hydroxymorpholine was not available, thus the identified *N*-hydroxymorpholine could not be quantified. Hence detailed data for piperazine and morpholine are still missing and will need further elucidation.

OH radical ($^{\bullet}$OH). The reaction of ozone with the *N*-heterocyclic compounds can lead to $^{\bullet}$OH (von Sonntag & von Gunten, 2012) according to the suggested reactions in Scheme 1 if ozone reacts via a radical mechanism, e.g., electron transfer or H-abstraction with the compounds (pathways 2 and 3). Besides electron transfer and H-abstraction $^{\bullet}$OH can also be formed via $O_2^{\bullet-}$, which itself is formed from the decay of the insertion product (pathway 4). In order to calculate the $^{\bullet}$OH yield the sum of methanesulfinic and methanesulfonic acid is in all cases plotted against the ozone concentration (see Experimental part, Figure 4 and Supporting Information Text S6 and Scheme S7).

The slope of the resulting graph (Figure 4) indicates $^{\bullet}$OH yields of 28 – 33% for the *N*-heterocyclic compounds (shown in Table 2). On account of these high values a second abundant oxidation pathway is in all cases a radical mechanism (e.g., electron transfer (pathway 2), H-abstraction (pathway 3) or insertion with subsequent radical formation (pathway 4)). With present data at hand a distinction between these primary radical reaction pathways based on $^{\bullet}$OH yield is not possible.

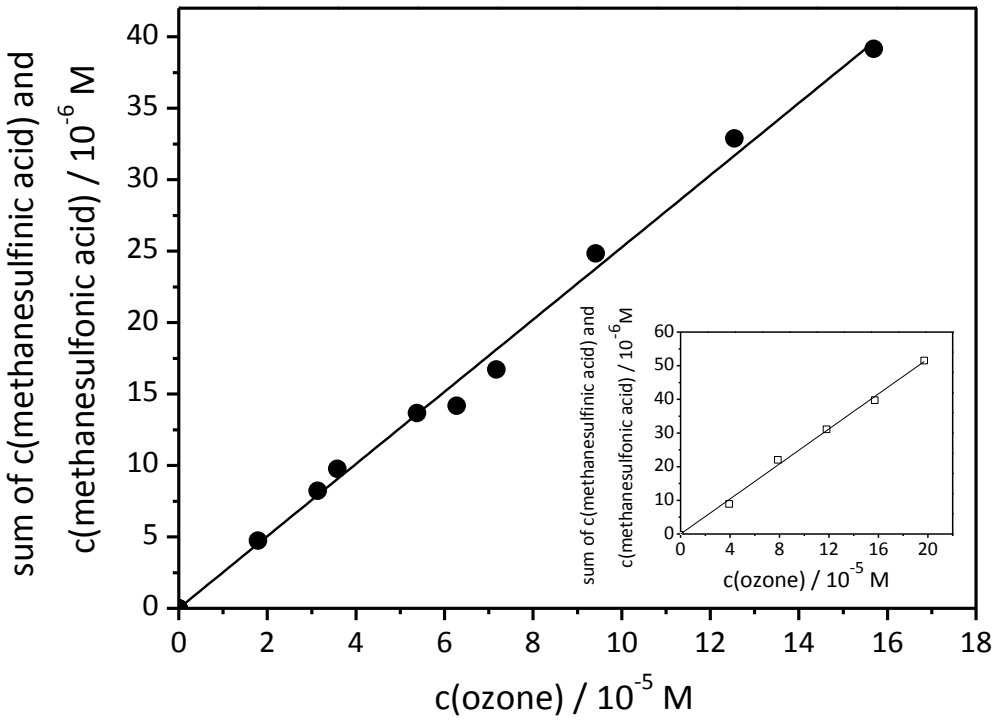

Figure 4. $^{\bullet}$OH yield in the reaction of piperidine $c_0(1 \times 10^{-3}$ M) (main graph) (pooled data of two individual experiments) and piperazine $c_0(1 \times 10^{-3}$ M) (inset) with ozone in the presence of DMSO $c_0(0.1$ M). The sum of the concentrations of methanesulfinic acid and methanesulfonic acid are plotted vs. the ozone concentration. Note, that the sum of both acids represents 92% of $^{\bullet}$OH yield (Flyunt et al., 2001a & 2003a, Veltwisch et al., 1980).

Formaldehyde, hydroxylamine and hydrogen peroxide. In the ozonation of the investigated amines, major secondary products can potentially be formaldehyde, hydrogen peroxide and hydroxylamine. The product yields of those compounds in every individual experiment (without pH adjustment, pH 9.8 – 11.2) and with varying ozone concentrations were calculated and averaged (see Experimental part and Supporting Information Text S7 and Figure S6). The corresponding data are summarized in Table 2. A plot of the concentration of generated formaldehyde vs. ozone concentration in the scavenged and non scavenged system allows quantifying yields by a linear regression as illustrated in Figure 5 for piperazine and morpholine. The slope represents the product yield of formaldehyde. In the case of piperazine (10 and 19% in non scavenged and scavenged system) and morpholine (4.3 and 8.2%)

substantial formaldehyde yields are deduced (Table 2). In contrast, in the piperidine reaction with ozone hardly any formaldehyde is formed (1.2 and 2.5%).

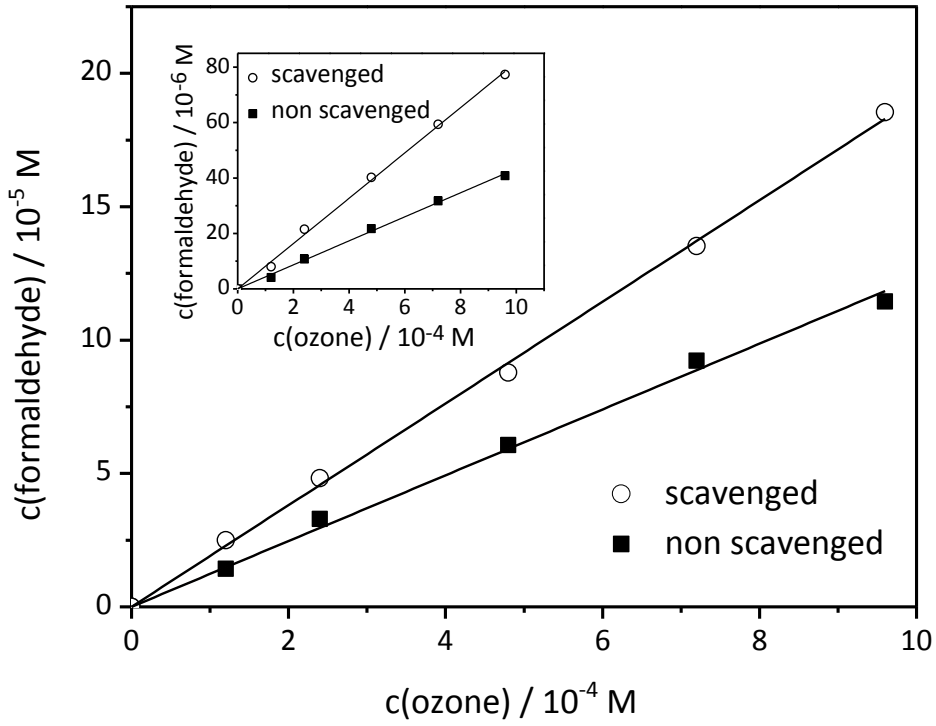

Figure 5. Main graph: Formaldehyde yield in the reaction of piperazine $c_0(1 \times 10^{-3}$ M) with ozone by Hantzsch method. Inset: Formaldehyde yield in the reaction of morpholine $c_0(1 \times 10^{-3}$ M) with ozone by Hantzsch method. Formaldehyde concentrations in the presence and absence of DMSO (0.1 M) as radical scavenger are plotted vs. the ozone concentration.

If hydrogen peroxide yields are plotted against the ozone concentration (in the presence of t-BuOH) the relation is sometimes not linear with increasing ozone concentration in the whole range. Nevertheless, according to this analysis, the yields of H_2O_2 calculated from the linear range as shown in Figure 6 are low (Table 2), while piperazine with a value of 7.2% displays the highest yield for hydrogen peroxide. In all three cases of ozone-compound systems the formaldehyde and hydrogen peroxide yield is higher in the presence of scavenger than in its absence.

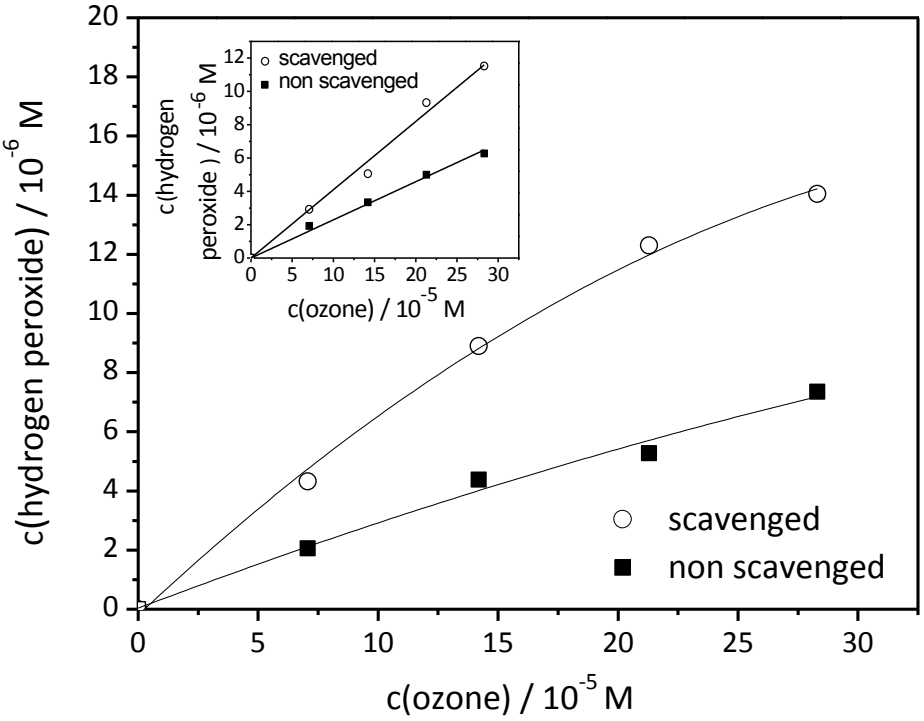

Figure 6. Hydrogen peroxide yield in the reaction of piperazine $c_0(1 \times 10^{-3}$ M) with ozone (main graph). Hydrogen peroxide yield in the reaction of morpholine (inset) $c_0(1 \times 10^{-3}$ M) with ozone. Hydrogen peroxide concentrations in the presence and absence of tertiary butanol c_0(0.1 M) are potted vs. the ozone concentration.

For hydroxylamine in all cases low yields (< 10%) were deduced (see Table 2) from the slope of the resulting graph, which at all points increased linearly with increasing ozone concentration (see Figure 7 with the example of piperazine and morpholine). In comparison piperazine reacts with ozone resulting in the highest hydroxylamine yield (7.8%). Surprisingly, in contrast to hydrogen peroxide and formaldehyde the hydroxylamine yield is lower in the presence of scavenger than in its absence, however, the difference is not really significant.

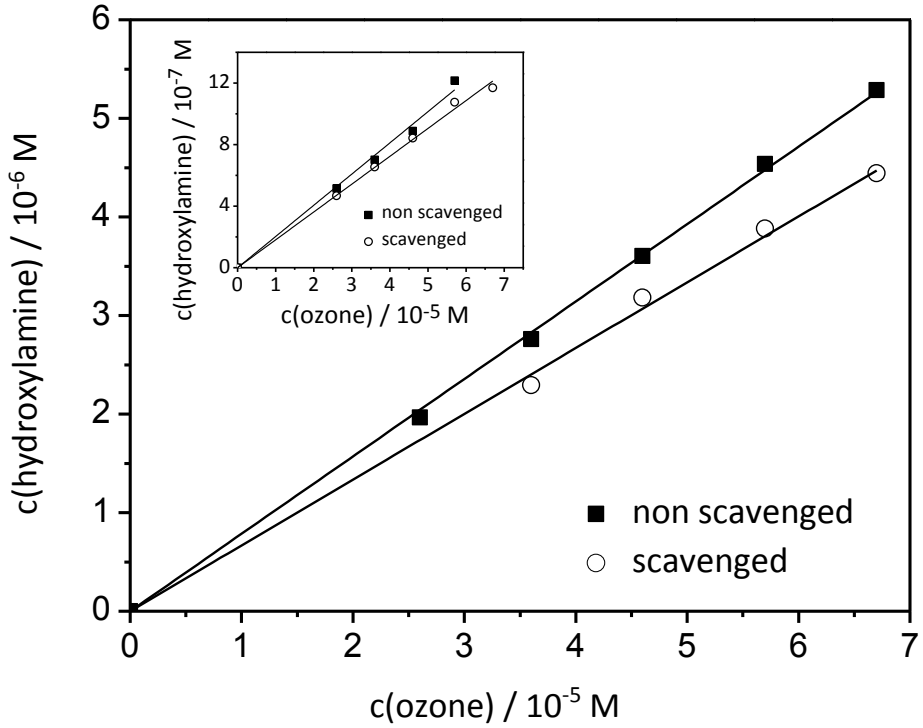

Figure 7. NH_2OH yield in the reaction of piperazine $c_0(1 \times 10^{-3}$ M) (main graph) and morpholine $c_0(1 \times 10^{-3}$ M) (inset) with ozone. Hydroxylamine concentrations in the presence and absence of tertiary butanol $c_0(0.1$ M) are plotted vs. the ozone concentration.

The observation of formaldehyde, hydroxylamine and hydrogen peroxide formation requires a mechanistic explanation. This is shown exemplarily for morpholine in Scheme 3 (products emphasized clearly with product yields in %, calculation see below). Formaldehyde can potentially be released from compound decomposition according to reactions (21) – (25). Due to the high formaldehyde yield in reference to compound degradation in the reaction of morpholine (27%) and piperazine (71%) with ozone (listed in Table 2), it is suggested that in these cases based on the pathway 2 the aminyl radical cation (reaction (22)) can rearrange into the corresponding carbon-centered radical. Such reactions are analogous to the well-documeted 1,2-H shift reactions of alkoxyl radicals (von Sonntag & von Gunten, 2012). $^{\bullet}OH$ (generated in high $^{\bullet}OH$ yield, see above) can react with the compounds under study at the C-H bond (Asmus et al., 1973) via H-abstraction (reaction (27)). This H-abstraction reaction also gives rise to C-centered radicals, which could react rapidly with oxygen (Tauber & von Sonntag, 2000) (for further information see Supporting Information Text S2). Since all

experiments are performed in air saturated solution the oxygen concentration is sufficiently high to largely favor the addition of oxygen to C-centered radicals (reaction (23)). The resulting short-lived peroxyl radical may cleave $O_2^{\bullet-}$ (reaction (24), Das et al., 1987), which furthermore can react with ozone (reaction (26)). Subsequently the developed C-centered cation can react with water (reaction (25)). The successive (base and acid catalysed) hydrolysis releases formaldehyde (see Scheme 3) in analogy to aliphatic amines (Das & von Sonntag, 1986) and can result in oxazolidine (imidazolidine in the case of piperazine, reaction not shown) according to reaction (25). For the ozone-piperidine system this reaction appears as well, but obviously does not play an important role.

The formation of hydrogen peroxide is as well an indication that after ozone or $^{\bullet}OH$ attack and subsequent O_2 addition unstable peroxidic intermediates are formed (Schuchmann & von Sonntag, 1979, von Sonntag & Schuchmann, 1997). These short-lived peroxyl radicals could in principle undergo dimerization to form short-lived tetraoxides (see Scheme 3, reaction (28), well established in organic solvents, Bennett et al., 1970). The hydrogens can take part in the decay of the tetraoxides by forming two equivalent of morpholin-2-one (in the case of morpholine) and one equivalent of hydrogen peroxide (reaction (29)) according to the Bennett mechanism (Bennett & Summers, 1974, Bothe & Schulte-Frohlinde, 1978). For the reactions ozone-morpholine and ozone-piperazine this reaction pathway can play an important role. In the reaction of piperidine with ozone the absence of significant amounts of hydrogen peroxide indicates that the Bennett mechanism and thus also the subsequent reactions are not relevant. In principle the formation of hydrogen peroxide may occur from an insertion process leading to hydrogen peroxide radical, $HO_2^{\bullet}$ (see pathway 4). The hydrogen peroxide radical can combine with another hydrogen peroxide radical to hydrogen peroxide (Bielski et al., 1985; von Sonntag and von Gunten, 2012). A similar, however, non radical reaction is described for *N*-phenylmorpholine in organic solvents (Suarez-Bertoa et al., 2012). In our system these reactions can be ruled out on the one hand due to basic experimental conditions (pK_a ($HO_2^{\bullet}$) = 4.8, refer to Introduction, Bielski et al., 1985) and on the other hand because of the hydrogen at the nitrogen in contrast to *N*-phenylmorpholine.

Hydroxylamine can be formed from compound decomposition of the generated *N*-hydroxyheterocycles (e.g., for *N*-hydroxymorpholine this is shown in Scheme 3, reactions (30) – (36)) in analogy to the above-documented reaction of morpholine (or piperazine) with ozone or $^{\bullet}OH$ (Scheme 3, reactions (21) – (25)). For example unstable peroxidic intermediates (reaction (33)) can be formed from *N*-hydroxymorpholine (detected with LC-HRMS) after ozone or $^{\bullet}OH$ attack and subsequent O_2 addition.

In the same way the short-lived peroxyl radicals can give rise to C-centered cation (reaction (34)) and subsequently release formaldehyde to generate *N*-hydroxy-oxazolidine (reaction (35)). If *N*-hydroxyoxazolidine undergoes a fast further decomposition, hydroxylamine (see Table 2, found in relative amounts) and 2*H*-oxet (reaction (36)) are formed. In analogous manner this reaction pathway may occur with *N*-hydroxypiperazine. Thus, hydroxylamine is also found in high relative amounts (Table 2), so that after the release of formaldehyde from the generated *N*-hydroxyimidazolidine hydroxylamine and azacyclobutene could be formed. In a minor extent this reaction pathway might equally occur with *N*-hydroxypiperidine by releasing the appropriate *N*-hydroxypyrrolidine and cyclobutene. The higher formaldehyde and hydroxylamine yield in the case of piperazine and consequential high decomposition of the *N*-hydroxypiperazine can possibly explain why in contrast to *N*-hydroxypiperidine and *N*-hydroxymorpholine no *N*-hydroxypiperazine could be detected in LC-HRMS analysis. Furthermore, the results of the hydroxylamine yield also might explain that the addition reaction (pathway 1) takes place to a minor extent in the ozonation of morpholine and piperazine, however, the generated *N*-hydroxy products are decomposed in further reactions (Scheme 3). Since pure compounds of imidazolidine and *N*-hydroxyimidazolidine were not available (neither oxazolidine, *N*-hydroxyoxazolidine and *N*-hydroxypyrrolidine) the reactions could not definitely be proven, but seem very likely. Not surprisingly, it has to be noted that in the reaction of piperidine with ozone no pyrrolidine (which was commercially available) has been found. The reason for the differences in the ozone reactions of piperidine, piperazine and morpholine are not fully understood, yet.

Scheme 3. Formation of formaldehyde, hydrogen peroxide and hydroxylamine in the reaction of morpholine with ozone.

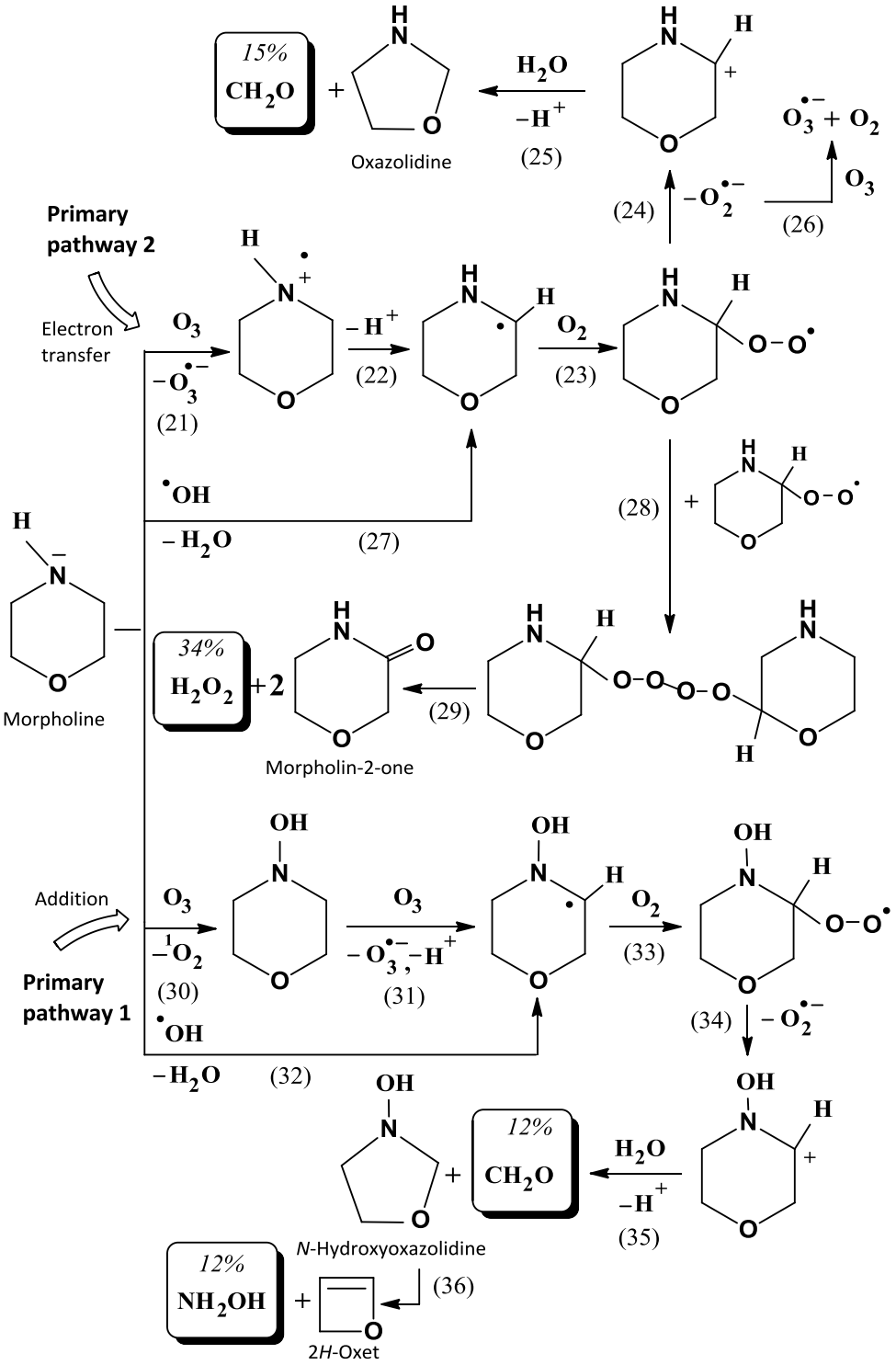

The above mechanistic considerations cannot rationalize why *N*-hydroxypiperidine formation is so largely favored over the formation of *N*-hydroxypiperazine and *N*-hydroxymorpholine. One reason could be that the latter oxidation products react faster with ozone compared to their precursors, or •OH reacts to a larger extent with

N-hydroxymorpholine and *N*-hydroxypiperazine. There is evidence that without scavenging an additional attack of $^{\bullet}OH$ forms more hydroxylamine (Table 2). It has to be noted that *N*-hydroxypiperidine reacts with ozone more or less in the same manner as piperidine based on kinetic and stoichiometry results (refer to Table 2).

3.4.4 Mass balances and mechanistic considerations

From data of all products and their yields (in mole per mole of ozone and mole compound) compiled in Table 2 it can be seen that in the case of piperidine and piperazine a closed mass balance has been obtained, whereas it is around 60% complete in the case of morpholine. The reason for the incomplete mass balance in this case is probably the missing *N*-hydroxymorpholine quantification, which could close the gap. The sum is computed with formaldehyde and hydrogen peroxide but without hydroxylamine, since it is formed in the same reaction sequence as formaldehyde (see Scheme 3). The ratio of the product yield in absence and presence of scavenger is in all cases in good accordance with the ratio of the compound consumption in absence and presence of scavenger.

In the reaction of piperidine with ozone, addition as a non radical pathway is the preferred primary reaction (more than 90%). Only less than 10% are transformed through primary radical reactions. In the case of morpholine, ozone addition may be at least a feasible primary pathway, based on the detected *N*-hydroxymorpholine and 12% hydroxylamine release (see Scheme 3). Another main primary reaction pathway may proceed after ozone attack via a radical mechanism (see Scheme 3, reaction (21)) with an extent of around 50%. This is evaluated from the corresponding secondary products: hydrogen peroxide (34%) and formaldehyde (15%, calculated from the total formaldehyde yield (27%, see Table 2) minus hydroxylamine yield in %, see above) of the pathway 2 (shown in Table 2 and Scheme 3). The reaction of piperazine with ozone resembles that of morpholine, however, the primary radical reaction pathway (e.g., electron transfer) occurs to a higher extent (around 60%, secondary products: hydrogen peroxide (44%) and formaldehyde (15%, calculation see above) shown in Table 2). Ozone addition could also occur (around 50%) deduced from the high hydroxylamine yield, in spite of the not detected *N*-hydroxypiperazine. Based on the lower formaldehyde and hydrogen peroxide yield (in reference to compound

consumption, see Table 2) in the case of morpholine and piperazine in the non scavenged system, $^{\bullet}$OH attack to the C-H bond of the genuine compound should play a subordinate role (reaction (27)). However, because of the sufficient difference in hydroxylamine yield between the scavenged and the non scavenged system, $^{\bullet}$OH attack to the C-H bond of *N*-hydroxy products should be more important (reaction (32)). In all of the above mentioned reactions $^{\bullet}$OH could be formed in primary (reaction (21)) and secondary reactions (reactions (24), (31) and (34)) and just as well consumed (reactions (27) or (32)), so that the $^{\bullet}$OH yield cannot be considered in the mass balance.

3.5 Conclusions

The present study shows that upon ozonation of piperidine, piperazine and morpholine as secondary amines in aqueous solution several radical and nonradical processes take place. The mechanisms of the three investigated amines in their reaction with ozone could tentatively be proposed. Although there are considerable similarities between the selected amines in their reaction with ozone, there are also marked differences despite the structural similarity. The presented results may help to explain transformation kinetics and products in the reaction of more complex micropollutants containing an *N*-heterocyclic amine as structural unit.

3.6 References

Afkhami, A., Madrakian, T., Maleki, A., 2006. Indirect kinetic spectrophotometric determination of hydroxylamine based on its reaction with iodate. Analytica Sci 22, 329-331.

Allen, A. O., Hochanadel, C. J., Ghormley, J. A., Davis, T. W., 1952. Decomposition of water and aqueous solutions under mixed fast neutron and gamma radiation. J Phys Chem 56, 575-586.

Asmus, K.-D., Möckel, H., Henglein, A., 1973. Pulse radiolytic study of the site of $^{\bullet}$OH radical attack on aliphatic alcohols in aqueous solution. J Phys Chem 77, 1218-1221.

Beltrán, F. J., Encinar, J. M., Alonso, M. A., 1998. Nitroaromatic hydrocarbon ozonisation in water: 1: single ozonation. Ind Eng Chem Res 37, 25-31.

Benitez, F. J., Acero, J. L., Real, F. J., Roldan, G., Casas, F., 2011. Comparison of different chemical oxidation treatments for the removal of selected pharmaceuticals in water matrices. Chem Eng J 168, 1149–1156.

Benner, J., Salhi, E., Ternes, T. A., von Gunten, U., 2008. Ozonation of reverse osmosis concentrate: kinetics and efficiency of beta blocker oxidation. Wat Res 42, 3003-3012.

Benner, J., Ternes, T. A., 2009a. Ozonation of metoprolol: elucidation of oxidation pathways and major oxidation products. Environ Sci Technol 43, 5472-5480.

Benner, J., Ternes, T. A., 2009b. Ozonation of propranolol: formation of oxidation products. Environ Sci Technol 43, 5086-5093.

Bennett, J. E., Brown, D. M., Mile, B., 1970. Studies by electron spin resonance of the reactions of alkylperoxy radicals. Part 2. Equilibrium between alkylperoxy radicals and tetroxide molecules. Trans Faraday Soc 66, 397-405.

Bennett, J. E., Summers, R., 1974. Product studies of the mutual termination reactions of sec-alkylperoxy radicals: evidence for non-cyclic termination. Can J Chem 52, 1377-1379.

Benotti, M. J., Trenholm, R. A., Vanderford, B. J., Holady, J. C., Stanford, B. D., Snyder, S. A., 2009. Pharmaceuticals and endocrine disrupting compounds in US drinking water. Environ Sci Technol 43, 597-603.

Bielski, B. H. J., Cabelli, D. E., Arudi, R. L., Ross, A. B., 1985. Reactivity of HO_2/O_2^- radicals in aqueous solution. J Phys Chem Ref Data 14, 1041-1100.

Bothe, E., Schulte-Frohlinde, D., von Sonntag, C., 1978. Radiation chemistry of carbohydrates. Part 16. Kinetics of $HO_2^\bullet$ elimination from peroxyl radicals derived from glucose and polyhydric alcohols. J Chem Soc, Perkin Trans 2, 416-420.

Boxall, A., Keller, V. D. J., Straub, J. O., Monteiro, S. C., Fussell, R., Williams, R. J., 2014. Exploiting monitoring data in environmental exposure modelling and risk assessment of pharmaceuticals. Environ Int 73, 175-185.

Bühler, R. E., Staehelin, J., Hoigné, J., 1984. Ozone decomposition in water studied by pulse radiolysis. HO_2/O_2^- and HO_3/O_3^- as intermediates. J Phys Chem 88, 2560-2564.

Buxton, G. V., Greenstock, C. L., Helman, W. P., Ross, A. B., 1988. Critical review of rate constants for reactions of hydrated electrons, hydrogen atoms and hydroxyl radicals (OH/O^-) in aqueous solution. J Phys Chem Ref Data 17, 513-886.

Cocheci, V., Gerasimov, E., Csunderlik, C., Cotarca, L., Nov, A., 1989. Ozone oxidation of alkylamines in aqueous solution. - I. Rate constants of ozone reactions with primary, secondary and tertiary amines. Revue roumaine de chimie, 749-57.

Das, S., von Sonntag, C., 1986. Oxidation of trimethylamine by OH radicals in aqueous solution as studied by pulse radiolysis, ESR and product analysis. The reactions of the alkylamine radical cation, the aminoalkyl radical and the protonated aminoalkyl radical. Z Naturforsch B 41, 504-513.

Das, S., Schuchmann, M. N., Schuchmann, H.-P., von Sonntag, C., 1987. The production of the superoxide radical anion by the OH radical-induced oxidation of trimethylamine in oxygenated aqueous solution. The kinetics of the hydrolysis of (hydroxymethyl)-dimethylamine. Chem Ber 120, 319-323.

Deblonde, T., Cossu-Leguille, C., Hartemann, P., 2011. Emerging pollutants in waste-water: a review of the literature. Int J Hyg Environ Health 214, 442-448.

Dodd, M. C., Buffle, M.-O., von Gunten, U., 2006a. Oxidation of antibacterial molecules by aqueous ozone: moiety-specific kinetics and application to ozone-based wastewater treatment. Environ Sci Technol 40, 1969-1077.

Doré, M., Langlais, B., Legube, B., 1980. Mechanism of the reaction of ozone with soluble aromatic pollutants. Ozone Sci Eng 2, 39-54.

Dowideit, P., von Sonntag, C., 1998. The reaction of ozone with ethene and its methyl- and chlorine-sustituted derivatives in aqueous solution. Environ Sci Technol 32, 1112-1119.

Elliot, A. J., McCracken, D. R., 1989. Effect of temperature on $O^{\bullet-}$ reactions and equilibria: a pulse radiolysis study. Radiat Phys Chem 33, 69-74.

Elmghari-Tabib, M., LaPlanche, A., Venien, F., Martin, G., 1982. Ozonation of amines in aqueous solutions. Wat Res 16, 223-229.

Flyunt, R., Makogon, O., Schuchmann, M. N., Asmus, K.-D., von Sonntag, C., 2001a. The OH-radical-induced oxidation of methanesulfinic acid. The reactions of the methyl-sulfonyl radical in the absence and presence of dioxygen. J Chem Soc, Perkin Trans 2, 787-792.

Flyunt, R., Theruvathu, J. A., Leitzke, A., von Sonntag, C., 2002. The reactions of thymine and thymidine with ozone. J Chem Soc, Perkin Trans 2, 1572-1582.

Flyunt, R., Leitzke, A., Mark, G., Mvula, E., Reisz, E., Schick, R., von Sonntag, C., 2003a. Determination of $^{\bullet}OH$ and $O_2^{\bullet-}$, and hydroperoxide yields in ozone reactions in aqueous solutions. J Phys Chem B 107, 7242-7253.

Flyunt, R., Leitzke, A., von Sonntag, C., 2003b. Characterisation and quantitative determination of (hydro)peroxides formed in the radiolysis of dioxygen-containing systems and upon ozonolysis. Radiat Phys Chem 67, 469-473.

Forni, L., Bahnemann, D., Hart, E. J., 1982. Mechanism of the hydroxide ion initiated decomposition of ozone in aqueous solution. J Phys Chem 86, 255-259.

Gabet-Giraud, V., Miège, C., Choubert, J. M., Ruel, S. M., Coquery, M., 2010. Occurrence and removal of estrogens and beta blockers by various processes in wastewater treatment plants. Sci Total Environ 408, 4257-4269.

Gilbert, E., Zinecker, H., 1980. Ozonization of aromatic amines in water. Ozone Sci Eng 2, 65-74.

Hart, E. J., Sehested, K., Holcman, J., 1983. Molar absorptivities of ultraviolet and visible bands of ozone in aqueous solutions. Anal Chem 55, 46-49.

Hoigné, J., Bader, H., 1983a. Rate constants of reactions of ozone with organic and inorganic compounds in water. - I. Non-dissociating organic compounds. Wat Res 17, 173-183.

Hoigné, J., Bader, H., 1983b. Rate constants of reactions of ozone with organic and inorganic compounds in water. - II. Dissociating organic compounds. Wat Res 17, 185-194.

Huber, M. M., Canonica, S., Park, G.-Y., von Gunten, U., 2003. Oxidation of pharamceuticals during ozonation and advanced oxidation processes. Environ Sci Technol 37, 1016-1024.

Huber, M. M., Ternes, T. A., von Gunten, U., 2004. Removal of estrogenic activity and formation of oxidation products during ozonation of 17α-ethinylestradiol. Environ Sci Technol 38, 5177-5186.

Huber, M. M., Göbel, A., Joss, A., Hermann, N., Löffler, D., McArdell, C. S., Ried, A., Siegrist, H., Ternes, T. A., von Gunten, U., 2005. Oxidation of pharmaceuticals during ozonation of municipal wasterwater effluents: a pilot study. Environ Sci Technol 39, 4290-4299.

Huggett, D. B., Brooks, B. W., Peterson, B., Foran, C. M., Schlenk, D., 2002. Toxicity of select beta adrenergic receptor-blocking pharmaceuticals (B-blockers) on aquatic organisms. Arch Environ Contam Toxicol 43, 229–235.

Kim, I. H., Yamashita, N., Kato, Y., Tanaka, H., 2009. Discussion on the application of UV/H2O2, O3 and O3/UV processes as technologies for sewage reuse considering the removal of pharmaceuticals and personal care products. Wat Sci Tech 59, 945–955.

Kitsuka, K., Mohammad, A. M., Awad, M. I., Kaneda, K., Ikematsu, M., Iseki, M., Mushiake, K., Ohsaka, T., 2007. Simultaneous spectrophotometric determination of ozone and hydrogen peroxide. Chem Letters 36, 1396-1397.

Küster, A., Alder, A. C., Escher, B. I., Duis, K., Fenner, K., Garric, J., Hutchinson, T. H., Lapen, D. R., Péry, A., Römbke, J., Snape, J., Ternes, T. A., Topp, E., Wehrhan, A., Knackerk, T., 2010. Environmental risk assessment of human pharmaceuticals in the European union: a case study with the B-blocker atenolol. Integr Environ Assess Manag 6, 514–523.

Lee, Y., von Gunten, U., 2010. Oxidative transformation of micropollutants during municipal wastewater treatment: comparison of kinetic aspects of selective (chlorine, chlorine dioxide, ferrateVI and ozone) and non-selective oxidants (hydroxyl radical). Wat Res 44, 555-566.

Leitzke, A., Flyunt, R., Theruvathu, J. A., von Sonntag, C., 2003. Ozonolysis of vinyl compounds, CH_2=CH-X, in aqueous solution – the chemistries of the ensuing formyl compounds and hydroperoxides. Org Biomol Chem 1, 1012-1019.

Lipari, F., Swarin, S. J., 1982. Determination of formaldehyde and other aldehydes in automobile exhaust with an improved 2,4-dinitrophenylhydrazine method. J Chrom 247, 297-306.

Martínez Bueno, M. J., Ulaszewska, M. M., Gomez, M. J., Hernando, M. D., Fernández-Alba, A. R., 2012. Simultaneous measurement in mass and mass/mass mode for accurate qualitative and quantitative screening analysis of pharmaceuticals in river water. J Chrom A 1256, 80–88.

Merényi, G., Lind, J., Naumov, S., von Sonntag, C., 2010b. The reaction of ozone with the hydroxide ion. Mechanistic considerations based on thermokinetic and quantum-chemical calculations. The role of HO_4^- in superoxide dismutation. Chem Eur J 16, 1372-1377.

Muñoz, F., von Sonntag, C., 2000a. Determination of fast ozone reactions in aqueous solution by competition kinetics. J Chem Soc, Perkin Trans 2, 661-664.

Muñoz, F., von Sonntag, C., 2000b. The reaction of ozone with tertiary amines including the complexing agents nitrilotriacetic acid (NTA) and ethylenediaminetetra-acetic acid (EDTA) in aqueous solution. J Chem Soc, Perkin Trans 2, 2029-2033.

Muñoz, F., Mvula, E., Braslavsky, S. E., von Sonntag, C., 2001. Singlet dioxygen formation in ozone reactions in aqueous solution, J Chem Soc, Perkin Trans 2, 1109-1116.

Mvula, E., von Sonntag, C., 2003. Ozonolysis of phenols in aqueous solution. Org Biomol Chem 1, 1749-1756.

Nash, T., 1953. The colorimetric estimation of formaldehyde by means of the Hantzsch reaction. Biochem J 55, 416-421.

Naumov, S., von Sonntag, C., 2010. Quantum chemical studies on the formation of ozone adducts to aromatic compounds in aqueous solution. Ozone Sci Eng 32, 61-65.

Naumov, S., von Sonntag, C., 2011a. Standard Gibbs free energies of reactions of ozone with free radicals in aqueous solution − Quantum chemical calculations. Environ Sci Technol 45, 9195-9204.

Naumov, S., von Sonntag, C., 2011b. The reaction of $^{\bullet}OH$ with O_2, the decay of $O_3^{\bullet-}$ and the pK_a of $HO_3^{\bullet-}$ − Interrelated questions in aqueous free-radical chemistry. J Phys Org Chem 24, 600-602.

Neta, P., Huie, R. E., Ross, A. B., 1988. Rate constants for reactions of inorganic radicals in aqueous solution. J Phys Chem Ref Data 17, 1027-1284.

Nöthe, T., Hartmann, D., von Sonntag, J., von Sonntag, C., Fahlenkamp, H., 2007. Elimination of the musk fragrances galaxolide and tonalide from wastewater by ozonation and concomitant stripping. Wat Sci Tech 55, 287-292.

Nöthe, T., Fahlenkamp, H., von Sonntag, C., 2009. Ozonation of wastewater: rate of ozone consumption and hydroxyl radical yield. Environ Sci Technol 43, 5990-5995.

Pietsch, J., Hampel, S., Schmidt, W., Brauch, H.-J., Worch, E., 1996. Determination of aliphatic and alicyclic amines in water by gas and liquid chromatography after derivatisation by chloroformates. Fresenius J Anal Chem 355, 164-173.

Pietsch, J., Schmidt, W., Brauch, H.-J., Worch, E., 1999. Kinetic and mechanistic studies of the ozonation of alicyclic amines. Ozone Sci Eng 21, 23-37.

Pryor, W. A., Giamalva, D. H., Church, D. F., 1984. Kinetics of ozonation. 2. Amino acids and model compounds in water and comparison to rates in non polar solvents. J Am Chem Soc 106, 7094-7100.

Ragnar, M., Eriksson, T., Reitberger, T., 1999a. Radical formation in ozone reactions with lignin and carbohydrate model compounds. Holzforschung 53, 292-298.

Schmidt, C. K., Brauch, H.-J., 2008. *N,N*-Dimethylsulfamide as precursor for *N*-nitrosodimethylamine (NDMA) formation upon ozonation and its fate during drinking water treatment. Environ Sci Technol 42, 6340-6346.

Schuchmann, M. N., von Sonntag, C., 1979. Hydroxyl radical-induced oxidation of 2-methyl-2-propanol in oxygenated aqueous solution. A product and pulse radiolysis study. J Phys Chem 83, 780-784.

Schwarzenbach, R. P., Escher, B. I., Fenner, K., Hofstetter, T. B., Johnson, C. A., von Gunten, U., Wehrli, B., 2006. The challenge of micropollutants in aquatic systems. Science 313, 1072-1077.

Sehested, K., Holcman, J., Hart, E. J., 1983. Rate constants and products of the reactions of e^-, O_2^- and H with ozone in aqueous solutions. J Phys Chem 87, 1951-1954.

Sehested, K., Holcman, J., Bjergbakke, E., Hart, E. J., 1984. A pulse radiolytic study of the reaction OH + O_3 in aqueous medium. J Phys Chem 88, 4144-4147.

Sein, M. M., Zedda, M., Tuerk, J., Schmidt, T. C., Golloch, A., von Sonntag, C., 2008. Oxidation of diclofenac with ozone in aqueous solution. Environ Sci Technol 42, 6656-6662.

Shang, N.-C., Yu, Y.-H., 2001. Toxicity and color formation during ozonation of mono-substituted aromatic compounds. Environ Technol 23, 43-52.

Staehelin, J., Hoigné, J., 1982. Decomposition of ozone in water: rate of initiation by hydroxide ions and hydrogen peroxide. Environ Sci Technol 16, 676-681.

Staehelin, J., Bühler, R. E., Hoigné, J., 1984. Ozone decomposition in water studied by pulse radiolysis. 2. OH and HO_4 as chain intermediates. J Phys Chem 88, 5999-6004.

Staehelin, J., Hoigné, J., 1985. Decomposition of ozone in water in the presence of organic solutes acting as promoters and inhibitors of radical chain reactions. Environ Sci Technol 19, 1206-1213.

Suarez-Bertoa, R., Saliu, F., Bruschi, M., Rindone, B., 2012. Reaction products and mechanism of the regioselective oxidation of *N*-phenylmorpholine by ozone. Tetrahedron 68, 8267-8275.

Takacs-Novak, K., Box, K. J., Avdeef, A., 1997. Potentiometric pK(a) determination of water-insoluble compounds: validation study in methanol/water mixtures. Int J Pharm 151, 235-248.

Tauber, A., von Sonntag, C., 2000. Products and kinetics of the OH-radical-induced dealkylation of atrazine. Acta Hydrochim Hydrobiol 28, 15-23.

Ternes, T. A., 1998. Occurrence of drugs in german sewage treatment plants and rivers. Wat Res 32, 3245-3260.

Ternes, T. A., Meisenheimer, M., McDowell, D., Sacher, F., Brauch, H.-J., Haist-Gulde, B., Preuss, G., Wilme, U., Zulei-Seibert, N., 2002. Removal of pharmaceuticals during drinking water treatment. Environ Sci Technol 36, 3855-3863.

Ternes, T. A., Joss, A., 2006. Human pharmaceuticals, hormones and fragrances. The challenge of micropollutants in urban water management. IWA Publishing, London, New York.

Ternes, T. A., Joss, A., Oehlamann, J., 2015. Occurrence, fate, removal and assessment of emerging contaminants in water in the water cycle (from wastewater to drinking water). Wat Res 72, 1-2.

Theruvathu, J. A., Flyunt, R., Aravindakumar, C. T., von Sonntag, C., 2001. Rate constants of ozone reaction with DNA, its constituents and related compounds. J Chem Soc, Perkin Trans 2, 269-274.

Tyupalo, N. F., Yakobi, Y. A., 1980. The reactions of ozone with manganese(II) and manganese(III)ions in sulphuric acid. Russ J Inorg Chem 25, 865-868.

Veltwisch, D., Janata, E., Asmus, K.-K., 1980. Primary processes in the reactions of $^{\bullet}OH$ radicals with sulphoxides. J Chem Soc, Perkin Trans 2, 146-153.

von Gunten, U., 2003a. Ozonation of drinking water. Part I. Oxidation kinetics and product formation. Wat Res 37, 1443-1467.

von Gunten, U., 2003b. Ozonation of drinking water. Part II. Desinfection and by-product formation. Wat Res 37, 1469-1487.

von Gunten, U., Salhi, E., Schmidt, C. K., Arnold, W. A., 2010. Kinetics and mechanisms of *N*-nitrosodimethylamine formation upon ozonation of *N*,*N*-dimethylsulfamide-containing waters: bromide catalysis. Environ Sci Technol 44, 5762-5768.

von Sonntag, C., 2007. The basics of oxidants in water treatment. Part A: OH radical reactions. Wat Sci Tech 55, 19-23.

von Sonntag, C., 2008. Advanced oxidation processes: mechanistic aspects. Wat Sci Tech 58, 19-23.

von Sonntag, C., Schuchmann, H.-P., 1997. Peroxylradicals in aqueous solution. In: Peroxyl Radicals, Z. B. Alfassi (ed.), Wiley, Chichester, 173-234.

von Sonntag, C., von Gunten, U., 2012. Chemistry of ozone in water and wastewater treatment. From basic principles to applications. IWA Publishing

Zimmermann, S. G., Schmukat, A., Schulz, M., Benner, J., von Gunten, U., Ternes, T. A., 2012. Kinetic and mechanistic investigations of the oxidation of tramadol by ferrate and ozone. Environ Sci Technol 46, 876-884.

3.7 Acknowledgment

The authors are deeply thankful for the expert advice of Prof. Clemens von Sonntag. With his great knowledge and vast experience, he supported the present study.

3.8 Supporting Information of Chapter 3

Ozonation of piperidine, piperazine and morpholine: Kinetics, stoichiometry, product formation and mechanistic considerations

Agnes Tekle-Röttering, Kevin S. Jewell, Erika Reisz, Holger V. Lutze,
Thomas A. Ternes, Winfried Schmidt, Torsten C. Schmidt

Water research (2016), 88, 960-971

25 pages of Supporting Information, including 8 narrations, 8 figures, 9 schemes and 1 table

Text S1. Chemicals 140
Text S2. Sample preparation 141
Text S3. Reaction kinetics (including experimental conditions and determination of formaldehyde) 143
Text S4. Reaction stoichiometry 150
Text S5. Identification of products with LC-HRMS 152
Text S6. Determination of OH radicals ($^{\bullet}$OH) 154
Text S7. Determination of secondary products 156
Text S8. Singlet oxygen 159

Figure S1. Degree of dissociation (α) of piperazine, piperidine and morpholine
Figure S2. Calibration curves for reaction stoichiometry experiments of piperidine and piperazine in the derivatization with FMOC-Cl
Figure S3. HPLC chromatogram and mass spectrum of *N*-hydroxypiperidine in the reaction of piperidine with ozone

Figure S4. HPLC chromatogram and mass spectrum of *N*-hydroxymorpholine in the reaction of morpholine with ozone
Figure S5. Calibration curves of methanesulfinic acid and methanesulfonic acid
Figure S6. Calibration curves of formaldehyde and nitrite. Formation of nitrite from hydroxylamine in its reaction with iodate
Figure S7. Compound degradation and product yield relating to ozone consumption in the ozonation of piperidine, piperazine and morpholine in scavenged system
Figure S8. Product yield relating to compound degradation in the reaction of piperidine, piperazine and morpholine with ozone in non scavenged system

Scheme S1. Scavenging of $^{\bullet}OH$ with tertiary butanol
Scheme S2. Calculation of the rate constant if the compound is present at different protonation states
Scheme S3. Degree of dissociation (α) of the corresponding acids of the amine bases in the case of piperidine and morpholine
Scheme S4. Degree of dissociation (α) of the corresponding acids of the amine bases in the case of piperazine
Scheme S5. Competition in the reaction of piperidine and 3-buten-2-ol with ozone plus derivatization of the developed formaldehyde with DNPH
Scheme S6. Derivatization of the remained compound with FMOC-Cl in the reaction of piperidine with ozone in the ozone consumption experiment
Scheme S7. Determination of $^{\bullet}OH$ with dimethyl sulfoxide
Scheme S8. Reaction of hydroxylamine with iodate by forming nitrite
Scheme S9. Determination of hydrogen peroxide in its reaction with iodide

Table S1. Compilation of ozone rate constants of heterocyclic compounds in aqueous solution

Text S1. Chemicals

Piperidine (99%), piperazine (99%) and morpholine (99%) (all from Merck, Darmstadt, Germany) were used for investigation. For product quantification *N*-hydroxypiperidine

(96%, Aldrich, Seelze, Germany) and pyrrolidine (99%, Merck) were available as reference material. Tertiary butanol (t-BuOH) (p.a. Merck) and dimethyl sulfoxide (DMSO) (99.9%, J.T. Baker, Griesheim, Germany) were applied as radical scavenger. Cephalexin (97%) and 3-buten-2-ol (97%) (both from Alfa Aesar, Karlsruhe, Germany) were used for competition experiments. 9-Fluorenylmethyl chloroformate (FMOC-CL) (p.a.), potassium carbonate (p.a.), ammonia (25%), t-butyl methyl ether (p.s.) and toluene (p.a.) (all from Merck) were used for derivatization in compound degradation experiments. Potassium iodate (p.a.) and hydroxylamine hydrochloride (p.s.) (both from Merck) were applied for measuring hydroxylamine. Ammonium acetate (p.a.), acetic acid (100%), acetylacetone (99%), 2,4-dinitrophenylhydrazine (DNPH) (p.a.) (all from Merck) and perchloric acid (70%, p.a. Aldrich) were applied for measuring formaldehyde. Potassium hydrogen phthalate (99.5%), potassium iodide (99.5%) and ammonium heptamolybdate (99%) (all from Merck) were used for measuring hydrogen peroxide. Methanesulfinic acid (95%, Alfa Aesar) and methanesulfonic acid (p.s., Merck) were used for quantification of OH radicals. Phosphoric acid, sodium dihydrogen phosphate, sodium hydrogen phosphate and sodium hydroxide (all from Merck) were required for pH adjustment.

Text S2. Sample preparation

Glass test tubes, bottles or volumetric flasks (20 − 25 mL) closed with ground-in glass stoppers were used as reaction vessels. In order to limit losses of ozone, the flasks were kept closed during all the experimental time. The ozone solution was added (with a glass syringe, under rapid mixing) to the reaction solution containing the investigated compounds resulting in ozone to compound ratios of 1:0.1 – 1:10 at given pH (pH of the aqueous solutions with the investigated amines at the applied concentration) or adjusted pH (with sodium hydroxide or phosphate buffer, denoted later as alkalinized or buffered). Most samples were prepared without phosphate buffer (excluding kinetic experiments), because the relevant buffer species scavenge $^{\bullet}OH$ (Andreozzi et al., 2000). Dominant species and the corresponding rate constants change with pH from $H_2PO_4^-$ ($k(H_2PO_4^- + {}^{\bullet}OH) = 2.0 \times 10^4\ M^{-1}\ s^{-1}$, Buxton, 1988) in the pH range of 3.0 – 5.0 to HPO_4^{2-} ($k(HPO_4^{2-} + {}^{\bullet}OH) = 5.0 \times 10^6\ M^{-1}\ s^{-1}$, Staehelin & Hoigné, 1982) at pH around 7 to PO_4^{3-} ($k(PO_4^{3-} + {}^{\bullet}OH) = 1.0 \times 10^4\ M^{-1}\ s^{-1}$, Buxton, 1988) at pH around 12. The pH of

experimental solutions was measured by a Metrohm 620 pH meter with a glass electrode (Metrohm, Filderstadt, Germany), calibrated every time before use.

The systematic exclusion of $^{\bullet}OH$ reactions was conducted by choosing $^{\bullet}OH$ scavenger whichever react slowly with ozone but fast with $^{\bullet}OH$ (von Sonntag, 2007). In the teriary butanol (t-BuOH) assay (k(t-BuOH + $^{\bullet}OH$) = 6×10^8 M^{-1} s^{-1}) OH radicals are scavenged by their reaction with t-BuOH to formaldehyde (see Scheme S1) (Schuchmann & von Sonntag, 1979, Buxton et al., 1988, Reisz et al., 2003). Besides this, tertiary butanol (k (t-BuOH + O_3) = 0.003 M^{-1} s^{-1}) reacts with ozone at negligible rates even if present at reasonable excess (Flyunt et al., 2003a). Taking into account the concentration of t-BuOH (at most 0.1 M) and substrate (at least 1×10^{-4} M and k(piperazine + O_3) = 1.9×10^4 M^{-1} s^{-1}, lowest k in this study) in their reaction with ozone (k_{app}(t-BuOH + O_3) = 3×10^{-4} s^{-1} and k_{app}(piperazine + O_3) = 1.9 s^{-1}) the latter is still favored. For the use of DMSO see Text S6.

Scheme S1. Scavenging of $^{\bullet}OH$ with tertiary butanol

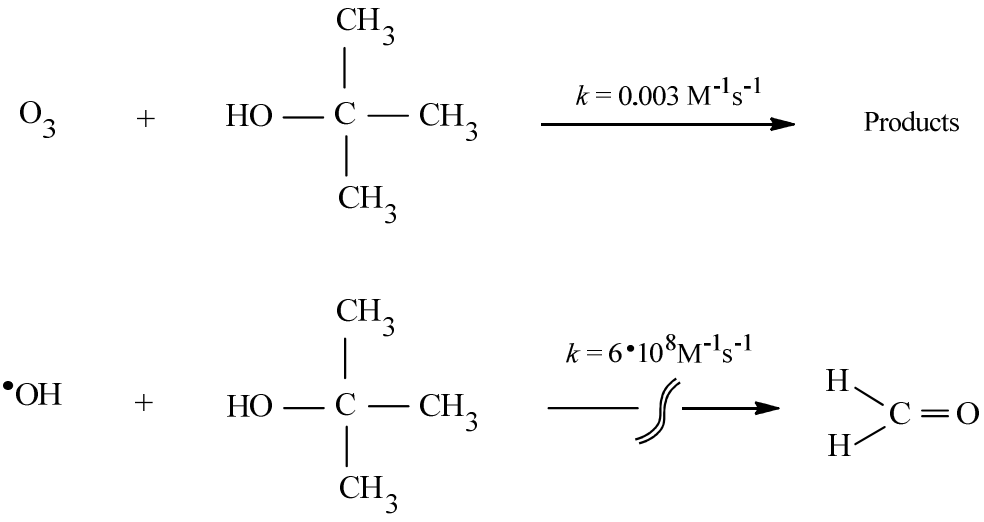

In particular, in its reaction with free radicals, ozone has to compete with oxygen. Yet, oxygen reacts only with few radical types (e.g. C-centered radicals) rapidly and irreversibly (von Sonntag & Schuchmann, 1997). Thus, ozone reacts with many free radicals effectively, despite the fact that oxygen is typically present in large excess over ozone (von Sonntag & von Gunten, 2012). Water does not react with ozone (k (H_2O + O_3) < 10^{-7} M^{-1} s^{-1}, Neta et al., 1988), but its conjugate base, OH^-, does, (Forni et al.,

1982, see Experimental part), albeit slowly and gives rise to $^{\bullet}$OH radicals (Staehelin & Hoigné, 1982, 1984, Merényi et al., 2010b). Hence, based on the possible importance of radical reactions in ozonation, in addition to the pH effects on the speciation of amines, pH is probably a main variable (Gilbert & Zinecker, 1980, Staehelin & Hoigné, 1985, Beltrán et al., 1998, von Sonntag & von Gunten, 2012). Decomposition of ozone at pH higher than 10 (reaction of $^{-}$OH with ozone gives rise to $^{\bullet}$OH, see Experimental part) is irrelevant due to the high rate constants of the amines with ozone (see Table S1). Taking into account the concentration of the hydroxide ion (e.g. 10^{-2} M at adjusted pH of 12 with sodium hydroxide) in its reaction with ozone ($k_{app}(^{-}OH + O_3)$ = 0.48 s^{-1} or 0.70 s^{-1}) this reaction can be neglected since the reaction of ozone with the amines (usually 1 × 10^{-3} M but at least 1 × 10^{-4} M and k(piperazine + O_3) = 1.9 × 10^4 M^{-1} s^{-1}, lowest k in this study) that occurs in competition is sufficiently faster (k_{app}(piperazine + O_3) ≥ 1.9 s^{-1}) under all investigated conditions and therefore still favored. Thus, $^{\bullet}$OH formation from this reaction should be low.

Text S3. Reaction kinetics (including experimental conditions and determination of formaldehyde)

Competition experiments require the measurement of only a single endpoint P, which is typically the degradation of a reactant or the formation of a product resulting from oxidation of either the compound (M) or the competitor (C). The evaluation of the reaction rate constants were conducted using equation 1 (Muñoz & von Sonntag, 2000a, Dodd et al., 2006a, Zimmermann et al., 2012),

$$\frac{[P]_0}{[P]} = 1 + \frac{k_{O_3,M}\,[M]_0}{k_{O_3,C}\,[C]_0} \qquad (1)$$

where $[P]_0$ represents the measured endpoint yield in the absence of competitor obtained from controls and [P] represents the endpoint yield in the presence of varying doses of competitor.

The rate constant of the investigated compound was determined from the slopes of plots of equation 2.

$$\frac{[P]_0}{[P]} - 1 = f\left(\frac{[M]_0}{[C]_0}\right) \qquad (2)$$

The competition kinetic method was applied because a direct determination of the rate constants according to Bader & Hoigné (1981) was not successful.

Due to the fact that ozone reacts fast with the free electron pair at nitrogen (see Introduction), protonation of amines reduces the ozone reactivity, which therefore depends on pH (von Sonntag & von Gunten, 2012). Due to the high pK_a values (see Table S1) of the investigated amines some experiments were carried out in a high pH range from 11 to 12.5 to ensure deprotonation of the corresponding acids of the amines. Under these conditions, 96% of piperidine and 100% of piperazine and morpholine are present as free amines according to Scheme S2, S3, S4 and Figure S1.

Scheme S2. Calculation of the rate constant if the compound is present at different protonation states

$$d(c(HA_{total}))/dt = (\alpha_{HA} \cdot k(O_3 + HA) + (1 - \alpha_{HA}) \cdot k(O_3 + A^-)) \cdot c(HA_{total}) \cdot c(O_3)$$

$$d(c(H_2A_{total}))/dt = (\alpha_{H_2A} \cdot k(O_3 + H_2A) + (\alpha_{HA^-} \cdot k(O_3 + HA^-) + (\alpha_{A^{2-}} \cdot k(O_3 + A^{2-})) \cdot c(H_2A_{total}) \cdot c(O_3)$$

If the compounds HA or H_2A are in equilibrium with their anions (see equilibriums below), the compounds react with ozone according to Scheme S2, where α is the degree of dissociation of the corresponding species. The degree of dissociation (see

Scheme S3, S4 and Figure S1) can be calculated on the basic of the acid dissociation constant (K_a) and the pH (von Sonntag & von Gunten, 2012).

Scheme S3. Degree of dissociation (α) of the corresponding acids of the amine bases in the case of piperidine and morpholine

$$HA + H_2O \rightleftharpoons H_3O^+ + A^-$$

$$\alpha = \frac{K_a}{c(H_3O^+) + K_a}$$

Scheme S4. Degree of dissociation (α) of the corresponding acids of the amine bases in the case of piperazine

$$H_2A + H_2O \rightleftharpoons H_3O^+ + HA^-$$

$$HA^- + H_2O \rightleftharpoons H_3O^+ + A^{2-}$$

$$\alpha_{H_2A} = \frac{c(H_3O^+)^2}{c(H_3O^+)^2 + K_{a1} \cdot c(H_3O^+) + K_{a1} \cdot K_{a2}}$$

$$\alpha_{HA^-} = \frac{K_{a1} \cdot c(H_3O^+)}{c(H_3O^+)^2 + K_{a1} \cdot c(H_3O^+) + K_{a1} \cdot K_{a2}}$$

$$\alpha_{A^{2-}} = \frac{K_{a1} \cdot K_{a2}}{c(H_3O^+)^2 + K_{a1} \cdot c(H_3O^+) + K_{a1} \cdot K_{a2}}$$

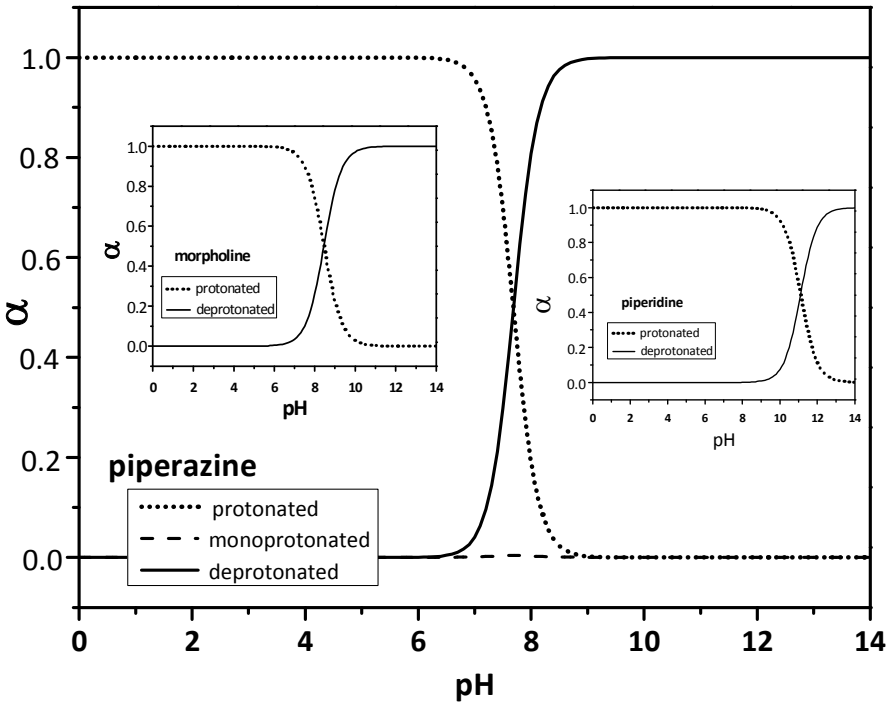

Figure S1. Degree of dissociation (α) of piperazine (main graph), piperidine and morpholine (insets)

In their reactions with ozone, nitrogen-containing compounds, e.g., amines (according to Scheme 1, pathway 2 and 3) can give rise to the formation of $^{\bullet}$OH (Muñoz & von Sonntag, 2000b) and the ensuing $^{\bullet}$OH-induced reactions can influence the kinetics considerably. For this reason, an $^{\bullet}$OH scavenger was added to test whether its presence has an influence on the rate of reaction. If 3-buten-2-ol is used as competitor tertiary butanol can no longer be added as an $^{\bullet}$OH scavenger, since t-BuOH also yields formaldehyde in $^{\bullet}$OH-induced reactions. Therefore, dimethyl sulfoxide (DMSO) was chosen as scavenger instead. Unfortunately, there were interferences in the DNPH system with DMSO, so that formaldehyde concentrations from 3-buten-2-ol were further determined with the Hantzsch method. By buffering with phosphate, there were interferences too and the use of DMSO was just as impossible, so that the experiments with DMSO were only alkalinized. Due to a higher formaldehyde formation (see paper, Table 2, description see under product formation) in the reaction of piperazine and morpholine with ozone the competition with 3-buten-2-ol potentially could yield unreliable values, even if the values were corrected for the formaldehyde obtained from substrate. In order to corroborate the rate constants

with further methods a competition with cephalexin was carried out, however, in this case in presence and absence of tertiary butanol as $^{\bullet}OH$ scavenger and buffered with phosphate.

Formaldehyde as product from the competition reaction of ozone with 3-buten-2-ol (as selected reference compound) was determined with different methods. One approach was the Hantzsch method in which diacetyldihydrolutidine (DDL) (Nash et., al 1953) was determined, another the determination as their 2,4-dinitrophenyl-hydrazones by HPLC-DAD after derivatization with 2,4-dinitrophenylhydrazine (DNPH) (Lipari & Swarin, 1982, Olson & Swarin, 1985) according to Scheme S5.

Scheme S5. Competition in the reaction of piperidine and 3-buten-2-ol with ozone plus derivatization of the developed formaldehyde with DNPH

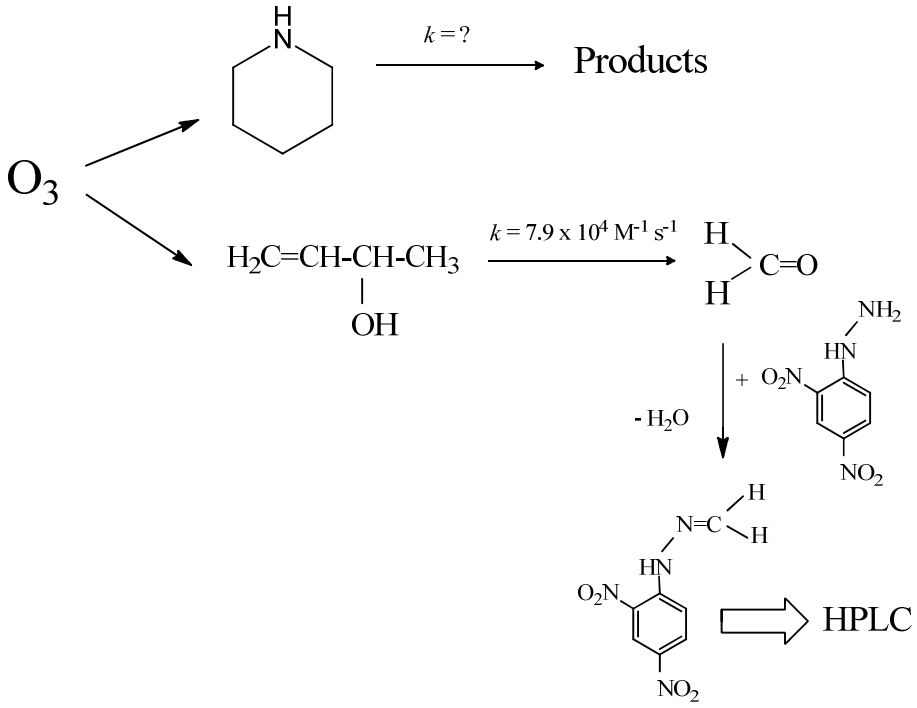

The experiments were carried out in a series of volumetric flasks (20 mL) each containing 1 mL of 3-buten-2-ol (10^{-2} – 10^{-3} M) as competitor and different volumes (0–8 mL) of compound solution (10^{-2} – 10^{-3} M) to obtain various ratios of $[M]:[C]_0$ (both in at least 10-fold molar excess to ozone). After adding appropriate volumes of

pure water to complete the solution volume to 9 mL, 1 mL ozone solution was added with a glass syringe under rapid mixing. All experiments were performed at room temperature, sometimes scavenged and at different pH values (given pH and pH 11−12.5, alkalinized with sodium hydroxide or buffered with phosphate buffer, see Text S2). After complete ozone consumption the developed formaldehyde was determined in the Hantzsch method by following its reaction with acetylacetone and ammonium ion, when a yellow compound characterized by ε(412 nm) = 7700 M^{-1} cm^{-1} (Nash, 1953) was formed. When measuring with this method, 5 mL sample were withdrawn from the batch and transferred into a volumetric flask. After that 2 mL of reagent solution (25 g ammonium acetate, 3 mL acetic acid and 0.2 mL acetylacetone filled up to 100 ml with H_2O) and 3 mL H_2O were added. The samples were heated 30 minutes in a water bath at 50°C and then measured spectrophotometrically at room temperature. For measuring the formaldehyde with DNPH (according to Scheme S5) 1.5 mL sample were withdrawn from the batch and transferred into HPLC-vials. After that 0.2 mL 2,4-dinitrophenylhydrazine solution (30 mg / 25 mL acetonitrile) and 0.1 mL $HClO_4$ (0.1 M) were added. After a reaction time of 45 minutes (in the dark) the formed 2,4-dinitrophenylhydrazone was measured by HPLC (LC20, Shimadzu, Duisburg, Germany) and DAD at a wavelength of 353 nm. The separation occurs on a C_{18} column (Prontosil, NC-04, 250 mm x 4.0 mm I.D., 5.0 µm, Bischoff, Leonberg, Germany) with the following gradient: water/acetonitrile (ACN): 35% ACN/ 2 min, 45% ACN/ 5 min, 100% ACN.

Experiments with cephalexin were carried out as described above, however, with cephalexin (10^{-2} − 10^{-3} M) as competitor, only buffered at pH 12.5. After complete ozone consumption the residual cephalexin was determined with HPLC-DAD (LC20, Shimadzu) at a wavelength of 200 nm. The separation was carried out on a C_{18} column (Synergi Hydro-RP 80 A, 150 mm x 3.0 mm I.D., 4.0 µm, Phenomenex) with the following gradient: water/acetonitrile (ACN): 10% ACN/ 10 min, 45% ACN/ 15 min, 100% ACN. The elution flow rate in both methods was 0.5 mL min^{-1} and the injection volume was 50 µL for all samples. In all cases blanks were processed in the same manner with water instead of ozone solution to determine the initial concentration.

Table S1. Compilation of ozone rate constants of heterocyclic compounds in aqueous solution, when following competitors are used: a)1: 3-buten-2-ol (for formaldehyde quantification using DNPH method) a)2: 3-buten-2-ol (for formaldehyde quantification using Hantzsch method) b) cephalexin. When using 3-buten-2-ol and cephalexin, OH radicals are scavenged with DMSO and tertiary butanol, respectively.

Compound	***k*** / M^{-1} s^{-1}	**pH conditions** (in brackets the resulting deprotonated amine yield)	pK_a (of corres-ponding acid)
Piperidine	4.13 (± 0.31) × 10^4 a)1	given, pH 11.2, (56%)	11.1*
	1.97 (± 0.52) × 10^5 a)1	alkalinized, pH 11.5, (72%)	
	1.10 (± 0.70) × 10^5 a)2	buffered, pH 12.5, (96%)	
	1.56 (± 0.79) × 10^5 a)2	alkalinized, pH 11.5, (72%)	
	8.26 (± 0.40) × 10^4 a)2	alkalinized, scav., pH 11.5, (72%)	
	4.85 (± 2.45) × 10^5 b)	buffered, pH 12.5, (96%)	
	1.50 (± 0.74) × 10^5 b)	buffered, scav., pH 12.5, (96%)	
N-Hydroxy-piperidine	9.36 (± 0.27) × 10^4 a)2	alkalinized, pH 11.5,	
	6.32 (± 0.38) × 10^4 a)2	alkalinized, scav., pH 11.5	
Piperazine	2.48 (± 0.36) × 10^4 a)1	given pH 10.1, (99%)	9.80*
	2.72 (± 0.39) × 10^4 a)1	alkalinized, pH 11.5, (100%)	pK_{a2}:
	2.62 (± 0.14) × 10^4 a)2	buffered, pH 12.5, (100%)	5.57**
	2.72 (± 0.14) × 10^4 a)2	alkalinized, pH 11.5, (100%)	
	1.62 (± 0.05) × 10^4 a)2	alkalinized, scav., pH 11.5, (100%)	
	2.21 (± 0.08) × 10^4 b)	buffered, pH 12.5, (100%)	
	2.19 (± 0.05) × 10^4 b)	buffered, scav., pH 12.5, (100%)	
Morpholine	9.16 (± 0.80) × 10^4 a)1	given pH 9.8, (96%)	8.36*
	8.32 (± 0.26) × 10^4 a)1	alkalinized, pH 11.5, (100%)	
	6.73 (± 0.30) × 10^4 a)2	buffered, pH 12.5, (100%)	
	5.49 (± 0.11) × 10^4 a)2	alkalinized, pH 11.5, (100%)	
	4.12 (± 0.15) × 10^4 a)2	alkalinized, scav., pH 11.5, (100%)	

	1.15 (± 0.37) × 10^{5} b) 8.27 (± 0.35) × 10^{4} b)	buffered, pH 12.5, (100%) buffered, scav., pH 12.5, (100%)	
Literature Piperidine Piperazine Morpholine	9.8 – 36.2 (4 – 7.2) × 10^{3} (2.9 – 5) × 10^{3} (Pietsch et al., 1999)	buffered, pH 7 (0.0079%) buffered, pH 7 (4%)*** buffered, pH 7 (3.4%)	

* Handbook of Chemistry and Physics, David R. Lide, 89th Edition, 2008-2009

** (chemie-online (D`Ans-Lax))

*** 4% for completely deprotonated species at pH 7 from pK_{a1} and pK_{a2} (see Figure S1)

Text S4. Reaction stoichiometry

For determination the stoichiometry of the reaction, that is to say the amount of ozone needed for compound degradation lower compound concentrations have to be used, because consumption yields can only be measured at a reasonable transformation of the substrate, otherwise the deviation from the untreated sample is too small (Mvula & von Sonntag, 2003). Hence for these experiments a substrate concentration around 10^{-4} M was used, resulting in ozone to compound molar concentration ratios of 1:0.3 – 1:3. To exclude $^{\bullet}$OH reactions all samples were prepared in parallel as described above but containing tertiary butanol (0.05 – 0.1 M) as a radical scavenger.

The experiments were carried out in a series of volumetric flasks (20 mL) each containing 1 mL of the investigated compound solution, with and without tertiary butanol and different volumes (0 – 8 mL) of ozone solution to obtain various ozone concentrations. Appropriate volumes of pure water were added to complete the solution volume to 10 mL. All experiments were performed at room temperature and

at a pH of 11.5, alkalinized with sodium hydroxide. After complete ozone consumption the quantification was realized in the batch sample through compound-degradation. Since the original compounds do not absorb in the UV spectrum the consumption experiments were implemented by derivatization with 9-fluorenylmethyl chloro-formate (FMOC-Cl) to the corresponding carbamate derivatives as previously described by Pietsch et al., 1996 according to Scheme S6.

Scheme S6. Derivatization of the amines with FMOC-Cl, shown for the reaction of piperidine with ozone in the reaction stoichiometry experiment

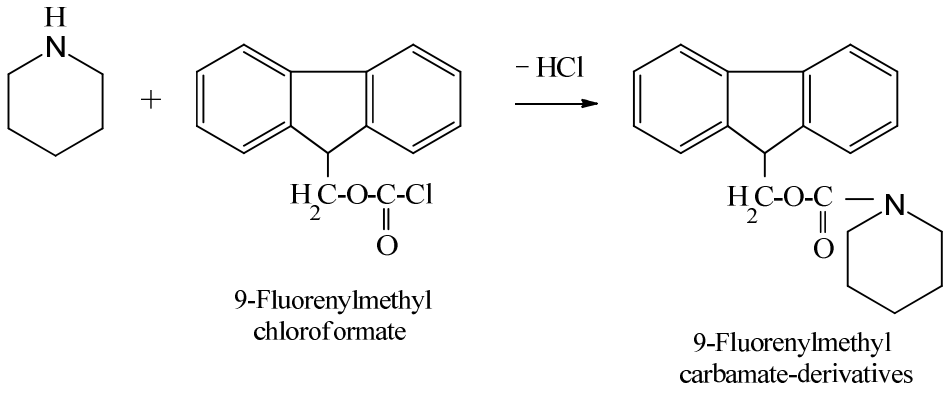

For derivatization 10 mL sample were withdrawn from the batch and transferred into Erlenmeyer flasks. After the addition of 1 g potassium carbonate and 0.2 mL FMOC-Cl reagent (0.06 g / 20 mL acetone) and rapidly stirring for 20 min the carbamate derivatives were extracted with tertiary butyl methyl ether / toluene (ratio 2:1) in the presence of ammonium (0.25%). After repeated rapid stirring for 20 min the organic phase was separated and evaporated. The residual was resolved in 1 mL acetonitrile and measured with HPLC-DAD (LC20, Shimadzu, Duisburg, Germany), equipped with a C_{18} column (Prontosil, NC-04, 250 mm x 4.0 mm I.D., 5.0 µm, Bischoff, Leonberg, Germany). The compounds were eluted with a water/acetonitrile gradient system (35% ACN/ 2 min, 45% ACN/ 5 min, 55% ACN/ 10 min, 65% ACN/ 15 min, 75% ACN/ 20 min, 85% ACN/ 30 min, 100% ACN) at a flow rate of 0.5 mL min^{-1} and an injection volume of 50 µL in all samples. The carbamate derivatives were verified by retention time and UV-spectra at 264 nm. In these measurements a fluorescence detector was also tested, but with UV- detection the quantified peaks are improved resolved under these conditions, thus all experiments were carried out with UV detection. Blanks were processed in the same manner with water instead of ozone solution to

determine the initial concentration. Calibration experiments (Figure S2) were performed in the same manner with the investigated compounds as reference materials.

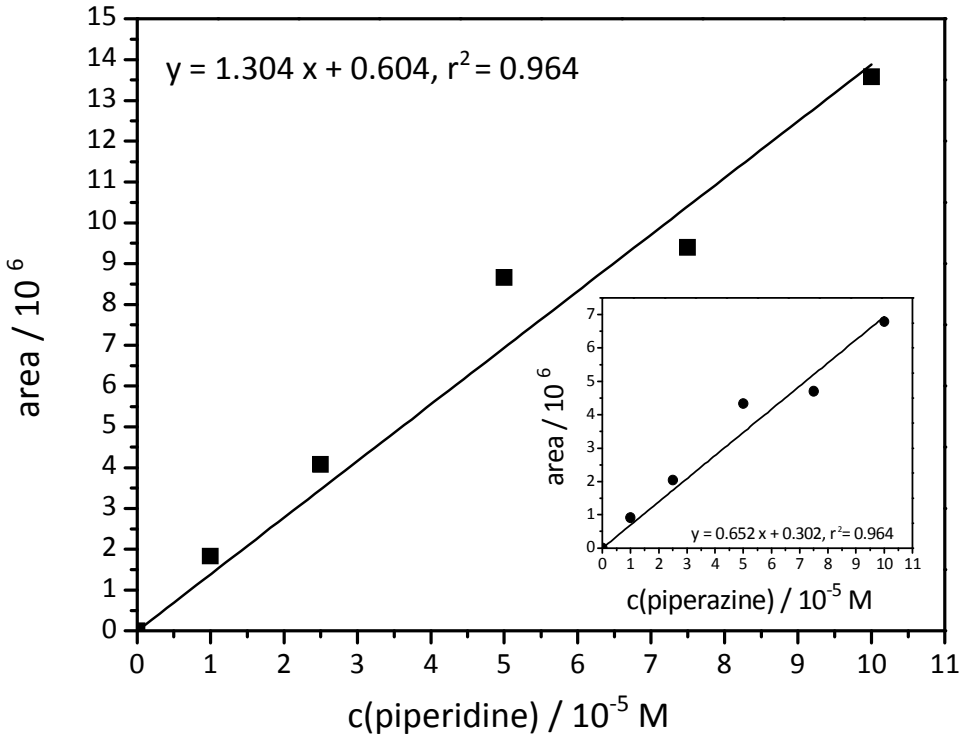

Figure S2. Calibration curves for reaction stoichiometry experiments of piperidine (main graph) and piperazine (inset) in the derivatization with FMOC-Cl. Areas are plotted vs. amine concentrations

Text S5. Identification of products with LC-HRMS

The molecular weights and hence sum formulae of the oxidation products were performed with Q1 scans in positive and negative mode. Structural elucidation of the oxidation products was based on their MS^2 fragmentation pathways obtained from product ions. The MS system (FTMS: Fourier transformation mass spectrometer) was equipped with an electrospray ionisation source (ESI) and an atmospheric pressure chemical ionisation (APCI). Since, the oxidation products were more sensitively detected in positive ionisation and with electrospray ionisation source, all following MS measurements were only performed in positive mode using ESI interface (see Figure S3).

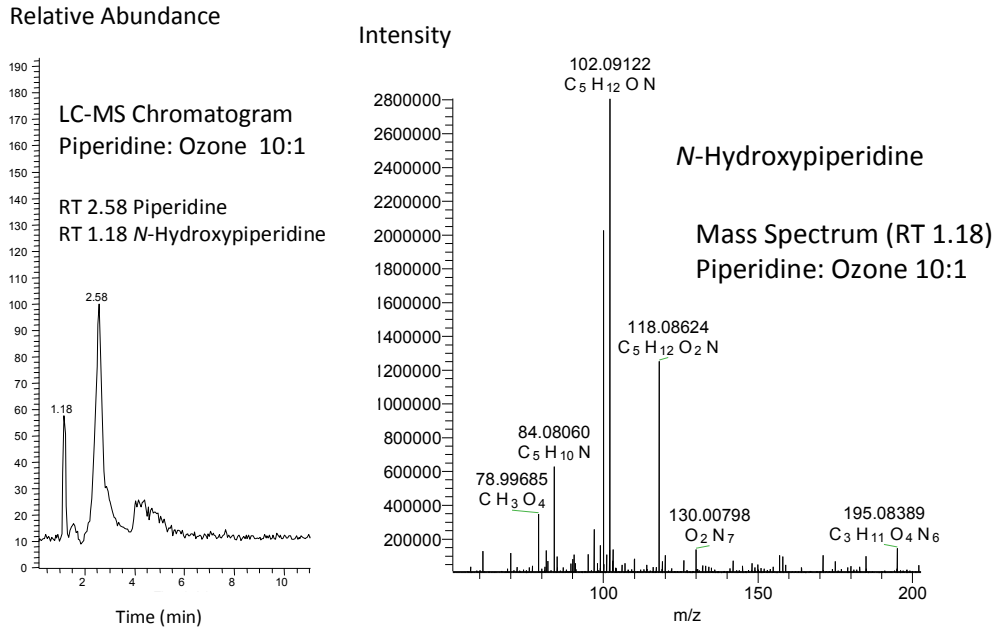

Figure S3. HPLC chromatogram and mass spectrum (TIC F: FTMS + pESI Full ms 50.00-500.00) of *N*-hydroxypiperidine (RT: 1.18) (calculated mass: 102.1558) in the reaction of piperidine (RT: 2.58) with ozone (in the absence of $^{\bullet}$OH scavenger).

The excitation energy was optimized for each experiment and varied between 20−100 V, with a collision energy spread of 5 V. In the LC system the sample compounds were separated on a C_{18} column (Synergi Hydro-RP 80 A, 150 mm x 3.0 mm I.D., 4.0 µm, Phenomenex, Aschaffenburg, Germany) at 25°C. As eluents ultra-pure water and acetonitrile, both containing 0.5% aqueous formic acid (HCOOH) were used in a gradient system (10% ACN/ 10 min, 45% ACN/ 15 min, 100% ACN). In addition fractionation of oxidation products were made, in particular to separate oxidation products from the original compound in large excess. The experiments were performed with direct injection of eluent fractions to obtain fragmentation patterns of MS^2 from product ion scans. The fractionation was carried out with HPLC (time wise fractionation (HIP-ALS-SL, Agilent, Waldbronn, Germany)) using C_{18} column (Synergi Hydro-RP 80 A, see above). Freeze drying of fractions was avoided to prevent any possible loss or degradation of oxidation products during this step. Unfortunately, MS^2

spectra showed no fragment signals, most likely because the fragment masses were too small to be detected.

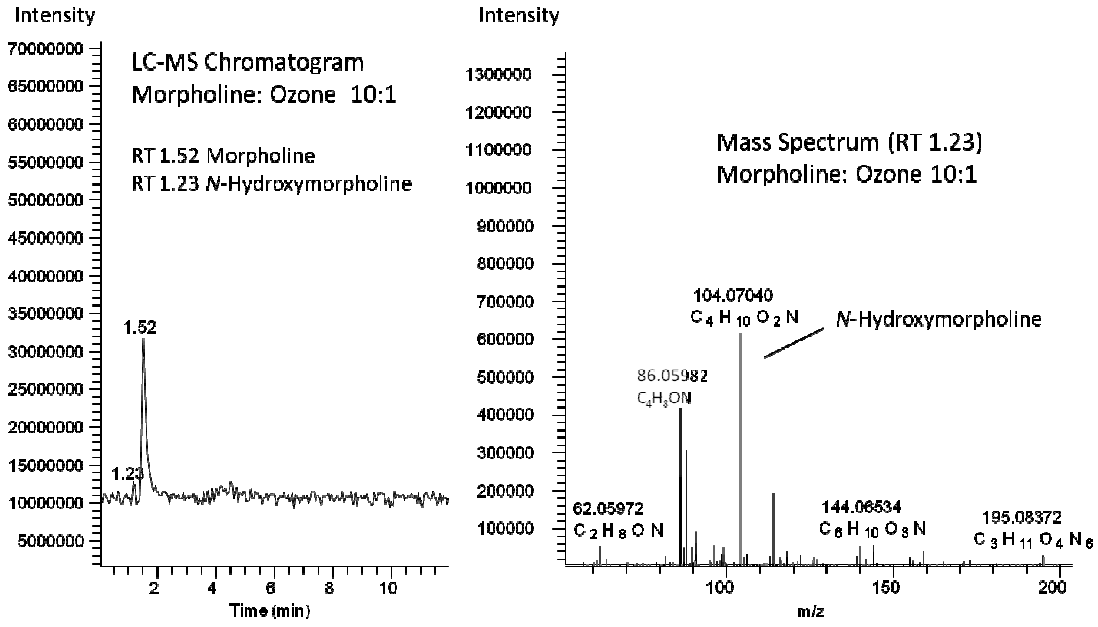

Figure S4. HPLC chromatogram and mass spectrum (TIC F: FTMS + pESI Full ms 50.00-500.00) of *N*-hydroxymorpholine (RT: 1.23) (calculated mass: 104.1280) in the reaction of morpholine (RT: 1.52) with ozone (in the presence of $^{\bullet}$OH scavenger)

Quantification of *N*-hydroxypiperidine was carried out with HPLC-DAD in the same way as reaction stoichiometric experiments described above, however with different separation conditions (35% ACN/ 2 min, 45% ACN/ 5 min, 100% ACN) and without derivatization since *N*-hydroxypiperidine absorb in the UV-range. In this HPLC analytics the elution flow rate was 0.5 mL min^{-1} and the injection volume was 50 µL in all samples.

Text S6. Determination of OH radicals ($^{\bullet}$OH)

The dimethyl sulfoxide (DMSO) method was applied because the use of tertiary butanol as an $^{\bullet}$OH scavenger is not recommended due to adequate formaldehyde yields in the reaction of ozone with the investigated *N*-heterocycles (see paper, values in Table 2). In the tertiary butanol assay formaldehyde is measured to quantify $^{\bullet}$OH (see sample preparation above). DMSO use is limited to highly ozone-reactive

substrates, which is given for the investigated *N*-heterocycles (see Table S1), since DMSO itself reacts with ozone with a rate constant of 8.2 M^{-1} s^{-1} (Veltwisch et al., 1980). The DMSO assay leads to methanesulfinic acid, which can be further oxidized to methanesulfonic acid by ozone (see Scheme S7 and Flyunt et al., 2001a, 2003a).

Scheme S7. Determination of $^{\bullet}OH$ with dimethyl sulfoxide

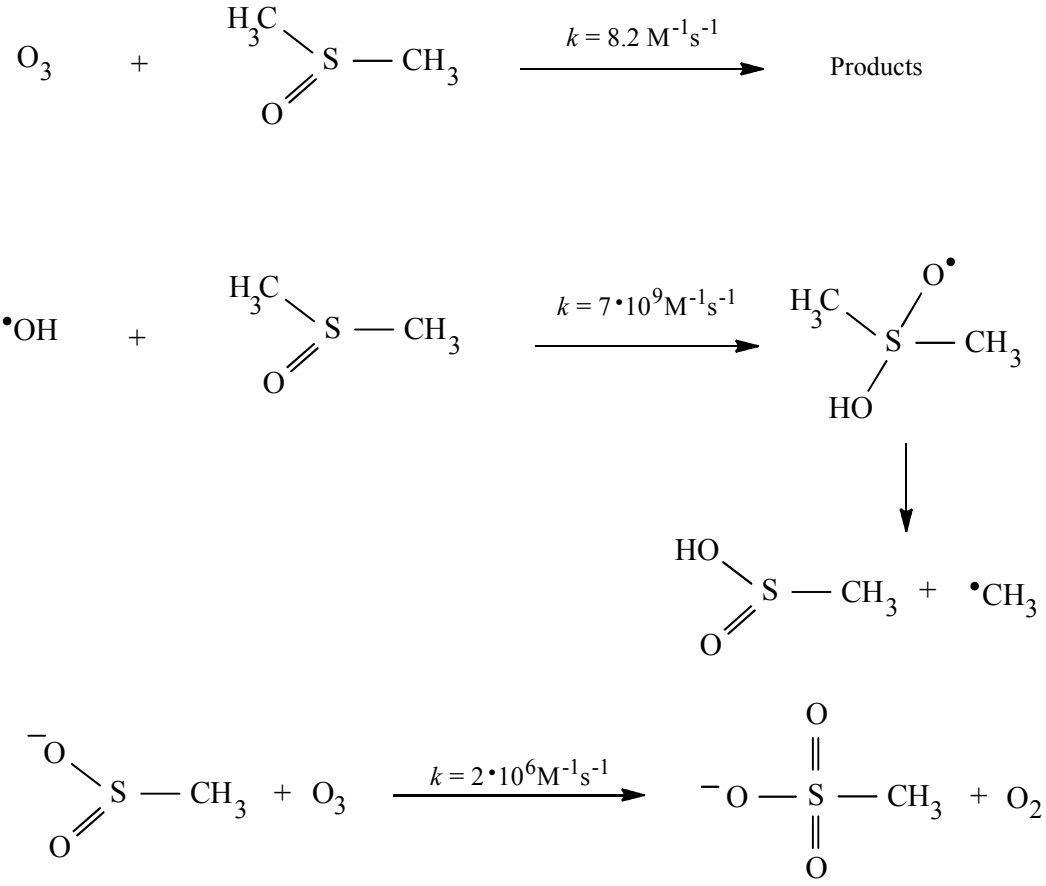

In addition, methanesulfinic acid ($k(O_3 + MSIS) = 2 \times 10^6$ M^{-1} s^{-1}) reacts fast with ozone (Flyunt et al., 2001a, Veltwisch et al., 1980). Thus, in these experiments the substrate was in constant high concentration (at least 10^{-2} M) and DMSO in large excess (0.1 M) over ozone (1×10^{-4} M − 4×10^{-4} M) to avoid ozone reaction with the acid and $^{\bullet}OH$. Taken into account the concentration of methanesulfinic acid (at most 2×10^{-5} M) in the reaction with ozone ($k_{app}(O_3 + MSIS) = 40$ s^{-1}), the reaction of piperazine with ozone ($k(O_3 + piperazine) = 1.9 \times 10^4$ M^{-1} s^{-1}, lowest *k* in this study and at least 10^{-2} M) is still favored ($k_{app}(O_3 + piperazine) = 190$ s^{-1}). In due consideration in the reaction of DMSO (0.1 M) with ozone ($k_{app}(O_3 + DMSO) = 0.82$ s^{-1}) or with $^{\bullet}OH$ ($k_{app}(^{\bullet}OH + DMSO) = 7 \times 10^8$

s^{-1}) the reaction of ozone with piperazine and the reaction of DMSO with $^{\bullet}OH$ radicals are clearly favored. The acids were quantified by ion chromatography (Metrohm 883 basic), equipped with a conductivity detector and ion suppression. The separation was performed on an anion exchange column with quaternary ammonium groups (Metrosep A Supp 4, 250/4.0 mm) with the following eluent: Na_2CO_3: 1.8×10^{-3} M, $NaHCO_3$: 1.7×10^{-3} M, at a flow rate of 1 mL min^{-1} and injection volume of 2 mL. Calibration experiments (Figure S5) with methanesulfinic acid and methanesulfonic acid were performed in the same manner.

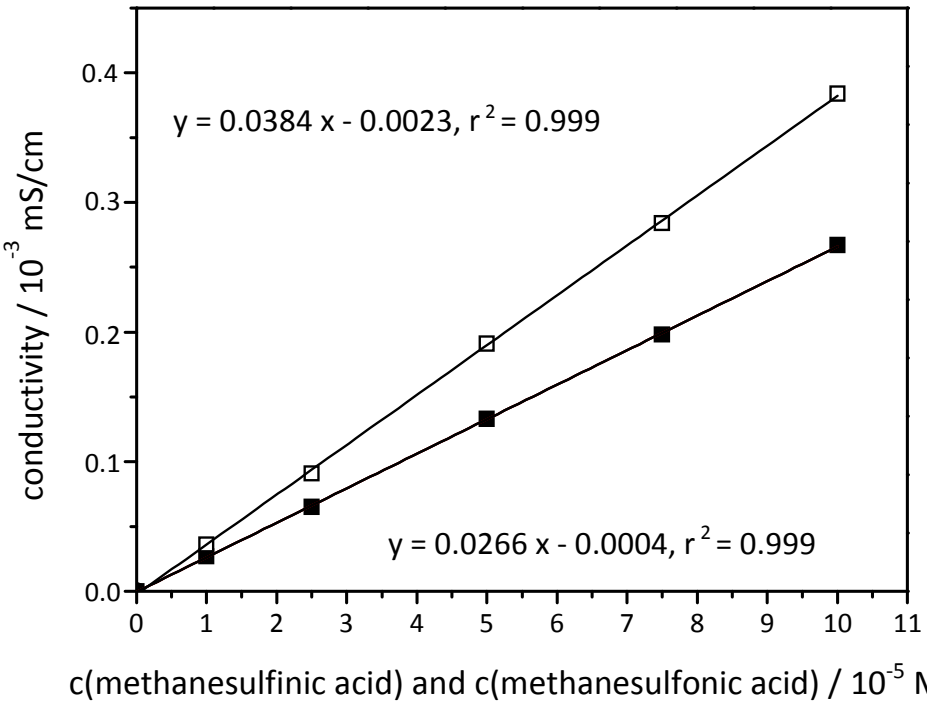

Figure S5. Calibration curves of methanesulfinic acid (■) and methanesulfonic acid (□). Conductivity is plotted vs. concentrations.

Text S7. Determination of secondary products

Formaldehyde ($k(CH_2O + O_3)$ = 0.1 M^{-1} s^{-1}, Hoigné & Bader, 1983a) and hydrogen peroxide ($k(H_2O_2 + O_3)$ = 0.01 M^{-1} s^{-1}, pK_a = 11.6, Staehelin & Hoigné 1982, Merényi et al., 2010a) react with ozone at low rates, even if ozone is present at reasonable excess. However, the hydrogen peroxide anion reacts with a much higher rate ($k(HO_2^- + O_3)$ = 5.5×10^6 M^{-1} s^{-1}, Staehelin & Hoigné 1982). In the experiments with a pH of about 11 around 50% of hydrogen peroxide is in the anionic form. Hydroxylamine (k (NH_2OH +

O_3) = 2 × 10^4 M^{-1} s^{-1}, Neta et al., 1988, Hoigné et al., 1985) reacts with ozone at high rates. Thus, in all of these experiments the substrate was in large excess to reduce ozone reaction with formaldehyde, hydrogen peroxide and hydroxylamine. Taking into account the concentration of formaldehyde (at most 6 × 10^{-5} M) and hydroxylamine (at most 5 × 10^{-5} M) in their reaction with ozone (k_{app}(O_3 + CH_2O) = 6 × 10^{-6} s^{-1}, k_{app}(O_3 + NH_2OH) = 1.1 s^{-1}) and the reaction of piperazine with ozone (k (O_3 + piperazine) = 1.9 × 10^4 M^{-1} s^{-1}, lowest k in this study and at least with substrate concentration of 10^{-3} M) the latter (k_{app}(O_3 + piperazine) = 19 s^{-1}) is still favored. In due consideration the concentration of hydrogen peroxide but rather of the hydroperoxide ion (at most 5 × 10^{-6} M) in the reaction with ozone (k_{app}(O_3 + HO_2^-) = 28 s^{-1}) and the ozone-piperazine reaction (see above) the reaction of ozone with piperazine is not favored, but rather both reactions are equally important. In parallel in experiments quantified hydrogen peroxide and hydroxylamine, tertiary butanol is added as $^{\bullet}$OH scavenger to test whether its presence has an influence on the reactions. In experiments quantified formaldehyde, dimethyl sulfoxide (DMSO) was chosen as scavenger, in consideration the fact, that tertiary butanol also yields formaldehyde in $^{\bullet}$OH-induced reactions (see above) so that it can not be added as an $^{\bullet}$OH scavenger. Due to the interferences of the DNPH system with DMSO, quantification of formaldehyde were made only with the Hantzsch method (see description above, competition method). By using DMSO, formaldehyde can also be generated (Yurkova et al., 1999). However, in these experiments it can be neglected, because with concentrations of 0.1 M DMSO only 0.5% formaldehyde could be formed. So that the formaldehyde yield in scavenged system results from substrate and not from DMSO. To confirm the unexpected high formaldehyde yields (see Table 2) in addition to the Hantzsch method a Hach-Lange test kit for formaldehyde was used, both of which led to comparable results. In all cases blanks and calibrations (Figure S6, inset) were performed in the same manner.

For hydroxylamine determination, the iodate method was chosen. Here, hydroxylamine is determined by its oxidation with iodate (IO_3^-, 4.7 × 10^{-2} M) to nitrite (Afkhami et al., 2006) according to Scheme S8.

Scheme S8. Reaction of hydroxylamine with iodate by forming nitrite

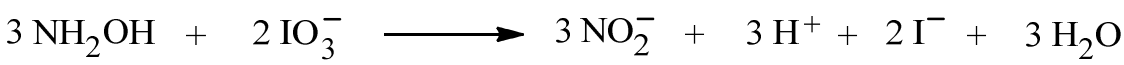

The nitrite yield was quantified by ion chromatography (see description above, however with different eluent conditions: Na_2CO_3: 1.8 × 10^{-4} M, $NaHCO_3$: 1.7 × 10^{-4} M). In the present study neutral conditions (pH 7.5) were chosen for the separation, because high sulfuric acid or hydrochloric acid concentrations disturbed the measurement by ion chromatography, so that in this case the nitrite yield represents 50% of the hydroxylamine yield. In the same manner, blanks and calibrations (with hydroxylamine hydrochloride, 6.6 × 10^{-4} M and nitrite) were performed (Figure S6). *N*-hydroxypiperidine was used as reference standard to test for potential nitrite formation in the analytical preparation without ozonation, however, no nitrite was detected in this case.

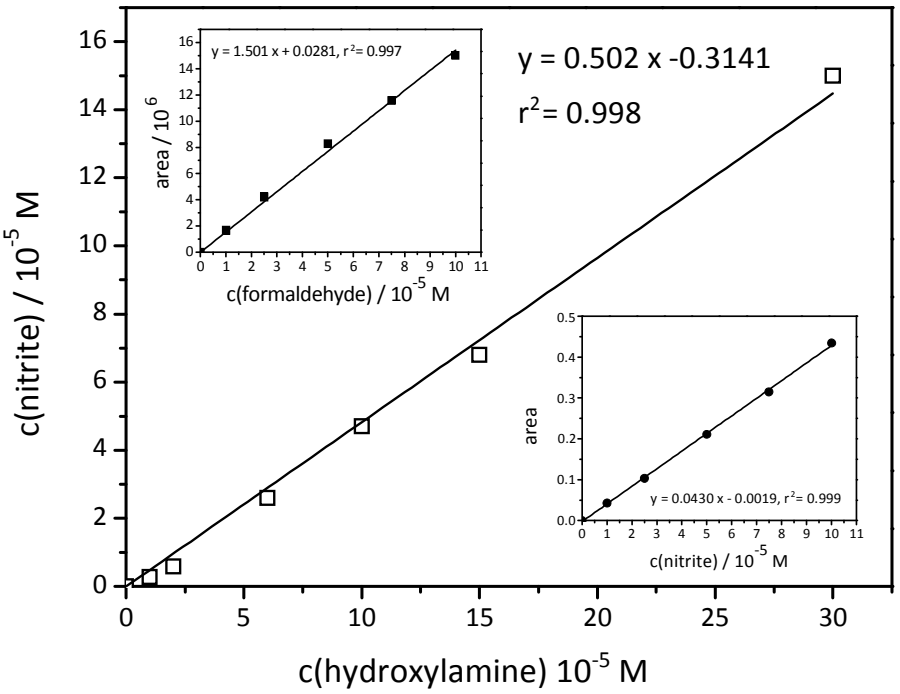

Figure S6. Calibration curves of the formation of nitrite from hydroxylamine (main graph) in its reaction with iodate. Nitrite concentrations are plotted vs. hydroxylamine concentrations. Calibration curves of formaldehyde (inset 1) and nitrite (inset 2). Areas in the insets are plotted vs. concentrations.

Hydrogen peroxide (H_2O_2) was quantified spectrophotometrically with Allen`s reagent (molybdate-activated iodide) (Allen et al., 1952, Kitsuka et al., 2007). Hydroperoxides oxidize molybdate activated iodide ions to iodine, which can be detected as triiodide ion (I_3^-) according to Scheme S9. The kinetics of this reaction is complex, but organic hydroperoxides can be distinguished from H_2O_2 by their reaction with molybdate-activated iodide (Dowideit & von Sonntag 1998, Flyunt et al., 2003b).

Scheme S9. Determination of hydrogen peroxide in its reaction with iodide

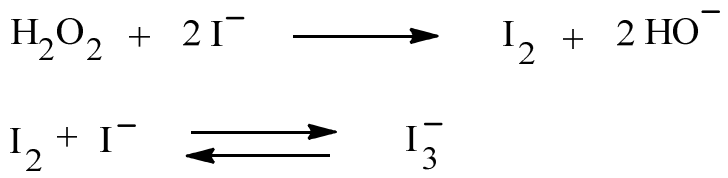

In all cases the method was carried out by pipetting into UV-cells (1 cm path length) as follows: 1 mL Allen´s reagent A (1 g NaOH + 33 g KI + 0.1 g $(NH_4)_6Mo_7O_{24} \cdot H_2O$ filled up to 500 mL ultra-pure water) plus 1 mL Allen´s reagent B (10 g potassium hydrogen phthalate (KHP) dissolved in 500 mL ultra-pure water) plus 1 mL sample. After mixing the absorbance was detected spectrophotometrically at 350 nm (absorption coefficient at this wavelength is 25500 M^{-1} cm^{-1}). In all analytical methods blanks were performed in the same manner with ultra-pure water instead of ozone solution.

Text S8. Singlet oxygen

Triplet oxygen is the ground state of molecular oxygen. The electron configuration of the molecule has two unpaired electrons occupying two degenerate molecular orbitals with parallel spin. Singlet oxygen has two higher-energy species of molecular oxygen, in which the electrons are paired. Since the ground state of the ozone adduct is a singlet state, the overall spin multiplicity of the products must also be a singlet. As a consequence, this spin conservation rules demands that oxygen is released in its excited singlet state ($^1O_2$), which lies 95.5 kJ mol^{-1} above the triplet ground state ($^3O_2$) (Muñoz et al., 2001, von Sonntag & von Gunten, 2012).

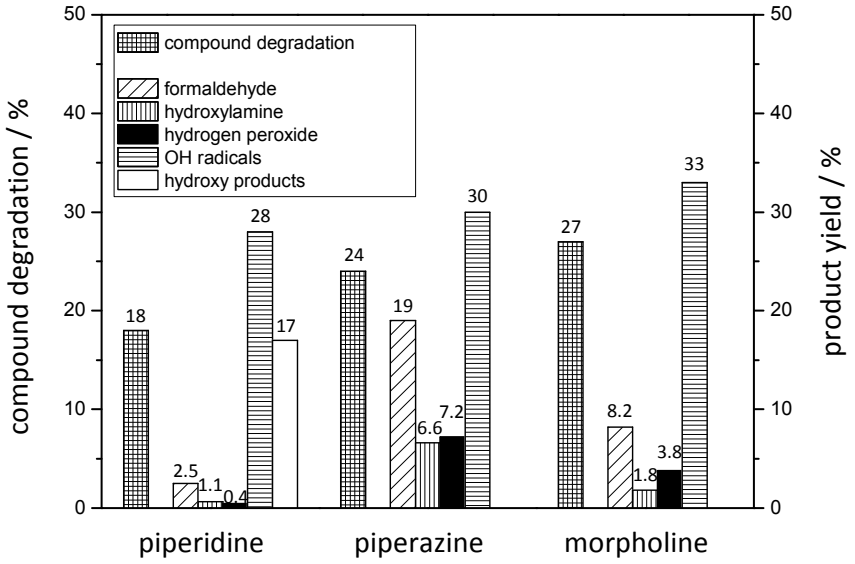

Figure S7. Compound degradation (%) and product yield (%) relating to ozone consumption in the ozonation of piperidine, piperazine and morpholine in scavenged system.

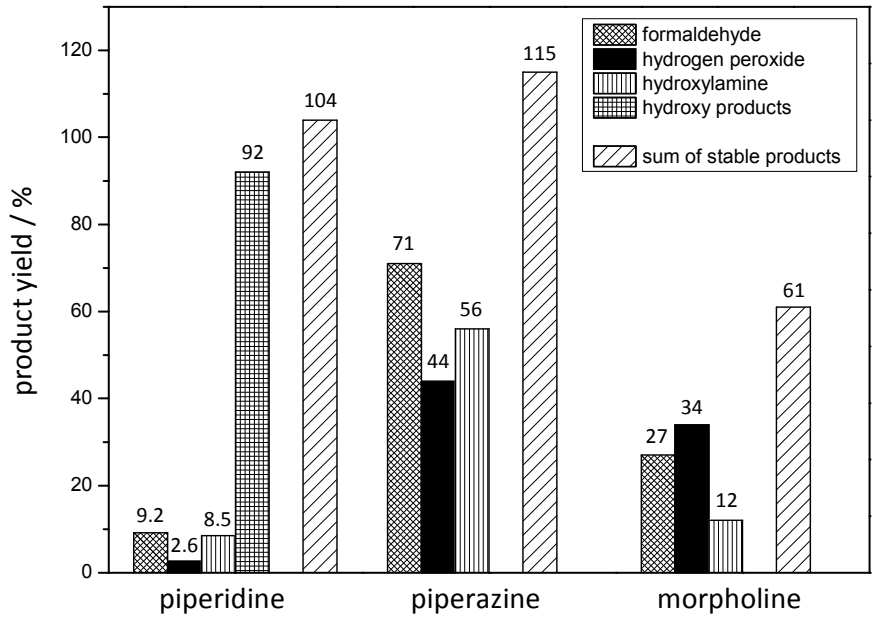

Figure S8. Product yield (%) relating to compound degradation in the reaction of piperidine, piperazine and morpholine with ozone in non scavenged system.

References

Andreozzi, R., Caprio, V., Insola, A., Marotta, R., 2000. The oxidation of metol (N-methyl-*P*-aminophenol) in aqueos solution by UV/H2O2 photolysis. Wat Res 34, 463-472.

Afkhami, A., Madrakian, T., Maleki, A., 2006. Indirect kinetic spectrophotometric determination of hydroxylamine based on its reaction with iodate. Analytica Sci 22, 329-331.

Allen, A. O., Hochanadel, C. J., Ghormley, J. A., Davis, T. W., 1952. Decomposition of water and aqueous solutions under mixed fast neutron and gamma radiation. J Phys Chem 56, 575-586.

Bader, H., Hoigné, J., 1981. Determination of ozone in water by the indigo method. Wat Res 15, 449-456.

Beltrán, F. J., Encinar, J. M., Alonso, M. A., 1998. Nitroaromatic hydrocarbon ozonisation in water: 1: Single ozonation. Ind Eng Chem Res 37, 25-31.

Buxton, G. V., Greenstock, C. L., Helman, W. P., Ross, A. B., 1988. Critical review of rate constants for reactions of hydrated electrons, hydrogen atoms and hydroxyl radicals (OH/O^{-}) in aqueous solution. J Phys Chem Ref Data 17, 513-886.

Dodd, M. C., Buffle, M.-O., von Gunten, U., 2006a. Oxidation of antibacterial molecules by aqueous ozone: moiety-specific kinetics and application to ozone-based wastewater treatment. Environ Sci Technol 40, 1969-1077.

Dowideit, P., von Sonntag, C., 1998. The reaction of ozone with ethene and its methyl- and chlorine-sustituted derivatives in aqueous solution. Environ Sci Technol 32, 1112-1119.

Flyunt, R., Makogon, O., Schuchmann, M. N., Asmus, K.-D., von Sonntag, C., 2001a. The OH-radical-induced oxidation of methanesulfinic acid. The reactions of the methyl-sulfonyl radical in the absence and presence of dioxygen. J Chem Soc, Perkin Trans 2, 787-792.

Flyunt, R., Leitzke, A., Mark, G., Mvula, E., Reisz, E., Schick, R., von Sonntag, C., 2003a. Determination of $^{\bullet}OH$ and $O_2^{\bullet-}$, and hydroperoxide yields in ozone reactions in aqueous solutions. J Phys Chem B 107, 7242-7253.

Flyunt, R., Leitzke, A., von Sonntag, C., 2003b. Characterisation and quantitative determination of (hydro)peroxides formed in the radiolysis of dioxygen-containing systems and upon ozonolysis. Radiat Phys Chem 67, 469-473.

Forni, L., Bahnemann, D., Hart, E. J., 1982. Mechanism of the hydroxide ion initiated decomposition of ozone in aqueous solution. J Phys Chem 86, 255-259.

Gilbert, E., Zinecker, H., 1980. Ozonization of aromatic amines in water. Ozone Sci Eng 2, 65-74.

Hoigné, J., Bader, H., 1983a. Rate constants of reactions of ozone with organic and inorganic compounds in water. - I. Non-dissociating organic compounds. Wat Res 17, 173-183.

Hoigné, J., Bader, H., Haag, W. R., Staehelin, J., 1985. Rate constants of reactions of ozone with organic and inorganic compounds in water. - III. Inorganic compounds and radicals. Wat Res 19, 993-1004.

Kitsuka, K., Mohammad, A. M., Awad, M. I., Kaneda, K., Ikematsu, M., Iseki, M., Mushiake, K., Ohsaka, T., 2007. Simultaneous spectrophotometric determination of ozone and hydrogen peroxide. Chem Letters 36, 1396-1397.

Lipari, F., Swarin, S. J., 1982. Determination of formaldehyde and other aldehydes in automobile exhaust with an improved 2,4-dinitrophenylhydrazine method. J Chrom 247, 297-306.

Merényi, G., Lind, J., Naumov, S., von Sonntag, C., 2010a. The reaction of ozone with hydrogen peroxide (peroxone process). A revision of current mechanistic concepts based on thermokinetic and quantum-mechanical considerations. Environ Sci Technol 44, 3505-3507.

Merényi, G., Lind, J., Naumov, S., von Sonntag, C., 2010b. The reaction of ozone with the hydroxide ion. Mechanistic considerations based on thermokinetic and quantum-chemical calculations. The role of HO_4^- in superoxide dismutation. Chem Eur J 16, 1372-1377.

Muñoz, F., von Sonntag, C., 2000a. Determination of fast ozone reactions in aqueous solution by competition kinetics. J Chem Soc, Perkin Trans 2, 661-664.

Muñoz, F., von Sonntag, C., 2000b. The reaction of ozone with tertiary amines including the complexing agents nitrilotriacetic acid (NTA) and ethylenediaminetetra-acetic acid (EDTA) in aqueous solution. J Chem Soc, Perkin Trans 2, 2029-2033.

Muñoz, F., Mvula, E., Braslavsky, S. E., von Sonntag, C., 2001. Singlet dioxygen formation in ozone reactions in aqueous solution. J Chem Soc, Perkin Trans 2, 1109-1116.

Mvula, E., von Sonntag, C., 2003. Ozonolysis of phenols in aqueous solution. Org Biomol Chem 1, 1749-1756.

Nash, T., 1953. The colorimetric estimation of formaldehyde by means of the Hantzsch reaction. Biochem J 55, 416-421.

Neta, P., Huie, R. E., Ross, A. B., 1988. Rate constants for reactions of inorganic radicals in aqueous solution. J Phys Chem Ref Data 17, 1027-1284.

Olson, K. L., Swarin, S. J., 1985. Determination of aldehydes and ketones by derivatization and liquid chromatography- mass spectrometry. J Chrom 333, 337-347.

Pietsch, J., Hampel, S., Schmidt, W., Brauch, H.-J., Worch, E., 1996. Determination of aliphatic and alicyclic amines in water by gas and liquid chromatography after derivatisation by chloroformates. Fresenius J Anal Chem 355, 164-173.

Reisz, E., Schmidt, W., Schuchmann, H.-P., von Sonntag, C., 2003. Photolysis of ozone in aqueous solution in the presence of tertiary butanol. Environ Sci Technol 37, 1941-1948.

Schuchmann, M. N., von Sonntag, C., 1979. Hydroxyl radical-induced oxidation of 2-methyl-2-propanol in oxygenated aqueous solution. A product and pulse radiolysis study. J Phys Chem 83, 780-784.

Staehelin, J., Hoigné, J., 1982. Decomposition of ozone in water: Rate of initiation by hydroxide ions and hydrogen peroxide. Environ Sci Technol 16, 676-681.

Staehelin, J., Bühler, R. E., Hoigné, J., 1984. Ozone decomposition in water studied by pulse radiolysis, 2. OH and HO_4 as chain intermediates. J Phys Chem 88, 5999-6004.

Staehelin, J., Hoigné, J., 1985. Decomposition of ozone in water in the presence of organic solutes acting as promoters and inhibitors of radical chain reactions. Environ Sci Technol 19, 1206-1213.

Veltwisch, D., Janata, E., Asmus, K.-K., 1980. Primary processes in the reactions of $^{\bullet}$OH radicals with sulphoxides. J Chem Soc, Perkin Trans 2, 146-153.

von Sonntag, C., 2007. The basics of oxidants in water treatment. Part A: OH radical reactions. Wat Sci Tech, 19-23.

von Sonntag, C., Schuchmann, H.-P., 1997. Peroxylradicals in aqueous solution. In: Peroxyl Radicals, Z.B. Alfassi (ed.), Wiley Chichester, 173-234.

von Sonntag, C., von Gunten, U., 2012. Chemistry of ozone in water and wastewater treatment. From basic principles to applications. IWA Publishing.

Yurkova, I. L., Schuchmann, H.-P., von Sonntag, C., 1999. Production of OH radicals in the autooxidation of the Fe(II)-EDTA system. J Chem Soc, Perkin Trans 2, 2049-2052.

Zimmermann, S. G., Schmukat, A., Schulz, M., Benner, J., von Gunten, U., Ternes, T. A., 2012. Kinetic and mechanistic investigations of the oxidation of tramadol by ferrate and ozone. Environ Sci Technol 46, 876-884

4 Ozonation of pyridine and other *N*-heterocyclic aromatic compounds: Kinetics, stoichiometry, identification of products and elucidation of pathways

Agnes Tekle-Röttering, Erika Reisz, Kevin S. Jewell, Holger V. Lutze,
Thomas A. Ternes, Winfried Schmidt, Torsten C. Schmidt

4.1 Abstract

Pyridine, pyridazine, pyrimidine and pyrazine were investigated in their reaction with ozone. These compounds are archetypes for heterocyclic aromatic amines, a structural unit that is often present in pharmaceuticals, pesticides and dyestuffs (e.g., enoxacin, pyrazineamide or pyrimethamine). The investigated target compounds react only slowly with ozone, with rate constants ranging from 0.37 to 57 M^{-1} s^{-1}, hampering their degradation during ozonation. In OH radical scavenged systems the reaction of ozone with pyridine and pyridazine is characterized by high transformation (per ozone consumed) of 55 and 54%, respectively. In non scavenged system the transformation drops to 52 and 12%, respectively. However, in the reaction of pyrimidine and pyrazine with ozone this is reversed. Here, in an OH radical scavenged system the compound transformation is much lower (2.1 and 14%, respectively) than in non scavenged one (22 and 25%, respectively). This is confirmed by corresponding high *N*-oxide formation in the ozonation of pyridine and pyridazine, but probably low formation in the reaction of pyrimidine and pyrazine with ozone. With respect to reaction mechanisms, it is suggested that ozone adduct formation at nitrogen is the primary step in the ozonation of pyridine and pyridazine. On the contrary, ozone adduct formation to the aromatic ring seems to occur especially in the ozonation of pyrimidine as inferred from

hydrogen peroxide yield. However, also OH radical reactions are supposed processes in the case of pyrimidine and in particular for pyrazine, albeit negligible OH radical yields are obtained. The low compound transformation in OH radical scavenged system can prove this. As a result of negligible OH radical yields in all cases (less than 6%) electron transfer as primary reaction pathway plays a subordinate role.

4.2 Introduction

Nitrogen is frequently present in micropollutants, since many biologically active compounds, e.g., pharmaceuticals or pesticides, contain aromatic and aliphatic amino groups. The micropollutants can reach the environment through several input paths according to their manifold uses. However, pharmaceuticals in particular are mainly emitted via municipal wastewater treatment plant (WWTP) effluents (Huber et al., 2005, Gabet-Giraud et al., 2010). Hence, there is a major concern about the occurrence of micropollutants in surface water and ground water that are used as source waters for drinking water supply (Nöthe et al., 2007, Ternes, 2015). In surface water micropollutants can be harmful to aquatic life, even at low concentrations (Huggett et al., 2002, Küster et al., 2010). Therefore, a polishing treatment of WWTP effluents by ozonation or activated carbon is currently discussed to minimize a discharge of micropollutants to receiving waters (Ternes et al., 2002, Huber et al., 2003, Snyder et al., 2006, Schwarzenbach et al., 2006, Benner et al., 2008, Hollender et al., 2009, Benitez et al., 2011, Zimmermann et al., 2012). However, during ozonation the oxidation of micropollutants is in competition with ozone reactions of the water matrix. Only micropollutants with high ozone rate constants are easily eliminated (Lee & von Gunten, 2010). For this reason, the determination of ozone rate constants of micropollutants is essential. OH radicals ($^{\bullet}$OH), being an important oxidant in ozonation, have gained attention as a tool to transform micropollutants during treatment of not only drinking water but also wastewater (von Gunten, 2003, Snyder et al., 2006). Hence, $^{\bullet}$OH yield is a relevant reaction parameter. In addition, the knowledge of the quantity of ozone used for full compound degradation (reaction stoichiometry) will allow the assessment of the treatment e.g., the dosage rate (Nöthe et al., 2009). Oxidative treatment does not typically result in full mineralization, but rather leads to transformation products (TPs). For a comprehensive environmental

assessment it is crucial to elucidate the transformation pathways, since it cannot be ruled out, that TPs may be more toxic to aquatic life than their precursors (Shang & Yu, 2002, Huber et al., 2004, Schmidt & Brauch, 2008, Boxall et al., 2014).

In this study, the reactions of ozone with pyridine, pyridazine, pyrimidine and pyrazine were investigated in aqueous solution. Those investigations can help to elucidate the chemical mechanisms involved in the oxidation of micropollutants by ozone, in particular for aromatic heterocyclic amines (e.g. the antibacterial agent enoxacin or pyrazineamide and the antimalarial drug pyrimethamine (Ternes & Joss, 2006). Quite a lot of papers already deal with reactions of ozone with aromatic compounds (Tyupalo et al., 1974, Tyupalo & Bernashevskii, 1980, Gilbert & Zinecker, 1980, Hoigné & Bader, 1979, 1983a, b, Gilbert & Hoffmann-Glewe, 1992, Pan et al., 1993, Mvula & von Sonntag, 2003, Naumov & von Sonntag, 2010), amines (Elmghari-Tabib et al., 1982, Cocheci et al., 1989, Andreozzi et al., 1990, 1991, Muñoz & von Sonntag, 2000b, Sein et al., 2008) and nucleobases (Flyunt et al., 2002). Thus, what ozone reactions with aromatic heterocyclic amines concerns, some basic principles are well established. Relating to the amine moiety, ozone reacts predominantly with activated amines. Since the free electron pair has to be available for reaction with ozone, the amines show pH-dependent kinetics (von Sonntag & von Gunten, 2012). Compounds that contain two amino groups (such as EDTA), show a high rate constant, when both amino groups are deprotonated, but reaction rates drop when one of them is protonated. Protonation of one of the nitrogens, apparently, also influences the electron density of the other, thereby reducing its reactivity towards ozone (Muñoz & von Sonntag, 2000b, von Sonntag & von Gunten, 2012). Considering ozone reactions of aromatic compounds the ozone-reactive site is the electron-rich aromatic ring (von Sonntag & von Gunten, 2012). In addition, ozone is a highly selective reactant and its rate constants with aromatic compounds (Neta et al., 1988), nitrogen-containing compounds (von Sonntag & von Gunten, 2012), electron-rich and electron-deficient olefins (Dowideit & von Sonntag, 1998) vary by ten orders of magnitude.

For the ozonation of *N*-heterocyclic aromatic compounds several studies in aqueous solution are presented in the literature. Some studies investigating the ozonation of atrazine, simazine and benzotriazoles (Legube et al., 1987, Yao & Haag, 1991, Acero et

al., 2000, Karpel vel Leitner & Roshani, 2010), as well as caffeine (Kolonko et al., 1979), quinoline (Andreozzi et al., 1992, Wang et al., 2004), imidazole (Pryor et al., 1984, Hoigné & Bader, 1983b) and pyridine (Andreozzi et al., 1991, Hoigné & Bader, 1983b). In the literature several primary ozone reactions with a wide range of compounds have been discussed (Doré et al., 1980, Muñoz et al., 2001, von Sonntag, 2008, von Gunten et al., 2010, von Sonntag & von Gunten, 2012), so that on the basis of these studies several conceivable primary processes are feasible for the four investigated compounds in aqueous solution. A mechanistic demonstration is shown in theoretical background in the Scheme 1, reactions (1) – (15). The examples in Scheme 1 are shown for pyridine, but these reactions can also be applied for pyridazine, pyrimidine and pyrazine. However, these studies and even the most comprehensive textbook (von Sonntag & von Gunten, 2012) have not discussed in detail the ozonation of the investigated amines. Thus, in the present paper the kinetics, stoichiometry and product formation in the reaction of ozone with pyridine, pyridazine, pyrimidine and pyrazine are investigated. The investigated *N*-heterocyclic aromatic compounds could be used as archetypes for more complex micropollutants. Finally, reaction mechanisms (e.g., most abundant primary pathways of scheme 1 and advanced oxidation pathways) are postulated based on stoichiometry data, identified oxidation products and available information from literature.

4.2.1 Theoretical background

In the reactions of the investigated *N*-heterocyclic aromatic compounds with ozone the ozone-reactive site of the amines could be the lone electron pair at nitrogen and the electron-rich aromatic ring as mentioned above. Since, for the investigated compounds the lack of hydrogen at nitrogen disables H-abstraction and ozone insertion, the ozone is forced to addition (see pathway 1) and electron transfer (pathway 2). The addition reaction at nitrogen can lead to *N*-oxides (reaction (1) – (2)) and singlet oxygen ($^1O_2$, see Supporting Information Text S8) as final products (Tyupalo et al., 1980, Andreozzi et al., 1991, Muñoz et al., 2001). In competition, the ozone adduct may undergo electron transfer by dissociating into an amine radical cation and an ozonide radical anion ($O_3^{\bullet-}$). This reaction may also occur immediately via an outer sphere electron transfer, without adduct formation (reaction (3)). However, the outer sphere electron

transfer and electron transfer after adduct formation cannot be distinguished experimenttally. The $O_3^{\bullet-}$ reacts with water giving rise to $^{\bullet}OH$ (reaction (4), Bühler et al., 1984).

Scheme 1. Primary reaction pathways of pyridine in the reaction with ozone (all pathways are just as effectual for pyridazine, pyrimidine and pyrazine).

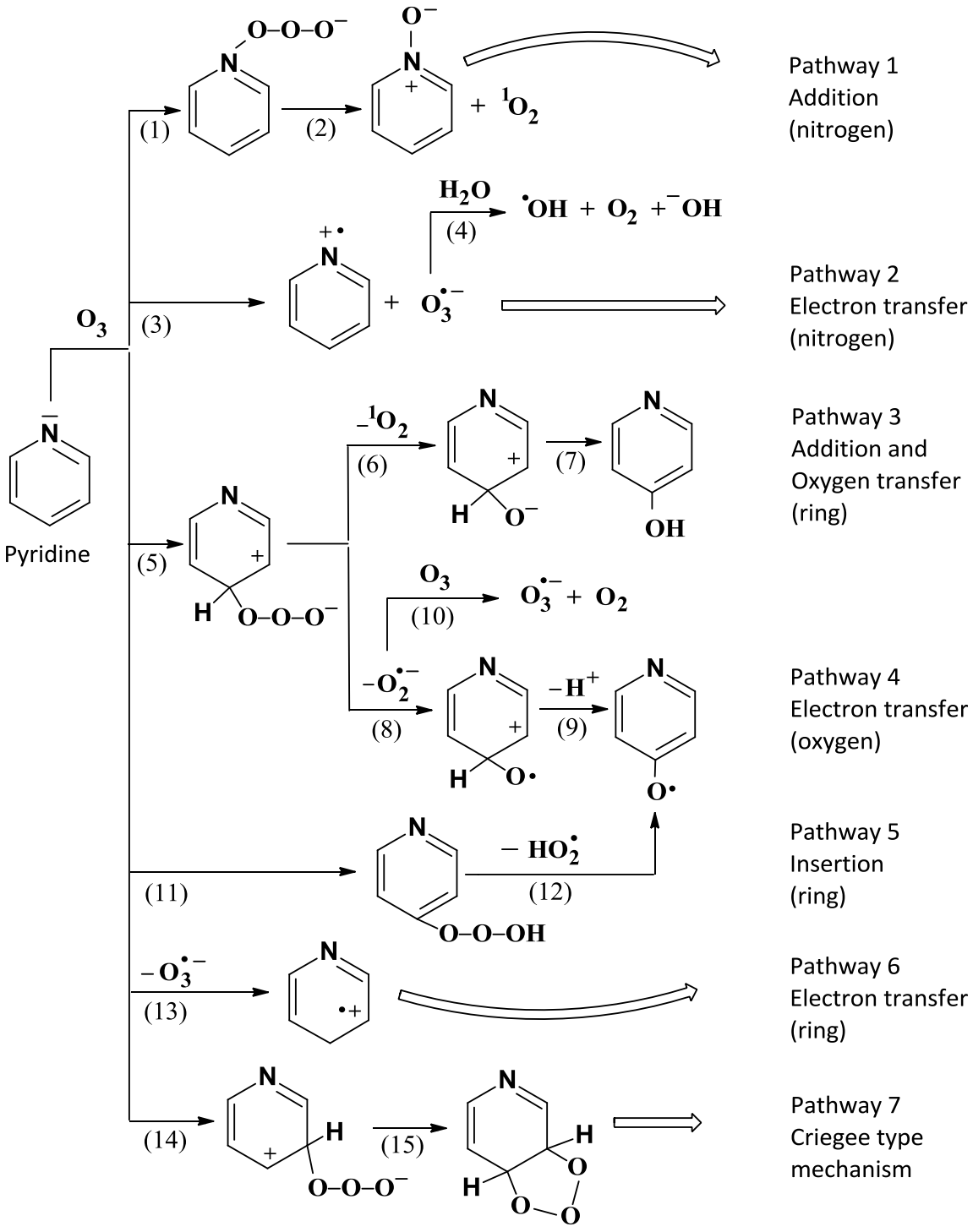

Furthermore, ozone addition can also take place at the slightly activated aromatic ring (reaction (5)). From the subsequent ozone adduct formation a hydroxylation can occur (reaction (6) – (7)). The formed adduct can release a singlet oxygen ($^1O_2$). The decay of the ozone adduct into a phenoxyl radical and a superoxide radical anion ($O_2^{\bullet-}$) is feasible as well (reaction (8) – (9), Ragnar et al., 1999a, b). The $O_2^{\bullet-}$ reacts with ozone to the $O_3^{\bullet-}$ (reaction (10), Sehested et al., 1983), an precursor of $^{\bullet}OH$ (see above). From the ozone attack an insertion process can still proceed (reaction (11)). One further radical pathway after insertion is the subsequent formation of a phenoxyl radical by releasing a hydroperoxyl radical ($HO_2^{\bullet}$) (reaction (12)). The latter is in equilibrium with its conjugate base, the super oxide radical anion, $O_2^{\bullet-}$ (pK_a ($HO_2^{\bullet}$) = 4.8, Bielski et al., 1985, Ragnar et al., 1999a, b). An electron transfer process at the aromatic ring into a radical cation and $O_3^{\bullet-}$ is feasible as well (reaction (13)). A further process that can occur from ozone attack at the aromatic ring is the formation of an ozonide that is well-documented in the reaction of olefins with ozone (reaction (14) – (15)), Criegee, 1975). Which of the above mentioned primary reactions takes place preferentially, may be inferred from products that are formed in the ozone-compound reactions.

4.3 Experimental part

4.3.1 Chemicals and materials

All chemicals were commercially available of analytical grade (> 95%) and used as received. Further information on chemicals is given in Supporting Information in Text S1. Ozone solutions (max. 1×10^{-3} M) were freshly prepared by bubbling ozone-containing gas from an oxygen-fed ozonator through ultra-pure water (Sander, Uetze-Eltze, Germany, oxygen 6.0 from Linde). If high ozone concentrations were required ice-bath-cooled water was used. The ozone concentration of this solution was determined spectrophotometrically taking ε(260nm) = 3200 M^{-1} cm^{-1} (Forni et al., 1982, Hart et al., 1983) using a Shimadzu UV 1800 device.

4.3.2 Methods

Sample preparation. Batch experiments were performed with 10^{-4} – 10^{-1} M solutions of investigated compounds. Solutions containing the investigated compounds with or without additives were made up in ultra-pure water (Merck Millipore, Darmstadt,

Germany) or water in HPLC-grade (Merck) and mixed in various ratios with ozone solutions. All experiments were carried out at room temperature in duplicate or triplicate. The samples were analyzed 3 − 5 h after the addition of ozone to ensure that no residual ozone was present, sometimes tested with indigotrisulfonate. The exclusion of $^{\bullet}OH$ reactions was conducted by choosing tertiary butanol (t-BuOH) as $^{\bullet}OH$ scavenger which reacts slowly with ozone but fast with $^{\bullet}OH$ (k(t-BuOH + O_3) = 0.003 M^{-1} s^{-1} and k(t-BuOH + $^{\bullet}OH$) = 6 × 10^8 M^{-1} s^{-1}, von Sonntag, 2007, Schuchmann & von Sonntag, 1979, Buxton et al., 1988, Flyunt et al., 2003a, Reisz et al., 2003). Further details are given in Supporting Information in Text S2.

Reaction kinetics. The rate constants of the ozone-compound reactions were determined by using the competition methods or by following ozone decay with the indigo method (Bader & Hoigné, 1981). In the indigo method indigotrisulfonate is bleached by ozone and the extent of bleaching is quantified. In this approach the reactions were carried out under pseudo-first-order conditions with substrate in excess, where $[substrate]_0$:$[ozone]_0$ was at least 10:1 (typically greater) (see Supporting Information Text S3). In the competition methods, the ozone decay (ozone under substoichiometric conditions) was followed by quenching with competitor substrate. Here, a competition with 3-buten-2-ol (k = 7.9 × 10^4 M^{-1} s^{-1}, Muñoz & von Sonntag, 2000a, Dowideit & von Sonntag, 1998) and atrazine (k = 24 M^{-1} s^{-1}, Yao & Haag, 1991, k = 7.9 M^{-1} s^{-1}, Brambilla et al., 1995, k = 6.0 M^{-1} s^{-1}, Acero et al., 2000) was selected, since these competitors and the investigated *N*-heterocycles are expected to have similar reactivity towards ozone. The competitor 3-buten-2-ol reacts with ozone to formaldehyde, which was determined with the 2,4-dinitrophenylhydrazine (DNPH) method (Lipari & Swarin, 1982, see Supporting Information Text S3 and Scheme S1). Experiments with atrazine (taking k = 6.0 M^{-1} s^{-1}, Acero et al., 2000) as competitor were carried out by determination of the residual atrazine after complete ozone consumption with HPLC-DAD (LC20, Shimadzu, Duisburg, Germany, see Supporting Information Text S3).

Reaction stoichiometry. The stoichiometry of the ozone reactions was determined by quantifying the residual compounds after complete ozone consumption, measured with a HPLC–DAD system using an external calibration (see Supporting Information Text S4).

Product formation. Product identification was performed via high resolution mass spectrometry (HRMS), in which the detected oxidation products can be identified by exact masses and fragmentation pattern from product ion scans. The spectra were obtained either on an IT-Orbitrap-MS (LTQ Orbitrap Velos) coupled to an Accela HPLC (Thermo Scientific, Bremen, Germany) or on QToF 5600 (SCIEX, Darmstadt, Germany) equipped with a G1312B HPLC system (Agilant, Waldbronn, Germany) via ESI in positive and negative ionization mode. The HPLC systems were equipped either with a Hydro-RP column or a Zorbax Eclipse Plus column running a standard gradient (for more details see Supporting Information Text S5). Quantification of the identified products, for which reference compounds were available, was performed with HPLC-DAD, method as described for the stoichiometric experiments above (refer to Supporting Information Text S5). Determination of $^{\bullet}OH$ yields was carried out with the tertiary butanol assay as $^{\bullet}OH$ scavenger present in excess (see above and Flyunt et al., 2003a, Reisz et al., 2003, Schuchmann & von Sonntag, 1979, Buxton et al., 1988). The tertiary butanol assay leads to formaldehyde, whose yield can be measured readily with the Hantzsch method (Nash et al., 1953). As a rule of thumb, the $^{\bullet}OH$ yield is twice the formaldehyde yield (Flyunt et al., 2003a, see Supporting Information Text S6 and Scheme S5). Formaldehyde (CH_2O) from the ozone-compound reaction was also determined with the Hantzsch method as well as with the DNPH (2,4-dinitrophenyl-hydrazine) method (see description above, kinetics). Hydrogen peroxide (H_2O_2) was quantified with Allen`s approach (Allen et al., 1952, Flyunt et al., 2003b, Kitsuka et al., 2007, see Supporting Information Text S7). Indication of phenolic compounds was carried out with a Hach-Lange test kit (LCK 345). In all analytical methods blanks were performed in the same manner with ultra-pure water instead of ozone solution to determine the initial concentration. Calibration experiments for product determination were performed in the same manner.

4.4 Results and Discussion

4.4.1 Rate constants

The rate constants of the nitrogen-containing heterocyclic compounds range between 0.37 and 57 M^{-1} s^{-1} (for deprotonation ratio (mostly near 100%) depending on apparent pH between 5 and 8 refer to Supporting Information Text S3, paragraph 3). Table 1

summarizes the fitted rate constants. All are very low, but still vary by two orders of magnitude. For pyridine the low rate constant (k = 3.2 M^{-1} s^{-1}) is consistent with previously reported findings suggesting that our method yields reliable kinetic data (k = ~3 M^{-1} s^{-1}, Hoigné & Bader, 1983b, k = 2.0 M^{-1} s^{-1}, Andreozzi et al., 1991). By buffering the samples with phosphate (pH 6.5) and using tertiary butanol (0.05 M) to scavange $^{\bullet}$OH the rate constants ranged between 1.6 and 0.066 M^{-1} s^{-1} (see Figure 1 and Table 1 and refer to Supporting Information Text S2, paragraph 2). These values are almost 10 times lower than without scavenging $^{\bullet}$OH, except for pyridine, where the rate was halfed.

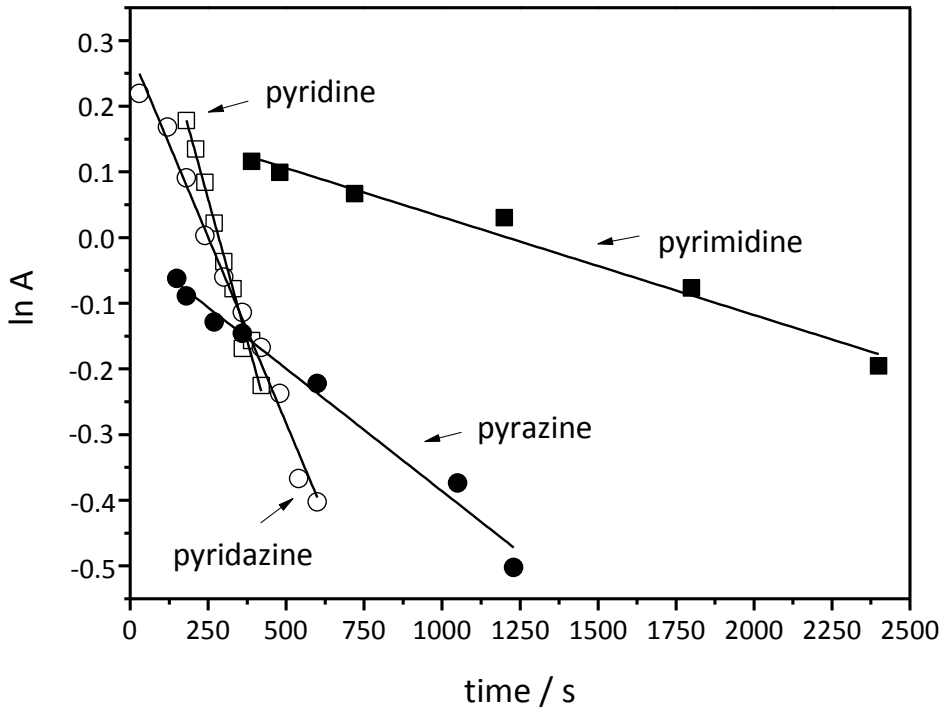

Figure 1. Determination of the rate constants in the reaction of the investigated *N*-heterocyclic compounds c_0(1 - 2 × 10^{-2} M) with ozone in the presence of tertiary butanol (0.05 M) and phosphate buffer (pH 6.5). The absorption of the indigo reagent in logarithmic scale is plotted against reaction time (see Supporting Information Text S3).

The rate constants of the corresponding *N*-oxides are around 10-fold higher, excluding pyridazine-*N*-oxide, than the rate constants of the original *N*-heterocycles (see Table 1). However, the rate constants of the *N*-oxides are very similar (between 28 and 35 M^{-1} s^{-1}). Only pyrimidine-*N*-oxide showed a 4 up to 5-fold lower rate constant. By

buffering and addition of the $^{\bullet}OH$ scavenger the rate constants of the *N*-oxides ranged between 0.45 and 2.1 M^{-1} s^{-1}, which differs up to 50-fold compared with the non scavenged system. Here, the rate constants of the *N*-oxides are also very similar, only pyridazine-*N*-oxide shows a higher rate constant (up to 5-fold).

In summary, the *N*-oxides mostly react somewhat faster with ozone in the presence of $^{\bullet}OH$. So it looks as if $^{\bullet}OH$ reactions are more important in this case. Contrary to all investigated heterocyclic compounds, pyrimidine is oxidized very slowly in particular by scavenging $^{\bullet}OH$. Albeit, $^{\bullet}OH$ reactions are presumably fast (cf. k ($^{\bullet}OH$ + pyrimidine) = 1.6×10^8 M^{-1} s^{-1}, pH 6-7, Buxton et al., 1988) due to the low $^{\bullet}OH$ yield in this experiment, the real $^{\bullet}OH$ reaction rate is slower (k_{app} ($^{\bullet}OH$ + pyrimidine = 3.2×10^3 s^{-1}), but nonetheless faster than the ozone reaction (k_{app} (O_3 + pyrimidine = 3.7×10^{-2} s^{-1} at highest c_0(10^{-1} M). Nevertheless, it should be mentioned that in the absence of $^{\bullet}OH$ the rate constant of all investigated *N*-heterocycles with ozone are all in all low (Table 1). As a consequence the reaction of ozone with the aromatic *N*-heterocycles is slow by comparison to aliphatic *N*-heterocyles ($1.9 \times 10^4 - 2.4 \times 10^5$ M^{-1} s^{-1}, Tekle-Röttering et al., 2016). The low ozone rate constants can be explained by the sp^2 hybridisation of nitrogen in comparison to the sp^3 hybridisation of anilines and aliphatic *N*-heterocycles. Under the assumption that ozone attack takes place on nitrogen or the aromatic ring, the lone nitrogen electron pair of the nitrogen is presumably not very accessible as well as the aromatic ring is less activated for electrophilic attack. This is in accordance to the low pK_a values (see Table 1), but not in accordance to the descending order of pK_a values, because increasing pK_a values do not consequently lead to increasing rate constants. However, in scavenged systems in line from pyridine to pyrazine, the rate constants are more compatible to pK_a values with the exception of pyrimidine. Therefore it is evident that the availability of the lone electron pair is not the only possibility for the reaction of ozone with the aromatic heterocyclic compounds. Moreover, the rate constants of pyridazine and pyridazine-*N*-oxide are appreciably higher in the non scavenged system than the others and in the case of pyrimidine and pyrimidine-*N*-oxide they are considerably lower. Thus, it seems that the effect of the second nitrogen atom on the rate constant depends very much on its position relative to N1. In *ortho* position the rate constant relative to pyridine is

increased, in *meta* position decreased and in *para* position the effect is not significant. Indeed, in the scavenged system, these relations are different.

Table 1. Compilation of ozone rate constants, reaction stoichiometry (in %) plus products and their yields (related to ozone consumed or to compound consumed) in the reaction of ozone with nitrogen-containing heterocyclic compounds in the presence and absence of tertiary butanol (standard deviation in parenthesis). Sum of products in relation to 100% oxidized compound are presented in rectangular brackets.

Compounds	k / $M^{-1} s^{-1}$	**Compound degradation / %** (Per ozone consumed)	**Product yield / %** First column: Per ozone consumed. Second column: Calculated per degraded compound. In rectangular brackets: Sum of stable products per degraded compound		pK_a #
Pyridine	3.2 (± 0.39)	52* (± 6.1)		[53]	5.23
	1.6 (± 0.17)•	55 (± 7.2)•		[94]•	
Pyridine-*N*-oxide	29 (± 0.94)	27 (± 1.8)	25* (± 1.1)	48	
	0.78 (± 0.15)•	4.6 (± 0.24)•	51 (± 6.4)•	93•	
•OH			1.7 (± 0.19)		
Formaldehyde			0.31 (± 0.025)	0.59	
Hydrogen peroxide			1.5 (± 0.23)	4.2	
			0.68 (± 0.071)•	1.2•	
Pyridazine	57 (± 4.9)	12 (± 2.1)		[21]	2.24
	1.4 (± 0.11)•	54 (± 4.0)•		[99]•	
Pyridazine-*N*-oxide	35 (± 0.99)	21 (± 1.5)	0.70 (± 0.011)	5.8	
	2.1 (± 0.68)•	1.6 (± 0.66)•	49 (± 1.7)•	91•	
•OH			5.7 (± 0.17)		

Formaldehyde Hydrogen peroxide			0.52 (± 0.045) 1.4 (± 0.064) 4.1 (± 0.76)*•	4.3 11 7.6•	
Pyrimidine Pyrimidine-*N*-oxide •OH Formaldehyde Hydrogen peroxide	0.37 (± 0.58) 0.066 (± 0.013)• 7.1 (± 0.14) 0.99 (± 0.15)•	25 (± 3.2) 14 (± 5.2)• 14 (± 2.7) 3.0 (± 0.50)•	 detected, not quantified 4.8 (± 0.51) 0.21 (± 0.013) 15 (± 2.1) 9.7 (± 1.7)•	[60] [69]• 0.84 59 69•	1.23
Pyrazine Pyrazine-*N*-oxide •OH Formaldehyde Hydrogen peroxide	1.3 (± 0.14) 0.17 (± 0.021)• 28 (± 0.56) 0.45 (± 0.071)•	22 (± 2.1) 2.1 (± 1.6)• 19 (± 0.82) 1.6 (± 0.94)•	 detected, not quantified 3.6 (± 0.15) 0.13 (± 0.021) 3.9 (± 0.28) 2.0 (± 0.41)•	[18] [95]• 0.59 17 95•	0.65

(Determination of formaldehyde with Hantzsch assay)

• Scavenged with t-BuOH and buffered (sometimes) with phosphate

* Calculated for the linear range

pK_a of corresponding acid, pK_a – values from Katritzky et al., 1984

In contrast, the rate constants of some *N*-heterocycles with resembling composition e.g., atrazine (7.9 ± 0.62 M^{-1} s^{-1} Brambilla et al., 1995, 6.0 ± 0.3 M^{-1} s^{-1}, Acero et al., 2000) simazine (11.9 ± 0.50 M^{-1} s^{-1}) and terbutylazine (8.9 ± 0.39 M^{-1} s^{-1}, Brambilla et al., 1995) are more similar to each other than the investigated *N*-heterocycles. On the contrary the rate constants of some benzotriazole, e.g., 1*H*-benzotriazole (35 M^{-1} s^{-1}), 5-chlorobenzotriazole (13 M^{-1} s^{-1}), 5-methylbenzotriazole (164 M^{-1} s^{-1}) and 5,6-dimethylbenzotriazole (880 M^{-1} s^{-1}, Lutze et al., 2015) vary by more than one order of magnitude due to the nature of substituents. In comparison to other aromatic compounds such as benzene and quinoline the rate constant of pyridine is as low as

that of benzene (*k* = 2.0 M^{-1} s^{-1}, Hoigné & Bader, 1983a) and little lower than for quinoline (*k* = 51 M^{-1} s^{-1}, Wang et al., 2004).

4.4.2 Reaction stoichiometry

Despite the moderate to low ozone rate constants, stoichiometry of the reaction between ozone with the nitrogen-containing heterocyclic compounds is of special interest for detailed mechanistic studies. The reaction stoichiometry, the amount of ozone needed for compound degradation was determined after complete ozone consumption by quantification of the residual compounds quantities. At apparent pH value (the pH of the initial solution of the selected amines was in the range of 5 – 8) and different ozone-compound molar ratios (1:0.7 – 1:7, in scavenged and non scavenged systems) the compound dissipation increased linear with ozone concentration (see Figure 2, using the examples pyridazine (main graph) and pyrazine (inset)). An exception is pyridine in the non scavenged system, for which the calculation is made only for the linear range until an ozone-compound molar ratio of 1:1.7 (see Figure 4). Further details are given in Supporting Information Text S4. The stoichiometric data for the reaction of ozone with the nitrogen-containing heterocyclic compounds are compiled in Table 1.

The data in Table 1 show that in the reaction of ozone with pyridine 0.52 moles of pyridine are degraded per mole ozone (in absence of an $^{\bullet}OH$ scavenger). Thus, after complete ozone consumption only 52% of that ozone attack yields the degradation of pyridine. Much less pyridazine (12%), pyrimidine (25%) and pyrazine (22%) have been degraded per ozone. In presence of the $^{\bullet}OH$ scavenger tertiary butanol, the efficiency of pyridine degradation nearly remains the same (55%). In the case of pyridazine a much higher difference of 42% in compound degradation between the presence and absence of the $^{\bullet}OH$ scavenger can be observed (Table 1). Therefore, in particular for pyridazine a higher ozone dosage is required for compound elimination when the radical scavenger is absent.

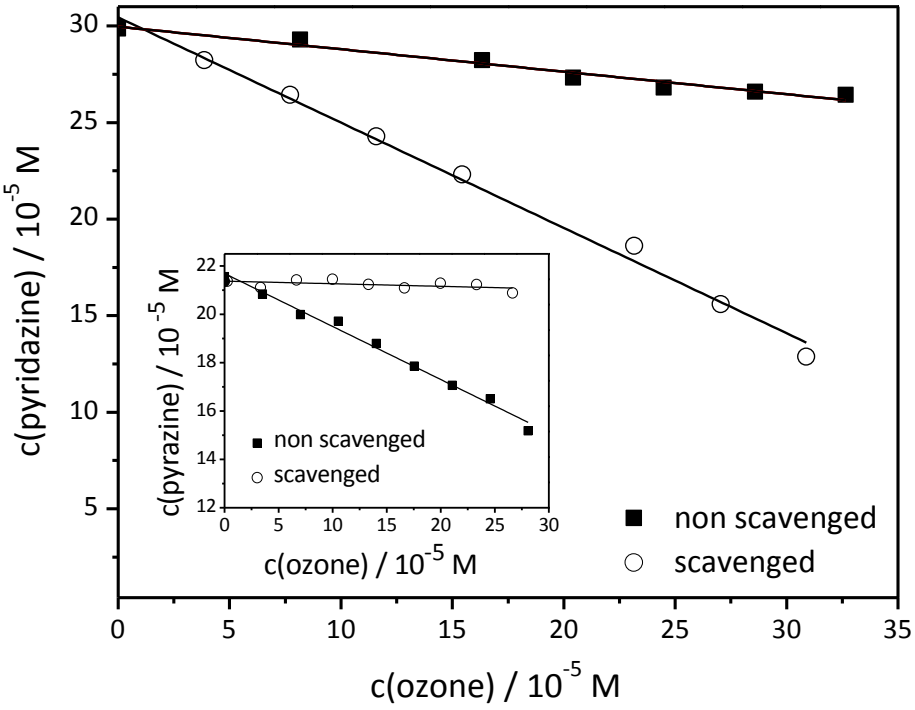

Figure 2. Correlation of amine degradation and ozone consumption in the ozone reaction of pyridazine $c_0(2.9 \times 10^{-4}$ M) and pyrazine $c_0(2.1 \times 10^{-4}$ M). Residual pyridazine and pyrazine concentrations after complete ozone consumption are plotted vs. the ozone concentration for experiments in the presence and absence of tertiary butanol. Main graph: pyridazine. Inset: pyrazine.

The difference in compound degradation between scavenged and non scavenged system indicates that ozone consuming reactions, which do not contribute to compound degradation are much more important in the presence of $^{\bullet}$OH. Even though reaction (3) (see Scheme 1, Table 1 and description below) should be a minor reaction (less $^{\bullet}$OH yields are determined, refer to Chapter $^{\bullet}$OH yields) and thus less free radicals may be developed, the low amine degradation could be reasonably explained by a chain reaction, similar to diclofenac (Sein et al., 2008). There it has been proposed, that aminyl radicals, whose are additionally formed by $^{\bullet}$OH, consume ozone in competition with the original compound (von Gunten, 2003, Sehested et al., 1984). The presence of a probably radical chain reaction in the pyridazine-ozone reaction as opposed to the pyridine-ozone reaction needs to explain. The $^{\bullet}$OH can react with pyridine and pyridazine by forming radicals (refer to Scheme 2, reaction (16) and (20),

respectively). In the case of pyridine the resulting radical can only undergo a radical-shift from nitrogen to carbon (reaction (17)). The resulting C-centered radical is expected to undergo a rapid reaction with oxygen (Tauber & von Sonntag, 2000) that are in high concentration in our systems.

Scheme 2. Reactions of $^{\bullet}$OH with pyridine and pyridazine by inducing a chain reaction in the case of pyridazine.

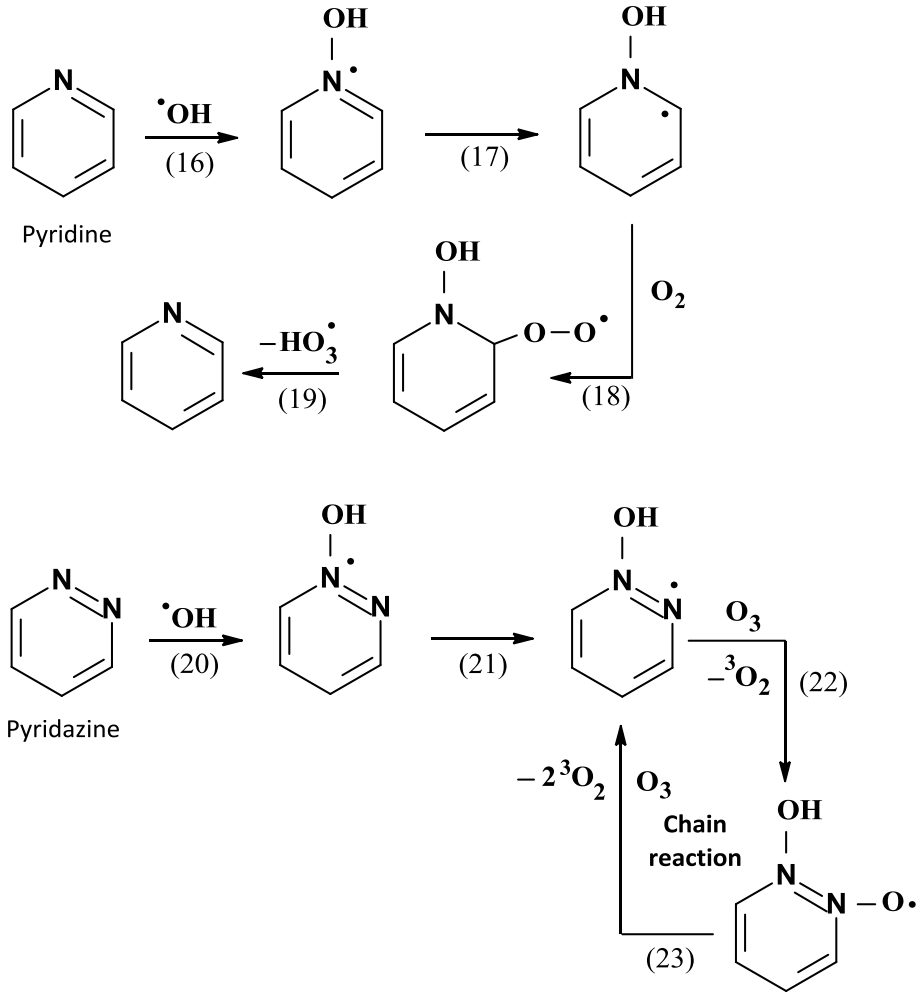

The composing short-lived peroxyl radical (reaction (18)) can subsequently cleave a hydrotrioxyl radical by back-forming the pyridine (reaction (19)). Thus, the radical reaction is terminated even if the resulting hydrotrioxyl radical decomposes by forming $^{\bullet}$OH again. Pyridazine can react in the same reaction type such as pyridine by forming a C-centered radical. However, this radical can also undergo a radical-shift from nitrogen to the adjacent nitrogen (reaction (21)) by forming an aminyl radical. Aminyl radicals as

N-centered radicals do not react with O_2, but can react with ozone. Thus, these aminyl radicals can initiate a chain reaction that consume ozone (see above and reaction (22) – (23)) without further compound degradation.

Surprisingly, pyrimidine (14%) and pyrazine (2.1%) react completely differently in that there is a marginal degradation with the use of $^{\bullet}OH$ scavenger (see Figure 2 for pyrazine (inset) and Table 1). These results point out, that particularly pyrazine mainly reacts with $^{\bullet}OH$, because scavenging $^{\bullet}OH$ leads to extremely low compound degradation. This is in accordance with Andreozzi et al., 1990. Here, it is demonstrated that in the ozonation of pyrazine (pH 5) it is only sensitive to a radical attack in contrast to quinoxaline. In the case of pyrimidine both reactions, ozone and $^{\bullet}OH$ reactions seem equally important since without $^{\bullet}OH$ the ozone reaction leads to more or less half the compound degradation than if both oxidants are present.

The low compound degradation while high ozone consumption in the absence of $^{\bullet}OH$ in particular for pyrazine indicates further ozone consuming reactions as well. Some feasible ozone consuming reactions (24) – (31) are presented in Scheme 3. In this scheme the decay of the ozone adduct into superoxide and phenoxyl radicals (Ragnar et al., 1999a, b) based on primary reaction pathway 4 is suggested. Phenoxyl radicals barely react with oxygen, but can react with ozone (von Sonntag & von Gunten, 2012). Thus, both of these radicals, the superoxide radical (reaction (27) – (29)) and the phenoxyl radical (reaction (30) and (31)) can consume ozone in further processes (von Sonntag & von Gunten, 2012). The reaction of $^{\bullet}OH$ with ozone, formulated as an O-transfer, can generally consume ozone. Although, this reaction is fast (k ($^{\bullet}OH + O_3$) = 3×10^9 M^{-1} s^{-1}, Bahnemann & Hart, 1982, or 1.1×10^8 M^{-1} s^{-1}, Sehested et al., 1984) $^{\bullet}OH$ is in principle in competition with other free radicals, which react with ozone in some cases close to the diffusion-controlled limit. Indeed, the $^{\bullet}OH$ reaction with ozone is also in competition with the ozone-compound reaction, which usually reacts faster because in normal case the compounds are present in higher concentration. In this case, however, the reaction of $^{\bullet}OH$ with ozone is faster than the reaction of ozone with the *N*-heterocycles (see Supporting Information Text S6). Certainly, the reaction of pyrazine or pyrimidine with $^{\bullet}OH$ should be faster, since $^{\bullet}OH$ interact very fast with the

N-heterocycles (e.g., k ($^{\bullet}$OH + pyridine) = 4.5×10^9 M^{-1} s^{-1}, pH 5.9, k ($^{\bullet}$OH + pyrimidine) = 1.6×10^8 M^{-1} s^{-1}, pH 6-7, k ($^{\bullet}$OH + pyridine-*N*-oxide) = 3.0×10^8 M^{-1} s^{-1} at pH 6-7, Buxton et al., 1988). Hence, the highest observed rate constants of ozone with pyridine and the other investigated compounds (see Kinetics) are many orders of magnitude lower than the rate constants in their reaction with $^{\bullet}$OH.

Scheme 3. Proposed reaction pathways for ozone consuming reactions in the case of pyrazine (which also holds for all *N*-heterocycles under study).

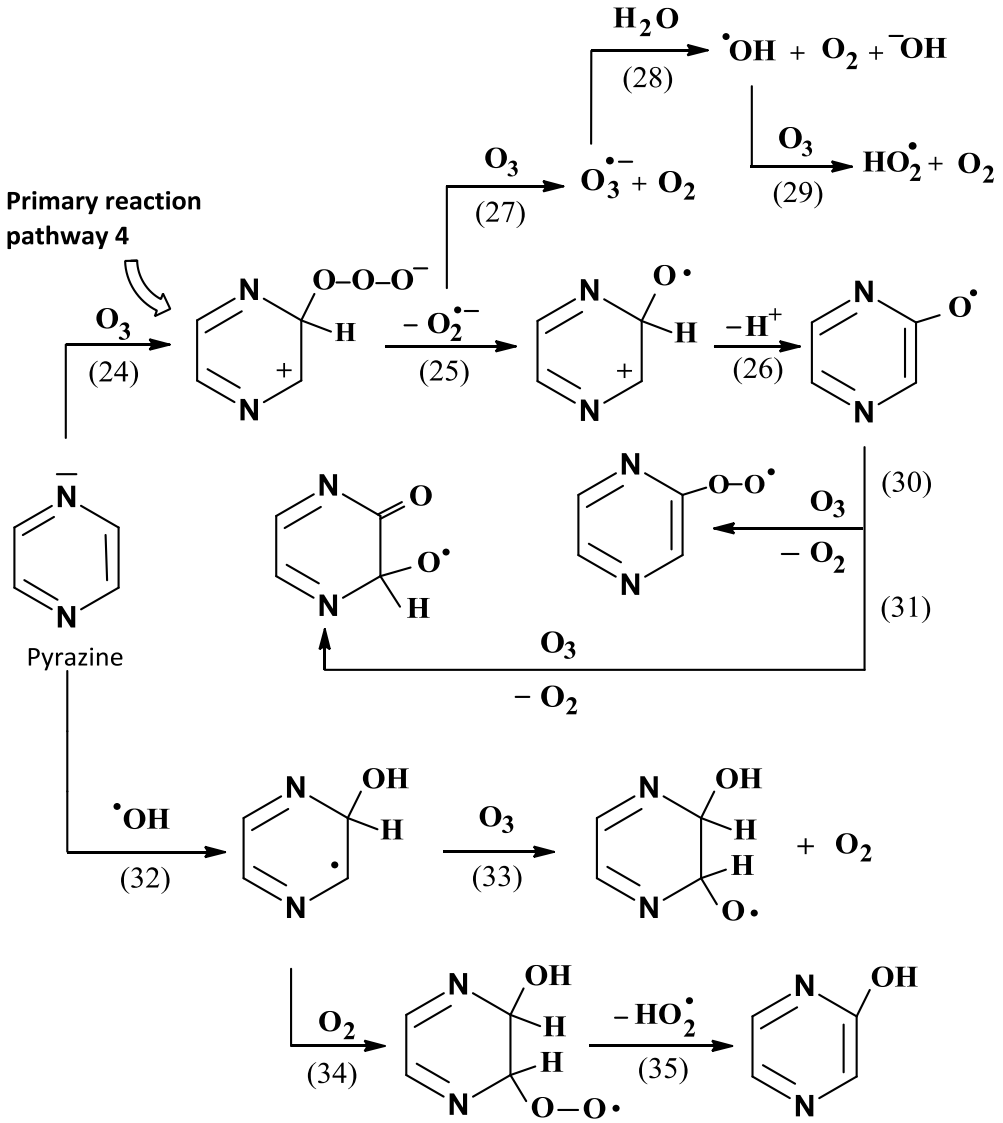

Thus, it would principally be conceivable that $^{\bullet}$OH may compete in the reaction of pyrazine and pyrimidine with ozone, even when the $^{\bullet}$OH concentration is low (e.g., k_{app} ($^{\bullet}$OH + pyrimidine) = 3.2×10^3 s^{-1}). In the non scavenged system $^{\bullet}$OH can create

hydroxycyclohexadienyl radicals (see Scheme 3, reaction (32), which further can consume ozone (reaction (33)). Certainly the hydroxycyclohexadienyl radicals may also react with oxygen by forming hydroperoxyl radical, $HO_2^{\bullet}$ (reaction (34) – (35)), which in turn can consume ozone (refer to theoretical background and (k ($O_2^{\bullet-}$ + O_3) = 1.5 × 10^9 M^{-1} s^{-1}, Sehested et al., 1983 or 1.6 × 10^9 M^{-1} s^{-1}, Bühler et al., 1984). In contrast to oxygen, which reacts reversibly with hydroxycyclohexadienyl radicals, ozone must react irreversibly (von Sonntag & von Gunten, 2012). It seems furthermore that no aminyl radicals should be formed for the same reason as in the case of pyridine, so that the ozone consuming aminyl radical chain reaction (see Scheme 2) is not observed in these systems.

In addition, the reaction stoichiometry of the *N*-oxides in the non scavenged and scavenged system has been investigated (see Table 1). Analysis of the samples with different ozone-compound molar ratios (see reaction stoichiometry for the *N*-heterocycles) show linear dependency of compound degradation (compiled in Table 1) upon the reaction with ozone (see Figure 3 for pyridazine-*N*-oxide and pyrimidine-*N*-oxide) and indicates the same transformation reaction for all *N*-oxides with ozone. In all cases (except pyridazine-*N*-oxide in non scavenged system) the degradation of the *N*-oxides is lower than for the corresponding *N*-heterocycles and yielded to 14% to 27% (Table 1) in the presence $^{\bullet}$OH.

In the absence of $^{\bullet}$OH, the degradation of all *N*-oxides leads to even much lower transformation values. Here, *N*-oxides degradation of 1.6 – 4.6% (Table 1) was observed. These results indicate that mainly $^{\bullet}$OH reacts with the *N*-oxides. Therefore, the *N*-oxides are similarly reactive towards ozone as like pyrazine and pyrimidine. For the *N*-oxides, this reactivity can be explained by their missing lone electron pair at nitrogen, which is already bound to oxygen and not available for the electrophilc ozone.

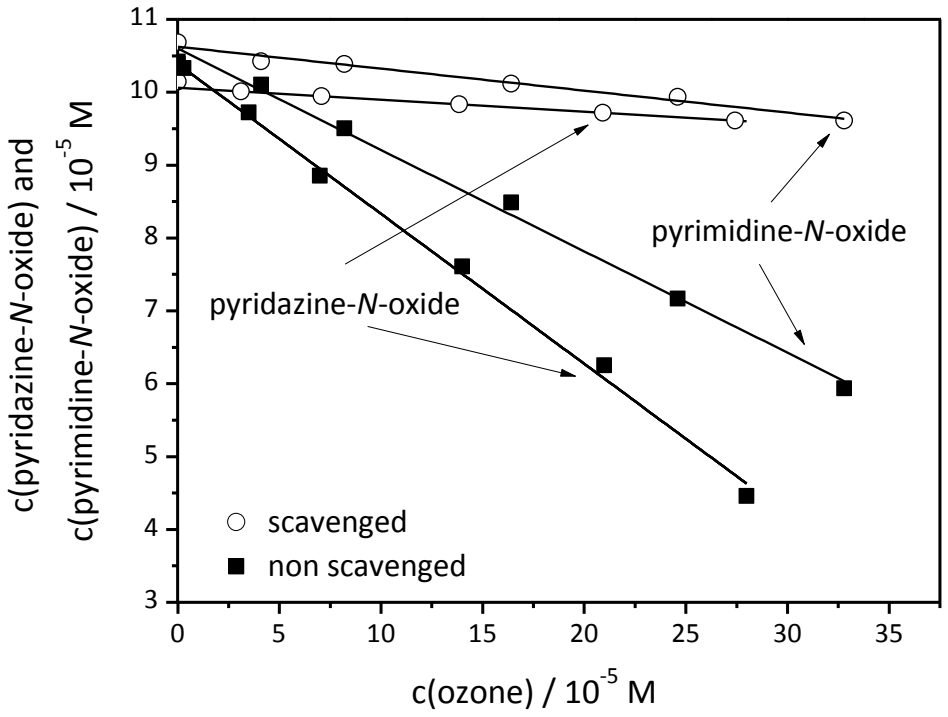

Figure 3. Reaction stoichiometry in the ozonation of pyridazine-*N*-oxide $c_0(1 \times 10^{-4}$ M) and pyrimidine-*N*-oxide $c_0(1 \times 10^{-4}$ M). Pyridazine-*N*-oxide and pyrimidine-*N*-oxide concentrations in the presence and absence of tertiary butanol are plotted vs. the ozone concentration.

4.4.3 Product formation

***N*-oxides and hydroxy products**. The *N*-heterocycles can react with ozone to their appropriate *N*-oxides according to the suggested primary reaction pathway 1 in Scheme 1 (e.g., reaction (1) – (2) illustrates the reaction with pyridine (Andreozzi et al., 1991). This is also similar to the *N*-oxide formation in the reaction of tertiary amines with ozone (Muñoz & von Sonntag, 2000b, Lange et al., 2006, Zimmermann et al., 2012). Indeed, in the reaction of pyridine and pyridazine with ozone the main oxidation products in each case is pyridine-*N*-oxide and pyridazine-*N*-oxide (for further details see supporting information Text S5, paragraph 1), which are formed in the presence and absence of $^{\bullet}$OH scavenger. The *N*-oxide yields increased linearly with the ozone dose. An exception is pyridine-*N*-oxide in the non scavenged system, for which the calculation was made only for the linear range up to an ozone-compound molar ratio of 1:3.2 (see Figure 4).

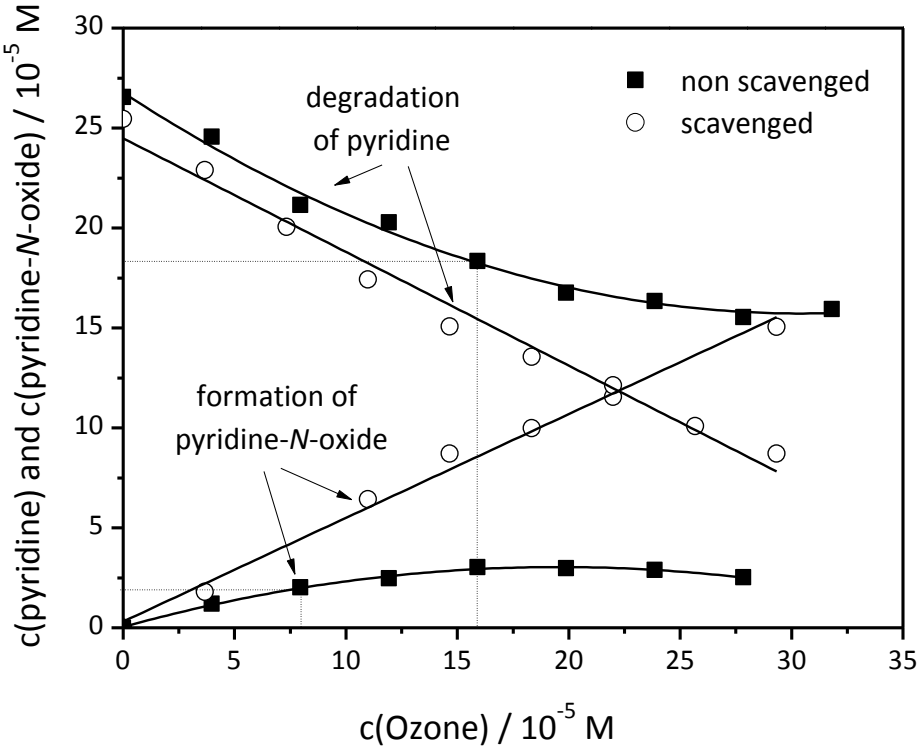

Figure 4. Ozonation of pyridine c_0(2.7 × 10^{-4} M) leading to the degradation of pyridine and formation of pyridine-*N*-oxide. Pyridine and pyridine-*N*-oxide concentrations in the presence and absence of tertiary butanol are plotted vs. the ozone concentration. In the absence of tertiary butanol calculation was made only for the linear range (see dotted line).

In Figure 4 it is seen that pyridine-*N*-oxide concentration is affected by its competition with pyridine for available ozone in the non scavenged system. This leads to a corresponding increase in ozone dose necessary to consume pyridine. The determined pyridine-*N*-oxide and pyridazine-*N*-oxide yields are 51% and 49%, respectively in scavenged system (calculated from the slope of the resulting graph see Figure 4 and Table 1). In absence of an $^{\bullet}$OH scavenger the pyridine-*N*-oxide yield decreased to 25% with respect to ozone, while a dramatically low yield of 0.7% in the case of pyridazine-*N*-oxide was determined. This is consistent with lower compound transformation in the absence of $^{\bullet}$OH scavenger in both cases (see reaction stoichiometry). However, this does not explain, the very low *N*-oxide yield in the case of pyridazine (Table 1).

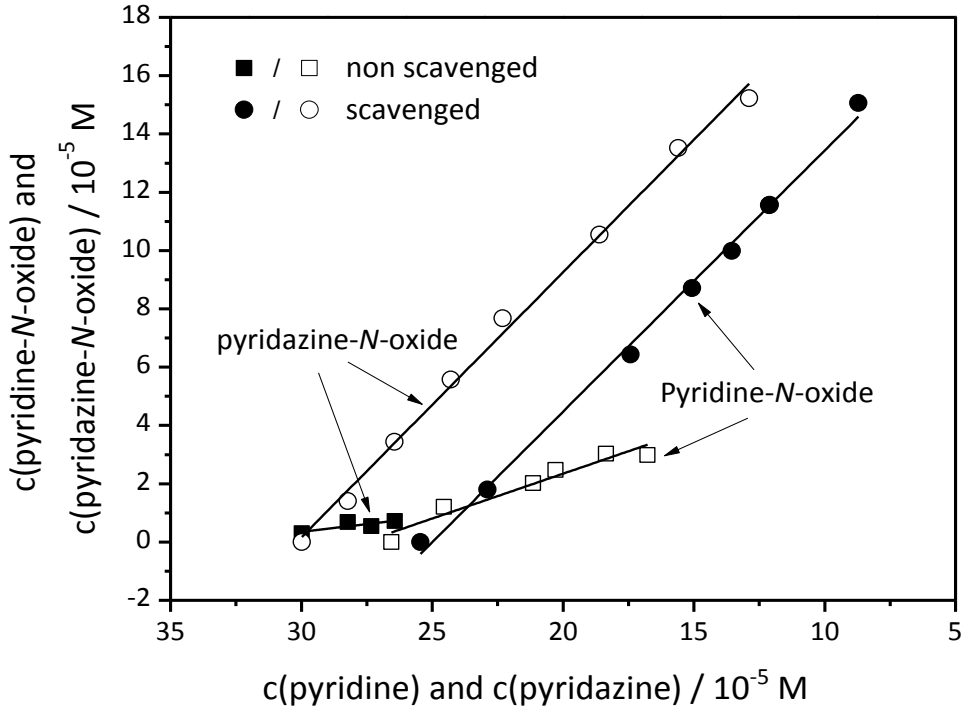

Figure 5. Formation of pyridine-*N*-oxide and pyridazine-*N*-oxide in the reaction of pyridine and pyridazine c_0(2.8×10^{-4} M) with ozone. Pyridine-*N*-oxide and pyridazine-*N*-oxide concentrations in the presence and absence of tertiary butanol are plotted vs. the oxidized compound concentration.

With respect to compound degradation the calculation provided a yield of 93% of pyridine-*N*-oxide and 91% of pyridazine-*N*-oxide in scavenged system (the slopes in Figure 5 indicate the yields). In the non scavenged system the yield of pyridine-*N*-oxide reached still almost the half (48%), while for pyridazine-*N*-oxide only 5.8% were calculated. The existence of high *N*-oxide yields (in the absence of $^{\bullet}$OH) indicate that the most favored reaction of ozone with pyridine and pyridazine is an ozone attack at nitrogen as suggested in Scheme 1 (see above and primary pathway 1). This electrophilic mechanism leads to an ozone adduct at nitrogen followed by an oxygen transfer yielding to *N*-oxide and singlet oxygen ($^1O_2$).

HPLC-DAD analysis did not indicate formation of *N*-oxides in the ozonation of pyrimidine and pyrazine, neither with nor without $^{\bullet}$OH scavenger. This is further evidence that apparently ozone attack does not take place preferentially at the nitrogen atom of pyrazine and pyrimidine. A reason for this could be the reduced

availability of the nitrogen lone pair, because the second ring-nitrogen shares the available π-electrons with the first and two nitrogen atoms further withdraw electron density from the ring carbon even more than one in pyridine. A reduced accessibility of the lone electron pair at nitrogen is also seen in the descending order of pK_a values from pyridine to pyrazine (see Table 1). Pyridazine, in contrast undergoes ozone attack at nitrogen much easier than pyrimidine and pyrazine, a result which is based on electron repulsion between the two immediately adjacent nitrogen lone pairs (Joule & Mills, 2010). For pyrimidine in turn the depletion of electron density at positions α or γ to the ring-nitrogens has a greater importance, since the ring-*N*-atoms act in unison, than in pyrazine, where this is not the case (Tisler & Stanovnik, 1984).

The occurrence of two main products in the reaction of ozone with pyrimidine and pyrazine in HPLC-DAD results (eluted close to the dead time and without characteristic UV-spectrum, see above) suggest formation of polar compounds. In order to identify these oxidation products, LC-HRMS measurements (see Supporting Information Text S5, paragraph 2) in scavenged and non scavenged systems (only at apparent pH) were used. The experiments were also performed with direct injection of eluent fractions containing the oxidation products in order to obtain MS^2 spectra (see Supporting Information Text S5). However, LC-HRMS measurements by using IT-Orbitrap-MS provided only one MS^2 in the reaction of pyrazine with ozone (without $^{\bullet}OH$ scavenger), which was obtained for the molecular mass 147.04 (see Supporting Information Text S5, paragraph 3). Measurements with a time-of-flight mass spectrometry (LC-Q-ToF) as a more sensitive analytical technique supplied also a MS^2 for the molecular mass 147.0417 with same sum formula ($C_4H_7O_4N_2$), albeit with different fragmentation pattern (see Supporting Information Text S5, paragraph 4). However, different fragmentation pattern is expected when changing LC-MS system and is no absolute indication that this is a different compound. The MS^2 fragmentation spectrum from m/z 147 $[M+H]^+$ using IT-Orbitrap-MS suggests the presence of an hydroxyl and amine group (presented in Supporting Information Figure S2 and Scheme S2). From the fragmentation pattern and sum formula ($C_4H_7O_4N_2$) obtained from accurate mass measurements, 2,3,5,6-tetrahydroxypyrazine is proposed as a transformation product. A positive phenol test confirmed the presence of compounds with hydroxyl groups in this ozone reaction. In reaction stoichiometry experiments it is shown that the ozone

plus pyrazine reaction should plays a minor role. Thus, a transformation of pyrazine is more likely to be achieved by the reaction of $^{\bullet}$OH and pyrazine and 2,3,5,6-tetrahydroxypyrazine is a plausible product from such a reaction. For a decent mechanistic discussion see Scheme S3 in the Supporting Information. From measurements with LC-Q-ToF obtained fragmentation pattern of 147.0417 rather suggests a linear alkyl chain (refer to Supporting Information Figure S3 and Scheme S4). With respect to the transformation mechanism for the ozonation of pyrazine Scheme 4 illustrates a proposed reaction pathway for the structure of ethylene diamine 1,4-dicarboxylic acid as follows. The way ozone can react with pyrazine is depicted in the reaction sequence (36) – (39). In this scheme the reactions (36) – (37) are identical with the primary pathway 7 in Scheme 1 supplemented with reactions (38) – (39). Thus, in the ozonation of pyrazine a preferential ozone attack on the double bond could be suggested, followed by Criegee cleavage as described below. For though, after ozone addition the ozonide can breakdown into a hydroxyhydroperoxide (Dowideit & von Sonntag, 1998), which could be converted into ethylene diamine 1,4-dicarboxylic acid. Thus, the above mentioned HRMS results indicate that in minor side reactions pyrazine can react either with ozone to ethylene diamine 1,4-dicarboxylic acid and/or with $^{\bullet}$OH to 2,3,5,6-tetrahydroxypyrazine, respectively.

In addition, a mass of 97.0409 was found as a product of the reaction of both pyrazine and pyrimidine with ozone. From the fragmentation pattern and molecular mass (see Supporting Information Figure S4) the corresponding *N*-oxides could be identified (cf. Scheme 1, pathway 1). This indicates that also for pyrazine and pyrimidine ozone attack on nitrogen takes place. However, this probably plays a subsidiary role. Quantification of the identified oxidation products was not feasible because an authentic reference standard was not available. Hence, detailed data for the transformation products of pyrimidine and pyrazine with ozone are still missing and will need further elucidation. However, this was out of scope of the current work.

Scheme 4. Proposed reaction pathways for the formation of ethylene diamine 1,4-dicarboxylic acid in the reaction of pyrazine with ozone and the formation of hydrogen peroxide in the reaction of pyrimidine with ozone (this also holds for pyrazine, albeit in a minor degree).

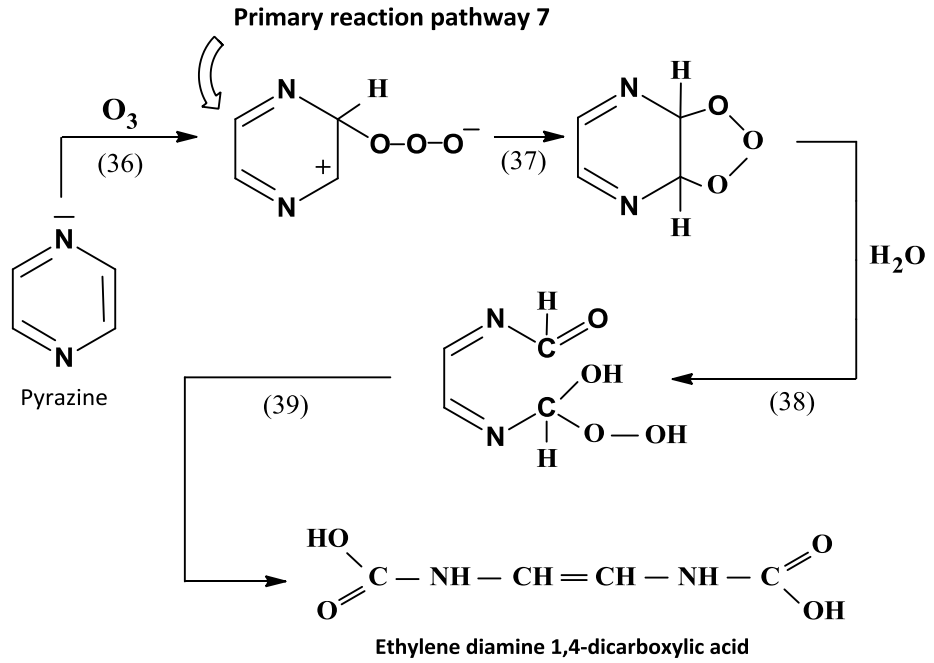

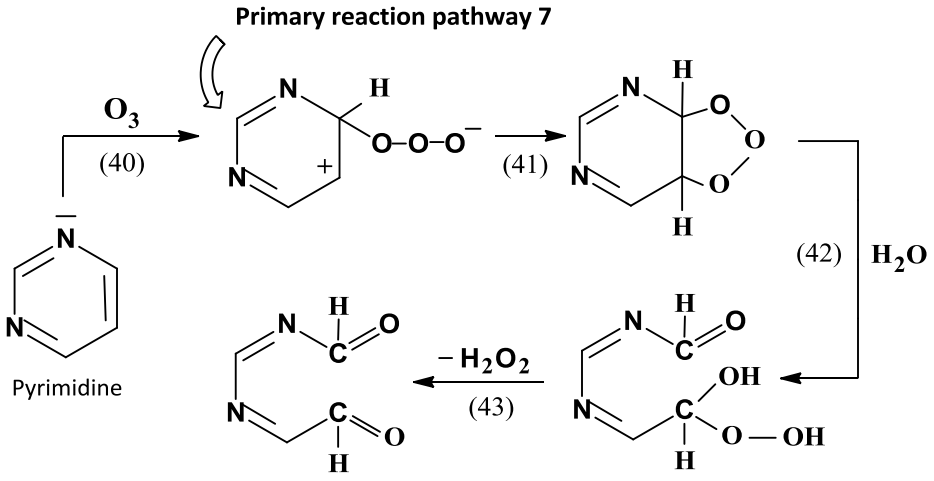

$^{\bullet}$OH yields. The reactions of ozone with aromatic *N*-heterocyclic compounds can generate $^{\bullet}$OH, if the primary pathways 2, 4, 5 and/or 6 (shown for pyridine in Scheme 1) take place (von Sonntag & von Gunten, 2012). Figure 6 shows that the $^{\bullet}$OH yields increase in all cases linearly with increasing ozone concentrations, when plotted against the ozone concentration (refer to supporting information Text S6). The slopes

in Figure 6 indicate very low •OH yields (1.7 – 5.7%) for the *N*-heterocyclic compounds by comparison with aliphatic *N*-heterocyles (28 – 33%, Tekle-Röttering et al., 2016). From the low values (shown in Table 1), it is suggested that electron transfer reactions are minor reactions in all cases. These reactions are shown as the primary pathways 2 and 6 in Scheme 1 in the case of pyridine, which are postulated to occur in an analogous manner for pyridazine, pyrimidine and pyrazine. However, these compounds can also initiate further radical reactions.

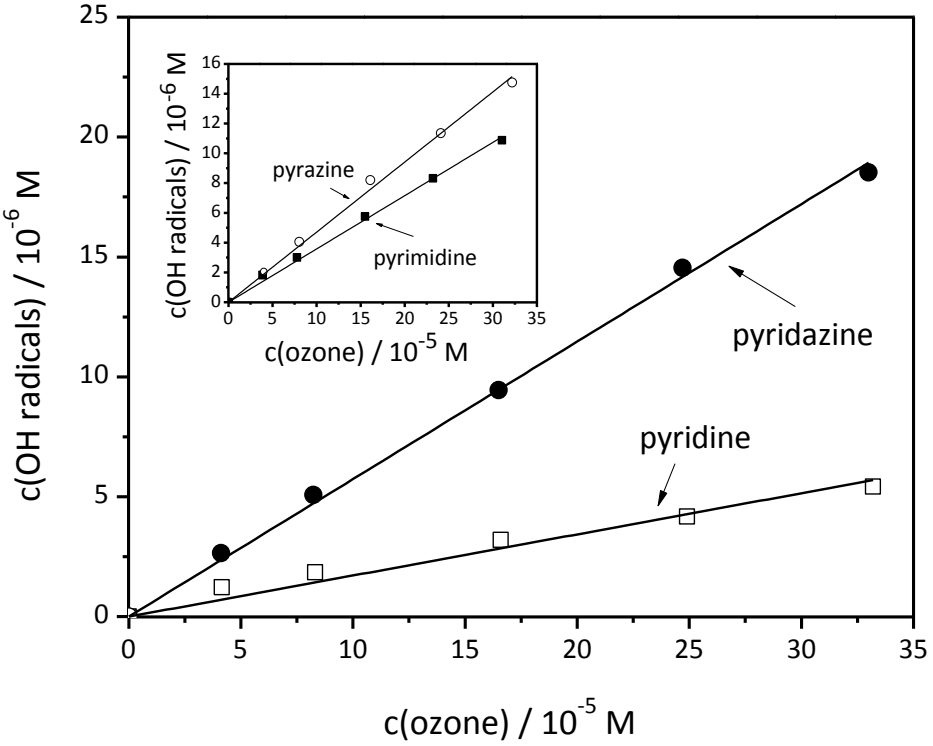

Figure 6. Formation of •OH in the reaction of *N*-heterocycles $c_0(3 \times 10^{-4}$ M) with ozone. •OH concentrations are potted vs. the ozone concentration. Main graph: pyridine and pyridazine. Inset: pyrimidine and pyrazine.

Formaldehyde and hydrogen peroxide yields. In ozonation experiments of the investigated amines secondary products can potentially be formaldehyde and hydrogen peroxide. The product yields of these compounds were calculated and the corresponding data are summarized in Table 1 (refer to Supporting Information Text S7). A plot of formaldehyde formation vs. ozone concentration in the non scavenged system allows quantifying yields by a linear regression. This leads in all cases to very low formaldehyde yields between 0.13 and 0.52%. On account of these low

formaldehyde yields mechanistic considerations are not meaningful. Furthermore, the $^{\bullet}OH$ determination is not adversely affected (refer to Supporting Information Text S6).

The formation of H_2O_2 could be an indication that after ozone attack at the aromatic ring of *N*-heterocyclic compounds ozonide formation and its breakdown can take place according to the suggested primary reaction pathway 7 (Criegee, 1975, Dowideit & von Sonntag, 1998). Ozone attack at the aromatic ring of pyrimidine as a result of substantial degradation in the absence of $^{\bullet}OH$ (see reaction stoichiometry) could proceed, even if only marginally. In all cases the hydrogen peroxide yields are plotted against the ozone concentration in scavenged (t-BuOH) and non scavenged systems. In the case of pyridazine (see Figure S5) this does not take place linear to ozone concentration in the non scavenged system. Thus, the calculation for pyridazine is only made for the linear range (up to 1.25×10^{-4} M ozone). In all other cases the hydrogen peroxide yields increase linearly with increasing ozone concentrations (see Figure 7 for the examples pyrimidine and pyrazine). The yields of H_2O_2 are mostly low (< 5%, see Table 1). An exception is pyrimidine. Here, a higher hydrogen peroxide yield of around 15% with respect to ozone concentration in the presence of $^{\bullet}OH$ was observed. Thus, mainly calculations for pyrimidine with respect to compound degradation are worthy to mention. Here, a hydrogen peroxide yield of 59% in non scavenged and 69% in scavenged system is deduced. In consideration to the fact that less amount of pyrazine is degraded in the scavenged system the calculation yields a value of 95%, whereas 17% in non scavenged system is deduced.

Mechanistic aspects relating to the yield of hydrogen peroxide will therefore be discussed particularly for the reaction of pyrimidine with ozone (similarly for pyrazine in the scavenged system). For pyrimidine, this is shown in scheme 4, reactions (40) – (43), (cf. also Scheme 1, suggested pathway 7, Criegee type mechanism). Here, in the first step ozone adds to the aromatic ring of pyrimidine and after ozone addition the ozonide can breakdown into a hydroxyhydroperoxide (Dowideit & von Sonntag, 1998). This cleaves off hydrogen peroxide (H_2O_2) by forming two carbonyl groups yielding to muconic compounds (described for methoxylated benzenes and phenols, Mvula & von Sonntag, 2003, Mvula et al., 2009). In the reaction of pyridine and pyridazine with ozone it could be proposed that the absence of significant amounts of hydrogen

peroxide indicates that the ozonide formation and thus also the subsequent reactions only take place to a minor degree.

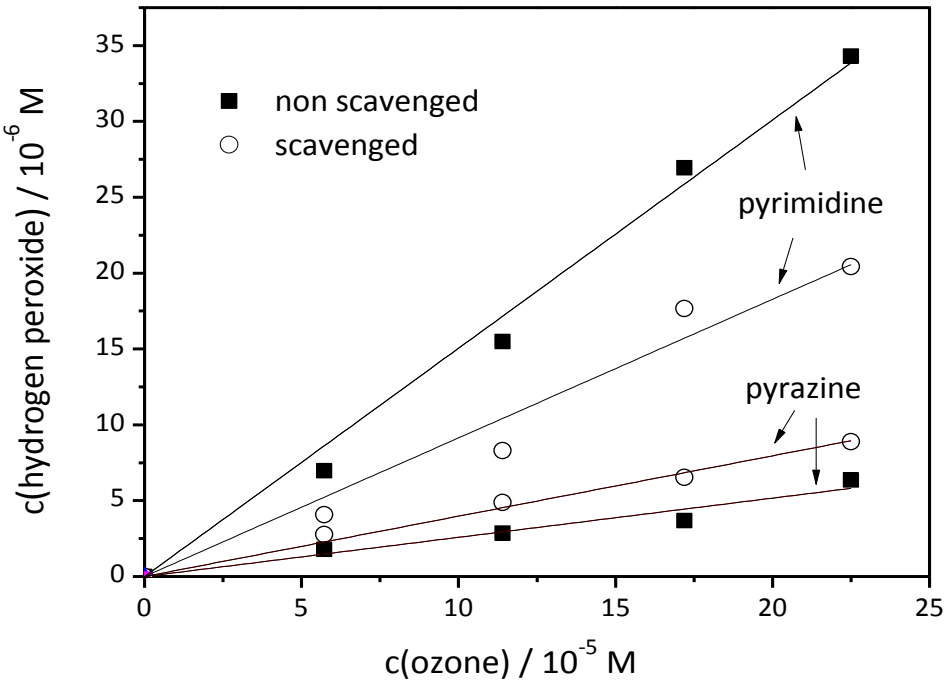

Figure 7. Formation of hydrogen peroxide in the reaction of pyrimidine $c_0(2.8 \times 10^{-4}$ M) and pyrazine $c_0(2.8 \times 10^{-4}$ M) with ozone. Hydrogen peroxide concentrations in the presence and absence of tertiary butanol are plotted vs. the ozone concentration.

4.4.4 Mass balances and mechanistic considerations

From the data of all target compounds and their yields (in mole per mole substrate) compiled in Table 1 (for a clearly arranged presentation see Figure S6 and S7 in Supporting Information) it can be seen that in the case of pyridine (94%) and pyridazine (99%) a closed mass balance has been obtained in the scavenged system. In the presence of $^{\bullet}$OH, however, it is around 50% in the case of pyridine and around 20% in the case of pyridazine. The sum is computed with *N*-oxide, formaldehyde and hydrogen peroxide. In comparison, in the case of pyrazine in the scavenged system a closed mass balance (95%) is received, too. However, a reason for this is the low compound transformation (see above). In contrast, in the case of pyrimidine (and pyrazine in the non scavenged system) closed mass balances were not obtained. Here, the sum is computed with formaldehyde and hydrogen peroxide. The reason for the

incomplete mass balance in the case of pyrazine (18%) and pyrimidine (60%) in presence of $^{\bullet}$OH is probably the missing quantification of the detected (or not identified) transformation products, which could close the gap. However, the results of incomplete mass balances obviously demonstrate the need of using further analytical techniques, e.g., besides HRMS also NMR measurements to identify further feasible products.

With respect to the reaction mechanism ozone addition as non radical pathway is the preferred primary reaction (closed to 100%) in the case of pyridine and pyridazine according to the primary reaction pathway 1. Only less than 6% are transformed via radical reactions (e.g., primary reaction pathways 2, 4, 5 and/or 6). These results are in accordance to quantum-chemical calculations, which indicate, that the *N*-adduct formation is highly exergonic (pyridine, ΔG^0 = -80 kJ mol^{-1}, pyridazine, ΔG^0 = -100 kJ mol^{-1}) whereupon electron transfer is endergonic (pyridine, ΔG^0 = +80 kJ mol^{-1}, pyridazine, ΔG^0 = +47 kJ mol^{-1}, Naumov, private communication). A reaction by ozone addition to the ring seems unlikely based on the low electron density (Morrison & Boyd, 1986) and in addition for pyridine a high positive Gibbs energy was calculated (ΔG^0 > + 158 kJ mol^{-1}, Naumov & von Sonntag 2011). With respect to the reaction mechanism in the reaction of pyrimidine and pyrazine with ozone a surprising effect is the different behavior compared with pyridine or pyridazine. For pyrimidine and pyrazine in addition to a slight ozone attack at nitrogen also ozone adduct formation at the aromatic ring (primary pathway 7) is a likely pathway. This is the one confirmed due to the high hydrogen peroxide yield (closed to 70%) in the case of pyrimidine and secondly due to ethylene diamine 1,4-dicarboxylic acid formation in the case of pyrazine (cf. Scheme 4). However, pyrazine does probably only react to a minor degree via addition of ozone to the aromatic ring, because of the low turnover efficiency, which is caused by radical reactions initiated by electron transfer reactions (cf. Scheme 3).

The different structure of the *N*-oxides under study does not neither affect the observed rate constant nor the reaction stoichiometry. However, the observed kinetics and stoichiometry are different in experiments in presence and absence of an $^{\bullet}$OH scavenger. All *N*-oxides are stable in direct ozone reactions (in absence of $^{\bullet}$OH),

whereas these compounds are degraded in presence of $^{\bullet}$OH. With respect to mechanisms it seems that $^{\bullet}$OH react with the *N*-oxides by means of addition reactions. This can be explained by the fact that the lone electron pair at nitrogen is already bound to oxygen and thus unavailable for the electrophilc ozone as mentioned above.

4.5 Conclusions

The present study shows that upon reaction of ozon with pyridine, pyridazine, pyrimidine, pyrazine and their corresponding *N*-oxides as aromatic *N*-containing heterocyclic compounds in aqueous solution several radical and non radical processes take place. The mechanisms of the investigated *N*-heterocycles in their reaction with ozone could tentatively be proposed. There are considerable similarities between pyridine and pyridazine in their reaction with ozone, however, also marked differences in comparison to pyrazine and pyrimidine despite the structural similarity. This illustrates how careful one must be in inferring on reaction mechanisms for seemingly closely related structures of *N*-heterocyclic aromatic compounds. If the aromatic *N*-heterocyles under study should be applied as archetypes for pharmaceuticals the ozone attack can be predicted for closely related structures. Thus, e.g., for pyrazineamide which containing only an aromatic *N*-heterocyclic moiety and an amide moiety (cf. Pryor et al., 1984) as structural unit, it could be said, that this molecule should be less susceptible to ozone attack.

4.6 References

Acero, J. L., Stemmler, K., von Gunten, U., 2000. Degradation kinetics of atrazine and its degradation products with ozone and OH radicals: a predictive tool for drinking water treatment. Environ Sci Technol 34, 591-597

Allen, A. O., Hochanadel, C. J., Ghormley, J. A., Davis, T. W., 1952. Decomposition of water and aqueous solutions under mixed fast neutron and gamma radiation. J Phys Chem 56, 575-586.

Andreozzi, R., Caprio, V., D`Amore, M. G., Insola, A., 1990. Quinoxaline ozonation in aqueous solution. Ozone Sci Eng 12, 329-340.

Andreozzi, R., Insola, A., Caprio, V., D`Amore, M. G., 1991. Ozonation of pyridine in aqueous solution: mechanistic and kinetic aspects. Wat Res 25, 655-659.

Andreozzi, R., Insola, A., Caprio, V., D`Amore, M. G., 1992. Quinoline ozonation in aqueous solution. Wat Res 26, 639-643.

Bader, H., Hoigné, J., 1981. Determination of ozone in water by the indigo method. Wat Res 15, 449-456.

Bahnemann, G., Hart, E. J., 1982. Rate constants of the reaction of the hydrated electron and hydroxyl radical with ozone in aqueous solution. J Phys Chem 86, 252-255.

Benitez, F. J., Acero, J. L., Real, F. J., Roldan, G., Casas, F., 2011. Comparison of different chemical oxidation treatments for the removal of selected pharmaceuticals in water matrices. Chem Eng J 168, 1149–1156.

Benner, J., Salhi, E., Ternes, T. A., von Gunten, U., 2008. Ozonation of reverse osmosis concentrate: kinetics and efficiency of beta blocker oxidation. Wat Res 42, 3003-3012.

Bielski, B. H. J., Cabelli, D. E., Arudi, R. L., Ross, A. B., 1985. Reactivity of HO_2/O_2^- radicals in aqueous solution. J Phys Chem Ref Data 14, 1041-1100.

Boxall, A., Keller, V. D. J., Straub, J. O., Monteiro, S. C., Fussell, R., Williams, R. J., 2014. Exploiting monitoring data in environmental exposure modelling and risk assessment of pharmaceuticals. Environ Int 73, 175-185.

Brambilla, A., Bolzacchini, E., Meinardi, S., Orlandi, M., Polesello, S., Rindone, B., 1995. Reactivity of organic micropollutants with ozone: a kinetic study. Proceedings Int Ozone Association 12, 43-52.

Bühler, R. E., Staehelin, J., Hoigné, J., 1984. Ozone decomposition in water studied by pulse radiolysis. HO_2/O_2^- and HO_3/O_3^- as intermediates. J Phys Chem 88, 2560-2564.

Buxton, G. V., Greenstock, C. L., Helman, W. P., Ross, A. B., 1988. Critical review of rate constants for reactions of hydrated electrons, hydrogen atoms and hydroxyl radicals (OH/O^-) in aqueous solution. J Phys Chem Ref Data 17, 513-886.

Criegee, R., 1975. Mechanismus der Ozonolyse. Angew Chem 87, 765-771.

Cocheci, V., Gherasimov, E., Csunderlik, C., Cotarca, L., Nov, A., 1989. Ozone oxidation of alkylamines in aqueous solution. - I. Rate constants of ozone reactions with primary, secondary and tertiary amines. Revue roumaine de chimie 1, 749-57.

Doré, M., Langlais, B., Legube, B., 1980. Mechanism of the reaction of ozone with soluble aromatic pollutants. Ozone Sci Eng 2, 39-54.

Dowideit, P., von Sonntag, C., 1998. The reaction of ozone with ethene and its methyl- and chlorine-substituted derivatives in aqueous solution. Environ Sci Technol 32, 1112-1119.

Elmghari-Tabib, M., LaPlanche, A., Venien, F., Martin, G., 1982. Ozonation of amines in aqueous solutions. Wat Res 16, 223-229.

Flyunt, R., Theruvathu, J. A., Leitzke, A., von Sonntag, C., 2002. The reactions of thymine and thymidine with ozone. J Chem Soc, Perkin Trans 2, 1572-1582.

Flyunt, R., Leitzke, A., Mark, G., Mvula, E., Reisz, E., Schick, R., von Sonntag, C., 2003a. Determination of $^{\bullet}OH$ and $O_2^{\bullet-}$, and hydroperoxide yields in ozone reactions in aqueous solutions. J Phys Chem B 107, 7242-7253.

Flyunt, R., Leitzke, A., von Sonntag, C., 2003b. Characterisation and quantitative determination of (hydro)peroxides formed in the radiolysis of dioxygen-containing systems and upon ozonolysis. Radiat Phys Chem 67, 469-473.

Forni, L., Bahnemann, D., Hart, E. J., 1982. Mechanism of the hydroxide ion initiated decomposition of ozone in aqueous solution. J Phys Chem 86, 255-259.

Gabet-Giraud, V., Miège, C., Choubert, J. M., Ruel, S. M., Coquery, M., 2010. Occurrence and removal of estrogens and beta blockers by various processes in waste-water treatment plants. Sci Total Environ 408, 4257-4269.

Gilbert, E., Zinecker, H., 1980. Ozonization of aromatic amines in water. Ozone Sci Eng 2, 65-74.

Gilbert, E., Hoffmann-Glewe, S., 1992. Ozonation of pyrimidines in aqueous solution. Wat Res 26, 1533-1540.

Hart, E. J., Sehested, K., Holcman, J., 1983. Molar absorptivities of ultraviolet and visible bands of ozone in aqueous solutions. Anal Chem 55, 46-49.

Hoigné, J., Bader, H., 1979. Ozonation of water: "Oxidation-competition values" of different types of water used in Switzerland. Ozone Sci Eng 1, 357-372.

Hoigné, J., Bader, H., 1983a. Rate constants of reactions of ozone with organic and inorganic compounds in water. - I. Non-dissociating organic compounds. Wat Res 17, 173-183.

Hoigné, J., Bader, H., 1983b. Rate constants of reactions of ozone with organic and inorganic compounds in water. - II. Dissociating organic compounds. Wat Res 17, 185-194.

Hollender, J., Zimmermann, S. G., Koepke, S., Krauss, M., McArdell, C. S., Ort, C., Singer, H., von Gunten, U., Siegrist, H., 2009. Elimination of organic micropollutants in a municipal wastewater treatment plant upgraded with a full-scale post-ozonation followed by sand filtration. Environ Sci Technol 43, 7862-7869.

Huber, M. M., Canonica, S., Park, G.-Y., von Gunten, U., 2003. Oxidation of pharmaceuticals during ozonation and advanced oxidation processes. Environ Sci Technol 37, 1016-1024.

Huber, M. M., Ternes, T. A., von Gunten, U., 2004. Removal of estrogenic activity and formation of oxidation products during ozonation of 17α-ethinylestradiol. Environ Sci Technol 38, 5177-5186.

Huber, M. M., Göbel, A., Joss, A., Hermann, N., Löffler, D., McArdell, C. S., Ried, A., Siegrist, H., Ternes, T. A., von Gunten, U., 2005. Oxidation of pharmaceuticals during ozonation of municipal wasterwater effluents: a pilot study. Environ Sci Technol 39, 4290-4299.

Huggett, D. B., Brooks, B. W., Peterson, B., Foran, C. M., Schlenk, D., 2002. Toxicity of select beta adrenergic receptor-blocking pharmaceuticals (b-blockers) on aquatic organisms. Arch Environ Contam Toxicol 43, 229–235.

Joule, J. A., Mills K., 2010. Heterocyclic chemistry. Blackwell Publishing. John Wiley & Sons LTD. The Atrium, Southern Gato, Chichester, West Sussex, United Kingdom.

Karpel vel Leitner, N., Roshani, B., 2010. Kinetic of benzotriazole oxidation by ozone and hydroxyl radical. Wat Res 44, 2058-2066.

Katritzky, A. R., 1984. Comprehensive heterocyclic chemistry, Pergamon Press, Oxford.

Kitsuka, K., Mohammad, A. M., Awad, M. I., Kaneda, K., Ikematsu, M., Iseki, M., Mushiake, K., Ohsaka, T., 2007. Simultaneous spectrophotometric determination of ozone and hydrogen peroxide. Chem Letters 36, 1396-1397.

Kolonko, K. J., Shapiro, R. H., Barkley, R. M., Sievers, R. E., 1979. Ozonation of caffeine in aqueous solution. J Org Chem 44, 3769-3778.

Küster, A., Alder, A. C., Escher, B. I., Duis, K., Fenner, K., Garric, J., Hutchinson, T. H., Lapen, D. R., Péry, A., Römbke, J., Snape, J., Ternes, T. A., Topp, E., Wehrhan, A., Knacker, T., 2010. Environmental risk assessment of human pharmaceuticals in the European union: a case study with the b-blocker atenolol. Integr Environ Assess Manage 6, 514–523.

Lange, F., Cornelissen, S., Kubac, D., Sein, M. M., von Sonntag, J., Hannich, C. B., Golloch, A., Heipieper, H. J., Möder, M., von Sonntag, C., 2006. Degradation of macrolide antibiotics by ozone: a mechanistic case study with clarithromycin. Chemosphere 65, 17-23.

Lee, Y., von Gunten, U., 2010. Oxidative transformation of micropollutants during municipal wastewater treatment: comparison of kinetic aspects of selective (chlorine, chlorine dioxide, ferrateVI, and ozone) and non-selective oxidants (hydroxyl radical). Wat Res 44, 555-566.

Legube, B., Guyon, S., Doré, M., 1987. Ozonation of aqueous solution of nitrogen heterocyclic compounds: benzotriazoles, atrazine and amitrole. Ozone Sci Eng 9, 233-246.

Lipari, F., Swarin, S. J., 1982. Determination of formaldehyde and other aldehydes in automobile exhaust with an improved 2,4-dinitrophenylhydrazine method. J Chrom 247, 297-306.

Lutze, H., Naumov, S., Peter, A., Liu, S., von Gunten, U., von Sonntag, C., Schmidt, T. C., 2015. Ozonation of benzotriazoles: rate constant and mechanistic aspects, in preparation.

Morrison, R. T., Boyd, R. N., 1986. Lehrbuch der organischen Chemie. Verlag Chemie, Weinheim, New York. (Organic Chemistry, Allyn & Bacon, Newton, MA, 1983)

Muñoz, F., von Sonntag, C., 2000a. Determination of fast ozone reactions in aqueous solution by competition kinetics. J Chem Soc, Perkin Trans 2, 661-664.

Muñoz, F., von Sonntag, C., 2000b. The reaction of ozone with tertiary amines including the complexing agents nitrilotriacetic acid (NTA) and ethylenediaminetetra-acetic acid (EDTA) in aqueous solution. J Chem Soc, Perkin Trans 2, 2029-2033.

Muñoz, F., Mvula, E., Braslavsky, S. E., von Sonntag, C., 2001. Singlet dioxygen formation in ozone reactions in aqueous solution. J Chem Soc, Perkin Trans 2, 1109-1116.

Mvula, E., von Sonntag, C., 2003. Ozonolysis of phenols in aqueous solution. Org Biomolec Chem 1, 1749-1756.

Mvula, E., Naumov, S., von Sonntag, C., 2009. Ozonolysis of lignin models in aqueous solution: anisole, 1,2-dimethoxybenzene, 1,4-dimethoxybenzene and 1,3,5-trimethoxy-benzene. Environ Sci Technol, 43, 6275-6282.

Nash, T., 1953. The colorimetric estimation of formaldehyde by means of the Hantzsch reaction. Biochem J 55, 416-421.

Naumov, S., von Sonntag, C., 2010. Quantum chemical studies on the formation of ozone adducts to aromatic compounds in aqueous solution. Ozone Sci Eng 32, 61-65.

Naumov, S., von Sonntag, C., 2011. Standard Gibbs free energies of reactions of ozone with free radicals in aqueous solution − Quantum chemical calculations. Environ Sci Technol 45, 9195-9204.

Naumov, S., 2015. Private communication

Neta, P., Huie, R. E., Ross, A. B., 1988. Rate constants for reactions of inorganic radicals in aqueous solution. J Phys Chem Ref Data 17, 1027-1284.

Nöthe, T., Hartmann, D., von Sonntag, J., von Sonntag, C., Fahlenkamp, H., 2007. Elimination of the musk fragrances galaxolide and tonalide from wastewater by ozonation and concomitant stripping. Wat Sci Tech 55, 287-292.

Nöthe, T., Fahlenkamp, H., von Sonntag, C., 2009. Ozonation of wastewater: rate of ozone consumption and hydroxyl radical yield. Environ Sci Technol 43, 5990-5995.

Pan, X-M., Schuchmann, M. M., von Sonntag, C., 1993. Oxidation of benzene by the OH radical. A product and pulse radiolysis study in oxygenated aqueous solution. J Chem Soc, Perkin Trans 2, 289-297.

Pryor, W. A., Giamalva, D. H., Church, D. F., 1984. Kinetics of ozonation. 2. Amino acids and model compounds in water and comparison to rates in nonpolar solvents. J Am Chem Soc 106, 7094-7100.

Ragnar, M., Eriksson, T., Reitberger, T., 1999a. Radical formation in ozone reactions with lignin and carbohydrate model compounds. Holzforschung 53, 292-298.

Ragnar, M., Eriksson, T., Reitberger, T., Brandt, P., 1999b. A new mechanism in the ozone reaction with lignin like structures. Holzforschung 53, 423-428.

Reisz, E., Schmidt, W., Schuchmann, H.-P., von Sonntag, C., 2003. Photolysis of ozone in aqueous solutions in the presence of tertiary butanol. Environ Sci Technol 37, 1941-1948.

Schmidt, C. K., Brauch, H.-J., 2008. *N*,*N*-Dimethylsulfamide as precursor for *N*-nitrosodimethylamine (NDMA) formation upon ozonation and its fate during drinking water treatment. Environ Sci Technol 42, 6340-6346.

Schuchmann, M. N., von Sonntag, C., 1979. Hydroxyl radical-induced oxidation of 2-methyl-2-propanol in oxygenated aqueous solution. A product and pulse radiolysis study. J Phys Chem 83, 780-784.

Schwarzenbach, R. P., Escher, B. I., Fenner, K., Hofstetter, T. B., Johnson, C. A., von Gunten, U., Wehrli, B., 2006. The challenge of micropollutants in aquatic systems. Science 313, 1072-1077.

Sehested, K., Holcman, J., Hart, E. J., 1983. Rate constants and products of the reactions of e^-, O_2^- and H with ozone in aqueous solutions. J Phys Chem 87, 1951-1954.

Sehested, K., Holcman, J., Bjergbakke, E., Hart, E. J., 1984. A pulse radiolytic study of the reaction OH + O_3 in aqueous medium. J Phys Chem 88, 4144-4147.

Sein, M. M., Zedda, M., Tuerk, J., Schmidt, T. C., Golloch, A., von Sonntag, C., 2008. Oxidation of diclofenac with ozone in aqueous solution. Environ Sci Technol 42, 6656-6662.

Shang, N.-C., Yu, Y.-H., 2002. Toxicity and color formation during ozonation of mono-substituted aromatic compounds. Environ Technol 23, 43-52.

Snyder, S. A., Wert, E. C., Rexing, D. J., Zegers, R. E., Drury, D. D., 2006. Ozone oxidation of endocrine disrupters and pharmaceuticals in surface water and waste-water. Ozone Sci Eng 28, 445-460.

Tauber, A., von Sonntag, C., 2000. Products and kinetics of the OH-radical-induced dealkylation of atrazine. Acta Hydrochim Hydrobiol 28, 15-23.

Tekle-Röttering, A., Jewell, K. S., Reisz, E., Lutze, H., Ternes, T. A., Schmidt, W., Schmidt, T. C., 2016. Ozonation of piperidine, piperazine and morpholine: Kinetics, stoichiometry, product formation and mechanistic considerations. Wat Res 88, 960-971.

Ternes, T. A., Meisenheimer, M., McDowell, D., Sacher, F., Brauch, H.-J., Haist-Gulde, B., Preuss, G., Wilme, U., Zulei-Seibert, N., 2002. Removal of pharmaceuticals during drinking water treatment. Environ Sci Technol 36, 3855-3863.

Ternes, T. A., Joss, A., 2006. Human pharmaceuticals, hormones and fragrances. The challenge of micropollutants in urban water management. IWA Publishing, London, New York.

Ternes, T. A., 2015. Occurrence, fate, removal and assessment of emerging contaminants in water in water cycle (from wastewater to drinking water). Wat Res 72, 1-2.

Tisler, M., Stanovnik, B., 1984. Pyridazines and their benzo derivatives. In: Katritzky, A. R., 1984. Comprehensive heterocyclic chemistry / the structure, reactions, synthesis and uses of heterocyclic compounds, Pergamon Press, Oxford, 1-56.

Tyupalo, N. F., Jacobi, W. A., Stepanjan, A. A., Bernashevskii, N. W., Budennaja, I. F., Kozlorezov, A. Z., 1974. Reactions of ozone with alkyl derivatives and condensed heteroatomic compounds. Kataliticeske reakcii v zidkoj faze 4, 593-594.

Tyupalo, N. F., Bernashevskii, N. W., 1980. Study of the reactions of ozone with pyridine homologs in aqueous solution. Doklady Akad Nauk SSSR 253, 896-898.

von Gunten, U., 2003. Ozonation of drinking water. Part I. Oxidation kinetics and product formation. Wat Res 37, 1443-1467.

von Gunten, U., Salhi, E., Schmidt, C. K., Arnold, W. A., 2010. Kinetics and mechanismus of *N*-nitrosodimethylamine formation upon ozonation of *N*,*N*-dimethylsulfamide-containing waters: bromide catalysis. Environ Sci Technol 44, 5762-5768.

von Sonntag, C., 2007. The basics of oxidants in water treatment. Part A: OH radical reactions. Wat Sci Tech, 19-23.

von Sonntag, C., 2008. Advanced oxidation processes: mechanistic aspects. Wat Sci Tech 58, 19-23.

von Sonntag, C., von Gunten, U., 2012. Chemistry of ozone in water and wastewater treatment. From basic principles to applications. IWA Publishing

Wang, X., Huang, X., Zuo, C., Hu, H., 2004. Kinetics of quinoline degradation by O_3/UV in aqueous phase. Chemosphere 55, 733-741.

Yao, C. C. D., Haag, W. R., 1991. Rate constants for direct reactions of ozone with several drinking water contaminats. Wat Res 25, 761-773.

Zimmermann, S. G., Schmukat, A., Schulz, M., Benner, J., von Gunten, U., Ternes, T. A., 2012. Kinetic and mechanistic investigations of the oxidation of tramadol by ferrate and ozone. Environ Sci Technol 46, 876-884.

4.7 Acknowledgment

The authors are deeply thankful for the expert advice of Prof. Clemens von Sonntag. With his great knowledge and vast experience, he supported the present study. The authors thank Sergej Naumov for his kind help by calculation of the Gibbs energies.

4.8 Supporting Information of Chapter 4

Ozonation of pyridine and other *N*-heterocyclic aromatic compounds: Kinetics, stoichiometry, identification of products and elucidation of pathways

Agnes Tekle-Röttering, Erika Reisz, Kevin S. Jewell, Holger V. Lutze,
Thomas A. Ternes, Winfried Schmidt, Torsten C. Schmidt

24 pages of Supporting Information, including 8 narrations, 6 schemes and 7 figures

Text S1. Chemicals 201
Text S2. Sample preparation 202
Text S3. Kinetics (indigo and competition method) 203
Text S4. Reaction stoichiometry 207
Text S5. Product quantification with HPLC-DAD and identification with LC-HRMS..... 209
Text S6. Determination of OH radical ($^{\bullet}$OH) with tertiary butanol..... 215
Text S7. Determination of secondary products..... 217
Text S8. Singlet oxygen 219

Figure S1. Calibration curves for reaction stoichiometry experiments of pyridine and pyrazine
Figure S2. HPLC chromatogram and mass spectrum in the reaction of pyrazine with ozone in the absence of scavenger
Figure S3. Mass spectrum in the reaction of pyrazine with ozone in the absence of scavenger obtained from LC-Q-ToF
Figure S4. Mass spectrum (MS^2 of 96.0409) in the reaction of pyrimidine with ozone in the absence of scavenger obtained from LC-Q-ToF
Figure S5. Formation of hydrogen peroxide in the reaction of pyridazine with ozone

Figure S6. Compound degradation and product yield relating to ozone consumption in the ozonation of pyridine, pyridazine, pyrimidine and pyrazine
Figure S7. Product yield relating to compound degradation in the reaction of pyridine, pyridazine, pyrimidine and pyrazine with ozone

Scheme S1. Competition in the reaction of pyridine and 3-buten-2-ol with ozone plus derivatization of the developed formaldehyde with DNPH
Scheme S2: MS^2 fragmentation pathway from m/z 147.04 $[M+H]^+$ obtained from IT-Orbitrap
Scheme S3: Proposed reaction pathway for the reaction of pyrazine with OH radicals by forming 2,3,5,6-tetrahydroxypyrazine
Scheme S4: MS^2 fragmentation pathway from m/z 147.04 $[M+H]^+$ obtained from LC-Q-ToF
Scheme S5. Determination of $^{\bullet}OH$ with tertiary butanol
Scheme S6. Determination of hydrogen peroxide in its reaction with iodide

Text S1. Chemicals

Pyridine (99.5%,), pyrazine (99%,), pyridazine (98%) and pyrimidine (99%) (all from Merck, Darmstadt, Germany) were used for investigation. For product quantification pyridine-*N*-oxide (95%, Aldrich, Seelze, Germany), pyridazine-*N*-oxide (97%, Aldrich), pyrimidine-*N*-oxide (97%, Aldrich), pyrazine-*N*-oxide (97%, Aldrich), 2-hydroxypyridine (p.s, Merck), 4-hydroxypyridine (95%, Aldrich), 2-pyridinecarboxylic acid (98%, Merck), 2-hydroxypyrimidine hydrochloride (98%, Aldrich), 2-hydroxypyrazine (97%, Aldrich), pyridazinone (96%, Alfa Aesar, Karlsruhe, Germany) and pyrimidinone (96%, Aldrich) were available as reference material. Tertiary butanol (t-BuOH) (p.a. Merck) was applied as radical scavenger. Potassium indigotrisulfonate (p.a. Aldrich) was required for the determination of the concentration of dissolved ozone in water for rate constant experiments. 3-buten-2-ol (97%, Alfa Aesar) and atrazine (p.a. Fluka, Buchs, Switzerland) were used for competitions experiments. Ammonium acetate (p.a.), acetic acid (100%), acetylacetone (99%), 2,4-dinitrophenylhydrazine (DNPH) (p.a.) (all from Merck) and perchloric acid (70%, p.a. Aldrich) were applied for measuring

formaldehyde. Potassium hydrogen phthalate (99.5%), potassium iodide (99.5%) and ammonium heptamolybdate (99%) (all from Merck) were used for measuring hydrogen peroxide. All further required chemicals were of analytical grade. Phosphoric acid, sodium dihydrogen phosphate, sodium hydrogen phosphate, sulphuric acid and sodium hydroxide (all from Merck) were required for pH adjustment. For chromatography acetonitrile (Fisher Scientific, Schwerte, Germany) and ultra-pure water (Merck Millipore) were used.

Text S2. Sample preparation

Glass test tubes, bottles or volumetric flasks (20 − 25 mL) closed with ground-in glass stoppers were used as reaction vessels. In order to limit losses of ozone, the flasks were kept closed during all the experimental time. Adding of the ozone solution (with a glass syringe, under rapid mixing) was resulting in ozone to compound ratios of 1:0.1 – 1:10 at apparent pH (pH of the aqueous solutions containing the investigated amines at the applied concentration) or adjusted pH (e.g. with phosphate buffer, denoted later as buffered)). Most samples were prepared without phosphate buffer (excluding kinetic experiments), because the relevant buffer species scavenge $^{\bullet}OH$ (Andreozzi et al., 2000). Dominant species and the corresponding rate constants change with pH from $H_2PO_4^-$ ($k(H_2PO_4^- + {}^{\bullet}OH) = 2.0 \times 10^4\ M^{-1}\ s^{-1}$, Buxton, 1988) in the pH range of 3.0 – 5.0 to HPO_4^{2-} ($k(HPO_4^{2-} + {}^{\bullet}OH) = 5.0 \times 10^6\ M^{-1}\ s^{-1}$, Staehelin & Hoigné, 1982) at pH around 7 to PO_4^{3-} ($k(PO_4^{3-} + {}^{\bullet}OH) = 1.0 \times 10^4\ M^{-1}\ s^{-1}$, Buxton, 1988) at pH around 12. The pH of experimental solutions was measured by a Metrohm 620 pH meter with a glass electrode (Metrohm, Filderstadt, Germany), calibrated every time before use.

To exclude $^{\bullet}OH$ reactions, for example the decomposition of ozone with $^{\bullet}OH$ (k ($^{\bullet}OH + O_3$) = $1.1 \times 10^8\ M^{-1}\ s^{-1}$, Buxton et al., 1988 or k ($^{\bullet}OH + O_3$) = $3.0 \times 10^9\ M^{-1}\ s^{-1}$, Staehelin & Hoigné, 1982) samples were prepared in parallel as described above but containing tertiary butanol (t-BuOH) (0.01 − 0.05 M) as a radical scavenger. Besides this, tertiary butanol (k (t-BuOH + O_3) = $0.003\ M^{-1}\ s^{-1}$) reacts with ozone at negligible rates even if present at reasonable excess (Flyunt et al., 2003a). Taking into account the concentration of tertiary butanol (at most 0.05 M) and substrate (usually 1×10^{-2} M and (k(pyrimidine + O_3) = $0.066\ M^{-1}\ s^{-1}$, lowest k in this study in scavenged system) in

their reaction with ozone (k_{app}(t-BuOH + O_3) = 1.5 × 10^{-4} s^{-1} and (k_{app}(pyrimidine + O_3) = 6.6 × 10^{-4} s^{-1}, the latter is still favored.

In particular, in its reaction with free radicals, ozone has to compete with oxygen. Yet, oxygen reacts only with few radical types (e.g. C-centered radicals) rapidly and irreversibly (von Sonntag & Schuchmann, 1997). Thus, ozone reacts with many free radicals effectively, despite the fact that oxygen is typically present in large excess over ozone (von Sonntag & von Gunten, 2012). Water does not react with ozone (k (H_2O + O_3) < 10^{-7} M^{-1} s^{-1}, Neta et al., 1988) but its conjugate base, OH^-, can react with ozone, (k (OH^- + O_3) = 48 M^{-1} s^{-1}, Forni et al., 1982 or 70 M^{-1} s^{-1}, Staehelin & Hoigné, 1982), albeit slowly and gives rise to $^{\bullet}OH$ (Staehelin & Hoigné, 1982, Merényi et al., 2010). However, this is only relevant at high pH. Thus in this experiments it does not play a role. Taking into account the concentration of the hydroxide ion (e.g. 10^{-6} M at pH of 8, highest pH in this experiments) in its reaction with ozone (k_{app}(OH^- + O_3) = 4.8 × 10^{-5} s^{-1} or 7.0 × 10^{-5} s^{-1}) this reaction can be neglected since the reaction of ozone with the amines (at least 1 × 10^{-3} M and k(pyrimidine + O_3) = 0.37 M^{-1} s^{-1}, lowest k in this study in non scavenged system) is sufficiently faster (k_{app}(pyrimidine + O_3) ≥ 3.7 × 10^{-4} s^{-1}) under all investigated conditions and therefore still favored. Thus, $^{\bullet}OH$ formation from this reaction does not take place.

Text S3. Kinetics (indigo and competition method)

Due to the fact, the investigated nitrogen-containing heterocyclic compounds absorb strongly in the UV-spectrum, the kinetics could not be followed by ozone decay spectrophotometrically at 260 nm. Hence other rate constant methods have to be applied. At first a competition with 3-buten-2-ol was carried out. However, it was seen that in this case this application was not a good qualified method, because the rate constant of 3-buten-2-ol (k = 7.9 × 10^4 M^{-1} s^{-1}, Muñoz & von Sonntag, 2000a, Dowideit & von Sonntag, 1998) differs with a large extent from the obtained rate constant of the selected *N*-heterocyclic compounds. As a result a competition with atrazine (k = 7.9 ± 0.62 M^{-1} s^{-1} Brambilla et al., 1995, k = 6.0 ± 0.3 M^{-1} s^{-1}, Acero et al., 2000) was used. To confirm this competition method and by its knowledge of low rate constants, a direct method in fact the indigo method (Bader & Hoigné, 1981) for components which react slow with ozone was applied. In this approach the indigotrisulfonate can use for the

determination of the residual ozone concentration. It has to be noted, that the indigo method for components which react fast with ozone was checked, however not successful (Bader & Hoigné, 1981). The rate constants determined by competition kinetics with atrazine agree well with the rate constants determined directly with the indigo method. Therefore, only the rate constant obtained with the indigo method are represented in this study. In all cases the compound concentration was in large excess (typically at 10^{-2} M) over ozone (near 10^{-3} M). Thus, under these conditions, ozone decay follows pseudo-first order kinetics.

In pseudo-first-order kinetic experiments ozone decay was followed at different substrate to ozone concentrations as a function of time (Bader & Hoigné 1981) according to equation 1. If substrate is added in large excess [S]>>>[O_3] in relation to the concentration of ozone, the change of substrate concentration due to reaction with ozone is negligible and can be considered stable. If this is applied to equation 1 it results in a pseudo-first-order rate according to equation 2. Integration of equation 2 leads to equation 3, which were applied for pseudo-first order rate constants determined from plots of ln([O_3]/[O_3]$_0$) vs. reaction time, resulting in a straight line with – $k_{O3,\,obs}$ as slope.

$$-\frac{d[O_3]}{dt} = k[S][O_3] \qquad (1)$$

$$\text{if } [S] >>> [O_3] \Longrightarrow \quad -\frac{d[O_3]}{dt} = k_{O_3,\,obs}[O_3] \qquad (2)$$

$$\ln\frac{[O_3]}{[O_3]_0} = -k_{O_3,\,obs}\cdot t \qquad \text{with } k_{O_3,\,obs} = k_{O_3,\,obs}[S] \qquad (3)$$

Pseudo-first order rate constants indicate an appreciable dependence upon pH (Muñoz & von Sonntag, 2000b). Due to the low pK_a values of the investigated amines (see Table 1) the degree of protonation at pH values around the neutral range is very low and negligible. Hence pH adjustment was not really necessary. Only for obtaining constant pH phosphate puffer was used. Thus, in the present study for setting up adequate conditions for the determination of the rate constant, experiments were carried out at the apparent pH of 5 – 8 or buffered at pH 6.5. Under these conditions,

almost 98.6% (95.8% by buffering at pH 6.5) of pyridine and 100% of pyridazine, pyrimidine and pyrazine are present as deprotonated amine.

In the indigo experiments an Erlenmeyer flask (50 mL) closed with ground-in glass stopper was used. In all cases ozone solutions were first pipetted and directly after that the compound solution with or without buffer and scavenger. Sampling was achieved in 10 – 600 s time intervals (sampling period around 300 – 3000 s). Aliquots of 10 mL were withdrawn (n=5−9) from the batch using a 10 mL glass syringe and were transferred into vessels containing 1.2 mL of phosphate buffered indigo reagent (10^{-3} M) to quench the residual ozone and stop the oxidation reaction. Stock solution of potassium indigotrisulfonate was prepared as previously described by Bader & Hoigné, 1981. The residual indigo concentration was spectrophotometrically measured at 600 nm at the end of the sampling method. Blanks were processed in the presence and absence of ozone and the absence of compound to control the initial concentration of indigo. As well pH values were measured at the end of the sampling method to check the stability. At the end the ozone rate constants were calculated by plotting the natural logarithm of the ratio of the residual ozone concentration vs. the initial ozone concentration $\ln([O_3]/[O_3]_0) = \ln A$ (measured by bleaching with the indigo reagent) against the reaction time.

Competition experiments require the measurement of only a single endpoint P, which is typically the formation of a product or the degradation of a reactant resulting from oxidation of either the compound (M) or the competitor (C). The evaluation of the reaction rate constants were conducted using equation 4 (Muñoz & von Sonntag, 2000a, Dodd et al., 2006, Zimmermann et al., 2012),

$$\frac{[\mathrm{P}]_0}{[\mathrm{P}]} = 1 + \frac{k_{\mathrm{O_3,M}}\ [\mathrm{M}]_0}{k_{\mathrm{O_3,C}}\ \ [\mathrm{C}]_0} \qquad (4)$$

where $[P]_0$ represents the measured endpoint yield in the absence of competitor obtained from controls and [P] represents the endpoint yield in the presence of varying doses of competitor.

The rate constant of the investigated compound was determined from the slopes of plots of equation 5.

$$\frac{[P]_0}{[P]} - 1 = f\left(\frac{[M]_0}{[C]_0}\right) \qquad (5)$$

In the competition experiments with 3-buten-2-ol (k = 7.9 × 10^4 M^{-1} s^{-1}, Muñoz & von Sonntag, 2000a, Dowideit & von Sonntag, 1998) the reaction product is formaldehyde. Formaldehyde was determined as their 2,4-dinitrophenylhydrazones after derivatisation with 2,4-dinitrophenylhydrazine (DNPH) (Lipari & Swarin, 1982, Olson & Swarin, 1985) according to scheme S1.

Scheme S1. Competition in the reaction of pyridine and 3-buten-2-ol with ozone plus derivatization of the developed formaldehyde with DNPH.

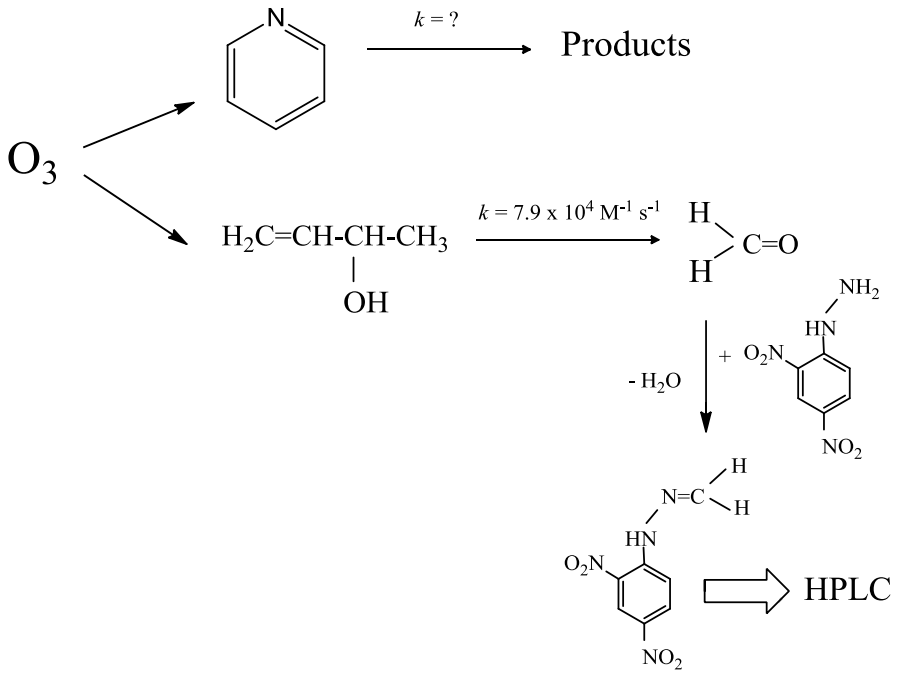

The experiments were carried out in a series of volumetric flasks (20 mL) each containing 1 mL of 3-buten-2-ol (10^{-2} – 10^{-3} M) as competitor and different volumes (0 – 8 mL) of compound solution (10^{-2} – 10^{-3} M) to obtain various ratios of $[M]:[C]_0$ (both in at least 10-fold molar excess of ozone). After adding appropriate volumes of pure water to complete the solution volume to 9 mL, a fixed dosage of 1 mL ozone solution was added with a glass syringe under rapid mixing. After complete ozone

consumption the developed formaldehyde was measured with DNPH (according to scheme S1). Here, 1.5 mL sample were withdrawn from the batch and transferred into HPLC-vials. After that 0.2 mL 2,4-dinitrophenylhydrazine solution (30 mg / 25 mL acetonitrile) and 0.1 mL $HClO_4$ (0.1 M) were added. After a reaction time of 45 minutes (in the dark) the formed 2,4-dinitrophenylhydrazone was measured by HPLC-DAD (LC20, Shimadzu, Duisburg, Germany) at a wavelength of 353 nm. The separation occurs on a C_{18} column (Prontosil, NC-04, 250 mm x 4.0 mm I.D., 5.0 µm, Bischoff, Leonberg, Germany) with the following gradient: water/acetonitrile (ACN): 35% ACN/ 2 min, 45% ACN/ 5 min, 100% ACN. All experiments were performed at the apparent pH.

Competition experiments with atrazine were carried out as described above however with atrazine (10^{-2} – 10^{-3} M) as competitor and buffered with phosphate. After complete ozone consumption the residual atrazine was determined with HPLC-DAD (LC20, Shimadzu) at a wavelength of 220 nm. The separation was carried out on a C_{18} column (Synergi Hydro-RP 80 A, 150 mm x 3.0 mm I.D., 4.0 µm, Phenomenex, Aschaffenburg, Germany) with the following gradient: water (pH 1.3 (0.1 M phosphoric acid))/acetonitrile (ACN): 10% ACN/ 2 min, 45% ACN/ 5 min, 100% ACN. The elution flow rate in both methods was 0.5 mL min^{-1} and the injection volume was 50 µL in all samples. In all cases blanks were processed in the same manner with water instead of ozone solution to determine the initial concentration.

Text S4. Reaction stoichiometry

Substrate concentration around 10^{-4} M with different ozone/compound molar ratios (1:0.7 – 1:7) was used. All samples were prepared in parallel as described above however with containing tertiary butanol (0.01 – 0.05 M) as radical scavenger to avoid $^{\bullet}OH$ reactions. All experiments were carried out in samples with solutions of the apparent pH at the applied concentration. Here, the pH of the initial solution of the selected amines was in the range of 5 – 8 and decreased gradually as the ozone was consumed to 4 – 7 as a function of the molar ratio of ozone to compound. Experiments by adjusting the pH with sulfuric acid to a value of 6 show no differences to experiments with apparent pH, thus no distinction in representing the results are made.

The experiments were carried out in a series of volumetric flasks (20 mL) each containing 1 mL of the investigated compound solution, with scavenger (1 mL) and without scavenger and different volumes (0 − 8 mL) of ozone solution to obtain various ozone concentration. Appropriate volumes of pure water were added to complete the solution volume to 10 mL. After complete ozone consumption the quantification was realized in the batch sample through compound-degradation using a HPLC – DAD system, equipped with a C_{18} column (Prontosil, as described above, Text S3). The compounds were eluted with a water/acetonitrile gradient system (35% ACN/ 5 min, 45% ACN/ 10 min, 100% ACN) and verified by retention time and the appropiate UV-spectra. The quantification was carried out at the following wavelengths: pyridine: 256 nm, pyridazine: 241 nm, pyrimidine: 242 nm, pyrazine: 260 nm, the appropriate *N*-oxides at 255 and 260 nm. Simultaneously, blanks were processed in the same manner with water instead of ozone solution to determine the initial concentration. Calibration experiments (Figure S1) were performed in the same manner with the investigated compounds as reference material.

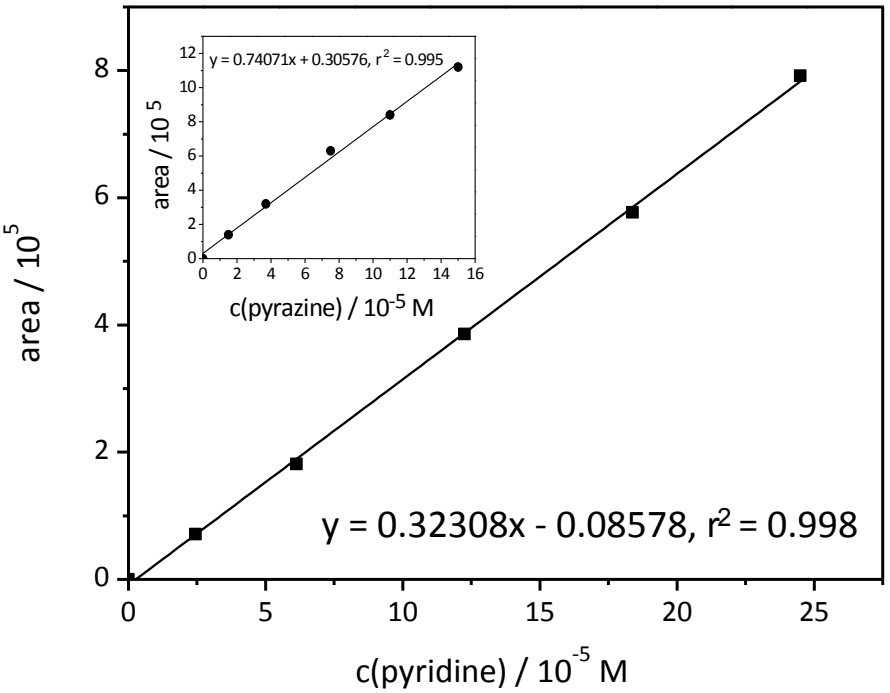

Figure S1. Calibration curves for reaction stoichiometry experiments of pyridine (main graph) and pyrazine (inset). Areas are plotted vs. amine concentrations.

Text S5. Product quantification with HPLC-DAD and identification with LC-HRMS

For product formation and quantification the compounds were present in large excess over ozone for guaranteeing that ozone reacts practically exclusively with the compounds and not in competition with the oxidation products. Thus, at 10^{-2} M compound, linear dose-yield relationships can be expected, despite the fact that the rate constant of ozone with the compounds is that low. Kinetic and reaction stoichiometry experiments showed that in the case of pyridine and pyridazine one main oxidation product (detected by HPLC-DAD with characteristic UV-spectrum) are formed in solution at apparent pH and in the presence or absence of tertiary butanol. In the ozonation of pyrimidine and pyrazine HPLC-DAD analysis revealed two main oxidation products, however, without characteristic UV-spectrum in scavenged as well in non scavenged system. The main oxidation product in ozonation experiments with pyridine and pyridazine (by adding tertiary butanol as $^{\bullet}$OH scavenger) are verified on the basis of retention time and characteristic UV-spectrum and quantified at appropriate wavelengths. The quantification was carried out with HPLC-DAD, using a C_{18} column (Prontosil, as described above) with the following separation conditions: 35% ACN/ 2 min, 45% ACN/ 5 min, 100% ACN. In this HPLC analysis the elution flow rate was 0.5 mL min^{-1} and the injection volume was 50 µL in all samples.

The molecular weights and hence sum formula of the transformation products were obtained by using two HRMS systems with performing Q1 scans in positive and negative mode. Structural elucidation of the oxidation products was based on their MS^2 fragmentation spectrum obtained from product ions (refer to Figure S2, S3 and S4 and see Scheme S2 and S4).

The first HRMS system (IT-Orbitrap-FTMS: Fourier transformation mass spectrometer) was equipped with an electrospray ionisation source (ESI) and an atmospheric pressure chemical ionisation (APCI). Since, the oxidation products were more sensitively detected in positive ionisation and with electrospray ionisation source, all following MS measurements were only performed in positive mode using ESI interface. The excitation energy was optimized for each experiment and varied between 20−100 V, with a collision energy spread of 5 V. In the LC system the sample compounds were

separated on a C_{18} column (Synergi Hydro-RP 80 A, 150 mm x 3.0 mm I.D., 4.0 µm, Phenomenex, Aschaffenburg, Germany) at 25°C. As eluents ultra-pure water and acetonitrile, both containing 0.5% aqueous formic acid (HCOOH) were used in a gradient system (10% ACN/ 10 min, 45% ACN/ 15 min, 100% ACN).

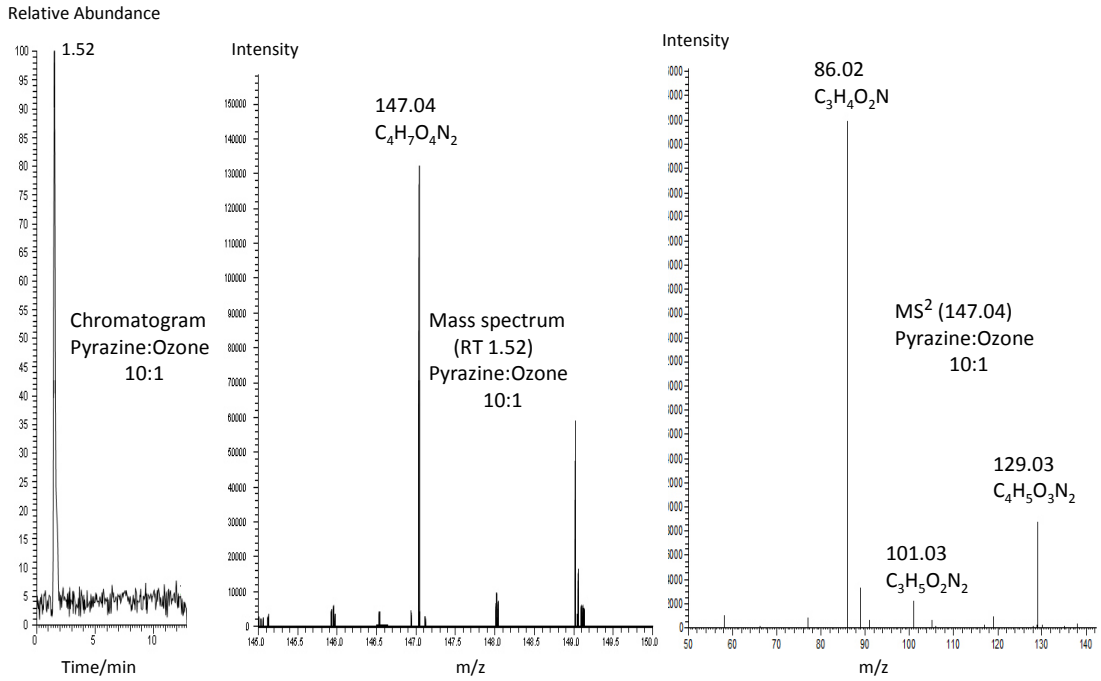

Figure S2. HPLC chromatogram and mass spectrum (MS and MS^2 of 147.04) in the reaction of pyrazine with ozone in the absence of scavenger (Orbitrap).

The second HRMS system was equipped with a LC system (Agilant, Waldbronn, Germany) connected to a SCIEX (Triple ToF 5600, Darmstadt, Germany) hybrid quadrupole time-of flight mass spectrometer(QToF) with a DuoSpray ion source and a TurboIonSpray probe for ESI experiments. To protect the HRMS system a postcolumn divert valve (Rheodyne, Darmstadt, Germany) directed the LC flow into the waste from 0 to 1 min and 20 to 27 min. Separation was achieved using a Zorbax Eclipse Plus C_{18} column (150 mm x 2.1 mm I.D., 3.5 µm, Agilent). The flow rate was set to 300 µL / min using a binary gradient of mobile phase A (ultra-pure water with 0.1% HCOOH) and phase B (acetonitrile with 0.1% HCOOH).

In addition fractionation of oxidation products were made, in particular to separate oxidation products from the original compound in large excess. The fractionation was carried out with HPLC (time wise fractionation (HIP-ALS-SL, Agilent, Waldbronn, Germany)) using C_{18} column (Synergi Hydro-RP 80 A, see above). Freeze drying of fractions was avoided to prevent any possible loss or degradation of oxidation products during this step.

Scheme S2: MS^2 fragmentation pathway from *m/z* 147.04 $[M+H]^+$ obtained from IT-Orbitrap.

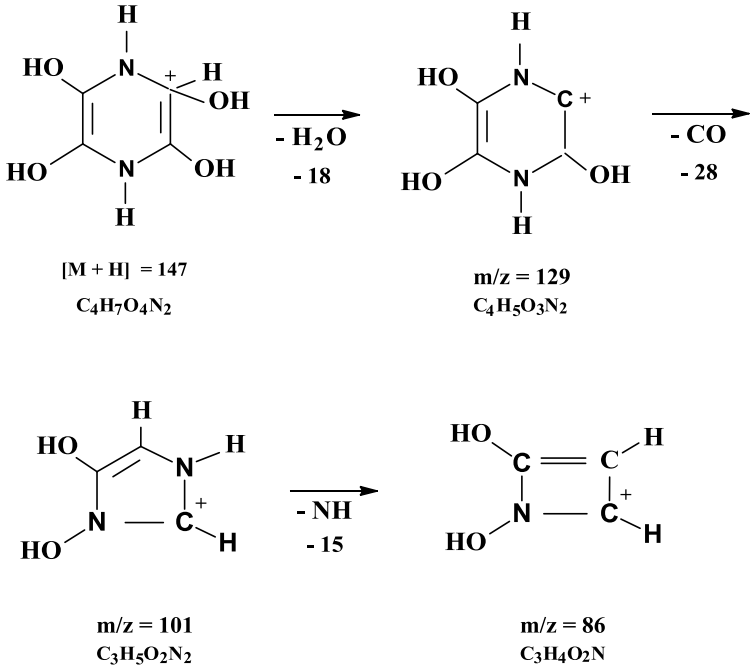

A proposed reaction pathway for the structure of 2,3,5,6-tetrahydroxypyrazine in the ozonation of pyrazine is presented in Scheme S3. The way $^{\bullet}OH$ can react with pyrazine to 2,3,5,6-tetrahydroxypyrazine is depicted in the reaction sequence (44) – (50). In the first step an $^{\bullet}OH$ adds to pyrazine, since addition reactions to C=C and C=N bonds belong to the most common and fastest $^{\bullet}OH$ reactions (Söylemez & von Sonntag, 1980, Veltwisch et al., 1980, von Sonntag & Schuchmann, 1991 & 1997, Andreozzi et al., 1999, von Sonntag, 2006). The first intermediate must be a π-complex complex as inferred from the kinetics of $^{\bullet}OH$ with benzene that subsequently collapses into σ-complex (Ashton et al., 1995, von Sonntag & von Gunten, 2012, reactions see there). Thus, the $^{\bullet}OH$ adduct can furthermore yield a C-centered radical (reaction (44)). This is

expected to undergo a rapid reaction (reaction (45)) with oxygen (see above and Tauber & von Sonntag, 2000). The resulting short-lived peroxyl radical can subsequently cleave a hydroperoxyl radical by forming 2-hydroxypyrazine (reaction (46)), which is in equilibrium with pyrazinone (reaction (47), Porter et al., 1984). Analogous consecutive reactions yield 2,3-dihydroxypyrazine (reaction (48)). In a third step the 2,3-dihydroxypyrazine can react with $^{\bullet}$OH by forming a C-centered radical in turn, which is assumed to undergo a H-shift from carbon to nitrogen (reaction (49)) in analogy to the well-documented 1,2-H-shift of alkoxyl radicals (Konya et al., 2000). In this reaction 2,3,5-trihydroxypyrazine is formed. This reacts with $^{\bullet}$OH in the same way yielding 2,3,5,6-tetrahydroxypyrazine (reaction (50)).

Scheme S3: Proposed reaction pathway for the reaction of pyrazine with OH radicals by forming 2,3,5,6-tetrahydroxypyrazine.

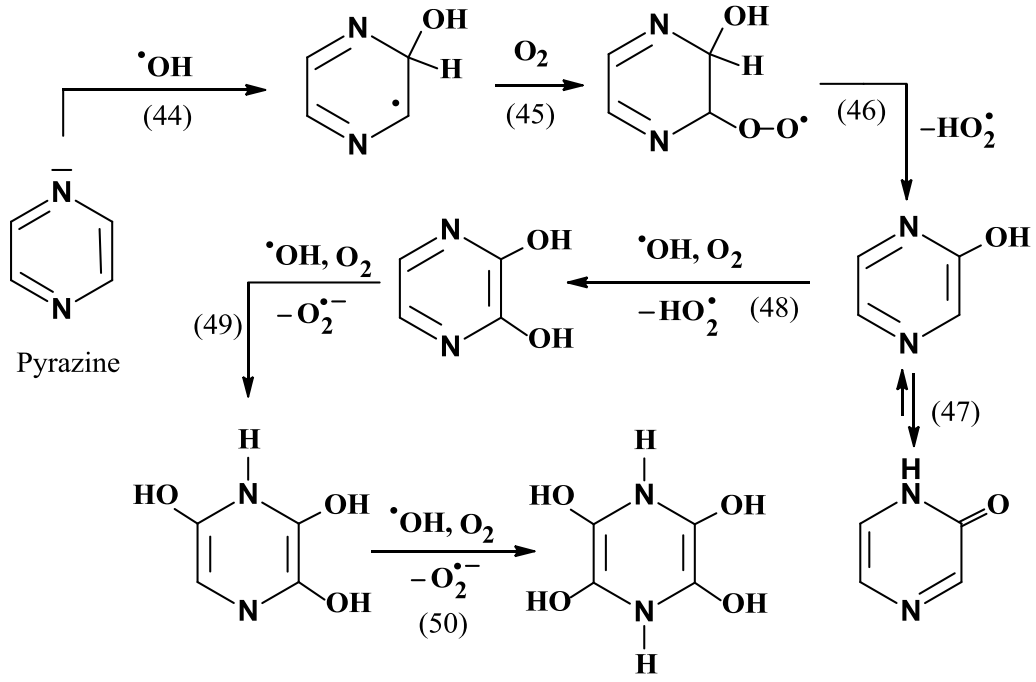

Besides, the hydroxylated pyrazine should react faster with $^{\bullet}$OH than pyrazine. Phenol as a hydroxylic compound of benzene reacts faster with $^{\bullet}$OH, albeit the effect is low (e.g., k ($^{\bullet}$OH + benzene) = 7.8×10^9 M^{-1} s^{-1}, k ($^{\bullet}$OH + phenol) = 1.8×10^{10} M^{-1} s^{-1}, Buxton et al., 1988). The same is seen in the case of pyridine (see above) by contrast with 3-pyridinol (e.g. k ($^{\bullet}$OH + 3-pyridinol) = 6.8×10^9 M^{-1} s^{-1}, pH 6.5, Buxton et al., 1988). The

faster reaction due to the presence of hydroxyl substituents should have a stronger effect when the compounds react with ozone, due to the activation effect of the hydroxyl groups and the high electrophilic character of ozone. Here, kinetic studies from the literature of reactions between ozone and phenol and ozone and benzene show rate constants of 1.3×10^3 M^{-1} s^{-1} and 2 M^{-1} s^{-1}, respectively (Hoigné & Bader, 1983a, b). It has to be noted, that 2-hydroxypyrazine (for which reference material was available) could not be detected in product formation experiments (the same is valid for 2-hydroxypyridine, 4-hydroxypyridine, 2-hydroxypyrimidine, pyridazinone and pyrimidinone). A reason could be that these products may directly react with $^{\bullet}OH$ or ozone and thus escape detection.

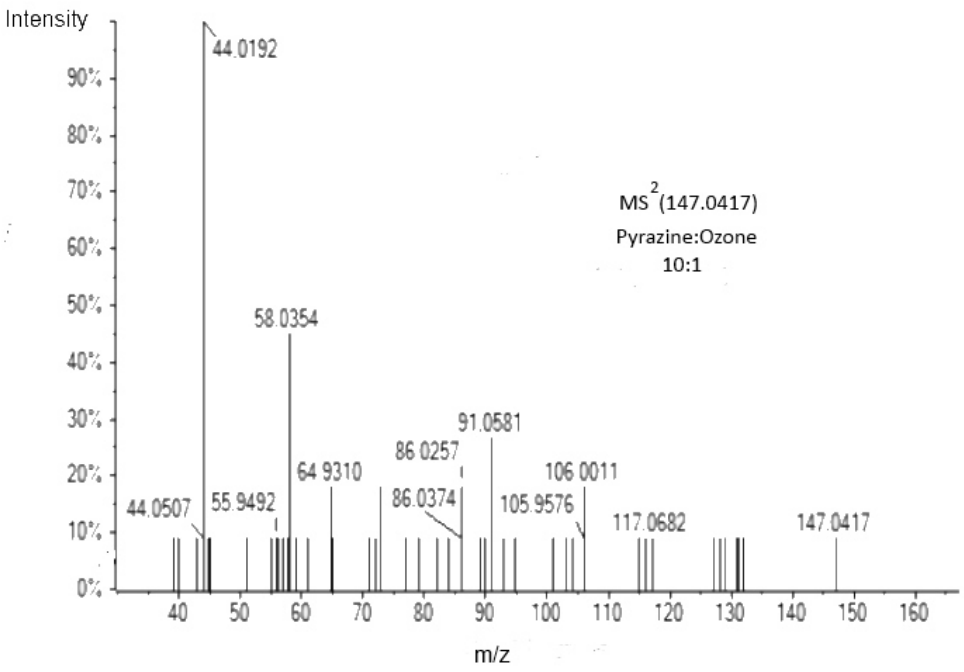

Figure S3. Mass spectrum (MS^2 of 147.0417) in the reaction of pyrazine with ozone in the absence of scavenger obtained from LC-Q-ToF.

Scheme S4: MS^2 fragmentation pathway from *m/z* 147.04 $[M+H]^+$ obtained from LC-Q-ToF.

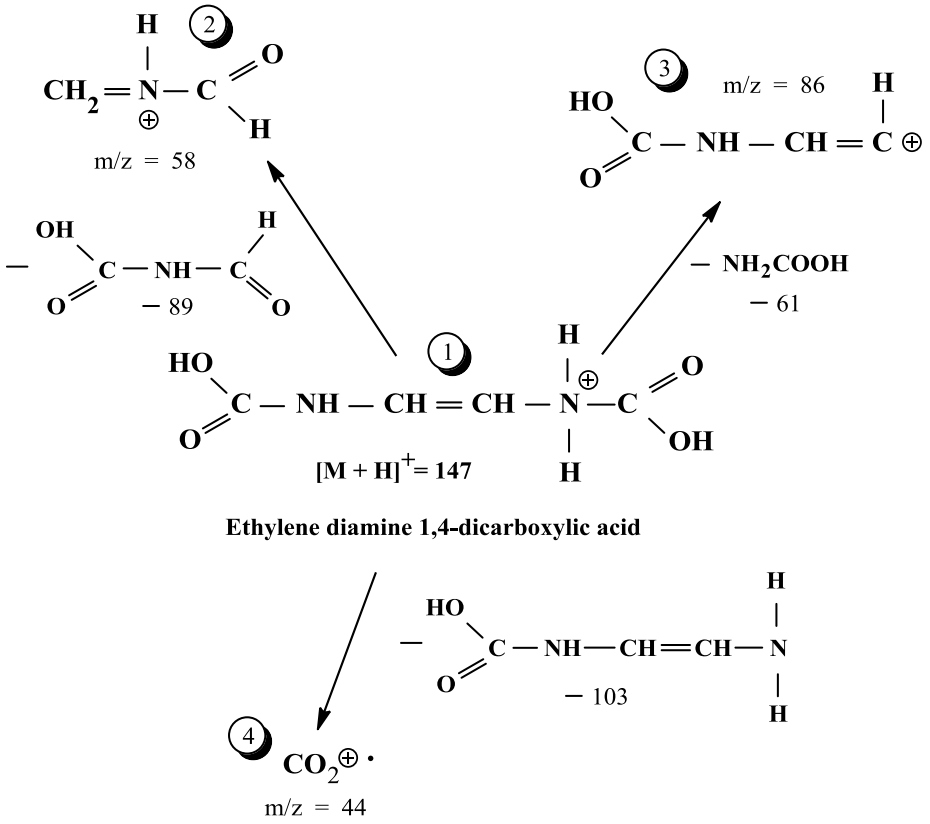

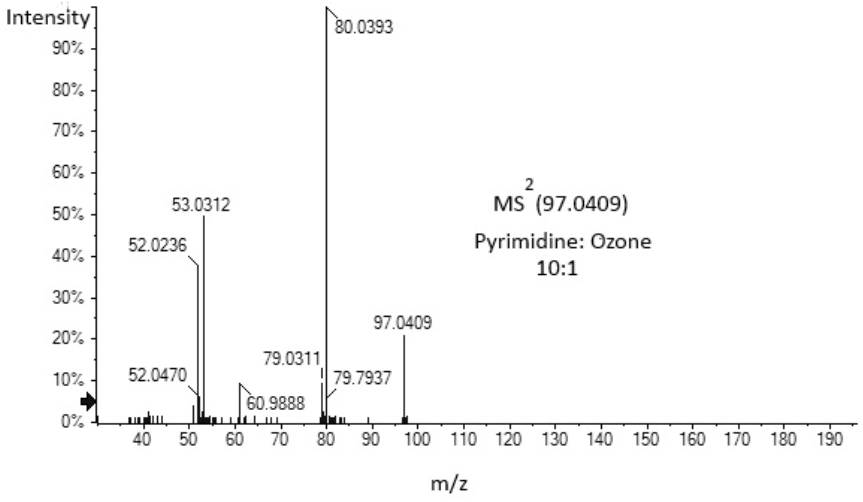

Figure S4. Mass spectrum (MS^2 of 96.0409) in the reaction of pyrimidine with ozone in the absence of scavenger obtained from LC-Q-ToF.

Text S6. Determination of OH radicals ($^{\bullet}$OH) with tertiary butanol

One method to determine $^{\bullet}$OH is to use $^{\bullet}$OH radical scavenger, for example dimethyl sulfoxide (DMSO) or tertiary butanol (t-BuOH). Due to the low ozone rate constants of the *N*-heterocyclic compounds (see Table 1), DMSO cannot be used as $^{\bullet}$OH scavenger in their reaction with ozone. DMSO use is limited to highly ozone-reactive substrates, since DMSO itself reacts with ozone with a rate constant of 8.2 M^{-1} s^{-1} (Veltwisch et al., 1980). Hence, tertiary butanol was applied as $^{\bullet}$OH scavenger (see Experimental and Scheme S5). The reaction of tertiary butanol with $^{\bullet}$OH leads to formaldehyde (in the presence of oxygen) and 2-hydroxy-2-methylpropanal, result from the bimolecular decay of the tertiary butanol-derived peroxyl radicals (Schuchmann & von Sonntag, 1979). To derive at the $^{\bullet}$OH yield in ozone reactions in this assay, the formaldehyde yield has to be approximately doubled, the yield of 2-hydroxy-2-methylpropanal is typically 1.3−1.4 times that of formaldehyde (Flyunt et al., 2003a).

The Hantzsch approach is a spectrophotometrically quantification of formaldehyde as diacetyldihydrolutidine (DDL) (Nash et al., 1953) by following its reaction with acetylacetone and ammonium ion, when a yellow compound characterized by ε(412 nm) = 7700 M^{-1} cm^{-1} was formed. By measuring with the Hantzsch method 5 mL sample were withdrawn from the batch and transferred into a volumetric flask. After that 2 mL of reagent solution (25 g ammonium acetat, 3 mL acetic acid and 0,2 mL acetylacetone mixed in 100 mL H_2O) and 3 mL H_2O was added. The samples were heated 30 minutes in a water bath at 50°C and than measured spectrophotometrically at room temperature.

Tertiary butanol reacts with ozone at a low rate constant (*k* (t-BuOH + O_3) = 0,003 M^{-1} s^{-1}, Flyunt et al., 2003b, or *k* (t-BuOH + O_3) = 0,011 M^{-1} s^{-1}, Reisz et al., 2014). Therefore, in the reaction of the nitrogen-containing heterocyclic compounds with ozone, where there was no interference with the Hantzsch method, $^{\bullet}$OH formation has been monitored with a large excess of tertiary butanol (0.05 M). A higher tertiary butanol concentration up to 0.1 M leads to a decrease of ozone concentration (Gurol & Nekouinaini, 1984), because it seems evident that in this case ozone reacts directly with t-BuOH in spite of the very low reaction rate constant. Therefore, one has to take into account the competition for ozone. Hence, in these experiments the substrate

was in constant high concentration (at least 10^{-1} M) over ozone (3×10^{-5} M – 3×10^{-4}M) to avoid ozone reactions with t-BuOH and $^{\bullet}$OH. Taking into account the concentration of pyrimidine (lowest *k* in this study in scavenged system and at least 1×10^{-1} M) in the reaction of pyrimidine (*k* (O_3 + pyrimidine) = 0.066 M^{-1} s^{-1}) with ozone (k_{app} (O_3 + pyrimidine) = 6.6×10^{-3} s^{-1}) and the reaction of t-BuOH with ozone (k_{app} (O_3 + t-BuOH) = 1.5×10^{-4} s^{-1}) the reaction of ozone with pyrimidine is still favored. In due consideration the reaction of t-BuOH with $^{\bullet}$OH (k_{app} ($^{\bullet}$OH + t-BuOH) = 3×10^{7} s^{-1}) and the reactions above, the reaction of t-BuOH with $^{\bullet}$OH is favored.

However, in non savenged system, taking into account the concentration of $^{\bullet}$OH (at most 2×10^{-5} M) in the reaction with ozone (k_{app} (O_3 + $^{\bullet}$OH) = 6×10^{4} s^{-1}) and the reaction of pyrazine (*k* (O_3 + pyrazine) = 1.3 M^{-1} s^{-1}) and pyrimidine (*k* (O_3 + pyrimidine) = 0.37 M^{-1} s^{-1}, in scavenged system and at least 10^{-2} M) with ozone (k_{app} (O_3 + pyrazine) = 1.3×10^{-2} s^{-1}) and (k_{app} (O_3 + pyrimidine) = 3.7×10^{-3} s^{-1}) the reaction of ozone with the *N*-heterocycles is absolutely not preferred.

Scheme S5. Determination of $^{\bullet}$OH with tertiary butanol.

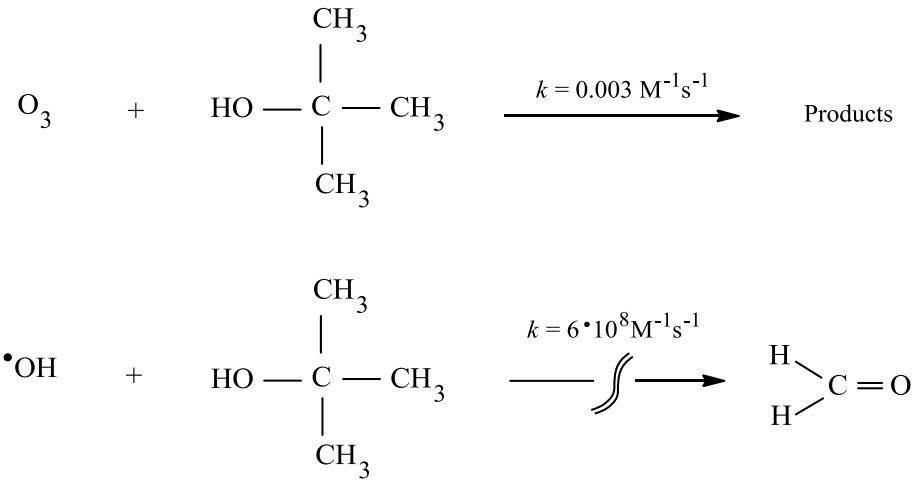

Besides, the above mentioned succession of ozone reactions tertiary butanol reacts with ozone at negligible rates even if present at reasonable excess (Flyunt et al., 2003b), however, isobutene (an impurity in t-BuOH) also give rise to formaldehyde (Dowideit & von Sonntag, 1998). On the one hand, formaldehyde formation yield is low (1%, Reisz et al., 2014) thus influences only little the slope of formaldehyde yield – ozone dose plot. On the other hand, due to the fact that the reaction is very fast,

formaldehyde formation occurs at the very beginning, i.e., it determines the apparition of a positive intercept but does not influence the slope of yield – dose line (Reisz et al., 2014).

Text S7. Determination of secondary products

In rate constant experiments with the competitor 3-buten-2-ol as well in experiments determining $^{\bullet}OH$ using tertiary butanol the extent of the formaldehyde yield in the reaction of nitrogen-containing heterocyclic compounds with ozone is necessary to know for the exclusion of interferences. The formaldehyde yields were determined in non scavenged system with the method of Hantzsch and the DNPH assay (see description above, competition kinetics, Text S3, determination of $^{\bullet}OH$, Text S6). Formaldehyde (k ($CH_2O + O_3$) = 0.1 M^{-1} s^{-1}, Hoigné & Bader, 1983a) reacts with ozone at low rates, even if present at reasonable excess. In addition, in these experiments the substrate was in constant high concentration (at least 10^{-2} M) to avoid ozone reaction with the formaldehyde. Thus, taking into account the concentration of formaldehyde (at most 2×10^{-5} M) in the reaction with ozone (k_{app} ($O_3 + CH_2O$) = 2×10^{-6} s^{-1}) and the reaction of pyrimidine (k (O_3 + pyrimidine) = 0.37 M^{-1} s^{-1}, lowest k in this study in non scavenged system and at least 10^{-2} M) with ozone (k_{app} (O_3 + pyrimidine) = 3.7×10^{-3} s^{-1}) the reaction of ozone with pyrimidine is still favored. In all cases blanks were performed in the same manner.

Scheme S6. Determination of hydrogen peroxide in its reaction with iodide.

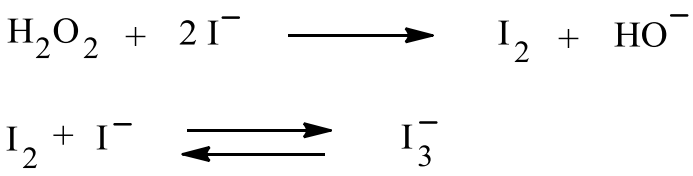

Hydrogen peroxide (H_2O_2) was determined spectrophotometrically with Allen`s reagent (molybdate-activated iodide) (Allen et al., 1952, Kitsuka et al., 2007). Hydroperoxides oxidize molybdate activated iodide ions to iodine, which can detected as I_3^- according to Scheme S6. The kinetics of this reaction is complex, but organic hydroperoxides can be distinguished from H_2O_2 by their kinetics with molybdate-activated iodide (Dowideit & von Sonntag, 1998, Flyunt et al., 2003b).

Hydrogen peroxide ($k(H_2O_2 + O_3)$ = 0.01 M^{-1} s^{-1}, pK_a = 11.6) reacts with ozone at low rates, even if present at suitable excess, however its anion, the hydroperoxide ion ($k(HO_2^- + O_3)$ = 5.5 × 10^6 M^{-1} s^{-1}) react with higher rates (Staehelin & Hoigné, 1982). But in these experiments with a pH of maximum 7 and the high pK_a value of hydrogen peroxide (see above) almost 100% of hydrogen peroxide is in the protonated form. Taking into account the concentration of hydrogen peroxide (at most 3.5 × 10^{-5} M) in the reaction with ozone (k_{app} ($O_3 + H_2O_2$) = 3.5 × 10^{-7} s^{-1}) and the reaction of pyrimidine with ozone (k (O_3 + pyrimidine) = 0.066 M^{-1} s^{-1}, lowest k in this study in scavenged system and at least 10^{-2} M, k_{app} (O_3 + pyrimidine) = 6.6 × 10^{-4} s^{-1}) the reaction of ozone with pyrimidine is still preferred.

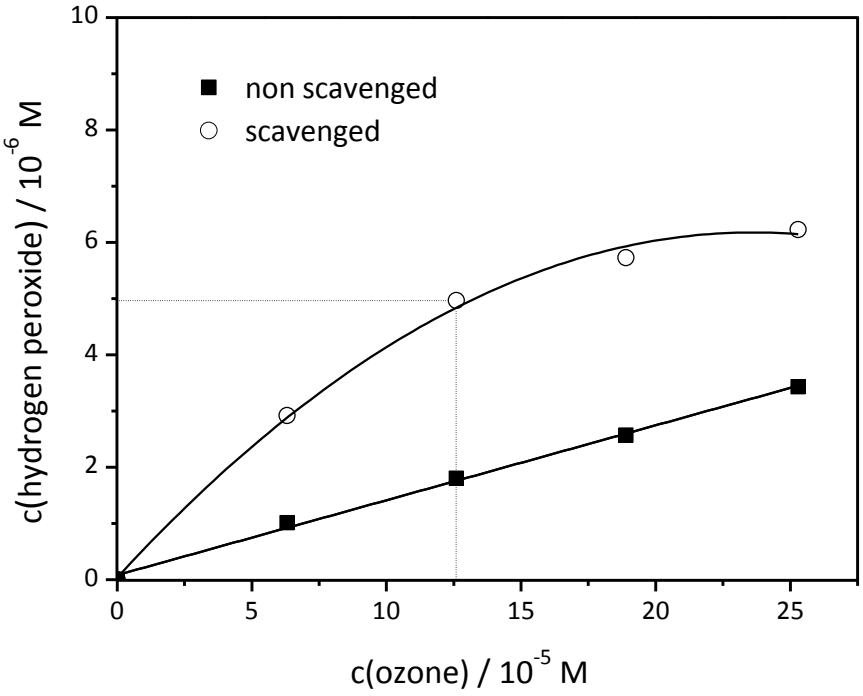

Figure S5. Formation of hydrogen peroxide in the reaction of pyridazine c_0(2.8 × 10^{-4}M) with ozone. Hydrogen peroxide concentrations in the presence and absence of tertiary butanol are plotted vs. the ozone concentration. In presence of tertiary butanol the calculation was made only for the linear range (see dotted line).

In all cases the Allen´s method was carried out by pipetting into UV-cells (1 cm path length) as follows: 1 mL Allen´s reagent A (1 g NaOH + 33 g KI + 0.1 g $(NH_4)_6Mo_7O_{24}$ · H_2O filled up to 500 mL ultra-pure water) plus 1 mL Allen´s reagent B (10 g potassium

hydrogen phthalate (KHP) dissolved in 500 mL ultra-pure water) plus 1 mL sample. After mixing the absorbance was detected spectrophotometrically at 350 nm (absorption coefficient at this wavelength is 25500 M^{-1} cm^{-1}). In all analytical methods blanks were performed in the same manner with ultra-pure water instead of ozone solution.

Text S8. Singlet oxygen

Triplet oxygen is the ground state of molecular oxygen. The electron configuration of the molecule has two unpaired electrons occupying two degenerate molecular orbitals with parallel spin. Singlet oxygen has two higher-energy species of molecular oxygen, in which the electrons are paired. Since the ground state of the ozone adduct is a singlet state, the overall spin multiplicity of the products must also be a singlet. As a consequence, this spin conservation rules demands that oxygen is released in its excited singlet state ($^1O_2$), which lies 95.5 kJ mol^{-1} above the triplet ground state ($^3O_2$) (Muñoz et al., 2001, von Sonntag & von Gunten, 2012).

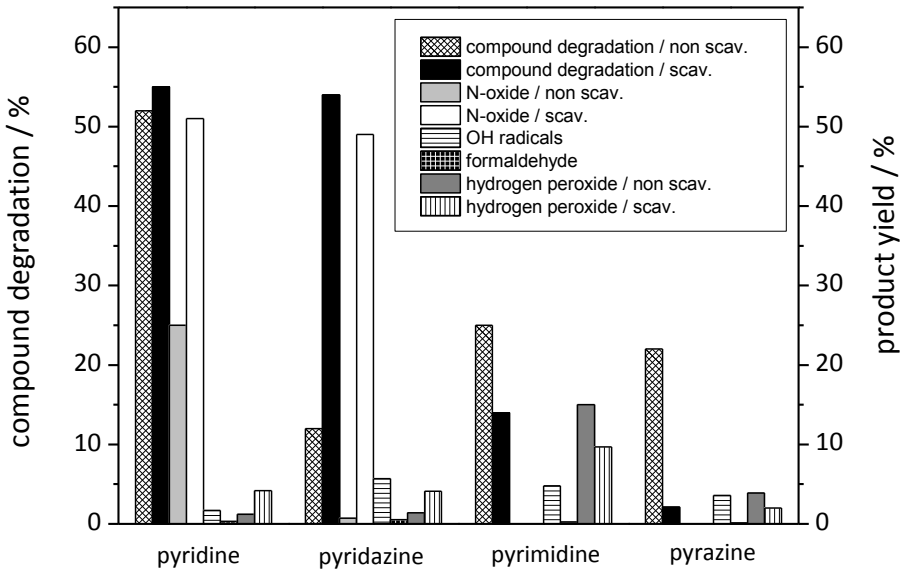

Figure S6. Compound degradation (%) and product yield (%) relating to ozone consumption in the ozonation of pyridine, pyridazine, pyrimidine and pyrazine in scavenged and non scavenged system.

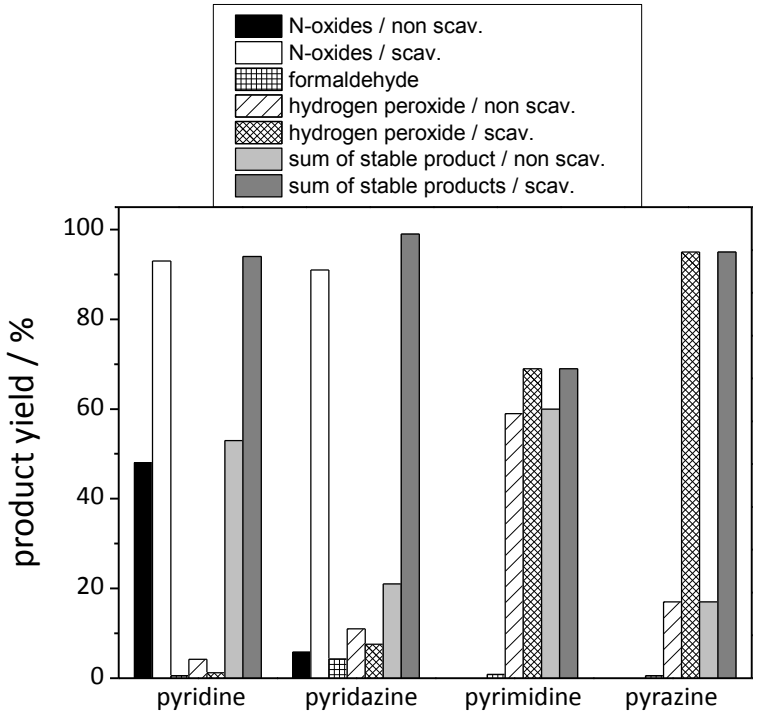

Figure S7. Product yield (%) relating to compound degradation in the reaction of pyridine, pyridazine, pyrimidine and pyrazine with ozone in scavenged and non scavenged system.

References

Acero, J. L., Stemmler, K., von Gunten, U., 2000. Degradation kinetics of atrazine and its degradation products with ozone and OH radicals: a predictive tool for drinking water treatment. Environ Sci Technol 34, 591-597

Allen, A. O., Hochanadel, C. J., Ghormley, J. A., Davis, T. W., 1952. Decomposition of water and aqueous solutions under mixed fast neutron and gamma radiation. J Phys Chem 56, 575-586.

Andreozzi, R., Caprio, V., Insola, A., Marotta, R., 2000. The oxidation of metol (*N*-methyl-*P*-aminophenol) in aqueos solution by UV/H2O2 photolysis. Wat Res 34, 463-472.

Andreozzi, R., Marotta, R., 1999. Ozonation of *p*-chlorophenol in aqueous solution. J Hazard Mater 69, 303-317.

Ashton, l., Buxton, G. V., Stuart, C. R., 1995. Temperature dependence of the rate of reaction of OH with some aromatic compounds in aqueous solution. J Chem Soc, Faraday Trans 91, 1631-1633.

Bader, H., Hoigné, J., 1981. Determination of ozone in water by the indigo method. Wat Res 15, 449-456.

Brambilla, A., Bolzacchini, E., Meinardi, S., Orlandi, M., Polesello, S., Rindone, B., 1995. Reactivity of organic micropollutants with ozone: a kinetic study. Proceedings Int Ozone Association 12, 43-52.

Buxton, G. V., Greenstock, C. L., Helman, W. P., Ross, A. B., 1988. Critical review of rate constants for reactions of hydrated electrons, hydrogen atoms and hydroxyl radicals (OH/O^-) in aqueous solution. J Phys Chem Ref Data 17, 513-886.

Dodd, M. C., Buffle, M.-O., von Gunten, U., 2006. Oxidation of antibacterial molecules by aqueous ozone: moiety-specific kinetics and application to ozone-based wastewater treatment. Environ Sci Technol 40, 1969-1077.

Dowideit, P., von Sonntag, C., 1998. The reaction of ozone with ethene and its methyl- and chlorine-substituted derivatives in aqueous solution. Environ Sci Technol 32, 1112-1119.

Flyunt, R., Leitzke, A., Mark, G., Mvula, E., Reisz, E., Schick, R., von Sonntag, C., 2003a. Determination of $^{\bullet}OH$ and $O_2^{\bullet-}$, and hydroperoxide yields in ozone reactions in aqueous solutions. J Phys Chem B 107, 7242-7253.

Flyunt, R., Leitzke, A., von Sonntag, C., 2003b. Characterisation and quantitative determination of (hydro)peroxides formed in the radiolysis of dioxygen-containing systems and upon ozonolysis. Radiat Phys Chem 67, 469-473.

Forni, L., Bahnemann, D., Hart, E. J., 1982. Mechanism of the hydroxide ion initiated decomposition of ozone in aqueous solution. J Phys Chem 86, 255-259.

Gurol, M., Nekouinaini, S., 1984. Kinetic behaviour of ozone in aqueous solutions of substituted phenols. Ind Eng Chem Fundamen 23, 54-60.

Hoigné, J., Bader, H., 1983a. Rate constants of reactions of ozone with organic and inorganic compounds in water. - I. Non-dissociating organic compounds. Wat Res 17, 173-183.

Hoigné, J., Bader, H., 1983b. Rate constants of reactions of ozone with organic and inorganic compounds in water. - II. Dissociating organic compounds. Wat Res 17, 185-194.

Kitsuka, K., Mohammad, A. M., Awad, M. I., Kaneda, K., Ikematsu, M., Iseki, M., Mushiake, K., Ohsaka, T., 2007. Simultaneous spectrophotometric determination of ozone and hydrogen peroxide. Chem Letters 36, 1396-1397.

Konya, K. G., Paul, T., Lin, S., Lusztyk, J., Ingold, K. U., 2000. Laser flash photolysis studies on the first superoxide thermal source. First direct measurements of the rates of solvent-assisted 1,2-hydrogen atom shifts and a proposed new mechanism for this unusual rearrangement. J Am Chem Soc 122, 1718-7527.

Lipari, F., Swarin, S. J., 1982. Determination of formaldehyde and other aldehydes in automobile exhaust with an improved 2,4-dinitrophenylhydrazine method. J Chrom 247, 297-306.

Merényi, G., Lind, J., Naumov, S., von Sonntag, C., 2010. The reaction of ozone with the hydroxide ion. Mechanistic considerations based on thermokinetic and quantum-chemical calculations. The role of HO_4^- in superoxide dismutation. Chem Eur J 16, 1372-1377.

Muñoz, F., von Sonntag, C., 2000a. Determination of fast ozone reactions in aqueous solution by competition kinetics. J Chem Soc, Perkin Trans 2, 661-664.

Muñoz, F., von Sonntag, C., 2000b. The reaction of ozone with tertiary amines including the complexing agents nitrilotriacetic acid (NTA) and ethylenediaminetetra-acetic acid (EDTA) in aqueous solution. J Chem Soc, Perkin Trans 2, 2029-2033.

Muñoz, F., Mvula, E., Braslavsky, S. E., von Sonntag, C., 2001. Singlet dioxygen formation in ozone reactions in aqueous solution. J Chem Soc, Perkin Trans 2, 1109-1116.

Nash, T., 1953. The colorimetric estimation of formaldehyde by means of the Hantzsch reaction. Biochem J 55, 416-421.

Neta, P., Huie, R. E., Ross, A. B., 1988. Rate constants for reactions of inorganic radicals in aqueous solution. J Phys Chem Ref Data 17, 1027-1284.

Olson, K. L., Swarin, S. J., 1985. Determination of aldehydes and ketones by derivatization and liquid chromatography- mass spectrometry. J Chrom 333, 337-347.

Porter, A. E. A., 1984. Pyrazines and their benzo derivatives. In: Katritzky, A. R., 1984. Comprehensive heterocyclic chemistry / the structure, reactions, synthesis and uses of heterocyclic compounds, Pergamon Press, Oxford, 157-199.

Reisz, E., Fischbacher, A., Naumov, S., von Sonntag, C., Schmidt, T. C., 2014. Hydride transfer: a dominating reaction of ozone with tertiary butanol and formate ion in aqueous solution. Ozone Sci Eng 36, 532-539.

Schuchmann, M. N., von Sonntag, C., 1979. Hydroxyl radical-induced oxidation of 2-methyl-2-propanol in oxygenated aqueous solution. A product and pulse radiolysis study. J Phys Chem 83, 780-784.

Söylemez, T., von Sonntag, C., 1980. Hydroxyl radical-induced oligomerization of ethylene in deoxygenated aqueous solution. J Chem Soc, Perkin Trans 2, 391-394.

Staehelin, J., Hoigné, J., 1982. Decomposition of ozone in water: rate of initiation by hydroxide ions and hydrogen peroxide. Environ Sci Technol 16, 676-681.

Tauber, A., von Sonntag, C., 2000. Products and kinetics of the OH-radical-induced dealkylation of atrazine. Acta Hydrochim Hydrobiol 28, 15-23.

Veltwisch, D., Janata, E., Asmus, K.-K., 1980. Primary processes in the reactions of •OH radicals with sulphoxides. J Chem Soc, Perkin Trans 2, 146-153.

von Sonntag, C., 2006. Free-radical-induced DNA damage and its repair. A chemical perspective. Springer Verlag, Heidelberg, Berlin

von Sonntag, C., Schuchmann, H.-P., 1991. The elucidation of peroxyl radical reactions in aqueous solution with the help of radiation-chemical methods. Angew Chem, Int Ed Engl 30, 1229-1253.

von Sonntag, C., Schuchmann, H.-P., 1997. Peroxylradicals in aqueous solution. In: Peroxyl Radicals, Z.B. Alfassi (ed.), Wiley Chichester, 173-234.

von Sonntag, C., von Gunten, U., 2012. Chemistry of ozone in water and wastewater treatment. From basic principles to applications. IWA Publishing.

Zimmermann, S. G., Schmukat, A., Schulz, M., Benner, J., von Gunten, U., Ternes, T. A., 2012. Kinetic and mechanistic investigations of the oxidation of tramadol by ferrate and ozone. Environ Sci Technol 46, 876-884.

5 General conclusions and outlook

In the thesis presented here ozonation of three classes of amines were investigated to assist the elucidation of mechanisms involved in the oxidation of micropollutants by ozone. Ozonation research is required to assess the risk potential in the urban water cycle by using ozonation techniques, due to the high number of micropollutants, in particular pharmaceuticals, which are estimated to be continuously released into the aquatic environment. To gain insight into ozonation processes ozone rate constants, reaction stoichiometry and product formation, including $^{\bullet}$OH yields are important reaction parameters.

The present study has depicted that transformation or degradation of anilines, aliphatic and aromatic *N*-heterocyles by ozonation, including $^{\bullet}$OH reactions is in principle feasible in aqueous solution. The rate constants of anilines and aliphatic *N*-heterocycles with ozone (around 10^6 M^{-1} s^{-1} for anilines and 10^5 M^{-1} s^{-1} for aliphatic *N*-hetrocycles) were so high that a reliable determination of rate constants could only be achieved by competition kinetics (refer to Chapter 2 and 3). This is consistent with the fact that amines contain a lone electron pair at the nitrogen and hence could be usually prone to electrophilic attack of ozone. In addition, in aromatic amines the free electron pair can conjugate into the aromatic ring system, which hence also could be more susceptible to ozone attack (refer to Chapter 1). The lower ozone rate constants for aromatic *N*-heterocycles (lower than 60 M^{-1} s^{-1}) can be explained by the sp^2 hybridisation of nitrogen in comparison to the sp^3 hybridisation of anilines and aliphatic *N*-heterocycles, whereby either the lone electron pair at nitrogen is less available or the aromatic ring is less activated for electrophilic attack (refer to Chapter 4). Although the ozone rate constants are rather high for most of the investigated amines except aromatic *N*-heterocyles, the demand of ozone for complete amine transformation is in all cases high too. Moreover, additional studies led to substantial $^{\bullet}$OH yields in the reaction of ozone with anilines (34-59%) and aliphatic *N*-heterocycles (near 30%), however, much lower $^{\bullet}$OH yields for the aromatic *N*-heterocycles (lower than 6%) are deduced. $^{\bullet}$OH reactions on the one hand take part in degradation of compounds, on the other hand participate in undesirable ozone degradation reactions. This and the very low amine degradation, in most cases attributed to the chain

reaction, which decomposes ozone without compound degradation, point out that ozonation techniques have to be applied very carefully in relation to ozone addition amount (refer to reaction stoichiometry in chapter 2, 3 and 4).

Considering the mechanism in the ozonation of anilines raises the question, whether the strongly electrophilic ozone attacks at the electron-rich aromatic ring rather than at the lone electron pair at nitrogen is the most favored reaction. The present study revealed, in detail for anilines (see Chapter 2), that the ozone attack takes place preferentially at the aromatic ring (see Scheme 1, reaction Ar 1 – 4) however, an addition to the nitrogen must also be envisaged (see Scheme 1, reaction An 1). Electron transfer reactions on nitrogen (Scheme 1, reaction ETn 1 – 2) as well as on the aromatic ring (Scheme 1, reaction ETr 1 – 2) have also be proven. In contrast, for the aliphatic *N*-heterocycles ozone attack occurs preferentially at the nitrogen, albeit with marked differences in reaction mechanisms for piperidine, piperazine and morpholine despite considerable similarities in the range of rate constants and stoichiometric ratio and the structural resemblance. The most favored reaction of ozone with piperidine is an electrophilic addition at nitrogen (see Scheme 1, reaction An 2). This also holds for morpholine (Scheme 1, reaction An 4), although to a lower extent. An ozone attack at nitrogen leading to the *N*-hydroxy product in the case of piperazine must also be envisaged (reaction An 3), because a significant hydroxylamine yield enables the formation and decomposition of the *N*-hydroxypiperazine. However this could not definitely be proven in this study. Further evidence of the temporary existence of this *N*-hydroxy product (cf. Scheme 1, reaction An 2) may be received by determination of the singlet oxygen yield (Scully & Hoigné, 1987). In literature several analytical techniques are described for the determination of singlet oxygen available (Hideg et al., 1994, Mishra et al., 1996, Telfer et al., 1999). Moreover, the ozone attack at nitrogen can also lead to electron transfer reactions, which is mainly assumed for piperazine and morpholine (Scheme 1, reaction ETr 1 – 2, see also Chapter 3). One further confirmation for these postulated reaction pathways could be the identification of the suggested products, like oxazolidine, *N*-hydroxyoxazolidine, imidazolidine and *N*-hydroxyimidazolidine e.g., with very sensitive analytical technique such as time-of-flight mass spectrometry (LC-Q-TOF).

Scheme 1. Primary reaction pathways of the amines under study denoted with the corresponding probability in percentage based on product yields with respect to compound transformation. In the absence of compound transformation results (missing reaction stoichiometry), the data are reported with a greater (>) sign.

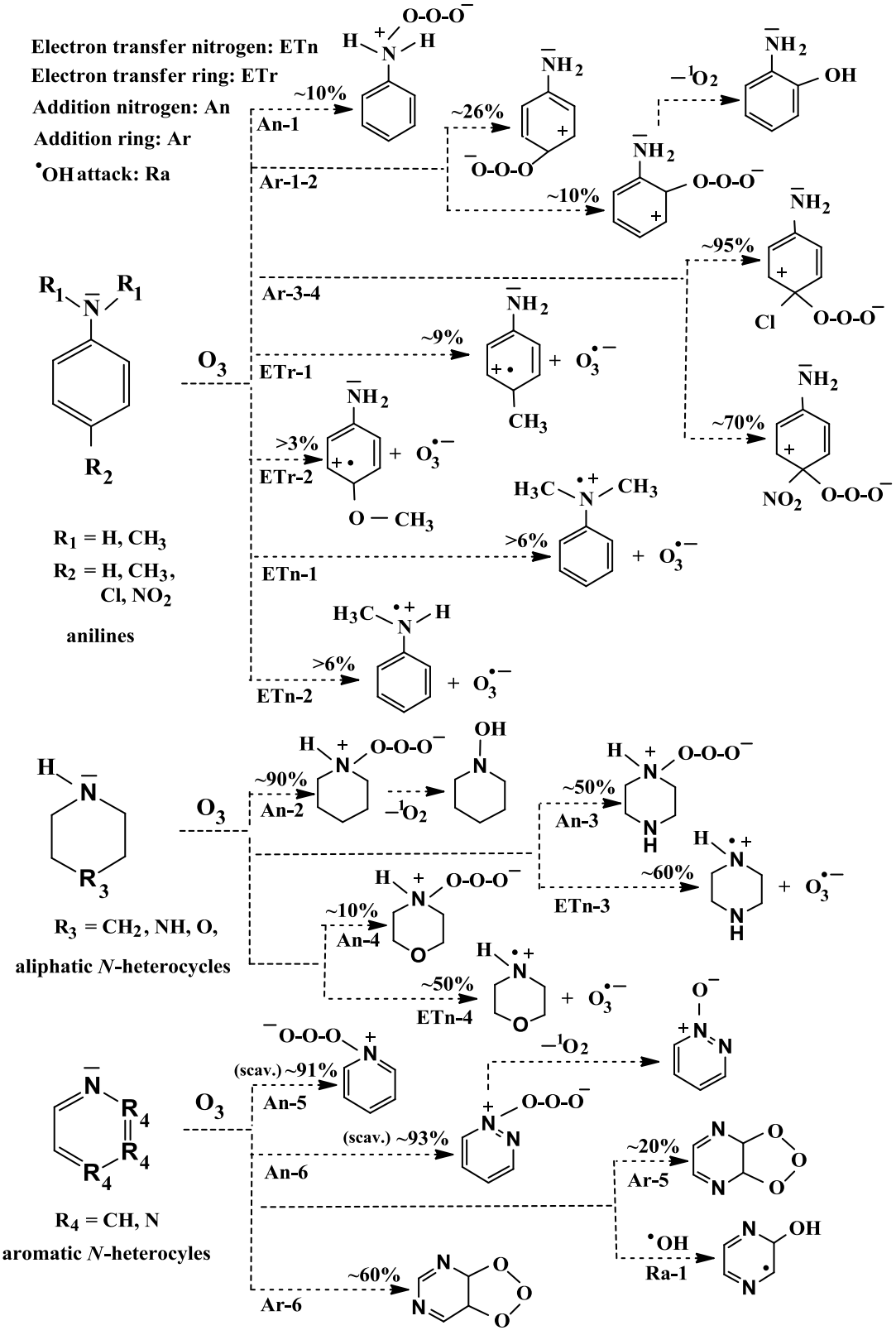

For the primary ozone reactions pathways of the aromatic *N*-heterocycles (see Chapter 4), the present study indicates that in spite of similarities in molecular structure, there are significant differences in rate constants (e.g., pyridazine 57 M^{-1}, s^{-1}, pyrimidine 0.37 M^{-1} s^{-1}), reaction stoichiometry (in particular with regard to scavenged and non scavenged system), product formation and consequently for drawing mechanistic conclusions. It was shown that for pyridine and pyridazine ozone preferable attacks at nitrogen to form the appropriate *N*-oxides (see Scheme 1, reaction An 5 – 6), whereas this reaction probably does only play a subsidiary role in the ozonation of pyrimidine and pyrazine. Considering the significant hydrogen peroxide yield ozone addition to the aromatic ring following the Criegee mechanism seems to occur mainly in the case of pyrimidine (presumably also for pyrazine, although to a lower extent (Scheme 1, reaction Ar 5 – 6)). For pyrimidine this is consistent with the unexpected stoichiometric ratio in scavenged and non scavenged systems, in contrast to pyridine and pyridazine. Further products confirming this reaction pathway have not been found. However, results from reaction stoichiometry suggest that for pyrazine mainly $^{\bullet}OH$ reactions followed by oxygen reactions should take place (see Scheme 1, reaction Ra 1). One further validation for the proposed reaction pathway in the pyrazine/ozone reaction could be the identification of products in the absence of oxygen. The same is valid for ozone reactions with the aliphatic *N*-heterocycles. It was additionally shown that the ozonation of the corresponding *N*-oxides indicate a different reaction behavior compared to the parent compounds. In principle, it was demonstrated that already slight structural difference in the chemical structure could be decisive for their degradation behavior. It is not yet known, why the structurally closely related aromatic (as well as aliphatic) *N*-heterocycles react in such different pathways. However, this consolidated knowledge is of great importance if the presented results should be transferred to more complex micropollutants and it should be addressed in coming-up studies. Calculations of the electron density, the probability of an electron being present at a specific location may help to foster our mechanistic understanding.

In the present study the mass balances for almost all investigated ozone-amine reactions were calculated. This is crucial to assess whether all relevant transformation products have been identified, quantified and to assure the mechanistic conclusions. With respect to mass balances, the results obtained highlight that in the case of

piperidine and piperazine the mass balance is closed, whereas it is around 60% complete for morpholine (see Scheme 1, reaction An 2 – 4 and ETn 3 – 4). To close this gap, a quantification of the commercially not available *N*-hydroxymorpholine should be done. The results from product formation of ozone reactions with anilines revealed a complete mass balance only for chloroaniline in systems without $^{\bullet}$OH scavenging (see Scheme 1, reaction Ar 3), whereas for nitroaniline at least 70% could be deduced (Scheme 1, reaction Ar 4). Indeed, for aniline itself, the mass balance is not complete, albeit in this case a comprehensive product determination was carried out. Here, a quantification of the identified 2-Amino-5-anilino-benzochinon-anil should close the gap. A complete mass balance was found for pyridine, pyridazine and pyrazine in $^{\bullet}$OH scavenged systems. The incomplete mass balance in non scavenged pyrazine/ozone reactions may be closed by quantification of the identified products. However, in general and in particular for pyrimidine the results of incomplete mass balances clearly highlight the necessity of using miscellaneous analytical techniques, e.g., besides high-resolution mass spectrometry (HRMS) also NMR measurements to identify further products. This should be addressed in further product studies. Additionally, it is proposed to synthesize the missing reference material for the quantification of the identified products to close the gap in mass balances. However, this comes with an enormous additional effort.

Finally it can be said that the mechanism of the investigated amines in their reaction with ozone could tentatively be proposed. Thereby, the results clearly highlight the necessity of comprehensive studies using several reaction parameters, since determination of the (pseudo) first order rate constants and product formation studies do not give a complete picture if, e.g., the stoichiometric ratio is not established. Another crucial outcome of this thesis is that the amines under study can be applied as archetypes for some kind of pharmaceuticals since the presented results may help to explain transformation kinetics and products in the reaction of more complex micropollutants containing an amine moiety as structural unit. Micropollutants e.g., owning a moiety of aniline or aliphatic *N*-heterocycles such as the pharmaceuticals clenbuterol or timolol, respectively (refer to Chapter 1) should be easily attack by ozone. In contrast, micropollutants carrying an aromatic *N*-heterocyclic moiety as well as an amide moiety (cf. Pryor et al., 1984) such as pyrazineamide should be less

susceptible to ozone attack. Pyrimethamine in turn in spite of containing an aromatic *N*-heterocyclic moiety should be indicated high reactivity to ozone due to the aniline moiety (for the structures of the pharmaceuticals refer to Chapter 1: Introduction). However, one needs to consider that even structurally closely related compounds can react very differently with ozone as was demonstrated in this work. Hence, pharmaceuticals, which were not examined for their reaction with ozone, can ultimately result in the formation of unknown transformation products. Nonetheless, research on ozonation of amines pointed out the relevance of fundamental studies to understand the elementary mechanisms. Not only some transformation products (as well how stable they are) and a few stoichiometric ratios for a couple of investigated compounds (e.g., for anilines) are still unknown but also numerous further aspects that still need further investigation. While ozone rate constants of the investigated amines are determined in this study, corresponding rate constants of $^{\bullet}$OH reactions are largely lacking. Further overarching studies of pH dependence (see Mvula & von Sonntag, 2003) of the ozone-amine reactions may help to improve the understanding of the amines. In addition, ozonation of structurally related *N*-containing compounds (e.g., pyrrolidine and pyrrol or pyrazol, imidazol and imidazolidine, quinoline and quinoxaline) should be addressed in future works in order to clarify different ozone mechanisms by comparing their reactions. All this data could complement the results of the present study for describing amine degradation and help to transfer the model to more complex micropollutants. Therefore, a stronger focus of coming-up studies should be on fundamental research. In particular ozonation studies of specific structural features of pharmaceuticals may contribute to a reliable prediction of transformation products and their prioritization for risk assessment. Moreover, it is strongly recommended to study the mechanism in clean water as well as in waste water matrix, in which the conditions are more complex.

As an overall conclusion for using ozonation in waste water treatment plants or waterworks, this technology is appropriate to remove nitrogen-containing compounds. However, ozonation can lead to the release of transformation products in the urban water cycle with unknown toxicity, whereas the complexity of transformation pathways can be further increased by $^{\bullet}$OH reactions and free radical reactions with oxygen. This can lead to reactive moieties that can be toxic to aquatic life such as

formaldehyde. Therefore, new mitigation strategies are crucial to upgrade waste water treatment plants and waterworks with advanced physico-chemical treatment. Besides ozonation, membrane filtration (such as nanofiltration and reverse osmosis), activated carbon treatment and advanced oxidation processes (AOP) have been proposed as end of pipe techniques (Joss et al., 2008). Even if, one has to consider the high costs for implementation of such technologies, the protection of the aquatic ecosystem should be a priority.

5.1 References

Hideg, E., Spetea, C., Vass, I., 1994. Singlet oxygen and free radical production during acceptor- and donor-side-induced photoinhibition. Studies with spin trapping EPR spectroscopy. BBA - Bioenergetics 1186, 143-152.

Joss, A., Siegrist, H., Ternes, T. A., 2008. Are we about to upgrade wastewater treatment for removing organic micropollutants? Water Sci Techol 57, 251-255.

Mishra, R. K., Mishra, N. P., Kambourakis, S., Orfanopoulos, M., Ghantokis, D. F., 1996. Generation and trapping of singlet oxygen during illumination of a photosystem II core complex. Plant Sci 115, 151-155.

Mvula, E., von Sonntag, C., 2003. Ozonolysis of phenols in aqueous solution. Org Biomolec Chem 1, 1749-1756.

Pryor, W. A., Giamalva, D. H., Church, D. F., 1984. Kinetics of ozonation. 2. Amino acids and model compounds in water and comparison to rates in non polar solvents. J Am Chem Soc 106, 7094-7100.

Scully, F. E., Hoigné, J., 1987. Rate constants for reactions of singlet oxygen with phenols and other compounds in water. Chemosphere 16, 681-694.

Telfer, A., Oldham, T. C., Phillips, D., Barber, J., 1999. Singlet oxygen formation detected by near-infrared emission from isolated photosystem II reaction centres: direct correlation between P680 triplet decay and luminescence rise kinetics and its consequences for photoinhibition. J Photochem Photobio B 48, 8-96.

6 Supplement

6.1 List of abbreviations

List of abbrivations in alphabetic order; latin follows greek; arabic numerals follows letters

Symbol/ Abbreviations	
α	degree of dissociation
A	absorbance (or peak area)
A_0	absorbance (or peak area) in the absence of competitor
A^-	monovalent anion
A^{2-}	bivalent anion
ACN	acetonitrile
ADHD	attention deficit hyperactivity disorder
amu	atomic mass unit
APCI	atmospheric pressure chemical ionisation
C	carbon
c	concentration
c_0	initial concentration
°C	degree Celsius
(C)	competitor
[C]	competitor concentration
$[C]_0$	initial competitor concentration
C_{18}	octadecyl carbon chain, $C_{18}H_{37}$ alkyl group
cf.	conferre, confer, compare
-CH-	benzene bridge
cm	centimetre
$-CH_2-$	methylene bridge
CH_20	formaldehyde
$-CH_3$	methyl group
-Cl	chlorine group
Cl^-	chloride
-C=N-	imine unit
-C=O	carbonyl unit
-COOH	carboxyl group
ΔG^0	standard Gibbs energy
DAD	dioden-array detector
DDL	diacetyldihydrolutidine
DFT	density functional theory
DMSO	dimethylsulfoxide
DNPH	2,4-dinitrophenylhydrazine
Ɛ	molar absorptions coefficient

E°	standard reduction potential
EDTA	ethylenediaminetetraacetic acid
e.g.	exempli gratia, for example
EI	electron ionisation
Eq	equation
ESI	electron spray ionisation
et al.	et alii, and others
eV	electron volt
FMOC-Cl	9-fluorenylmethyl chloroformate
FTMS	fourier transformation mass spectrometer
g	gram
GC	gas chromatography
h	hour
H	hydrogen
H_2A	biprotonated bivalent compound
HA	monoprotonated monovalent compound
HA^-	monoprotonated bivalent compound
HCl	hydrochloric acid
HCOOH	formic acid
H_2O	water
H_2O_2	hydrogen peroxide
H_3O^+	hydronium ion
HO_2^-	hydrogen peroxide anion
$HO_2^\bullet$	hydroperoxyl radical
$HO_3^\bullet$	hydrotrioxyl radical
HO_4^-	hydrotetraoxide anion
HO_5^-	hydropentaoxide anion
HPO_4^{2-}	hydrogen phosphate
$H_2PO_4^-$	dihydrogen phosphate
H_3PO_4	phosphoric acid
H_2SO_4	sulfuric acid
HPLC	high-performance liquid chromatography
HRMS	high-resolution mass spectrometry
IC	ion chromatography
I.D.	inside diameter
i.e.	id est
(-I)	electron-withdrawing inductive effect
(+I)	electron-releasing inductive effect
I_2	iodine
I^-	iodide ion
I_3^-	triiodide ion
IO_3^-	iodate
k	rate constant
k'	first order rate konstant
k''	second order rate constant
k_{app}	reaction rate
k_{obs}	first order rate konstant
K_a	acid dissociation constant
K_{a1}	first acid dissociation constant

K_{a2}	second acid dissociation constant
K_b	base dissociation constant
KHP	potassium hydrogen phthalate
KI	potassium iodide
λ	wave length
L	litre
LC	liquid chromatography
LFER	linear free energy relationships
ln	natural logarithm
log	logarithm
µg	microgram
µL	microlitre
µm	micrometre
m	mass
M	molar (usually in moles per liter)
(M)	compound
[M]	compound concentration
$[M]_0$	initial compound concentration
(-M)	electron-withdrawing mesomeric effect
(+M)	electron-releasing mesomeric effect
mg	milligram
min	minute
mL	millilitre
mm	millimetre
MS	mass spectrometry
MSIS	methanesulfinic acid
m/z	mass-to-charge ratio
N	nitrogen
Na_2CO_3	sodium carbonate
$NaHCO_3$	sodium bicarbonate
NaOH	sodium hydroxide
-NH-	amine bridge
$-NH_2$	amine group
NH_2OH	hydroxylamine
$(NH_4)_6Mo_7O_{24}$	ammonium heptamolybdate
nm	nanometre
NMR	nuclear magnetic resonance
$-NO_2$	nitrogen dioxide group
NO_2^-	nitrite
NO_3^-	nitrate
o	ortho
-O-	oxygen bridge
$O^{\bullet-}$	oxide radical anion
O_2	oxygen
$^1O_2$	singlet Oxygen
$^3O_2$	triplet Oxygen
O_2^-	superoxide anion
$O_2^{\bullet-}$	superoxide radical anion
O_3	ozone

$O_3^{\bullet-}$	ozonide radical anion
^{-}OH	hydroxyl ion
$^{\bullet}OH$	hydroxyl radical
-OH	hydroxyl group
π	pi
p	para
p.a.	pro analysis
[P]	endpoint yield in the presence of competitor
$[P]_0$	endpoint yield in the absence of competitor
PBF	poisson-boltzmann solver
PDMS	polydimethylsiloxane
pH	potentia hydrogenii, pH value
pK_a	logarithmic acid dissociation constant
pK_b	logarithmic base dissociation constant
p.s.	pro synthesis
PO_4^{3-}	phosphate
Q1	first quadrupole
r	correlation coefficient
RT	retention time
σ	hammett constants, substituent constant
sp	s(sharp)p(principal) hybrid orbitals
sp^2	s(sharp)2p(principal) hybrid orbitals
sp^3	s(sharp)3p(principal) hybrid orbitals
SPME	solid phase micro extraction
T	temperature
t	time
t-BuOH	tertiary butanol
TIC	total ion current
TPs	transformation products
UV	ultra violet light
V	volt
VIS	visible light
WWTP	waste water treatment plant
y = a x + b	linear equation

6.2 List of Publications

Publications in peer-reviewed journals

Tekle-Röttering, A., Jewell, K. S., Reisz, E., Lutze, H., Ternes, T. A., Schmidt, W. and Schmidt, T.C., (2016). **Ozonation of piperidine, piperazine and morpholine: Kinetics, stoichiometry, product formation and mechanistic considerations**. Wat Res, 88, 860-971.

Tekle-Röttering, A.,von Sonntag, C., Reisz, E., vom Eyser, C., Lutze, H., Türk, J., Naumov, S., Schmidt, W., Schmidt, T.C., **Ozonation of anilines: Kinetics, stoichiometry, product, identification and elucidation of pathways**, submitted to Water Research

Oral presentations and posters

Tekle-Röttering, A., Schmidt, W. and Schmidt, T. C.
Poster presentation: **Mechanistic considerations of ozone-amine reactions**,
May, 11. – 13., 2015, Wasser 2015-Jahrestagung der Wasserchemischen Gesellschaft, Schwerin, Germany

Tekle-Röttering, A., Schmidt, W. and Schmidt, T. C.
Poster presentation: **Mechanistic considerations of ozone-amine reactions**,
May, 03. – 07., 2015, SETAC Europe 25th Annual Meeting, Barcelona, Spain

Tekle-Röttering, A., Schmidt, W. and Schmidt, T. C.
Oral presentation: **Ozonation of heterocycles: Kinetics, stoichiometry, product formation and mechanistic considerations**, March, 26. 2015, KNUST, Kumasi, Ghana

Tekle-Röttering, A., Schmidt, W. and Schmidt, T. C.
Poster presentation: **Reactions of nitrogen-containing heterocycles with ozone**,
June, 03. – 04., 2013, International Conference, Pharmaceutical Products in the Environment, Nimes, France

Tekle-Röttering, A., Jewell, K. S., Ternes, T. A., Schmidt, W. and Schmidt, T. C.
Oral presentation: **Kinetic and mechanistic aspects of the oxidation of piperidine, piperazine and morpholine by ozone**, May, 26. – 28., 2014, Wasser 2014-Jahrestagung der Wasserchemischen Gesellschaft, Haltern am See, Germany

Tekle-Röttering, A., Jewell, K. S., Ternes, T. A., Schmidt, W. and Schmidt, T. C.
Short oral and poster presentation: **Kinetic and mechanistic aspects of the oxidation of piperidine, piperazine and morpholine by ozone**, September, 23. – 24. 2014, Tagung: Relevanz von Transformationsprodukten im urbanen Wasserkreislauf, Koblenz, Germany

Tekle-Röttering, A., Schmidt, W. and Schmidt, T. C.
Poster presentation: **Reactions of nitrogen-containing heterocycles with ozone**, May, 06. – 08., 2013, Wasser 2013-Jahrestagung der Wasserchemischen Gesellschaft, Goslar, Germany

Tekle-Röttering, A., Schmidt, W. Schmidt, T. C. and von Sonntag, C.
Short oral and poster presentation: **Kinetics and OH radical yield of the reaction of ozone with aniline and morpholine,** April, 23. – 24., 2012, Tagung: Relevanz von Transformationsprodukten im urbanen Wasserkreislauf, Koblenz, Germany
Koblenz, Germany

Tekle-Röttering, A., Schmidt, W., Schmidt, T. C. and von Sonntag, C.
Short oral and poster presentation: **Products and stoichiometry aspects in the reaction of aniline with ozone**, May, 14. – 16., 2012, Wasser 2012-Jahrestagung der Wasser-chemischen Gesellschaft, Neu-Ulm, Germany

Tekle-Röttering, A., Schmidt, W., Schmidt, T. C. and von Sonntag, C.
Poster presentation: **Kinetics and OH radical yield of the reaction of ozone with aniline and morpholine**, May, 30. – June 01., 2011, Wasser 2011-Jahrestagung der Wasserchemischen Gesellschaft, Norderney, Germany

6.3 Curriculum Vitae

Der Lebenslauf ist in der Online-Version aus Gründen des Datenschutzes nicht enthalten.

6.4 Acknowledgment

My sincere gratitude belongs to my research supervisor **Prof. Dr. Torsten C. Schmidt** for his excellent support and our critical and fruitful discussions and the chances he had given to me. Prof. Dr. Torsten C. Schmidt always encouraged me to go on in critical situations during my research activities.

Moreover, I want to thank **Prof. Dr. Winfried Schmidt** for his support and various discussions and the chance to do my doctoral thesis.

Many thanks to **Prof. Dr. Thomas A. Ternes** for his efforts to act as secondary assessor of this work and his support to do LC-HRMS-analytics at the Federal Institute of Hydrology (BfG) in Koblenz.

In particular, I thank **Kevin S. Jewell** from the Federal Institute of Hydrology in Koblenz for helping and assisting the LC-HRMS analytics.

I also thank **Claudia vom Eyser** and **Dr. Jochen Türk** for their support in doing LC-MS analytics at the Institute of Energy- and Environmental Technics (IUTA) in Duisburg.

Furthermore, I highly appreciate **Dr. Erika Reisz** from University "Politehnica" of Timişoara in Romania. Without her neverending support this work would not have been successful.

A great thank to my colleagues **Dr. Natalia Tabler** and **Jens Richter** form the Westphalian University for their translation of russian literature and support in computer problems, respectively.

I also thank all my colleagues at the Department of Instrumental Analytical Chemistry, University Duisburg-Essen, who have welcomed me heartily in their community. In particular I thank **Dr. Holger Lutze** for proofreading and fruitful discussions. As well as I thank **Alexandra Fischbacher**, **Alexandra Beermann**, **Dr. Christine Erger** and **Sarah Willach** for their help and assistance in laboratory work.

Last, but not least, posthymously, a great appreciation belongs to **Prof. Clemens von Sonntag** for sharing his great knowledge and vast experience with me and for professional discussions that changes my view.

Without many words: **My whole family** - Thank you.

6.5 Erklärung

Hiermit versichere ich, dass ich die vorliegende Arbeit mit dem Titel:

“Ozonation of amines: Kinetics, stoichiometry, product formation and mechanistic considerations“

selbst verfasst und keine außer den angegebenen Hilfsmitteln und Quellen benutzt habe, und dass die Arbeit in dieser oder ähnlicher Form noch bei keiner anderen Universität eingereicht wurde.

Düsseldorf, im Dezember 2015

Agnes Tekle-Röttering